Effects of Developmental Exposure to Selective Serotonin Reuptake Inhibitors: Impacts on Stress Axis Function and Screening Approaches in Zebrafish

Emmanuelle Monniez

Thesis submitted to the University of Ottawa
in partial fulfillment of the requirements for the
Doctorate in Philosophy degree in Biology

Department of Biology
Faculty of Sciences
University of Ottawa

© Emmanuelle Monniez, Ottawa, Canada, 2026

Acknowledgements

Coming to the end of this marathon, full of ups and downs, I would like to express my gratitude to everyone with whom I crossed paths and who, in their own way, contributed to bringing me to the finish line.

First and foremost, I would like to acknowledge both my supervisors, Dr. Vance L. Trudeau and Dr. Carole Yauk. Thank you for giving me the opportunity to pursue my academic path, but most of all, for your mentorship, guidance, friendship and support throughout this project. I have grown incredibly during this journey, both scientifically and personally, and I can only aspire to become as resilient and strong a scientist as you are. I am sure our friendship will last beyond this project and across the world.

I would like to thank my Ph.D. Thesis Advisory Committee, Dr. Kathleen Gilmour, Dr. Jan Mennigen, Dr. Jason O'Brien and Dr. Errol Thomson. Thank you for your time, insightful and valuable suggestions. I also would like to especially thank my external evaluator, Dr. Som Niyogi, for agreeing to serve on my evaluation committee. The time that you have allocated for this is greatly appreciated.

To my colleagues and friends in the TeamENDO.ca and GReAT Lab, both past and present members: it has been a pleasure to work alongside all of you; thank you for your support and the fun times. A special mention to David Eickmeyer, both my friend and a super lab technician; thank you for watching over my shoulder during library preparations. Thank you to Ridoy Uptal and Shirley Zeng for trusting me as your project mentor and for helping me at the lab bench. I hope you have gained as much from these experiences and working together as I did, learning to be a mentor. I wish you the best for the rest of your studies and future endeavours. To the CAREG 4th-floor team, thank you for always being there at lunchtime; the conversations, full of laughter and debates over opinions, were always welcome.

To my close friends I made here in Canada, Alex Hicks, Dr. Paul Agnani, Nicolas Bonin, Wyeth Blumberg, Mathieu Vilain (a.k.a., "the French Gang"), and many more: thank you for your friendship, the laughs, the very much needed coffee breaks and gym sessions. You helped me keep my balance throughout this journey. To all my friends back home, thank you for your support, even from afar.

Now, a very special thank you goes to my dear Dr. David M. Schuster. We met here, both freshly arrived in Canada, and colleagues in the GReAT Lab. We became partners along the way. I cannot imagine doing this without you by my side, you kept me afloat on the roughest seas. We will look back on these moments with nostalgia and pride in what we accomplished. Of course, you are so speedy you had to beat me to the finish line, but I look forward to joining you back in the Netherlands! I love you; life together is only starting. An honorary thank-you also goes to my little Calvin, the purrfect co-worker, for his feline support and companionship through many working hours.

Finally, to my family, whom I deeply love. Thank you to my parents, Pascal and Pascale Monniez, for raising me into the woman I am today. Deciding to do this PhD far from home on the other side of the pond was the boldest decision I ever made. But you never questioned it, supported me, and showed up with love and patience for the past 5 years. Your unconditional faith in me is one of my most prized possessions. Thank you to my little sisters, Cécile and Estelle. I have watched you grow, find your passions and carve your paths in life. I am proud to be your sister and look forward to being close by again.

Thank you all for your support throughout this journey. Collectively, you have shaped this experience and my path.

Abstract – English

Selective serotonin reuptake inhibitors (SSRIs) and serotonin-norepinephrine reuptake inhibitors (SNRIs), hereafter SS(N)RIs, are the most prescribed pharmacological treatments for depressive disorders and reach aquatic ecosystems through incomplete municipal wastewater treatment. Their therapeutic target is evolutionarily conserved in teleosts, and serotonergic signalling modulates the hypothalamic-pituitary-interrenal (HPI) axis, so teleost fish inadvertently exposed during early development may experience disruption of serotonin-modulated functions, such as disruption of the stress axis response. Standard ecotoxicological assessments are conducted under static, undisturbed conditions and rely mostly on apical endpoints, and most studies examine a single molecule at a time, mainly fluoxetine. The overarching goal of my thesis was to evaluate whether developmental exposure to SS(N)RIs disrupts the physiological and behavioural stress response, using the transgenic SR4G zebrafish (*Danio rerio*) in vivo screening model, and to link these apical effects to transcriptomic alterations. The SR4G line expresses eGFP under the control of six consecutive glucocorticoid response elements (GRE), providing a direct readout of glucocorticoid receptor (GR)-mediated transcription. The GRE-driven eGFP transcription closely tracks whole-body cortisol following an acute handling stress in 7 days post-fertilisation (dpf) larvae. Screening six SS(N)RIs and one common metabolite (0.001 to 1000 nM, 1 to 7 dpf) revealed no effect on basal or stress-induced reporter transcription at environmentally relevant concentrations. Effects were restricted to the highest concentration tested, where norfluoxetine and sertraline amplified stress-induced transcription 1.5- and 1.9-fold, respectively, and sertraline caused substantial mortality. Targeted RNA sequencing (TempO-Seq, Zebrafish S1500+ panel) of larvae exposed to fluoxetine, norfluoxetine, or sertraline showed that these three compounds alter transcriptional profiles in a compound- and context-dependent manner. Fluoxetine and norfluoxetine suppressed up to 13 immediate-early genes and disrupted the transcription of genes involved in lipid metabolism only in stressed larvae, whereas 1000 nM sertraline induced a protein-, tissue-damage, and cytotoxicity signature associated with morbidity. Integrating apical, behavioural, and molecular endpoints to further study sertraline within a light/dark challenge, I observed no effect on survival, hatching, or malformation frequency up to 500 nM, but concentration-dependent hypoactivity during dark phases

from 50 nM and increased GRE-driven transcription at 100 and 500 nM following the challenge, while basal transcription remained unaffected. These results highlight the necessity of an acute stress challenge to unmask neuroendocrine disruption that is otherwise undetectable under static conditions, and, by showing divergent molecular responses among compounds of the same pharmacological class, highlight the limitations of focusing studies on a single model SSRI. Collectively, this thesis contributes to the development of an integrative *in vivo* testing platform to evaluate neuroactive contaminants acting as stress-response disruptors and indicates that individual SS(N)RI concentrations currently reported in surface waters are unlikely to impair HPI axis responsiveness at this early life stage.

Abstract – Français

Les inhibiteurs sélectifs de la recapture de la sérotonine (ISRS) et les inhibiteurs de la recapture de la sérotonine et de la noradrénaline (IRSN), ci-après IS(N)RS, constituent le traitement pharmacologique le plus prescrit contre les troubles dépressifs et atteignent les écosystèmes aquatiques en raison du traitement incomplet des eaux usées municipales. Leur cible thérapeutique est conservée au cours de l'évolution chez les téléostéens, et la signalisation sérotoninergique module l'axe hypothalamo-hypophyso-interrénalien (HHI) ; les poissons exposés de façon involontaire au cours du développement pourraient donc subir une perturbation de la réponse de l'axe du stress. Les évaluations écotoxicologiques courantes sont menées en conditions statiques et non stressantes, reposant principalement sur des paramètres apicaux, et la plupart des études portent sur une seule molécule à la fois, principalement la fluoxétine. L'objectif général de ma thèse était de déterminer si l'exposition aux IS(N)RS au cours du développement perturbe la réponse physiologique et comportementale au stress, en utilisant le modèle poisson-zèbre transgénique SR4G (*Danio rerio*) comme outil de criblage *in vivo*, et de relier ces effets apicaux à des altérations transcriptomiques. La lignée SR4G exprime l'eGFP sous le contrôle de six éléments de réponse aux glucocorticoïdes (GRE) consécutifs, ce qui permet une lecture directe de la transcription médiée par le récepteur des glucocorticoïdes (GR). Les niveaux de transcription de l'eGFP sous contrôle des GRE suivent étroitement ceux du cortisol corporel total après un stress aigu induit par la manipulation chez des larves de 7 jours post-fécondation (jpf). Le criblage de six IS(N)RS et d'un métabolite commun (0,001 à 1000 nM, de 1 à 7 jpf) n'a révélé aucun effet sur la transcription du rapporteur, basale ou induite par le stress, aux concentrations environnementales pertinentes. Les effets se sont limités à la plus forte concentration testée, où le traitement avec la norfluoxétine ou la sertraline a amplifié la transcription induite par le stress de 1,5 et 1,9 fois respectivement, et où la sertraline a entraîné une mortalité importante. Le séquençage ciblé de l'ARN (TempO-Seq, panel Zebrafish S1500+) de larves exposées à la fluoxétine, à la norfluoxétine ou à la sertraline a montré que ces trois composés modifient les profils transcriptionnels de manière dépendante du composé et du contexte. La fluoxétine et la norfluoxétine ont réprimé jusqu'à 13 gènes précoces immédiats et perturbé les voies du métabolisme lipidique uniquement chez les larves stressées, tandis que la sertraline à 1000 nM a induit

une signature de dommage des protéines, de cytotoxicité et de lésion tissulaire associée à une morbidité. En intégrant plusieurs paramètres apicaux, comportementaux et moléculaires pour étudier la sertraline dans le cadre d'une épreuve lumière/obscurité, je n'ai observé aucun effet sur la survie, la fréquence des malformations ou le succès d'éclosion jusqu'à 500 nM, mais une hypoactivité dépendante de la concentration pendant les phases sombres dès 50 nM, ainsi qu'une augmentation de la transcription induite par les GRE à 100 et 500 nM après l'épreuve, la transcription basale demeurant inchangée. L'ensemble des résultats souligne la nécessité d'une épreuve de stress aigu pour révéler une perturbation neuroendocrinienne autrement indétectable en conditions statiques et, en montrant des réponses moléculaires divergentes entre composés d'une même classe pharmacologique, met en évidence les limites des études centrées sur un seul ISRS « modèle ». Dans l'ensemble, cette thèse contribue au développement d'une plateforme d'essai *in vivo* intégrative pour évaluer les contaminants neuroactifs agissant comme perturbateurs de la réponse au stress, et indique que les concentrations d'IS(N)RS, individuellement, rapportées dans les eaux de surface sont peu susceptibles d'altérer la réactivité de l'axe HHI à ce stade de vie.

Table of Contents

Acknowledgements ..... **ii**

Abstract – English ..... **iv**

Abstract – Français ..... **vi**

List of Abbreviations ..... **xii**

List of Figures ..... **xv**

List of Tables ..... **xvii**

List of Supplementary Figures ..... **xviii**

List of Supplementary Tables ..... **xix**

1. Chapter 1: General Introduction **1**

1.1. Pharmaceuticals as environmental contaminants 1

1.2. Serotonin and serotonin-norepinephrine reuptake inhibitors 2

1.2.1. Antidepressant drugs: historical overview *2*

1.2.2. Clinical mechanism of action *5*

1.2.3. Metabolism and pharmacological potency of metabolites *6*

1.3. Physiology of the teleost stress axis 7

1.3.1. Definition and concept of stress response *7*

1.3.2. Endocrine modulation of the hypothalamic-pituitary-interrenal (HPI) axis *8*

1.3.3. Glucocorticoid synthesis, transport, and mechanism of action at target cells *9*

1.3.4. Negative feedback regulation of glucocorticoid synthesis *13*

1.3.5. Interactions between serotonergic pathways and HPI axis modulation *13*

1.4. Ecotoxicology of SSRIs in non-target species 14

1.4.1. Conservation of therapeutic target and concerns for non-target species *14*

1.4.2. SSRI-induced disruption of the stress response *14*

1.4.3. SSRI-induced behavioural disruptions *15*

1.4.4. Other apical effects and implications for populations *16*

1.5. Zebrafish as a study model 16

1.6. Thesis overview 18

1.6.1. Rationale for the study *18*

1.6.2. Chapter-specific objectives *19*

2. Chapter 2: Developmental exposure to serotonin reuptake inhibitors does not impair stress response activation in a transgenic zebrafish reporter line 21

2.1. Statement of contributions 21

2.2. Introduction 22

2.3. Material and Methods 25

2.3.1. Animal care and husbandry 25

2.3.2. Chemicals and solution preparations 25

2.3.3. Exposure conditions and experimental design 27

2.3.4. Standardised stress protocol and sample collection 28

2.3.5. Whole-body cortisol extraction and measurement 28

2.3.6. Total RNA extraction, cDNA synthesis, and qPCR 29

2.3.7. Data processing and statistical analyses 30

2.4. Results 31

2.4.1. Malformation frequency and survival after exposure 31

2.4.2. Technical validation: acute handling stress increases both cortisol and eGFP expression levels in control larvae. 35

2.4.3. Overnight exposure to dexamethasone as a positive control for eGFP expression induction in unstressed larvae. 38

2.4.4. High sertraline and norfluoxetine concentrations elevate GRE-regulated transcription in stressed larvae. 41

2.4.5. Correlation between whole-body eGFP expression and cortisol levels. 44

2.5. Discussion 45

2.6. Conclusion 49

2.7. Funding sources and acknowledgements 50

2.8. Declaration on the use of artificial intelligence 50

3. Chapter 3: Developmental exposures to fluoxetine, norfluoxetine, and sertraline cause divergent, stress-dependent transcriptomic responses in zebrafish larvae 52

3.1. Statement of contributions 52

3.2. Introduction 53

3.3. Material and Methods 56

3.3.1. Animal care and husbandry 56

3.3.2. Chemicals and solution preparations *56*
3.3.3. Exposure conditions and experimental design *57*
3.3.4. Standardised stress protocol, sample collection and RNA extractions *57*
3.3.5. TempO-Seq library preparation, sequencing, and data preprocessing *58*
3.3.6. Differentially expressed genes and pathway analysis *60*
3.4. Results 60
3.4.1. Transcriptomic responses differ among SSRIs in unstressed larvae *60*
3.4.2. Transcriptomic shifts following acute handling stress and SSRI exposure *66*
3.4.3. High-concentration sertraline induces widespread proteotoxicity and divergent stress-responsive targets *72*
3.4.4. Pathway analysis *77*
3.5. Discussion 82
3.6. Conclusion 86
3.7. Funding sources and acknowledgements 87
3.8. Declaration on the use of artificial intelligence 87
4. Chapter 4: Sertraline disrupts photomotor behaviour and glucocorticoid-responsive transcription in transgenic zebrafish larvae 88
4.1. Statement of contributions 88
4.2. Introduction 89
4.3. Material and Methods 92
4.3.1. Zebrafish maintenance and husbandry *92*
4.3.2. Chemicals and solutions preparation *92*
4.3.3. Experimental design and exposure conditions *93*
4.3.4. Larval behaviour analysis *95*
4.3.5. Data processing and statistical analysis for apical endpoints *95*
4.3.6. Sample collection and preparation for gene expression analysis *96*
4.3.7. RT-qPCR analysis of eGFP reporter expression *97*
4.3.8. TempO-Seq library preparation, sequencing, and data preprocessing *98*
4.3.9. Differentially expressed genes and pathway analysis *99*
4.4. Results 101
4.4.1. Developmental effects *101*
4.4.2. Larval photomotor response (LPR) *102*
4.4.3. GRE-driven eGFP expression *107*

4.4.4. Targeted transcriptomics 109
4.5. Discussion 116
4.6. Conclusions 122
4.7. Funding sources and acknowledgment 122
4.8. Declaration on the use of artificial intelligence 123
5. Chapter 5: General discussion and future directions 124
5.1. Thesis summary and discussion 124
5.2. Significance and contribution to scientific knowledge 130
5.3. Future perspectives 131
List of References 134
Appendix 156
A. Supplementary materials of Chapter 2 156
B. Supplementary materials for Chapter 3 166
C. Supplementary materials for Chapter 4 200
D. Application of the integrative testing design to fluoxetine and norfluoxetine. 215
a. Summary of materials and methods 215
b. Results 217
i. Larval photomotor response at 4 dpf in response to fluoxetine and norfluoxetine 217
ii. Larval photomotor response at 5 dpf in response to fluoxetine and norfluoxetine 217
iii. Larval photomotor response at 5 dpf in response to overnight glucocorticoid treatment 218
iv. GRE-driven eGFP transcription at 5 dpf in response to fluoxetine and norfluoxetine treatment 219
v. GRE-driven eGFP transcription at 5 dpf in response to overnight glucocorticoid treatment 219
c. Figures 221

List of Abbreviations

5-HT	Serotonin (5-hydroxytryptamine)
5-HT1A	Serotonin receptor subtype 1A
5-HT2	Serotonin receptor subtype 2
5-HT4	Serotonin receptor subtype 4
ACTH	Adrenocorticotropic hormone
AIC	Akaike information criterion
ANOVA	Analysis of variance
APIs	Active pharmaceutical ingredients
cDNA	Complementary DNA
CI	Confidence interval
CIT	Citalopram
CNS	Central nervous system
CORT	Cortisol
CRF	Corticotropin-releasing factor
CRFRs	Corticotropin-releasing factor receptors
CYP450	Cytochrome P450 (isoenzyme family)
DA	Dopamine
DAT	Dopamine transporter
DEGs	Differentially expressed genes
DES	Desvenlafaxine
DEX	Dexamethasone
DMSO	Dimethyl sulfoxide
DNA	Deoxyribonucleic acid
dpf	Days post-fertilization
EC50	Effective concentration 50%
eGFP	Enhanced green fluorescent protein
ELISA	Enzyme-linked immunosorbent assay
EMMs	Estimated marginal means
ERK1/ERK2	Extracellular signal-regulated kinase 1/2
ESC	Escitalopram
FA	Formic acid
FC	Fold-change
FGF	Fibroblast growth factor
FLX	Fluoxetine
GCs	Glucocorticoids

gDNA	Genomic DNA
GLMMs	Generalized linear mixed-effects models
GO	Gene Ontology
GR	Glucocorticoid receptor
GRα / GRβ	GR alpha- and beta-isoforms
GRE	Glucocorticoid response element
GSEA	Gene set enrichment analysis
hpf	Hours post-fertilization
HPA (axis)	Hypothalamic-pituitary-adrenal axis
HPI (axis)	Hypothalamic-pituitary-interrenal axis
HSD	Hydroxysteroid dehydrogenase
HSP	Heat-shock protein
IEGs	Immediate-early genes
KEGG	Kyoto Encyclopædia of Genes and Genomes
LBD	Ligand-binding domain
LC50	Lethal concentration 50%
LPR	Larval photomotor response
MAPK	Mitogen-activated protein kinase
MC2R	Melanocortin type 2 receptor
MR	Mineralocorticoid receptor
mRNA	Messenger RNA
NE	Norepinephrine
NET	Norepinephrine transporter
NOR	Norfluoxetine
OECD	Organisation for Economic Co-operation and Development
ORA	Over-representation analysis
PCA	Principal component analysis
PCR	Polymerase chain reaction
POMC	Proopiomelanocortin
PPARs	Peroxisome proliferator-activated receptors
qPCR	Quantitative polymerase chain reaction
R-ODAF	Omics data analysis framework for regulatory application
RIN	RNA integrity number
RNA	Ribonucleic acid
SD	Standard deviation
SE	Standard error
SEM	Standard error of the mean

SER	Sertraline
SERT	Serotonin reuptake transporter
SLC	Solute carrier
SNRIs	Serotonin-norepinephrine reuptake inhibitors
SR4G	Stress Receptor 4-hour enhanced Green fluorescent protein (transgenic reporter line)
SS(N)RIs	Selective serotonin (and norepinephrine) reuptake inhibitors
SNRIs	Serotonin-norepinephrine reuptake inhibitors
SSRIs	Selective serotonin reuptake inhibitors
StAR	Steroidogenic acute regulatory (protein)
TCA (cycle)	Tricarboxylic acid cycle
VEN	Venlafaxine (hydrochloride)
WHO	World Health Organization
WWTPs	Wastewater treatment plants

List of Figures

Figure 1.1. Chemical structures of selective serotonin reuptake inhibitors. 4

Figure 1.2. Schematic representation of the hypothalamic-pituitary-interrenal axis in zebrafish. 12

Figure 2.1. A schematic representation of the experimental design. 27

Figure 2.2. Cumulative survival of 7 dpf larvae exposed to glucocorticoids. 32

Figure 2.3. Cumulative survival of 7 dpf larvae exposed to SS(N)RIs. 33

Figure 2.4. Correlation between whole-body cortisol levels and eGFP expression in 7 dpf SR4G larvae in control groups. 36

Figure 2.5. Relative eGFP expression fold-change in response to an overnight exposure to glucocorticoids in 7 dpf SR4G larvae. 39

Figure 2.6. Relative eGFP expression fold-change in response to SS(N)RI exposure for 6 days in SR4G larvae. 43

Figure 3.1. Differentially expressed genes (DEGs) summaries and overlaps across contrasts for fluoxetine, norfluoxetine, and sertraline exposure. 61

Figure 3.2. Effects of developmental exposure to sertraline on transcriptomic responses in 7 dpf unstressed and stressed SR4G larvae. 63

Figure 3.3. Similar effects of fluoxetine and norfluoxetine on the transcription of *agt* and *prg4b*. 65

Figure 3.4. Effects of developmental exposure to fluoxetine on transcriptomic responses in 7 dpf unstressed and stressed SR4G larvae. 67

Figure 3.5. Effects of developmental exposure to norfluoxetine on transcriptomic responses in 7 dpf unstressed and stressed SR4G larvae. 68

Figure 3.6. Similar effects of fluoxetine and norfluoxetine on the transcription of *fosab* and *fabp11b*. 70

Figure 3.7. Fluoxetine and norfluoxetine repress, whereas sertraline induces *fosl1a* and *atf3* transcription in stressed larvae. 73

Figure 3.8. Sertraline at high concentration alters transcription of monoaminergic and corticosteroidogenic regulators. 75

Figure 4.1. Overview of the experimental design. 94

Figure 4.2. Schematic representation of the different comparisons performed for the differentially expressed genes analysis. 100

Figure 4.3. Effects of sertraline on 4 dpf SR4G zebrafish photomotor response. 103

Figure 4.4. Effects of sertraline on 5 dpf SR4G zebrafish photomotor response. 105

Figure 4.5. Effects of sertraline and light/dark challenge on eGFP relative expression in 5 dpf SR4G zebrafish. 108

Figure 4.6. Differentially expressed genes (DEGs) overlap across contrasts testing the stimulus effect at each sertraline concentration. 112

Figure 5.1. SS(N)RI effects on the modulation of zebrafish stress responses across environmentally and pharmacologically relevant concentrations..... 133

List of Tables

Table 2.1. List of test compounds. 26

Table 2.2. Effects of treatment concentration on eGFP relative expression in unstressed and stressed 7 dpf SR4G larvae. 40

Table 2.3. Pearson correlation between whole-body cortisol and eGFP expression levels for each treatment. 44

Table 3.1. List of test compounds. 57

Table 3.2. Gene set enrichment analysis with WikiPathways, 7 dpf unstressed larvae exposed to fluoxetine, norfluoxetine, or sertraline. 78

Table 3.3. Gene set enrichment analysis with WikiPathways, 7 dpf stressed larvae exposed to fluoxetine, norfluoxetine, or sertraline. 80

Table 4.1. Effects of sertraline concentration on hatching success and mortality in larval SR4G zebrafish. 101

Table 4.2. Enriched biological pathways (over-representation analysis) associated with the overall effect of the light/dark challenge. 110

Table 4.3. Genes differentially expressed in response to the light/dark challenge across several concentration-specific contrasts. 113

Table 4.4. List of differentially expressed genes (DEGs) following sertraline exposure, in unstressed and stressed 5 dpf SR4G zebrafish. 115

List of Supplementary Figures

Supplementary Figure A.1. Relative eGFP expression fold-change in response to glucocorticoid treatment for 6 days in SR4G larvae. 164

Supplementary Figure A.2. Correlation between whole-body cortisol and relative eGFP expression levels in 7 dpf SR4G larvae across all complete pairs of samples. 165

Supplementary Figure B.1. Differentially expressed genes summary following dexamethasone exposure. 166

Supplementary Figure B.2. Variation between samples before batch effect normalization. 167

Supplementary Figure B.3. Variation between samples after batch effect normalization. 168

Supplementary Figure C.1. Variation between samples before batch effect normalisation. 201

Supplementary Figure C.2. Variation between samples after batch effect normalisation. 202

Supplementary Figure D.1. Effects of fluoxetine on 4 dpf SR4G zebrafish photomotor response. 221

Supplementary Figure D.2. Effects of norfluoxetine on 4 dpf SR4G zebrafish photomotor response. 223

Supplementary Figure D.3. Effects of fluoxetine on 5 dpf SR4G zebrafish photomotor response. 225

Supplementary Figure D.4. Effects of norfluoxetine on 5 dpf SR4G zebrafish photomotor response. 227

Supplementary Figure D.5. Effects of overnight cortisol treatment on 5 dpf SR4G zebrafish photomotor response. 229

Supplementary Figure D.6. Effects of overnight dexamethasone treatment on 5 dpf SR4G zebrafish photomotor response. 231

Supplementary Figure D.7. Effects of fluoxetine and norfluoxetine in combination with the light/dark challenge on eGFP relative expression in 5 dpf SR4G zebrafish. 233

Supplementary Figure D.8. Effects of overnight treatment with cortisol or dexamethasone and the light/dark challenge on eGFP relative expression in 5 dpf SR4G zebrafish. 234

List of Supplementary Tables

Supplementary Table A.1. Water sample analysis results of vehicle control and SS(N)RIs solutions. 156

Supplementary Table A.2. List of primers used for real-time qPCR on samples from 7 dpf SR4G larvae. 157

Supplementary Table A.3. Raw C_T values of the reference gene eef1a1l1 in 7 dpf SR4G larvae, per compound series. 158

Supplementary Table A.4. Summary table of the number and percentage of larvae affected by any malformation, and malformation counts per category, for each treatment. 159

Supplementary Table A.5. Survival rates of control groups, in both unstressed (uns) and stressed (str) conditions, across all experimental batches. 162

Supplementary Table A.6. Effects of treatment concentration and acute stress on the cumulative survival of SR4G larvae. 163

Supplementary Table B.1. List of differentially expressed genes following fluoxetine exposure, in unstressed and stressed 7 dpf SR4G zebrafish. 169

Supplementary Table B.2. List of differentially expressed genes following norfluoxetine exposure, in unstressed and stressed 7 dpf SR4G zebrafish. 171

Supplementary Table B.3. List of differentially expressed genes following sertraline exposure, in unstressed and stressed 7 dpf SR4G zebrafish. 173

Supplementary Table C.1. List of primers used for real-time qPCR on samples from 5 dpf SR4G larvae. 200

Supplementary Table C.2. Effects of sertraline exposure on hatching probability of SR4G zebrafish larvae. 203

Supplementary Table C.3. Effects of sertraline exposure on the mortality probability of 5 dpf SR4G zebrafish larvae. 204

Supplementary Table C.4. Malformation counts observed in 5 dpf SR4G larvae exposed to sertraline. 205

Supplementary Table C.5. List of all differentially expressed genes identified in 5 dpf SR4G zebrafish in response to the light/dark challenge. 206

Supplementary Table C.6. List of all differentially expressed genes identified in 5 dpf SR4G zebrafish in response to the light/dark challenge at each concentration tested. ... 211

1. Chapter 1: General Introduction

1.1. Pharmaceuticals as environmental contaminants

Active pharmaceutical ingredients (APIs) represent a class of emerging contaminants, with a wide range of compounds and metabolites detected across diverse environmental matrices. Pharmaceuticals are found in aquatic ecosystems worldwide across several environmental compartments including wastewater, wastewater sludge, surface water, groundwater and drinking water (aus der Beek et al., 2016; Fick et al., 2009; Kostich et al., 2014; Wilkinson et al., 2022). These bioactive compounds enter the aquatic environment through domestic and hospital wastewater discharges following human consumption and excretion, due to incomplete removal during conventional wastewater treatment processes, and via industrial runoff and improper disposal (Patel et al., 2019; Sanusi et al., 2023). Pharmaceuticals are biologically active compounds designed to induce physiological effects at low concentrations, raising concerns regarding their potential to cause adverse effects, including disruption of hormone-regulated processes in non-target aquatic wildlife (Knigge, 2024; Mennigen et al., 2011; Vaudin et al., 2022).

The distribution and detection of specific pharmaceutical categories in aquatic systems vary by region, depending on local consumption patterns, regulatory oversight, and wastewater infrastructure (Patel et al., 2019). Globally, antibiotics, analgesics, estrogens (e.g., estrone, estradiol, and ethinylestradiol), and lipid-lowering drug metabolites represent the most frequently detected pharmaceuticals (aus der Beek et al., 2016; Fick et al., 2009). A global-scale screening study of rivers across 104 countries identified several therapeutic classes across all continents, detecting anti-inflammatories, analgesics, β-blockers, antiepileptics, antihistamines, antidepressants, anticonvulsants, anaesthetics, and antimicrobials (Wilkinson et al., 2022).

Antidepressants, a category of particular concern, similarly enter the aquatic environment due to incomplete removal during wastewater treatment. Specifically, residues of selective serotonin (and norepinephrine) reuptake inhibitors (hereafter collectively referred to as SS(N)RIs) are widely detected in surface water, groundwater, and drinking water (Mole & Brooks, 2019; Silva et al., 2012). SS(N)RI occurrence and environmental concentrations show spatial and regional variations due to differences in

prescription rates, socioeconomic drivers, and local treatment efficiencies (Fernandes et al., 2020; S. L. Gould et al., 2021). The most frequently detected SS(N)RIs in surface waters are citalopram, fluoxetine, sertraline, and paroxetine, with environmental concentrations typically ranging from low nanograms per litre to several micrograms per litre (Mole & Brooks, 2019). This reflects the high rates of prescription and use of SS(N)RIs as the first line of pharmacological treatment for depressive and anxiety disorders today (Grohol & Wright, 2022; OECD, 2025; Peano et al., 2025), driving continuous release into surface waters, and thus the focus of this research will be on these two classes of antidepressants.

1.2. Serotonin and serotonin-norepinephrine reuptake inhibitors

1.2.1. Antidepressant drugs: historical overview

Major depressive disorder is a common and complex psychiatric condition resulting from interactions between genetic and environmental factors (Sullivan et al., 2000). The monoamine hypothesis postulates that the underlying mechanism for major depressive disorder development stems from deficits in monoaminergic neurotransmission, specifically norepinephrine (NE), dopamine (DA), and, later, serotonin (5-HT) (Albert et al., 2012; Coppen, 1967; Schildkraut, 1965). Consequently, pharmacological interventions primarily aim to restore neurotransmitter balance by targeting receptors and reuptake transporters of these monoamine systems (Laux, 2022a).

The first generation of antidepressants, introduced in the 1950s and 1960s, included monoamine oxidase inhibitors and tricyclic antidepressants (López-Muñoz & Álamo, 2016). Monoamine oxidase inhibitors, such as iproniazid, initially showed efficacy in improving the mood of depressed patients, but were largely withdrawn from the international market due to severe adverse effects, notably hepatotoxicity and hypertensive crises (Loomer et al., 1957; López-Muñoz & Álamo, 2016). Tricyclic antidepressants, such as imipramine, inhibit both serotonin and norepinephrine reuptake, but also exhibit broad, non-specific antagonist activity at histaminergic, cholinergic, and α-1-adrenergic receptors (Preskorn, 2012). This lack of pharmacological specificity, as well as factors such as inter-individual variability and significant adverse effects, drove the pursuit of safer, targeted pharmacological therapies (Hiemke & Härtter, 2000; López-Muñoz & Álamo, 2016).

Selective serotonin reuptake inhibitors (SSRIs) and serotonin-norepinephrine reuptake inhibitors (SNRIs) were introduced from the late 1980s onwards, quickly becoming the most prescribed pharmacological treatment for depressive disorders because of their high tolerability, efficacy, and purported few adverse side effects compared to previous antidepressants (Cipriani et al., 2018; Locher et al., 2017). Fluoxetine, the first SSRI approved in the United States (1987), remains widely prescribed for the treatment of depression, anxiety, and obsessive-compulsive disorders (Wong et al., 1995). The SSRI class currently includes citalopram, escitalopram, fluoxetine, fluvoxamine, paroxetine, and sertraline (Figure 1.1). While these compounds share similar pharmacodynamic mechanisms (i.e., their effects on the biological targets), they exhibit distinct pharmacokinetic profiles (i.e., absorption, distribution, metabolism, and excretion) (Hiemke & Härtter, 2000).

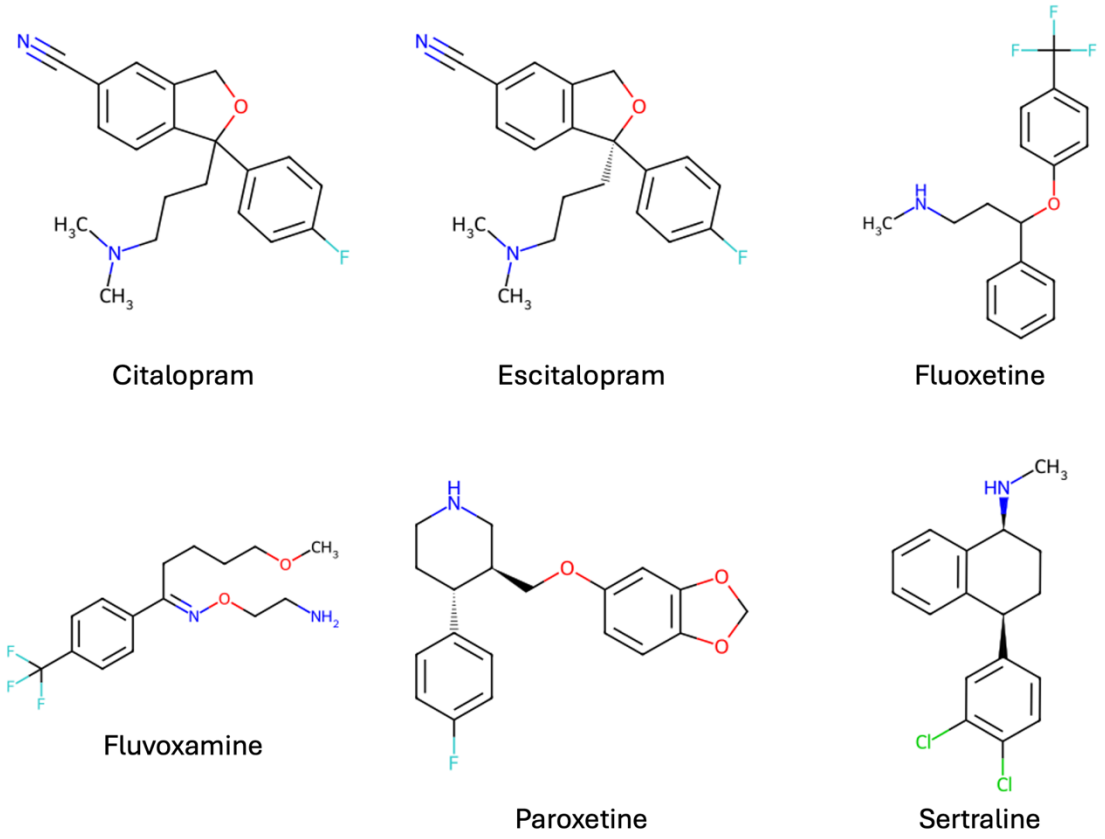

Figure 1.1. Chemical structures of selective serotonin reuptake inhibitors.

Images obtained from the ChemSpider website (*ChemSpider*, 2026).

1.2.2. Clinical mechanism of action

The primary therapeutic mechanism of SSRIs is the inhibition of the serotonin reuptake transporter (SERT; encoded by the *slc6a4* gene in humans), which terminates serotonergic signalling by returning extracellular serotonin (5-hydroxytryptamine, 5-HT) to the presynaptic terminal (Stahl, 1998). SERT is a member of the solute carrier 6 (SLC6) family of sodium-dependent neurotransmitter symporters; the translocation of 5-HT is an active transport, coupling the movement of one 5-HT+, one Na+ and one Cl- molecules, in exchange of one intracellular K+ ion (Stahl, 1998). SSRIs inhibit SERT competitively by occupying the central substrate-binding site, thereby preventing 5-HT translocation and increasing extracellular 5-HT. A second, lower-affinity allosteric site in the extracellular vestibule has also been described in the bacterial homologue LeuT and slows inhibitor dissociation. (Stahl, 1998; Zhou et al., 2009). This inhibition of SERT increases 5-HT levels in the synaptic cleft and at postsynaptic receptor sites, thereby enhancing serotonin signalling. SSRI binding and selectivity for SERT relies on specific halogen atoms. All clinically approved SSRIs possess electronegative halogen atoms, such as chlorine or fluorine (Figure 1.1), which interact with the hydrophobic halogen-binding pocket of the SERT (Zhou et al., 2009). Mutational analyses revealed that this pocket is the primary determinant of SSRI specificity for SERT over the norepinephrine (NET) or dopamine (DAT) transporters (Zhou et al., 2009).

Although SERT inhibition occurs immediately upon SSRI administration, clinical signs of improvement may take 14 to 21 days to appear. This latency reflects the time required for adaptive changes in 5-HT neurotransmission to occur (Blier & de Montigny, 1994; Castro et al., 2003). The acute increase in extracellular 5-HT following SERT inhibition stimulates 5-HT1A somatodendritic autoreceptors in the dorsal raphe nucleus, which in turn decreases the firing rate of serotonergic neurons and temporarily suppresses neurotransmitter release (Piñeyro & Blier, 1999; Stahl, 1998). With chronic SSRI administration, sustained elevation of extracellular 5-HT leads to desensitisation of these presynaptic 5-HT1A autoreceptors in the dorsal raphe nucleus, restoring firing rates and allowing sustained elevations of 5-HT within the synaptic cleft and enhanced postsynaptic 5-HT neurotransmission (Castro et al., 2003; Stahl, 1998).

1.2.3. Metabolism and pharmacological potency of metabolites

Cytochrome P450 (CYP450) isoenzymes play a major role in the hepatic metabolism of SSRIs, leading to high interindividual variability in drug clearance. While SSRIs undergo similar oxidative biotransformation pathways, the pharmacological potency of the resulting N-demethylated metabolites varies (Hiemke & Härtter, 2000). Fluoxetine undergoes N-demethylation catalysed by CYP2C9, CYP2D6, CYP2C19, and CYP3A4, forming norfluoxetine. Norfluoxetine retains pharmacological activity in an enantiospecific manner, with the (S)-enantiomer exhibiting approximately 20-fold greater potency for SERT inhibition compared to the (R)-enantiomer (Wong et al., 1995). Sertraline is N-demethylated to desmethylsertraline by CYP2D6, CYP2C9, CYP2B6, CYP2C19, and CYP3A4 (DeVane et al., 2002; Hiemke & Härtter, 2000). This metabolite is eliminated more slowly than its parent drug but retains only 5 to 10% of sertraline's *in vivo* potency (Hiemke & Härtter, 2000; Rudorfer & Potter, 1997). Citalopram and its isolated (S)-enantiomer, escitalopram, undergo N-demethylation mediated by CYP2C19, CYP3A4, and CYP2D6, resulting in the formation of desmethylcitalopram and didesmethylcitalopram (Hiemke & Härtter, 2000; Rao, 2007; Rochat et al., 1999). These metabolites have reduced SERT affinity, with S-desmethylcitalopram exhibiting only $1/7^{th}$ of the inhibitory potency of escitalopram, and is therefore considered a minor contributor to *in vivo* therapeutic effects (Hiemke & Härtter, 2000; Rao, 2007). The SNRI venlafaxine is primarily O-demethylated by CYP2D6 to O-desmethylvenlafaxine, which demonstrates equipotent serotonin and norepinephrine reuptake inhibition compared to the parent compound (Aryal et al., 2012; Suwała et al., 2019). In addition to acting as substrates, several SSRIs and their active metabolites interfere with CYP enzymatic activity. Paroxetine, and to a lesser extent fluoxetine and norfluoxetine, act as potent competitive inhibitors of CYP2D6, whereas fluvoxamine inhibits CYP1A2 and CYP2C19. This CYP inhibition alters the clearance of co-administered xenobiotics, increasing the potential for downstream drug-drug interactions (Hiemke & Härtter, 2000; Preskorn, 2012).

Given the role of serotonergic signalling in regulating the vertebrate stress response, understanding the organisation of the teleost stress axis is important for evaluating the potential effects of SSRIs and SNRIs in non-target fish species.

1.3. Physiology of the teleost stress axis

1.3.1. Definition and concept of stress response

The concept of stress response was built upon the principles of homeostasis and systemic adaptation. Homeostasis refers to the physiological processes by which organisms maintain internal stability in response to fluctuating environmental conditions and survive changes (Cannon, 1939). This framework was further expanded with the formulation of the General Adaptation Syndrome, which characterised the sum of non-specific responses to chronic challenges (three phases: alarm, resistance, exhaustion), directly linking prolonged neuroendocrine activation to the development of systemic pathologies (Godoy et al., 2018; Selye, 1946). Ambiguity around the term "stress" persists, as it is frequently used for three related concepts: the initiating stimulus, internal or external (stressor); the immediate physiological and behavioural responses activated (stress response); and the long-term pathological consequences of over-stimulation of these responses (chronic stress) (Le Moal, 2007; Romero, 2004).

To resolve some of this ambiguity, modern frameworks differentiate between internal parameters and the regulatory mechanisms required to preserve them. Allostasis is defined as the active process of maintaining stability (homeostasis) through physiological and behavioural adjustments (McEwen & Wingfield, 2003). Although the allostasis paradigm accounts for daily and seasonal physiological adjustments, its reliance on energy expenditure as a metric of allostatic load (i.e., the cumulative physiological cost and systemic exhaustion resulting from active adaptation to environmental and life challenges) limits its applicability to wild animals surviving in their natural habitats, as well as different strategies across taxa. In ectotherms such as teleosts, behavioural responses to acute stressors (e.g., freezing or tonic immobility) reduce overall metabolic demand and are not accurately captured by energy-centric models (Romero et al., 2009). To address this, the Reactive Scope Model integrates the concepts of homeostasis and allostasis while addressing weaknesses identified in earlier formulations of the allostasis paradigm. It defines a species-specific normal reactive scope, including predictive and reactive homeostatic ranges, bounded by pathological thresholds of homeostatic failure at the lower limit, and homeostatic overload at the upper limit (Romero et al., 2009).

In teleosts, the stress response (i.e., the physiological mechanisms used to maintain reactive scope) initiates a cascade of effects categorised into primary, secondary, and tertiary response phases (Barton, 2002; Wendelaar Bonga, 1997). The primary phase involves activation of the hypothalamic-sympathetic-chromaffin cell axis and the immediate release of catecholamines (epinephrine and norepinephrine) from chromaffin cells within seconds of perceiving a stressor, thereby mediating "fight or flight" reactions (Gesto et al., 2013; Wendelaar Bonga, 1997). Concurrently, the hypothalamic-pituitary-interrenal (HPI) axis is activated and secretes glucocorticoids (GCs), principally cortisol, which modulates sustained responses (Harris & Carr, 2016; Wendelaar Bonga, 1997). The secondary phase encompasses the downstream physiological and metabolic actions induced by these endocrine mediators at the tissue level (Mommsen et al., 1999; Wendelaar Bonga, 1997). Finally, the tertiary phase of the stress response represents the organism and population-level consequences of sustained energy reallocation, which can manifest as suppressed growth, compromised immune system, impaired reproductive capacity, and altered behaviours (Wendelaar Bonga, 1997).

1.3.2. Endocrine modulation of the hypothalamic-pituitary-interrenal (HPI) axis

The endocrine stress response in teleosts is mediated by the HPI axis, which is homologous to the mammalian hypothalamic-pituitary-adrenal (HPA) axis. Activation of the HPI axis culminates in the secretion of glucocorticoids, the corticosteroid hormones that mediate most aspects of the vertebrate stress response, with cortisol as the principal glucocorticoid in teleosts (Mommsen et al., 1999). Following stressor perception by neural circuits, the HPI axis is activated in the preoptic area and basal hypothalamus of teleost fish, where corticotropin-releasing factor (CRF) neurons, capable of *de novo* CRF synthesis, are activated (Wendelaar Bonga, 1997; Winberg et al., 1997). Unlike in mammals, where CRF is transported to the pituitary via the median eminence and the blood-portal system, teleost CRF neurons directly innervate the anterior pituitary (Trudeau & Somoza, 2020). Binding of CRF to its receptors (CRFRs) stimulates the secretion of the adrenocorticotropic hormone (ACTH) from corticotrope cells into the peripheral blood circulation. ACTH is derived from the prohormone proopiomelanocortin (POMC), which undergoes proteolytic cleavage into ACTH by prohormone convertases 1 and 2, but also produces other peptides, such as α-melanocyte-stimulating hormone and β-endorphins

(Bernier et al., 2009; Takahashi & Mizusawa, 2013). ACTH subsequently binds to the melanocortin type 2 receptor (MC2R) on interrenal cells located in the head kidney, triggering the synthesis and secretion of cortisol (Alsop & Vijayan, 2009a; Wendelaar Bonga, 1997). Circulating cortisol then binds to the glucocorticoid receptors (GR) expressed throughout the body to mediate systemic physiological adjustments and initiate negative feedback loops (Alsop & Vijayan, 2009a; Wendelaar Bonga, 1997).

1.3.3. Glucocorticoid synthesis, transport, and mechanism of action at target cells

The synthesis of glucocorticoids (GCs) occurs in the steroidogenic interrenal cells of teleosts and is driven by pathways functionally homologous to their mammalian counterparts (Mommsen et al., 1999; Schaaf et al., 2009). The synthesis cascade is initiated by ACTH binding to its receptor, MC2R, on the interrenal steroidogenic cell membrane, thereby stimulating the mobilisation or *de novo* synthesis of cholesterol, the primary steroidogenic substrate. Cholesterol is imported from the outer mitochondrial membrane to the inner mitochondrial membrane by the steroidogenic acute regulatory (StAR) protein. At the inner mitochondrial membrane, cytochrome P450 side chain cleavage (P450scc, CYP11A) catalyses the conversion of cholesterol to pregnenolone. While this step is mediated by CYP11A1 in mammals (Payne & Hales, 2004), zebrafish possess two paralogs: CYP11A2 is essential for the initiation and maintenance of interrenal steroidogenesis, whereas CYP11A1 is required during early embryonic development (Parajes et al., 2013).

Following its synthesis, pregnenolone is translocated to the endoplasmic reticulum, where it is metabolised into 17α-hydroxypregnenolone and subsequently 17α-hydroxyprogesterone by the enzymes CYP17 (17α-hydroxylase) and 3β-HSD (3β-hydroxysteroid dehydrogenase) (Mommsen et al., 1999; Parajes et al., 2013). In teleosts, the 17α-hydroxylation reaction is mediated by two isoenzymes, CYP17A1 and CYP17A2 (Pallan et al., 2015). The 3β-HSD1 isoform is involved in the steroidogenesis pathway in zebrafish, whereas the 3β-HSD2 isoform is involved in humans (J.-C. Lin et al., 2015; Miller, 2013). Final steps of cortisol synthesis involve the conversion of 17α-hydroxyprogesterone into 11-deoxycortisol by CYP21A2 (21-hydroxylase), and finally, 11-deoxycortisol is transported back to the inner mitochondrial membrane, where it is

converted into cortisol by CYP11B1 (11β-hydroxylase) (Mommsen et al., 1999; Payne & Hales, 2004).

Free cortisol released into the blood circulation binds to intracellular receptors, the glucocorticoid receptors (GR) and mineralocorticoid receptors (MR), which are ligand-activated transcription factors that mediate cellular responses in target tissues. Structurally, the GR shares the conserved organisation of the steroid receptor superfamily: a highly conserved central zinc-finger DNA-binding domain, a moderately conserved carboxyl-terminal ligand-binding domain (LBD), and a variable amino-terminal domain (Heitzer et al., 2007). In the absence of a ligand, the GR is localised in the cytoplasm and maintained inactive by a chaperone protein complex that includes heat-shock proteins 90 and 70 (HSP90, HSP70) (Weikum et al., 2017). The LBD mediates both receptor dimerisation and these protein-protein interactions with HSP90 (Heitzer et al., 2007). GC binding induces a conformational change in the GR, triggering dissociation of the chaperone complex and exposing nuclear localisation sequences within the hinge and LBD regions (Heitzer et al., 2007). Following nuclear translocation, the GR homodimerizes and binds to specific glucocorticoid response elements (GREs) in the genome. Once bound to DNA, the receptor recruits coregulatory complexes and other transcriptional regulatory factors to activate or repress the transcription of glucocorticoid-responsive genes (Heitzer et al., 2007; Weikum et al., 2017).

The structural and functional characteristics of the GR are highly conserved between teleosts and mammals. Notably, despite the teleost whole-genome duplication event, zebrafish carry only a single copy of the *gr* gene (Alsop & Vijayan, 2009a; Schaaf et al., 2009). Alternative splicing generates two distinct GR isoforms in both human and zebrafish: the GR α-isoform (GRα) and the GR β-isoform (GRβ). The amino acid sequence of the zebrafish GRα shares ~60% overall similarity with the human GRα, with particularly high conservation within the DNA- and ligand-binding domains (Schaaf et al., 2009; Schoonheim et al., 2010). The canonical GRα isoform functions as the primary ligand-dependent transcription factor (Chatzopoulou et al., 2015; Oakley & Cidlowski, 2013). Ligand-bound GRα translocates to the nucleus, dimerises, and binds glucocorticoid response elements (GREs) in the regulatory regions of target genes. Transcriptional output at these sites depends on the recruited coregulatory complex, which includes p160 family

coactivators, the histone acetyltransferases CBP and p300, and chromatin-remodelling SWI/SNF subunits that increase local chromatin accessibility, whereas NCoR and SMRT corepressor complexes reduce transcription at negatively regulated loci (Oakley & Cidlowski, 2013; Weikum et al., 2017). In contrast, the GRβ isoform diverges from the GRα at the C-terminus and carries alterations in the LBD that change its ligand-binding properties (Schaaf et al., 2008; Weikum et al., 2017). In zebrafish, GRβ act as a dominant-negative inhibitor, suppressing GRα-mediated transcriptional activity (Chatzopoulou et al., 2017; Schaaf et al., 2008). A schematic representation of the primary endocrine modulation of the HPI axis in teleosts is shown in Figure 1.2 below.

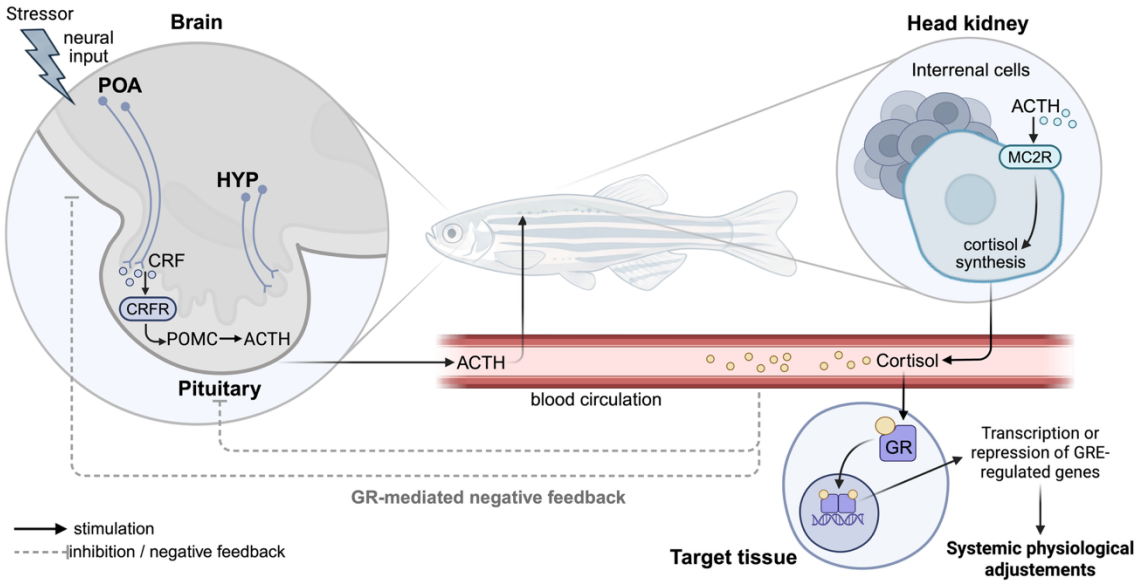

Figure 1.2. Schematic representation of the hypothalamic-pituitary-interrenal axis in zebrafish. The perception of a stimulus or stressor in the brain triggers the *de novo* synthesis of CRF from the preoptic area (POA) and hypothalamus (HYP). In teleosts, CRF neurons directly innervate the pituitary, where CRF is released. The binding and activation of CRF receptor (CRFR) stimulate the synthesis and release of ACTH from corticotrope cells in the anterior pituitary into the blood circulation. Following ACTH binding to its receptor, MC2R, on interrenal cells, cortisol is synthesised and released into the bloodstream. Cortisol then binds to its glucocorticoid receptor (GR) in target cells, where it modulates the transcription of genes regulated by GR-elements (GRE), resulting in physiological adjustments to address the stressor. The negative feedback mediated by cortisol at the POA and pituitary levels is also illustrated by dashed lines. Created with BioRender.com.

1.3.4. Negative feedback regulation of glucocorticoid synthesis

At the target-cell level, GC activity is regulated by 11β-hydroxysteroid dehydrogenase 2 (11β-HSD2), an enzyme that oxidises active cortisol into its inactive 11-keto form, cortisone. In mammals, cortisone can be recycled back into active cortisol via reduction by 11β-hydroxysteroid dehydrogenase 1 (11β-HSD1). However, zebrafish lack a functional 11β-HSD1 homologue capable of this reactivation. Consequently, cortisol inactivation is unidirectional and cortisone cannot be recycled in this species (Tsachaki et al., 2017; Wilson et al., 2013).

Systemically, circulating GCs regulate their own production through a negative feedback loop on the HPI axis, preventing prolonged exposure to elevated GC levels (Sapolsky et al., 2000). Cortisol binds to GR located in the preoptic area and the pituitary. This GR-mediated signalling downregulates the synthesis and secretion of CRF from hypophysiotropic neurons and ACTH from corticotropes, respectively (Mommsen et al., 1999). This transcriptional repression halts the steroidogenic cascade, ensuring an efficient return to homeostatic balance when the stress system is no longer challenged (Gallo-Payet et al., 2017; Sapolsky et al., 2000).

1.3.5. Interactions between serotonergic pathways and HPI axis modulation

Brain serotonergic (5-HT) pathways play a role in integrating and regulating the teleost stress response. Following stressor perception, 5-HT neurons in the raphe nuclei that project to the preoptic area and basal hypothalamus are activated (Lillesaar, 2011). This central 5-HT neurotransmission occurs within seconds of an acute stressor, preceding plasma cortisol elevations, and stimulates the HPI axis by promoting CRF synthesis and release (Gesto et al., 2013). This 5-HT modulation is mediated by specific 5-HT receptor subtypes (e.g., 5-HT1A, 5-HT2, and 5-HT4) expressed throughout the HPI axis. Centrally, 5-HT1A receptor activation triggers hypothalamic CRF expression and subsequent systemic cortisol secretion (Höglund et al., 2002; Medeiros et al., 2010; Winberg et al., 1997). Peripherally, 5-HT exerts paracrine control at the interrenal tissue level, with local activation of 5-HT4 receptors directly stimulating cortisol biosynthesis (Tea et al., 2025).

The interaction between serotonergic pathways and the HPI axis is bidirectional, and this crosstalk regulates phenotypic plasticity and behaviour (Herculano & Maximino,

2014a; Winberg & Thörnqvist, 2016). High circulating cortisol levels suppress central serotonergic activity by reducing 5-HT turnover and downregulating 5-HT1A receptor expression in the brain (Höglund et al., 2002; McDonald, 2017; Winberg & Nilsson, 1993). However, under chronic stress conditions, such as social subordination, this feedback loop can become dysregulated. Chronically defeated rainbow trout exhibit sustained elevations in brain serotonergic activity, indicated by high 5-HIAA/5-HT ratios, alongside elevated plasma cortisol (Winberg & Lepage, 1998; Winberg & Thörnqvist, 2016). Despite these high cortisol levels, pituitary POMC expression remains elevated, suggesting a state of glucocorticoid feedback resistance driven by chronic serotonergic overstimulation (Winberg & Lepage, 1998).

1.4. Ecotoxicology of SSRIs in non-target species

1.4.1. Conservation of therapeutic target and concerns for non-target species

The SSRIs and SNRIs elicit their pharmacological effects by blocking monoamine transporters. Because these primary targets (e.g., SERT) are highly conserved across vertebrates, non-target aquatic organisms are potentially susceptible to their neuroendocrine effects (S. L. Gould et al., 2021). In effluent-impacted surface waters, fluoxetine and its active metabolite accumulate in fish tissues. Measured plasma bioaccumulation factor, defined as the ratio of the compound concentration in plasma to the concentration in surrounding water, reach 386 L/kg in caged goldfish and up to 906 L/kg in wild populations, indicating plasma concentrations several hundred-fold above ambient water levels (Muir et al., 2017). This uptake pattern differs from humans' intermittent dosing with peak-and-trough kinetics over a treatment course, versus continuous lifetime exposure from embryo onwards. Fish in effluent-dominated systems are continuously exposed throughout their lives, so internal concentrations are governed by uptake and elimination kinetics. Furthermore, wild teleosts are chronically exposed to complex mixtures of antidepressants and other environmental contaminants, which can interact to drive population-level shifts in physiology, plasticity, and interspecies dynamics (Kostich et al., 2014; Rzymski et al., 2017; Saaristo et al., 2018; Wilkinson et al., 2022).

1.4.2. SSRI-induced disruption of the stress response

The teleost hypothalamic-pituitary-interrenal (HPI) axis is highly sensitive to serotonergic modulation, rendering it vulnerable to SSRI-induced disruption. Developmental exposure to fluoxetine (0.54 to 54 µg/L; 0 - 6 days post-fertilisation) alters transcriptomic profiles in the heads of 6 dpf zebrafish (*Danio rerio*), adult brains and interrenal glands, specifically disrupting networks associated with neuroendocrine signalling, the stress response, and epigenetic regulation (Nozari et al., 2022; Vera-Chang, Moon, et al., 2019). At the transcript level, early-life fluoxetine exposure notably downregulates *fkbp5*, a critical glucocorticoid-responsive gene (Park et al., 2012). This early-life transcriptomic disruption translates to permanent physiological deficits; adults exposed to fluoxetine exclusively during early development exhibit persistent hypocortisolism (Vera-Chang et al., 2018). This hypocortisolism phenotype is transgenerational, persisting for up to three consecutive unexposed generations in zebrafish lineages (Vera-Chang et al., 2018).

1.4.3. SSRI-induced behavioural disruptions

Neuroendocrine disruption by SSRIs and SNRIs frequently manifests as altered locomotion and anxiety-related behaviours in teleosts. During early life stages, acute and developmental exposures depress mobility. For example, citalopram exposure induces hypoactivity in zebrafish larvae at 144 hpf, with a behavioural EC50 of 471 µg/L (Bachour et al., 2020). Similarly, zygotic deposition and larval exposure to environmentally relevant concentrations of venlafaxine reduce spontaneous swimming and alter photomotor reactivity in zebrafish and fathead minnows (*Pimephales promelas*) (Thompson et al., 2017; Thompson & Vijayan, 2020a). These behavioural deficits are mechanistically linked to venlafaxine-induced reductions in brain serotonin (Thompson & Vijayan, 2020b). In adults, SSRI exposure has been reported to induce anxiolytic phenotypes in several species. Male fathead minnows exposed to sertraline (3 µg/L) exhibit reduced shelter-seeking behaviour, indicative of lowered anxiety (Valenti et al., 2012). Likewise, adult zebrafish developmentally exposed to fluoxetine display reduced exploratory behaviours, a phenotype that persists for up to two unexposed generations in males (Vera-Chang et al., 2018; Vera-Chang, St-Jacques, et al., 2019). Venlafaxine induces sex-specific long-term effects, reducing anxiety-like behaviours in juvenile zebrafish while triggering hyperactivity in adults (Thompson et al., 2022).

1.4.4. Other apical effects and implications for populations

Beyond the stress axis, prolonged inhibition of monoamine reuptake can alter feeding, growth, and reproduction. In yellow catfish (*Tachysurus fulvidraco*), environmental sertraline exposure downregulates brain transcripts of neuropeptide Y, somatostatin, growth hormone, and insulin-like growth factor 1, leading to decreased food intake and suppressed overall growth (H. Chen et al., 2021). Similar anorexigenic effects are observed in adult female goldfish, where fluoxetine suppresses the expression of feeding peptides and inhibits weight gain (Mennigen et al., 2009). However, apical outcomes can be species-specific; developmental exposure to citalopram in the three-spined stickleback (*Gasterosteus aculeatus*) increased both feeding and aggressive behaviours during adulthood (Kellner et al., 2018). Teleost reproductive and developmental physiology is also disrupted following SSRI exposure. In adult goldfish, fluoxetine disrupts the reproductive axis of both females and males (León-Olea et al., 2014; Mennigen et al., 2008, 2010). Finally, early-life exposures can induce severe developmental toxicity, with environmentally relevant concentrations of fluoxetine causing morphological deformities (Cunha et al., 2016) and accelerating both heart rates and hatching times in teleost embryos (Blahova et al., 2021).

1.5. Zebrafish as a study model

The zebrafish (*Danio rerio*), a teleost in the family Cyprinidae, is a widely used vertebrate model in toxicology, drug discovery, and risk assessment. Zebrafish embryos and larvae represent a bridge between *in vitro* models and *in vivo* mammalian models (Chakravarthy et al., 2014; Horzmann & Freeman, 2018). Several logistical and physiological advantages of this model compared to rodent models include high fecundity, external fertilisation, rapid development, short generation time, optical transparency, and relatively low-cost husbandry maintenance (Horzmann & Freeman, 2018). At the genomic level, approximately 70% of human genes have at least one zebrafish orthologue (Howe et al., 2013). Importantly, zebrafish possess orthologues to approximately 86% of human drug targets (Gunnarsson et al., 2008).

The suitability of this study model and developmental window rests on the timing of the two systems under study. The serotonergic system develops early in zebrafish: serotonergic neurons of the raphe nuclei and their descending projections are detectable from 24 to 48 hpf (hours post-fertilisation), and the major aminergic systems are in place shortly after hatching, by approximately 96 hpf (McLean & Fetcho, 2004; Norton et al., 2008). The two serotonin-transporter paralogues show distinct distributions, with *slc6a4a* broadly expressed and *slc6a4b* expression restricted to the brain (Norton et al., 2008). The serotonergic pathway maturation overlaps with the functional onset of the HPI axis. Maternal-deposited cortisol is largely depleted by hatching (48-72 hpf), and *de novo* cortisol synthesis is initiated; a stressor-induced cortisol response can first be detected at approximately 96, and glucocorticoid-mediated negative feedback is established by 120 hpf (Alsop & Vijayan, 2007, 2009b). The convergence of these two developmental timelines was used to define the 4 to 7 dpf period used across this thesis to study serotonergic modulation of stress-axis programming and reactivity, as well as the effects of xenobiotics.

The increasing availability of gene-editing tools and transgenic lines makes zebrafish an animal model of interest for high-throughput drug screening (Demin et al., 2021; McGrath & Li, 2008) and chemical risk assessment (Thunga et al., 2021). To evaluate stress-axis reactivity *in vivo*, this research employed the stress-inducible transgenic SR4G (Stress receptor 4-hour enhanced Green fluorescent protein) zebrafish reporter line (Krug et al., 2014). The SR4G line expresses a destabilised eGFP (d4EGFP, ~4 h half-life) under the transcriptional control of six consecutive glucocorticoid response elements (GREs). The short half-life of this reporter allows for the monitoring of glucocorticoid receptor activation dynamics in response to both acute and chronic exogenous agonists (Krug et al., 2014). It was developed to investigate environmental or genetic modifiers of stress-response signalling, and previous studies in our laboratory demonstrated that this line can be used as a rapid, *in vivo* screening assay to quantify the endocrine stress response following an acute handling stress (Nozari et al., 2021).

1.6. Thesis overview

1.6.1. Rationale for the study

SS(N)RIs are among the most highly prescribed classes of neuroactive pharmaceuticals and are frequently detected in urbanised watersheds. This category of antidepressants exerts its primary therapeutic action by inhibiting monoamine reuptake transporters, leading to elevated extracellular concentrations of serotonin and norepinephrine in the case of SNRIs. Because serotonergic pathways are highly conserved across vertebrates, these drugs may cause neuroendocrine disruption in non-target species, particularly affecting the HPI axis that coordinates the physiological stress response in teleost fish. Disruption of HPI axis function in teleosts is associated with altered baseline or stress-induced cortisol levels, disrupted metabolic capacity, and maladaptive behaviours, including impaired predator avoidance and locomotion. However, standard ecotoxicological assessments are usually conducted under static, unstressful conditions, which may fail to detect neuroendocrine and behavioural disruptions that may become apparent when the exposed organism is challenged.

Several knowledge gaps and limitations persist in our current understanding of the developmental impacts and environmental risks of SS(N)RIs in aquatic ecosystems. First, direct comparisons of multiple SS(N)RIs under standardised conditions remain sparse, with most studies focusing on one molecule at a time, mainly fluoxetine. Second, the molecular pathways underlying sublethal effects in teleosts are poorly characterised, as traditional ecotoxicological assessments focus primarily on apical endpoints rather than integrating molecular perturbations. Finally, there is a lack of standardised, reproducible *in vivo* screening methods that combine molecular, physiological, and behavioural endpoints within a dynamic challenge framework to evaluate disruption of the stress axis during early development. Consequently, comparative research integrating high-throughput molecular sequencing and behavioural assays is required to improve screening approaches and to better characterise how developmental exposure to SS(N)RIs may affect stress-axis responses. **The hypothesis I tested is that developmental exposure to SS(N)RIs will alter molecular, physiological, and behavioural components of the stress response in larval zebrafish compared with unexposed controls.**

1.6.2. Chapter-specific objectives

The thesis is organised into a series of distinct chapters that will serve as the basis for independent publications. Necessarily, these chapters have slightly different formats, and some level of redundancy in their introductions and methods is unavoidable. The results of the experiments performed throughout this doctoral research are described in the following chapters:

Chapter 2: Developmental exposure to serotonin reuptake inhibitors does not impair stress response activation in a transgenic zebrafish reporter line.

In this chapter, I aimed to confirm the use of transgenic zebrafish larvae (SR4G) as an *in vivo* screening tool for stress-disrupting compounds. I exposed transgenic zebrafish larvae to a range of concentrations of six SS(N)RIs or a common metabolite to evaluate glucocorticoid-responsive transcription under basal conditions and following an acute stressor (netting stress). Reporter transcription and cortisol levels were measured in both conditions using qPCR and ELISA, respectively.

Objectives:

1) Evaluate whether GRE-mediated eGFP reporter transcription accurately reflects whole-body cortisol fluctuations following an acute stressor in SR4G larvae.
2) Screen a panel of SS(N)RIs and a major metabolite for effects on basal and stress-induced GR-mediated transcription of the eGFP reporter to assess stress axis responsiveness.

Chapter 3: Developmental exposures to fluoxetine, norfluoxetine, and sertraline cause divergent, stress-dependent transcriptomic responses in zebrafish larvae.

In this chapter, I investigated the molecular mechanisms mediating SSRI effects and toxicity. The compounds and concentrations included in the study were based on the results of Chapter 2. Using TempO-Seq and the Zebrafish S1500+ panel assay, transcriptomic analyses were performed in larvae developmentally exposed to fluoxetine, norfluoxetine, or sertraline. I compared expression profiles for each compound at baseline and following a standardised netting stress and aimed to identify shared and compound-specific transcriptomic responses.

Objectives:

1) Determine if developmental exposure to fluoxetine, norfluoxetine or sertraline alters larval transcriptional responses under basal conditions and following an acute netting stress.
2) Identify shared and compound-specific transcriptomic responses to these three compounds.

<u>Chapter 4:</u> Sertraline disrupts photomotor behaviour and glucocorticoid-responsive transcription in transgenic zebrafish larvae.

In this chapter, I aimed to integrate physiological, behavioural, and transcriptomic endpoints to evaluate the effects of sertraline exposure. SR4G larvae were exposed to sub-lethal concentrations of sertraline until 5 dpf and subjected to a light/dark behavioural challenge. Development, survival, locomotion, and gene expression were measured, including the eGFP reporter transcription and transcriptomic analysis using TempO-Seq and the Zebrafish S1500+ panel assay.

Objectives:

1) Determine if developmental sertraline exposure affects larval survival and development.
2) Evaluate whether sertraline exposure disrupts locomotor behaviour and GR-mediated reporter transcription in response to a light/dark challenge.
3) Identify transcriptomic pathway perturbations associated with the observed behavioural and stress-response alterations.

2. Chapter 2: Developmental exposure to serotonin reuptake inhibitors does not impair stress response activation in a transgenic zebrafish reporter line

2.1. Statement of contributions

Submitted to: Environmental Pollution, in peer review.

Authors: Emmanuelle Monniez [1], Carole L. Yauk [1], Errol M. Thomson [2,3], Vance L. Trudeau [1]

Affiliations:

[1] Department of Biology, Faculty of Sciences, University of Ottawa, Ottawa, Canada

[2] Environmental Health Science and Research Bureau, Healthy Environments and Consumer Safety Branch, Health Canada, Ottawa, Canada

[3] Department of Biochemistry, Microbiology, and Immunology, Faculty of Medicine, University of Ottawa, Ottawa, Canada

Emmanuelle Monniez participated in the study design, conducted the experiments, analysed the data, and prepared the manuscript. Dr. Errol M. Thomson provided the platform for RT-qPCR experiments. Dr. Carole L. Yauk, Dr. Errol Thomson and Dr. Vance L. Trudeau obtained funding for the research, helped with the study design, and assisted with manuscript review and editing.

2.2. Introduction

Antidepressants, particularly selective serotonin reuptake inhibitors (SSRIs) and serotonin-norepinephrine reuptake inhibitors (SNRIs), are widely prescribed for the treatment of depression, anxiety, and mood disorders, and are often detected in aquatic environments worldwide (Castillo-Zacarías et al., 2021; Silva et al., 2012). These compounds exert their therapeutic effects by inhibiting monoamine reuptake transporters, notably the serotonin reuptake transporter (SERT), and in the case of SNRIs also the norepinephrine reuptake transporter (NET), leading to increased extracellular monoamine concentrations (Hiemke & Härtter, 2000; Lambert & Bourin, 2002). Because serotonergic and noradrenergic signalling pathways are highly conserved across vertebrates, these modes of action raise concerns regarding potential neuroendocrine disruption in non-target aquatic species.

Antidepressant use and environmental occurrence have increased in recent years, a trend amplified by the COVID-19 pandemic, which contributed to a 25% global rise in the prevalence of anxiety and depression, and increased antidepressant consumption in OECD countries (OECD, 2025; WHO, 2022). Recent studies indicate elevated occurrence of SSRIs in surface waters following the pandemic period (Diaz-Camal et al., 2022; Pappas et al., 2025). SSRI residues are routinely detected in surface water, groundwater, and drinking water (Mole & Brooks, 2019; Silva et al., 2012), with concentrations ranging from a few ng/L to several µg/L depending on compound, matrix, and geographic region (Fernandes et al., 2020; S. L. Gould et al., 2021; Kostich et al., 2014).

The central serotonergic system is conserved across vertebrates, raising concerns regarding the susceptibility of aquatic non-target species to SSRIs and SNRIs (S. L. Gould et al., 2021; Sehonova et al., 2018). The SERT protein shares, on average, 69% amino acid sequence homology, and up to 93% at amino acid residues critical for SSRI binding, between human and fish (McDonald, 2017; Mennigen et al., 2011). Therefore, SSRIs and SNRIs may increase extracellular serotonin levels in the brains of fish and induce a response where serotonin (and norepinephrine) receptors are present (McDonald, 2017; Mennigen et al., 2011).

Because serotonin plays a key role in modulating vertebrate neuroendocrine function, environmental exposure to SSRIs or SNRIs may disrupt physiological processes and behaviours in aquatic species. In teleost fish, serotonin modulates major neuroendocrine axes, including the hypothalamus-pituitary-interrenal (HPI) axis, which governs the endocrine stress response (McDonald, 2017). Like the mammalian HPA axis, the teleost HPI axis and endocrine stress response are activated upon triggering by a stimulus that disrupts homeostasis and result in the secretion of glucocorticoids (GCs) (Harris & Carr, 2016). Serotonin receptors are present at all levels of the HPI axis in teleost fish and are known to modulate it (Lillesaar, 2011; Winberg & Lepage, 1998; Winberg & Nilsson, 1993). Consistent with this, previous studies showed that developmental exposure to Fluoxetine in zebrafish (*Danio rerio*) induces persistent hypocortisolism, reduced exploratory and locomotor behaviours, and altered transcription of genes associated with steroidogenesis and HPI axis development, with effects that can persist across generations (Vera-Chang et al., 2018; Vera-Chang, Moon, et al., 2019; Vera-Chang, St-Jacques, et al., 2019). These findings suggest that developmental SSRI exposure can induce lasting alterations in stress axis regulation in fish, underscoring the need for direct *in vivo* assessment of HPI axis function across compounds.

Zebrafish are a well-established model in environmental toxicology and enable high-throughput screening of chemicals, particularly during embryonic and larval stages, which bridge *in vitro* and *in vivo* models (Chakravarthy et al., 2014; Horzmann & Freeman, 2018). Key advantages of this model include high fecundity, small, transparent larvae that facilitate *in vivo* observations and imaging, and short generation time, making it a cost-effective and ideal model for research in toxicology, drug discovery, and pharmaceutical risk assessment (Fitzgerald et al., 2020; Horzmann & Freeman, 2018). Zebrafish larvae support diverse biomonitoring approaches, including morphological assessment, gene expression analysis, behavioural assays, and fluorescence imaging of inducible transgenes (Bambino & Chu, 2017; Horzmann & Freeman, 2018; Thunga et al., 2021; von Hellfeld et al., 2020). Advances in gene-editing techniques have expanded the availability of transgenic lines for toxicological screening (Tanguay, 2018, 2025; Thunga et al., 2021).

In this study, we used the SR4G (Stress Receptor 4-hour enhanced Green fluorescent protein) transgenic line (Krug et al., 2014), which expresses a short half-life

green fluorescent protein (eGFP) under the control of six exogenous glucocorticoid response elements (GREs). This reporter provides a quantitative readout of glucocorticoid receptor (GR) activation and has been developed to detect environmental or genetic modifiers of stress signalling. Recent research in our laboratory demonstrated that SR4G larvae can be used as an *in vivo* tool to quantify blunted stress responses following chemical exposure, providing a proof of concept for its use as a screening tool (Nozari et al., 2021).

Although Fluoxetine disrupts the stress response in zebrafish, direct comparisons of multiple SSRIs and SNRIs on the HPI axis function under standardized conditions remain limited. Existing studies in zebrafish have focused on single compounds, mainly Fluoxetine, and have reported effects on basal and/or stress-induced cortisol levels (Abreu et al., 2014, 2017; Martinez et al., 2019; Nozari et al., 2021; Vera-Chang et al., 2018; Vera-Chang, Moon, et al., 2019). In contrast, other SSRIs have primarily been assessed using behavioural, neurochemical or transcriptomic endpoints, without direct measurement of HPI axis activity, making comparisons across compounds difficult (Park et al., 2012; Venkatachalam et al., 2023; Zindler et al., 2020). To address this gap, we compared multiple SSRIs, SNRIs, and their metabolites (hereafter collectively referred to as SS(N)RIs) under identical experimental conditions. Our objectives were to: (1) evaluate whether GRE-regulated eGFP reporter expression in SR4G larvae is a reliable proxy for whole-body cortisol levels in response to an acute stressor, and (2) screen SS(N)RIs for effects on basal and stress-induced GR-mediated transcription of the eGFP reporter to assess stress axis responsiveness.

2.3. Material and Methods

2.3.1. Animal care and husbandry

Colony maintenance and experimental procedures were approved by the University of Ottawa Animal Care Protocol Review Committee and comply with the guidelines of the Canadian Council on Animal Care for the use of animals in research. The SR4G zebrafish line (Tg(6xGRE:EGFP,myl7:TagBFP)mn48) (Krug et al., 2014) was housed in the Aquatic Facility of the University of Ottawa and maintained on an automatic flow-through ZebTEC rack system (Tecniplast, Montréal, QC, Canada), with water at 27-29 °C, pH = 7.4-7.5, conductivity 290-300 µS, dissolved oxygen >7 mg/L, and in a 14:10h light/dark photoperiod. Adults were fed a commercial food daily (Gemma Micro 300, Skretting, NB, Canada).

Zebrafish embryos were obtained by breeding adults in 1.7 L sloped breeding tanks (Tecniplast, Montréal, QC, Canada), at a ratio of 3F:2M per breeding tank. Breeding tanks were set up in the late afternoon the day prior, and females and males were separated for the night. The next morning, traps were transferred to tanks with clean facility water, separations were lifted between 09:00 and 09:30 am, and fish were allowed to spawn for an hour. Adults were then returned to the system, and embryos were collected in Petri dishes. Embryos were kept for 24 hours in an incubator set at 28 ± 0.5 °C, and unfertilized and dead embryos were removed. Before starting exposure, the viable embryos' surface was sanitized to remove potential pathogens as follows: 10 mins in diluted sodium hypochlorite (0.002%), 1 min in a sodium thiosulfate neutralization solution, and three rinses for 2 mins in embryo medium (facility water, 0.00003% methylene blue).

2.3.2. Chemicals and solution preparations

Chemicals were purchased from Tocris and TargetMol as powder stocks (Table 2.1). Stock solutions were prepared in DMSO and were diluted in 50 mL of embryo medium to obtain exposure solutions of 1000, 100, 10, 1, 0.1, 0.01, and 0.001 nM (nominal concentration; final concentration of vehicle DMSO 0.02% in all treatments). New stock solutions were prepared for each experimental replicate. Water samples were analysed to determine measured concentrations in the exposure medium. Samples (n = 3) consisted of 50 mL of 1000 nM (nominal concentration) for each SS(N)RI tested, as well as vehicle

controls (DMSO 0.02% v/v). Samples were sent to the Trent University Water Quality Centre for analysis by liquid chromatography-mass spectrometry. Analysis results are available in Supplementary Table A.1.

Table 2.1. List of test compounds.

Compound	Abbrev.	CAS#	Formula	Supplier	Purity[1]
Citalopram hydrobromide	CIT	59729-32-7	$C_{20}H_{21}FN_2O.HBr$	Tocris	≥99.9%
Desvenlafaxine	DES	93413-62-8	$C_{16}H_{25}NO_2$	TargetMol	99.65%
Dexamethasone	DEX	50-02-2	$C_{22}H_{29}FO_5$	Tocris	99.6%
Escitalopram oxalate	ESC	219861-08-2	$C_{20}H_{21}FN_2O.C_2H_2O_4$	Tocris	99.8%
Fluoxetine hydrochloride	FLX	56296-78-7	$C_{17}H_{19}ClF_3NO$	TargetMol	99.98%
Hydrocortisone	CORT	50-23-7	$C_{21}H_{30}O_5$	Tocris	99.5%
Norfluoxetine hydrochloride	NOR	57226-68-3	$C_{16}H_{17}ClF_3NO$	TargetMol	99.71%
Sertraline hydrochloride	SER	79559-97-0	$C_{17}H_{18}Cl_3N$	TargetMol	99.89%
Venlafaxine hydrochloride	VEN	99300-78-4	$C_{17}H_{27}NO_2.HCl$	Tocris	≥99.9%

[1] Reported in the supplier's certificate of analysis.

2.3.3. Exposure conditions and experimental design

For each "concentration" x "stress" group, 50 embryos were placed in 50 mL of exposure solution in glass Petri dishes. Embryos were exposed from 1 to 7 days post-fertilization (dpf) in an incubator set at 28 ± 0.5 °C, under a 14:10h light/dark photoperiod, with semi-static renewal of the exposure solutions. Exposures were performed in 3-4 independent biological replicates (separate experimental runs conducted on different spawning days) for each tested compound. Each replicate experiment included medium-only and vehicle controls (DMSO 0.02% v/v) (Figure 2.1). Embryos were checked daily for malformations (edema, trunk, tail) and survival under a microscope, and dead embryos were removed.

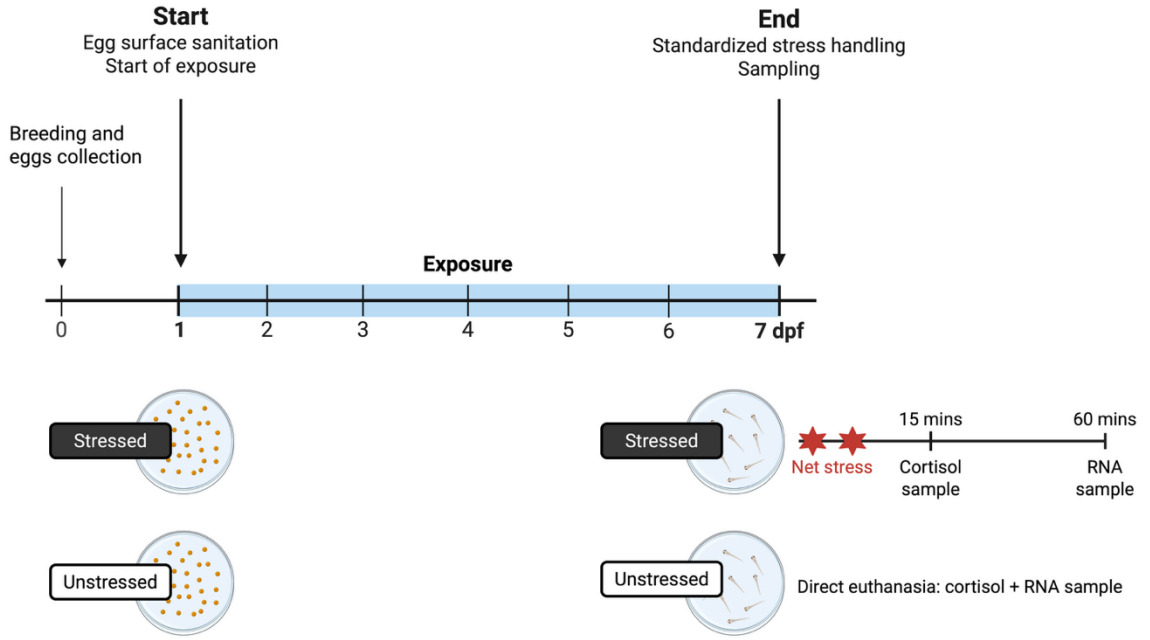

Figure 2.1. A schematic representation of the experimental design.

SR4G zebrafish embryos were exposed from 24 hours to 7 days post-fertilisation (dpf) to a concentration range of SSRI, SNRI, or metabolites. For each concentration tested, embryos were divided into two subgroups (unstressed and stressed) and raised in the same conditions. At the end of the exposure, the stressed groups underwent an acute handling stress, which consisted of catching the larvae with a brine shrimp net, exposing them to air for 1 min, followed by 3 min of rest in medium, and then another 1 min of air exposure. Larvae were returned to the medium for recovery and collected after 15 and 60 mins to assess cortisol and eGFP reporter mRNA levels, respectively. The corresponding unstressed group was directly euthanized to measure basal cortisol and eGFP mRNA levels. Created with BioRender.com: Monniez, E. (2026).

2.3.4. Standardised stress protocol and sample collection

At 7 dpf, stressed groups underwent a standardised stress protocol as previously described (Nozari et al., 2021). Briefly, larvae were caught using a brine shrimp net, exposed to air for 1 min, given 3 mins of rest in medium, and netted for another 1 min. Larvae were returned to Petri dishes filled with medium and placed back in the incubator before sampling. Within each experimental replicate, 20 larvae were sampled 15 min after the end of the stress protocol for cortisol quantification, and 20 larvae were sampled 60 min after the end of the stress protocol for eGFP mRNA levels. The unstressed groups were directly euthanised; as with the treatment conditions, 20 larvae were pooled for each endpoint (cortisol or mRNA levels) (Figure 2.1). Each pooled sample represented one biological replicate. Sampling order was randomised for each experimental replicate to avoid sampling-time bias. Euthanasia was conducted in two steps: first, a rapid chilling in 4 °C facility water, then larvae were collected and pooled in a 1.5 mL tube and kept on ice. Excess medium was removed and replaced with RNA*later* Stabilization Solution (Invitrogen, Thermo Fisher Scientific, Waltham, USA) in samples for RNA extraction, and samples for cortisol extraction were flash-frozen after removing excess medium. All samples were stored at -80 °C until further analysis.

2.3.5. Whole-body cortisol extraction and measurement

Whole-body cortisol was extracted from pools of 20 larvae using a solid-liquid phase extraction method (Lu et al., 2023). Briefly, samples were disrupted in 100 µL of homogenization buffer (90% MeOH, 1% AcOH) using a sonic dismembrator. Samples were centrifuged and the supernatant was collected in new tubes. Samples were evaporated to dryness (45 °C, 1 hr) (CentriVap Vacuum Concentration System, Labconco Corporation, Kansas City, USA) and stored overnight at 4 °C. Samples were resuspended in 100 µL of equilibrium solution (5% acetonitrile (ACN), 0.2% formic acid (FA), in water), vortexed, and then placed in a sonic water bath for 15 mins. Following resuspension, samples were run in solid-phase extraction columns prepared by packing 10 mg of ReproSil-Pur 120 C18-AQ powder (cat. no. r13.aq.0010, Dr. Maisch HPLC GmbH, Ammerbuch-Entringen, Germany) in filtered 96-well plate columns. Samples were purified by loading them onto the pre-packed, activated SPE plates and washing with the equilibrium solution. Elution

was performed by adding 20 µL of elution solution (75% ACN, 0.2% FA, in water) 6 times. Eluted samples were transferred to tubes, evaporated to dryness (45 °C, 1 hr), and kept at -20 °C until resuspension in 1X ELISA buffer.

Cortisol levels were measured using the Cayman Cortisol ELISA kit (cat. no. 500360, Cayman Chemicals, Michigan, USA) following the manufacturer's instructions. Samples were resuspended in 200 µL of 1X ELISA buffer and incubated at 4 °C for 24 hours, with 3 rounds of vortexing to fully resuspend the lipid extracts. Each sample was measured in technical duplicate on a single plate, and each plate included its own standard curve. The mean intra-assay coefficient of variation (CV) between technical duplicates was 6.4% (standard deviation 7.2%, median 4.1%). Samples from each experimental replicate were assayed on the same plate, except for re-assayed samples after dilution. Using spiked samples containing known amounts of cortisol (prepared with the cortisol standard solution provided in the kit), the extraction efficiency was estimated at ~80%, values were not corrected for extraction efficiency. Cortisol content was expressed in pg/larva by multiplying the sample concentration by the resuspension volume and dividing by the number of larvae in the sample pool.

2.3.6. Total RNA extraction, cDNA synthesis, and qPCR

RNA extractions were carried out using the RNeasy Mini kit, following the Qiagen User Manual guidelines (Qiagen, Toronto, Canada). Purified RNA extracts were quantified using a Qubit 4 Fluorometer and RNA Broad Range assay (Invitrogen, Thermo Fisher Scientific, Waltham, USA), and RNA integrity number (RIN) was measured using an automated electrophoresis system (Agilent Technologies Inc., Santa Clara, CA, USA). Only samples with RIN >8.0 were used in further analysis. For each sample, 500 ng of isolated RNA was converted to cDNA using the QuantiTect® Reverse Transcription kit with gDNA elimination (cat. no. 205313, Qiagen, Toronto, Canada), following the manufacturer's recommendations. Forward and reverse primer sequences for *d4egfp* (eGFP, enhanced green fluorescent protein) and *eef1a1l1* (eukaryotic translation elongation factor 1 alpha 1, like 1; housekeeping gene) were adopted from previous publications (Krug et al., 2014; Nozari et al., 2021) (Supplementary Table A.2).

All primers were synthesized by Integrated DNA Technologies (Coralville, Iowa, USA). Real-time quantitative polymerase chain reactions (qPCR) were performed using the PowerUp™ SYBR™ Green Master Mix (Applied Biosystems, Thermo Fisher Scientific, Waltham, USA), with 10 ng of cDNA and 400 nM of each primer, in a total volume of 10 µL/well. All reactions were performed in technical duplicates in a spectrofluorometric thermal cycler (Lightcycler 480, Roche Diagnostics, Laval, Quebec, Canada) following standard cycling parameters. A melt-curve analysis was performed at the end of each run to verify specificity and the absence of primer dimers. Each qPCR plate included "no RT" controls to ensure no gDNA contamination, as well as negative "no template" controls. Relative expression of the eGFP reporter was calculated using the $\Delta\Delta C_T$ method (Livak & Schmittgen, 2001) and the "tidyqpcr" analysis R package (https://github.com/ewallace/tidyqpcr) (Wallace & Haynes, 2022), with vehicle-unstressed samples as the reference group. Raw C_T values for *eef1a1l1* averaged 17.7 ± 0.8 (mean ± standard deviation, n = 440 samples total, 10 plates); mean C_T values of concentration and stress groups differed by at most 1.6 cycles within a compound series (Supplementary Table A.3), supporting its use for normalisation in this study.

2.3.7. Data processing and statistical analyses

Malformations were recorded over the 6 days of exposure. The recorded malformations included oedema (pericardiac, yolk sac), trunk malformations (scoliosis, kyphosis, lordosis), and tail malformations (short, crooked) (von Hellfeld et al., 2020). Malformation counts were summarised into three categories: oedema, trunk malformations, and tail malformations. The number of larvae affected by any malformation per treatment group was used to calculate the percentage of larvae affected. Cumulative survival at 7 dpf was expressed as the percentage of larvae alive at the end of the exposures, before euthanasia and sampling, relative to the number of embryos initially placed in exposure baths at 1 dpf.

Data processing, statistical analyses, and graphing were conducted using R (version 4.5.1) and RStudio (version 2025.09.1+401), or GraphPad Prism 10 (La Jolla, CA, USA). Data are presented as mean ± SEM. Whole-body cortisol levels were analysed both as raw content (pg/larva) and as fold-change values calculated relative to the mean of the vehicle-

unstressed group within each compound series (n = 3 or 4 pools). Raw values were log10-transformed to stabilise variance between unstressed and stressed larvae. For each compound, a two-way ANOVA (analysis of variance) was first used to test the effects of concentration, stress and their interaction, with experimental replicate as a blocking factor. The effect of concentration was then tested within each stress condition with a one-way ANOVA including the same blocking factor, followed by Dunnett's comparisons against the vehicle group. Repeating the comparisons on fold-change values gave the same conclusions for all concentration comparisons.

For eGFP relative expression, a two-way ANOVA was first used to assess the effects of concentration, stress and their interaction. When interaction effects were not significant, models were simplified to test main effects only, and pairwise comparisons were carried out with Tukey's post-hoc test when main effects were significant. In some cases, assumptions were still not met, so we separated the datasets into "unstressed" and "stressed" larvae and tested the effect of the concentration factor within each stress condition subgroup using a one-way ANOVA, followed by Dunnett's post-hoc test if the main effect was significant. To assess the correlation between cortisol and eGFP expression levels, the Pearson test was used. For every analyses, normality and homoscedasticity assumptions were assessed using the Shapiro-Wilk, Kolmogorov-Smirnov and Levene tests. The significance level for all analyses was set at $p < 0.05$.

2.4. Results

2.4.1. Malformation frequency and survival after exposure

To assess the effects of the tested compounds on embryonic development, we monitored malformations and survival. Malformations after exposure were rare, and the mean malformation frequency across all experimental replicates and treatments was <1% (0.61 ± 0.76 %). The highest percentages of larvae with at least one malformation after SS(N)RI exposure were observed in the Norfluoxetine 10 nM and 1000 nM treatments (2.3 ± 1.5 % and 2.3 ± 2.7 %, respectively) (Supplementary Table A.4). These results suggest that neither SS(N)RIs nor glucocorticoids, at the tested concentrations, affected malformation frequency in 7 dpf SR4G larvae.

Mean survival in control conditions exceeded 90% in both unstressed and stressed conditions (Supplementary Table A.5). There was no significant effect of the vehicle or acute handling stress on survival percentage (Treatment: $F_{(1, 104)} = 0.020$, $p = 0.89$; Stress: $F_{(1, 104)} = 0.037$, $p = 0.85$; Interaction: $F_{(1, 108)} = 0.110$, $p = 0.74$). Treatment with glucocorticoids for 6 days did not induce significant mortality in either unstressed or stressed conditions, compared with their respective controls (Figure 2.2, Supplementary Table A.6). For SS(N)RI exposures, survival percentages at the end of exposure were not significantly different across the following treatments: CIT, ESC, FLX, NOR, VEN, and DES, in either stressed or unstressed conditions (Figure 2.3, Supplementary Table A.6). SER concentration had a significant effect on larval survival but there was no significant effect of the stress factor (SER Concentration: $F_{(7, 39)} = 7.56$, $p < 0.001$; Stress: $F_{(1, 39)} = 0.44$, $p = 0.51$) (Figure 2.3). Tukey's post-hoc comparisons revealed a significant decrease in survival in larvae exposed to SER 1000 nM, in both unstressed and stressed larvae (Figure 2.3). Survival was 33% and 52% lower than in their vehicle control, respectively. Overall, SS(N)RIs or glucocorticoid treatment did not significantly affect the survival of SR4G larvae, except at the highest SER concentration tested.

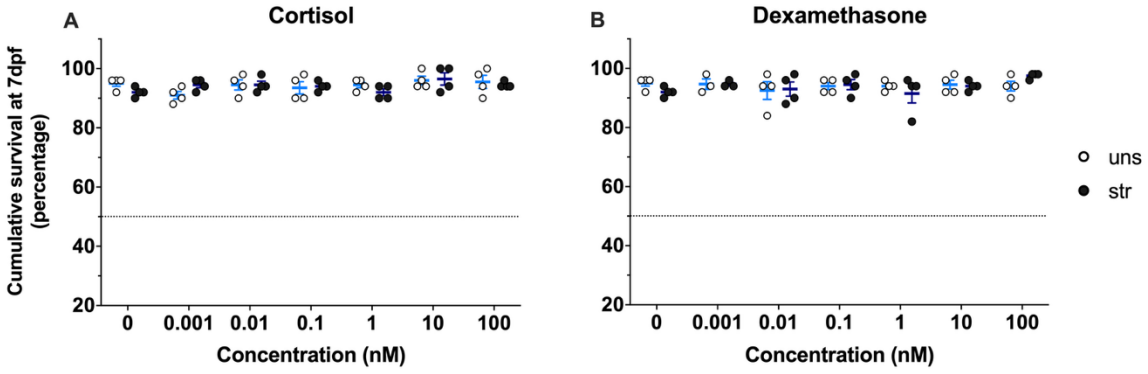

Figure 2.2. Cumulative survival of 7 dpf larvae exposed to glucocorticoids.

Panels show results for each compound: (A) Cortisol and (B) Dexamethasone. Cumulative survival represents the percentage of larvae alive at the end of the exposure period, calculated from the number of embryos initially placed in exposure baths at 24 hrs. post-fertilization. Bars and intervals represent mean ± SEM for each stress x concentration subgroup (n = 3-4), with individual observations overlaid (unstressed: white points, light-blue bars; stressed: black points, dark-blue bars). The dashed line indicates 50% survival. A two-way ANOVA tested the effects of the acute handling stress and treatment concentration.

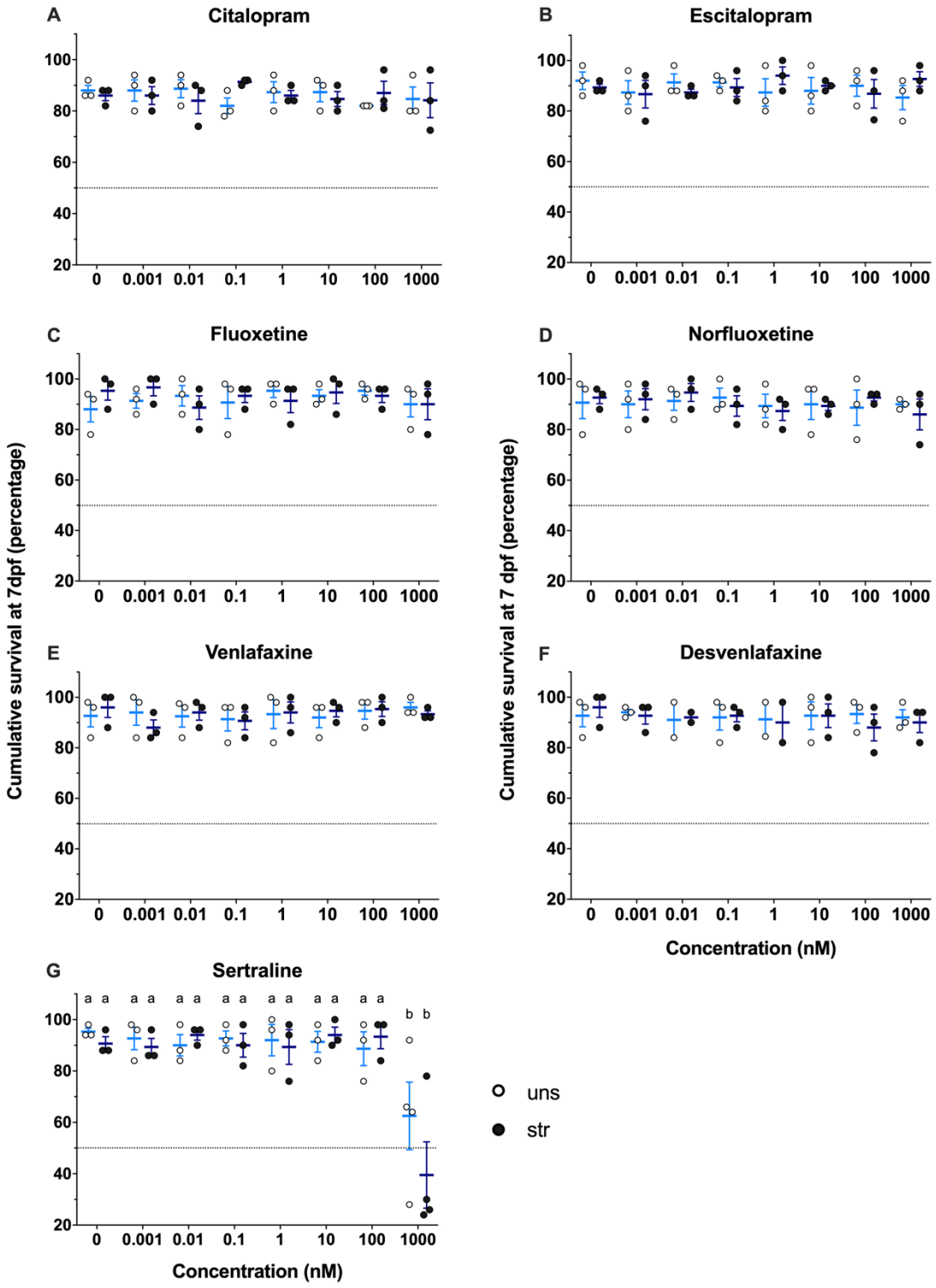

Figure 2.3. Cumulative survival of 7 dpf larvae exposed to SS(N)RIs.

Panels show results for each compound: (A) Citalopram, (B) Escitalopram, (C) Fluoxetine, (D) Norfluoxetine, (E) Venlafaxine, (F) Desvenlafaxine, and (G) Sertraline. Cumulative survival represents the percentage of larvae alive at the end of the exposure period, calculated from the number of embryos

initially placed in exposure baths at 24 hrs. post-fertilization. Bars and intervals represent mean ± SEM for each stress x concentration subgroup (n = 3-4), with individual observations overlaid (unstressed: white points, light-blue bars; stressed: black points, dark-blue bars). The dashed line indicates 50% survival. A two-way ANOVA tested the effects of the acute handling stress and treatment concentration, followed by Tukey's post-hoc test for pairwise comparisons. Different superscripts (a, b) display significant differences between groups (p-value < 0.05).

2.4.2. Technical validation: acute handling stress increases both cortisol and eGFP expression levels in control larvae.

Whole-body cortisol and eGFP relative expression were measured in 7 dpf larvae, both unstressed and stressed, to confirm that eGFP mRNA levels can serve as an alternative to cortisol measurements. In control larvae, whole-body cortisol levels increased significantly following acute handling stress, whereas the vehicle had no significant effect, and there was no significant interaction between factors (Stress: $F_{(1, 68)} = 228.7$, $p < 0.001$; Treatment: $F_{(1, 68)} = 0.011$, $p = 0.918$; Interaction: $F_{(1, 68)} = 0.166$, $p = 0.685$) (Figure 2.4). Baseline cortisol levels (unstressed larvae) were similar between larvae raised in medium-only and those exposed to vehicle control (1.10 ± 0.16 and 1.00 ± 0.07 fold-change, respectively). Similarly, cortisol levels following the acute stressor increased by the same magnitude in medium-only and vehicle-exposed larvae (5.68 ± 0.42 and 5.84 ± 0.42 fold-change, respectively) (Figure 2.4).

Relative eGFP expression levels were similar to whole-body cortisol levels, with no significant effect of the vehicle treatment and a strong, significant effect of the acute stressor (Stress: $F_{(1, 60)} = 264.6$, $p < 0.001$; Treatment: $F_{(1,60)} = 0.47$, $p = 0.496$; Interaction: $F_{(1, 60)} = 0.051$, $p = 0.822$) (Figure 2.4). Basal eGFP expression was low in both the medium-only and vehicle conditions (0.90 ± 0.12 and 1.03 ± 0.09 fold-change, respectively), and stress-induced expression increased by the same order of magnitude in both conditions (5.51 ± 0.42 and 5.77 ± 0.36 fold-change, respectively) (Figure 2.4). Finally, whole-body cortisol and eGFP reporter expression were positively correlated in SR4G larvae under control conditions (Pearson's $r = 0.809$, 95% confidence interval [0.701 – 0.880], $n = 63$ pairs) (Figure 2.4). These results support the use of eGFP mRNA expression as an alternative to cortisol measures in 7 dpf SR4G zebrafish larvae.

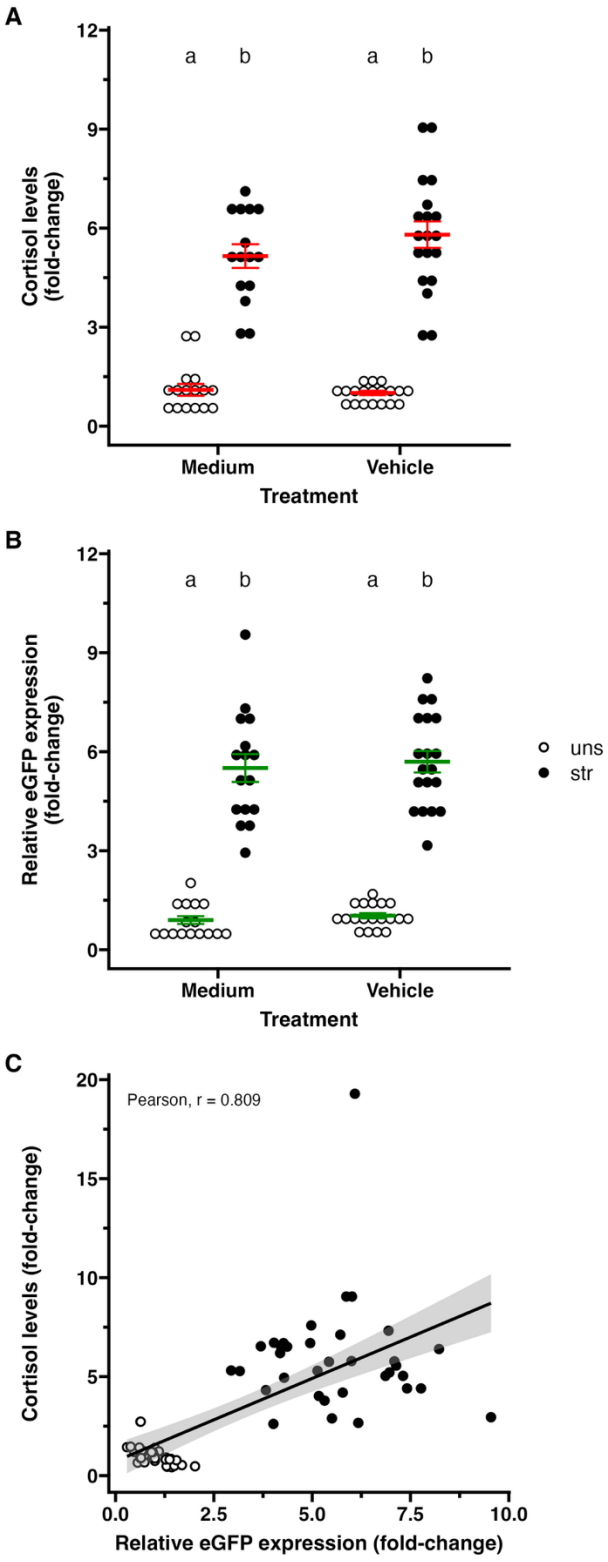

Figure 2.4. Correlation between whole-body cortisol levels and eGFP expression in 7 dpf SR4G larvae in control groups.

Panel (A) shows whole-body cortisol levels (fold-change), panel (B) shows relative eGFP expression levels (fold-change), and panel (C) shows the correlation between whole-body cortisol and relative eGFP expression levels. Medium represents larvae raised in embryo medium only, and vehicle represents larvae raised with 0.02% DMSO. Bars and intervals represent mean ± SEM (n = 16-18 biological replicates; sampling unit = 20 larvae/sample), with individual observations overlaid (unstressed: white points; stressed: black points). Two-way ANOVA tests were used to evaluate the effects of stress and treatment, followed by Tukey's post-hoc tests for pairwise comparisons. Different superscripts (a, b) display significant differences between groups (p-value < 0.05). The correlation between both endpoints was evaluated with the Pearson test.

2.4.3. Overnight exposure to dexamethasone as a positive control for eGFP expression induction in unstressed larvae.

To assess SR4G larval response dynamics to glucocorticoid agonists, we measured eGFP relative expression in unstressed and stressed larvae, following two different exposure scenarios: overnight exposure to 100 nM of either Cortisol (CORT) or Dexamethasone (DEX), or 6 days of exposure to a range of concentrations of each glucocorticoid.

In the overnight exposure scenario, we tested the effect of acute glucocorticoid treatment on eGFP expression in unstressed and stressed larvae separately. In unstressed larvae, we found a significant effect of the treatment ($F_{(2, 9)} = 8.24$, $p = 0.009$). Pairwise comparisons showed that overnight treatment with 100 nM of DEX significantly increased eGFP expression by 2.6-fold compared to vehicle control, while overnight treatment with 100 nM of CORT did not significantly increase basal eGFP expression (1.7-fold compared to vehicle) (Figure 2.5). In stressed larvae, there was no significant difference among the overnight treatments ($F_{(2, 9)} = 1.46$, $p = 0.282$). The relative eGFP expression fold-change in stressed larvae was 6.7 in vehicle, 7.8 in CORT 100 nM, and 8.5 in DEX 100 nM (Figure 2.5).

In the 6-day exposure scenario, we also tested the effect of each glucocorticoid concentration on eGFP expression levels in unstressed and stressed larvae, separately. There was no significant concentration-specific effect of both glucocorticoids on basal eGFP expression (CORT: $F_{(6, 21)} = 0.553$, $p = 0.777$; DEX: $F_{(6, 20)} = 1.06$, $p = 0.417$) (Table 2.2, Supplementary Figure A.1). Similarly, there was no significant effect of glucocorticoid concentrations on stress-induced eGFP relative expression (CORT: $F_{(6, 21)} = 1.84$, $p = 0.140$; DEX: $F_{(6, 20)} = 1.77$, $p = 0.157$) (Table 2.2, Supplementary Figure A.1). These results suggest that sub chronic exposure to 100 nM of glucocorticoid agonists, or less, is not sufficient to induce GRE-driven eGFP expression in 7 dpf SR4G larvae, nor to adversely affect the stress-induced levels, while overnight exposure to 100 nM of Dexamethasone increases basal GRE-driven expression.

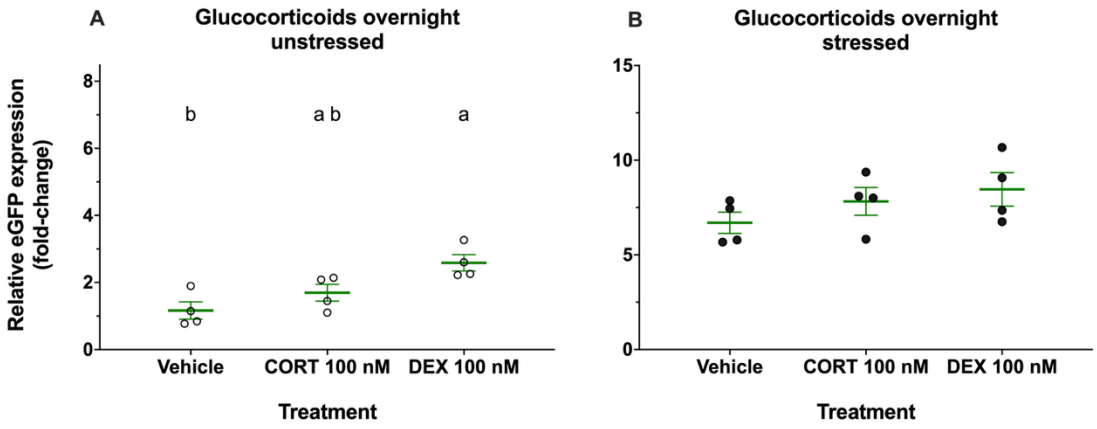

Figure 2.5. Relative eGFP expression fold-change in response to an overnight exposure to glucocorticoids in 7 dpf SR4G larvae.

Panels show results for each stress condition: (A) unstressed larvae, and (B) in stressed larvae. Larvae were raised with vehicle until 6 dpf and were exposed overnight to 100 nM of either hydrocortisone (CORT) or dexamethasone (DEX). Green bars and intervals represent mean ± SEM (n = 4 biological replicates; sampling unit = 20 larvae/sample), with individual observations overlaid (unstressed: white points; stressed: black points). A one-way ANOVA tested the effects of the treatment, followed by Tukey's post-hoc test for pairwise comparisons. Different superscripts (a, b) display significant differences between groups (p-value < 0.05).

Table 2.2. Effects of treatment concentration on eGFP relative expression in unstressed and stressed 7 dpf SR4G larvae.

Treatment	Mean sq. (residuals)	F statistic	df_1, df_2	*p*-value
Unstressed larvae				
Glucocorticoid agonists				
COR	0.104 (0.195)	0.533	6, 21	0.777
DEX	0.335 (0.315)	1.06	6, 20	0.417
SS(N)RIs				
CIT	0.218 (0.136)	1.60	7, 16	0.207
DES	0.076 (0.101)	0.750	7, 14	0.636
ESC	0.068 (0.178)	0.384	7, 16	0.898
FLX	0.113 (0.137)	0.826	7, 16	0.581
NOR	0.392 (0.794)	0.493	7, 16	0.826
SER	17.3 (0.357)	48.4	7, 16	**<0.0001**** [1]**
VEN	0.043 (0.064)	0.672	7, 16	0.693
Stressed larvae				
Glucocorticoid agonists				
COR	2.81 (1.53)	1.84	6, 21	0.140
DEX	5.80 (3.28)	1.77	6, 20	0.157
SS(N)RIs				
CIT	0.900 (3.37)	0.267	7, 16	0.958
DES	1.54 (2.54)	0.607	7, 14	0.741
ESC	0.734 (2.80)	0.262	7, 16	0.960
FLX	2.57 (1.39)	1.84	7, 16	0.147
NOR	2.84 (0.930)	3.06	7, 16	**0.0303***
SER	5.72 (1.94)	2.94	7, 16	**0.0349* [1]**
VEN	0.588 (2.62)	0.225	7, 16	0.974

Results from one-way ANOVA models testing the effect of the concentration within each stress condition (unstressed, or 60 mins after an acute net handling stress). Significant main effects are shown in bold (*$p < 0.05$, ****$p < 0.0001$).

[1] The dataset failed the normality of residuals using the Shapiro-Wilk test but passed the Kolmogorov-Smirnov test.

2.4.4. High sertraline and norfluoxetine concentrations elevate GRE-regulated transcription in stressed larvae.

We exposed developing SR4G larvae to a range of concentrations of several SSRIs, SNRIs, or their metabolites for 6 days. We measured both basal and stress-induced relative eGFP reporter expression to assess the stress axis responsiveness after exposure. In unstressed larvae, SSRI or SNRI treatments did not affect eGFP expression, except for SER ($F_{(7, 16)} = 48.4$, $p < 0.0001$) (Figure 2.6, Table 2.2). Post-hoc Dunnett's test identified a significant 7.6-fold increase in eGFP expression in SER 1000 nM relative to the vehicle control ($p < 0.0001$), while the relative eGFP expression varied between 0.5- and 0.9-fold changes in the other SER concentrations (Figure 2.6). Basal GRE-driven expression was not adversely affected by developmental exposure to SSRIs, SNRIs, or their metabolites at the tested concentrations, except for the SER 1000 nM treatment.

Following the acute stressor, NOR concentration significantly affected relative eGFP expression ($F_{(7, 16)} = 3.06$, $p = 0.0303$), as did SER concentration ($F_{(7, 16)} = 2.94$, $p = 0.0349$) (Figure 2.6, Table 2.2). Post-hoc comparisons showed that the highest concentrations in both treatments were significantly different from their respective vehicle groups (NOR 1000 nM: 8.2-fold vs. 5.3-fold increase in vehicle; SER 1000 nM: 8.2-fold vs. 4.3-fold increase in vehicle) (Figure 2.6). No other significant differences were observed in the stressed larvae exposed to the tested compounds (Figure 2.6, Table 2.2). Overall, stress-induced GRE-driven expression was unchanged following developmental exposure, except at the highest concentrations of NOR and SER, which produced greater eGFP induction than in vehicle controls.

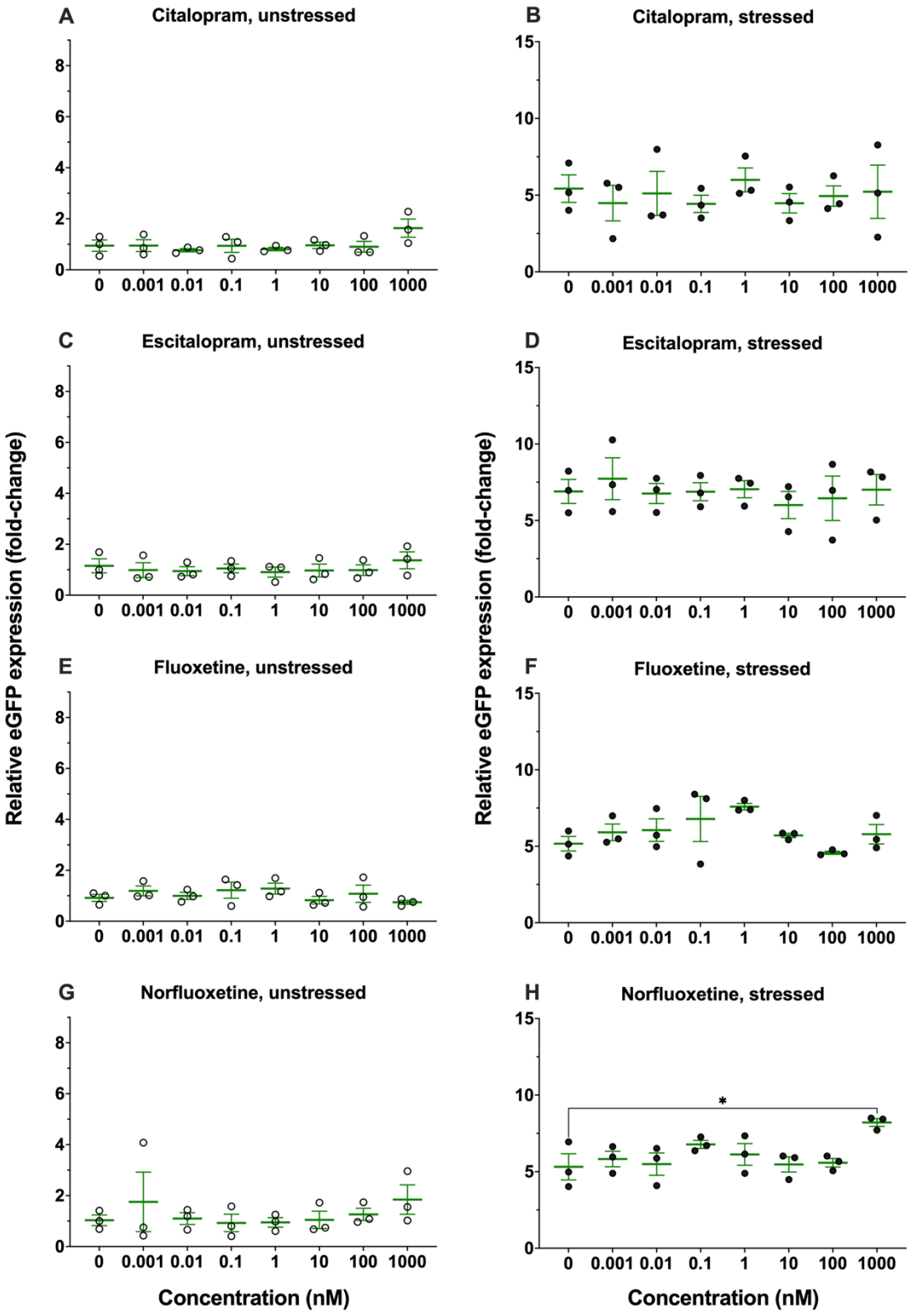
A
Citalopram, unstressed
B
Citalopram, stressed
C
Escitalopram, unstressed
D
Escitalopram, stressed
E
Fluoxetine, unstressed
F
Fluoxetine, stressed
G
Norfluoxetine, unstressed
H
Norfluoxetine, stressed
Relative eGFP expression (fold-change)
Concentration (nM)
0
0.001
0.01
0.1
1
10
100
1000
*

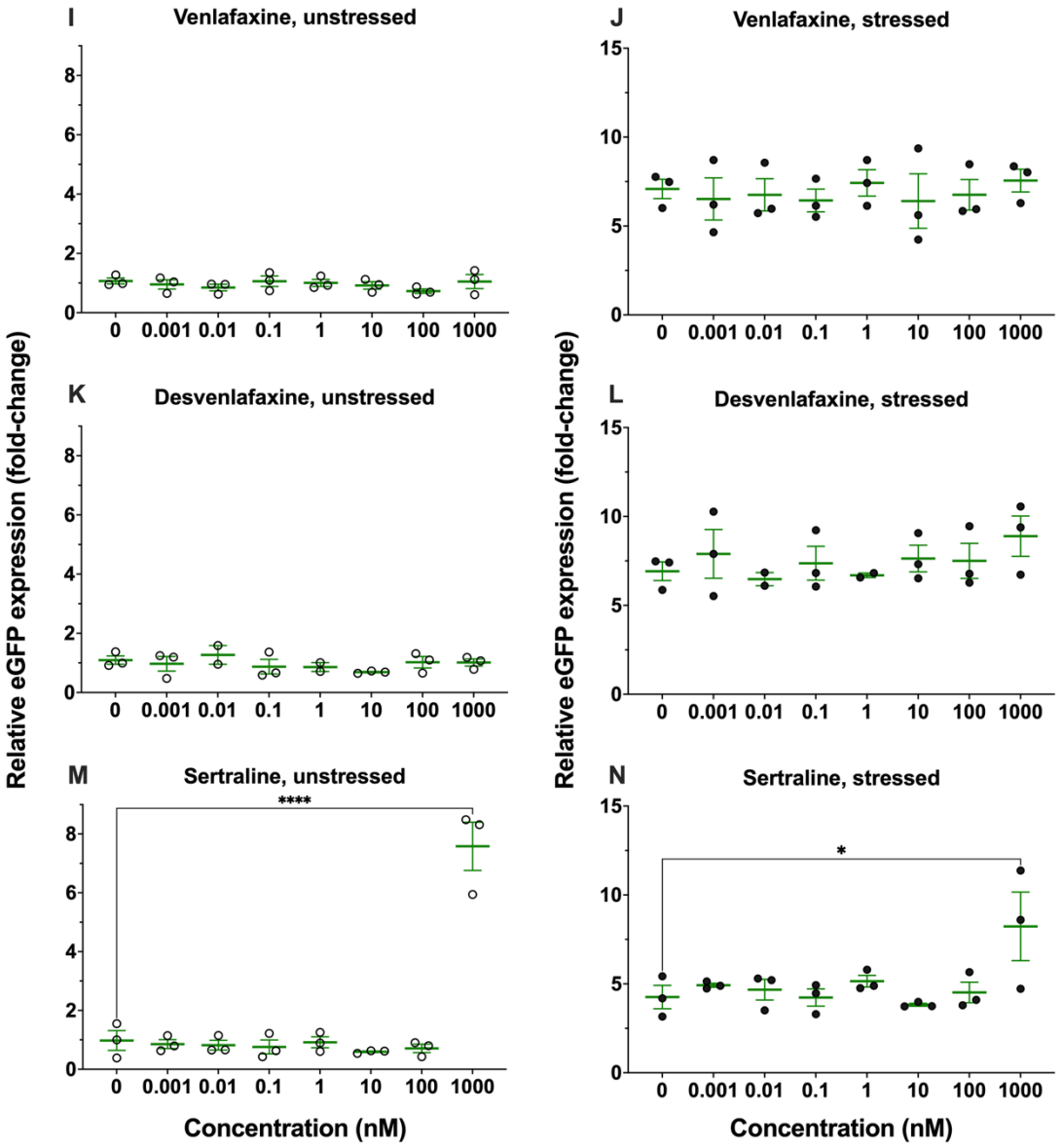

Figure 2.6. Relative eGFP expression fold-change in response to SS(N)RI exposure for 6 days in SR4G larvae.

Panels show results for each compound across rows, with unstressed larvae in the left column and stressed larvae in the right column: Citalopram (A – B), Escitalopram (C – D), Fluoxetine (E – F), Norfluoxetine (G – H), Venlafaxine (I – J), Desvenlafaxine (K – L), and Sertraline (M – N). Green bars and intervals represent mean ± SEM (N = 3 biological replicates; sampling unit = 20 larvae/sample), with individual observations overlaid (unstressed: white points; stressed: black points). One-way ANOVA, followed by Dunnett's post hoc test, were used to identify significant differences relative to the vehicle groups. Significant differences are represented by asterisks (**p*-value$_{adj.}$ < 0.05, ****p*-value$_{adj.}$ < 0.001).

2.4.5. Correlation between whole-body eGFP expression and cortisol levels.

To ensure that eGFP reporter expression remains an accurate surrogate for cortisol following chemical exposure in combination with the handling stressor, we calculated the correlation between whole-body eGFP mRNA expression and cortisol levels for each tested compound. Across all samples, the correlation between these endpoints was positive (Pearson's r = 0.746, 95% confidence interval [0.695 – 0.790], n = 335 pairs). There was no obvious grouping by treatment group (Vehicle, CIT, DES, ECS, FLX, NOR, SER, VEN, but rather by stress condition (unstressed vs. stressed) (Supplementary Figure A.2). Within each treatment group, the correlation between both endpoints was positive (Table 2.3). Correlation coefficients were r > 0.775 in each treatment, except for the ESC-treated larvae (r = 0.573). These results demonstrate consistent concordance between cortisol and eGFP relative expression across treatments.

Table 2.3. Pearson correlation between whole-body cortisol and eGFP expression levels for each treatment.

Treatment	Pearson r	95% confidence interval
Citalopram	0.807	0.679 – 0.888
Escitalopram	0.573	0.345 – 0.737
Fluoxetine	0.889	0.810 – 0.937
Norfluoxetine	0.936	0.887 – 0.965
Venlafaxine	0.815	0.665 – 0.902
Desvenlafaxine	0.806	0.649 – 0.897
Sertraline	0.775	0.634 – 0.867

2.5. Discussion

We characterized the effects of developmental exposure to SSRIs, SNRIs, and their metabolites on the stress axis using the SR4G transgenic zebrafish reporter line. We first established that GRE-regulated eGFP reporter expression closely tracks with whole-body cortisol measurement in response to acute handling stress in 7 dpf larvae. Screening seven SS(N)RI antidepressants or their metabolites revealed no effects on basal GRE-driven transcription, except at the highest Sertraline concentration tested. In contrast, following a standardized handling stress, we observed increased GRE-driven transcription at the highest concentrations of Norfluoxetine and Sertraline.

Our findings provide further evidence that GRE-driven eGFP expression in the SR4G reporter line is sensitive to acute handling stress, with changes comparable in magnitude to those observed in whole-body cortisol levels. In both the untreated and vehicle control groups, we observed a strong positive correlation (Pearson's $r = 0.809$) between these two endpoints. Cortisol and eGFP expression levels were low under basal conditions, but both increased approximately 5-fold following a standardized handling stressor. These results are consistent with a previous study that reported 5-fold and 3-fold increases in cortisol and eGFP mRNA levels, respectively, in DMSO-vehicle groups subjected to the same stressor (Nozari et al., 2021). These findings demonstrate that SR4G zebrafish larvae respond robustly to an acute physical stressor, as well as to acute glucocorticoid treatment, hyperosmotic stress, and circadian rhythm signalling, as previously described (Krug et al., 2014). Quantifying eGFP reporter expression by qPCR provides a higher-throughput alternative to cortisol immunoassays, avoiding issues of cross-reactivity and significant assay variability (El-Farhan et al., 2017; Jensen et al., 2014).

Developmental exposure to SSRIs, SNRIs or their metabolites did not alter basal GRE-driven eGFP expression, except for the highest Sertraline concentration, suggesting that baseline cortisol levels remain unaffected. Consistent with this observation, several studies in adult zebrafish reported no effect of FLX alone on basal cortisol following acute exposure (50 µg/L, < 20 mins), despite altered cortisol responses when combined with stress (Abreu et al., 2014). In contrast, chronic adult exposure to higher concentrations (100

μg/L FLX) has been shown to suppress basal cortisol levels (Egan et al., 2009), indicating a dependence on both dose and exposure duration. Evidence in zebrafish larvae is more limited and inconsistent. Developmental FLX exposure (0.54 and 54 μg/L) reduced basal cortisol levels between 4-6 dpf in AB strain larvae (Vera-Chang, Moon, et al., 2019), whereas 54 μg/L FLX had no effect on basal cortisol or GRE-driven eGFP expression in 6 dpf SR4G larvae (Nozari et al., 2021). By contrast, VEN exposure at 1 μg/L increased basal cortisol in 5 dpf AB larvae (Tang et al., 2021). Our findings support the hypothesis that SS(N)RI exposure does not consistently shift basal cortisol levels, but rather modulates the stress response, underscoring the importance of assessing of both basal and stress-induced states. While basal cortisol levels appear unaffected by developmental SS(N)RI exposure, treatment-stress interactions may reveal a different pattern.

To this end, we examined whether SS(N)RI exposure alters the GRE-driven transcriptional response to acute handling stress. Contrary to our predictions, developmental exposure to SSRIs, SNRIs, or their metabolites did not blunt the stress-induced GRE-driven transcriptional response. Instead, at the highest concentrations of Norfluoxetine and Sertraline, we observed enhanced GRE-driven eGFP expression. These results suggest that the HPI axis remains responsive to the acute stressor across most treatments. This observation contrasts with several studies reporting blunted cortisol responses following FLX exposure in both adult and larval zebrafish. In adults, short-term FLX ranging from 1-50 μg/L attenuated cortisol production following acute stressors such as net chasing, air exposure, and spatial restriction (Abreu et al., 2014, 2015, 2017), while a 7-day exposure to 0.01 mg/L reduced cortisol responses to unpredictable chronic stress (Marcon et al., 2016). Developmental FLX exposure (0.54 and 54 μg/L) similarly blunted cortisol increases following a swirling stress in 6 dpf AB larvae (Vera-Chang, Moon, et al., 2019). In the SR4G reporter line, 6-day exposure to 54 μg/L FLX blunted both cortisol and GRE-driven eGFP expression following netting stress(Nozari et al., 2021). In the present study, we observed a strong correlation between cortisol and eGFP reporter expression across treatments, reinforcing evidence that stress reactivity (cortisol production and mediated transcriptional effects) may not be abolished under challenging conditions.

Discrepancies across studies, whether in basal or stress-induced cortisol, are likely attributable to differences in exposure paradigms, tested concentrations, measurement

methods, and strain-specific sensitivities (Abreu et al., 2021; Maximino et al., 2013). It is also possible that subtle treatment-related effects were masked by the magnitude of the acute stress response in this assay. Indeed, previous studies using this transgenic line reported only a 1.7-fold increase in eGFP expression following a hyperosmotic stress (Krug et al., 2014) and a 3-fold increase in eGFP expression following the same net handling stress (Nozari et al., 2021), while we observed a 5.8- and 5.7-fold increase in cortisol production and eGFP mRNA levels following the net stress. Further research would be needed to explore alternative stress paradigms to capture more nuanced changes in GRE-driven eGFP expression in the line.

Surprisingly, we observed increased GRE-driven reporter expression in stressed larvae exposed to the highest concentration of Norfluoxetine and Sertraline, compared to their respective controls. The stress-induced eGFP expression levels were 1.5- and 1.9-fold higher in larvae treated with 1 μM of Norfluoxetine or Sertraline, respectively, than the response observed in vehicle controls. The mechanisms underlying elevated cortisol levels and GR-mediated transcription following SSRI exposure remain to be investigated. High serotonin may stimulate corticotropin-releasing hormone release and downstream adrenocorticotropic hormone production, as previously described in both mammals and teleost fish (Dinan, 1996; Jørgensen et al., 2002, 2003; Lowry & Lowry, 2002; Winberg & Lepage, 1998). Moreover, a 5-HT_{1A} receptor agonist increases plasma cortisol levels in rainbow trout (Winberg et al., 1997), and cortisol secretion by the interrenal cells is directly stimulated by serotonin in goldfish, via the 5-HT_{1A} and 5-HT_4 receptors, and rainbow trout via the 5-HT_4 receptor (Lim et al., 2013; Tea et al., 2025). Transcriptomic profiling of whole kidneys from male zebrafish developmentally exposed to FLX revealed disruptions in pathways associated with steroidogenesis and cortisol synthesis (Vera-Chang et al., 2018). Together, these findings suggest that the amplified GRE-driven eGFP expression at high Norfluoxetine and Sertraline concentrations is likely driven by upstream serotonergic activation of the HPI axis, or stimulation of cortisol release at the interrenal level.

Sertraline at 1 μM also increased basal GRE-driven transcription by 7.6-fold, a condition associated with 33% mortality. In the stressed groups, mortality increased to 52% following the acute stressor. Although only surviving larvae were sampled in both cases, the magnitude of the basal GRE-driven expression, combined with the high mortality,

suggests that this concentration may induce nonspecific toxicity or cytotoxic stress rather than a physiological endocrine response. This interpretation can be supported by lethality data from other aquatic species, with LC50 (lethal concentration 50%) values for Sertraline of 0.41 and 1.10 µM in 96-hr lethality assays (Minagh et al., 2009; Valenti et al., 2009), placing our highest tested concentration within a range known to cause acute toxicity.

In addition to mortality, we observed behavioural abnormalities in the 1 µM Sertraline treatments, including increased surfacing and reduced locomotion on the day prior to sampling. These behaviours were not quantified systematically but resemble hyperserotonergic phenotypes described in zebrafish larvae induced by 100 µM of the monoamine oxidase inhibitor deprenyl (Sallinen et al., 2009). A hyperserotonergic state and serotonergic overstimulation could contribute to the observed amplified GRE-driven expression. Alternatively, toxicants can activate whole-organism stress pathways, leading to elevated cortisol levels and, consequently, increased GR transcriptional activity (Mommsen et al., 1999; Wendelaar Bonga, 1997). However, because serotonin levels and behavioural endpoints were not quantified in this study, we cannot distinguish between serotonergic overstimulation and nonspecific cytotoxic stress as the driver of the effects observed at the highest Sertraline concentration. More broadly, because our study focused on the expression of a reporter of GR signalling, anchored to cortisol levels, we cannot exclude the possibility that downstream protein abundance, other neurotransmitters and physiological systems were affected and not captured in this targeted approach.

In this study, short-term (6-day) waterborne exposure to SS(N)RIs had minimal effects on GRE-driven transcription and cortisol levels in developing zebrafish, with detectable effects occurring only at the highest concentrations tested. Under the experimental conditions examined here (early-life stage, short-term exposure, and single-compound treatments), these results suggest that environmentally relevant concentrations of SS(N)RIs are unlikely to markedly alter stress-axis responsiveness in zebrafish larvae. Given the conserved organisation of the teleost stress axis, the SR4G zebrafish line offers a conservative screening approach that supports cautious extrapolation of stress-axis responses to other fish species. In this context, reported environmental concentrations generally fall below the effect thresholds observed here, although they vary widely across matrices and geographic regions. The highest levels are typically detected in wastewater

treatment effluents, where concentrations can reach 1930 – 9810 ng/L, whereas maximum concentrations reported in surface freshwater are considerably lower (426 ng/L for CIT, 330 ng/L for FLX, 80.5 ng/L for NOR, and 75 ng/L for SER) (Mole & Brooks, 2019). Correspondingly, mean measured environmental concentrations in surface waters are often in the low ng/L range, as illustrated by measurements in Portuguese rivers (1.87-28.9 ng/L for FLX, 67.9 ng/L for CIT, 5.4 ng/L for SER, 235-641 ng/L for VEN) (Fernandes et al., 2020) or in the Laurentian Great Lakes Basin (18.1 ng/L for FLX, 58.3 ng/L for NOR, 34.3 ng/L for CIT, 27.4 ng/L for SER, 34.2 ng/L for VEN) (Pappas et al., 2025).

However, extrapolation of these findings to fish more broadly is subject to several sources of uncertainty. Species-specific differences in stress physiology, sensitivity across life stages, and the influence of exposure timing and duration may modulate responses to SS(N)RIs (Ferreira et al., 2023; Thompson & Vijayan, 2022). In addition, environmentally realistic exposure scenarios often involve chemical mixtures, rather than single compounds. While individual antidepressants are commonly detected at low ng/L concentrations, summed mixtures in surface water can reach 200-700 ng/L (S. L. Gould et al., 2021), and a recent study in the Laurentian Great Lakes Basin reported a cumulative maximal concentration of 5000 ng/L in 2022 (Pappas et al., 2025). Antidepressant molecules are known to bioconcentrate and bioaccumulate in fish (Duarte et al., 2022, 2023), and mixture studies indicate additive effects, including SSRI-TCA mixtures in zebrafish larvae and TCA mixtures in common carp (Nowakowska et al., 2020; Sehonova et al., 2017; Venkatachalam et al., 2023). Together, these considerations suggest that while short-term exposure to individual SS(N)RIs at environmentally relevant concentrations did not impair basal or stress-induced HPI output in this model, mixture effects, accumulation, and long-term or context-dependent exposures may represent greater ecological risks and warrant further investigation.

2.6. Conclusion

This study demonstrates the utility of the SR4G transgenic zebrafish line as a tool for detecting chemically induced alterations in stress-axis responsiveness during early development. Across a range of SSRIs, SNRIs, and metabolites, environmentally relevant concentrations did not alter basal or stress-induced GRE-driven transcription and cortisol

levels in developing zebrafish larvae under short-term exposure conditions, indicating that typical surface freshwater concentrations are unlikely to impair HPI axis responsiveness in this life stage. Our findings highlight the importance of distinguishing pharmacological modulation at relevant exposure levels from toxicological effects that emerge at supraphysiological concentrations. Better characterization of SS(N)RIs' effective concentrations, species-specific sensitivity, mixture effects and bioaccumulation remains important for ecological risk assessment, as antidepressants co-occur in aquatic environments. Future studies integrating behavioural, metabolic, and transcriptomic endpoints will provide a more comprehensive understanding of how SS(N)RIs influence stress physiology across all levels of biological organization.

2.7. Funding sources and acknowledgements

This research was supported by the Natural Sciences and Engineering Research Council of Canada (Vance L. Trudeau: RGPIN-2021-03174; Carole L. Yauk: RGPIN-2021-02806) and by Health Canada through the Chemicals Management Plan (Errol M. Thomson), with infrastructure funding to Carole L. Yauk from the Canada Foundation for Innovation John Evans Leaders Fund (#233109, #43247) and the Ontario Research Fund (#40569, #43247). Vance L. Trudeau was supported by the University of Ottawa Research Chairs program, and Carole L. Yauk was also supported by the Canada Research Chairs program (CRC-2020-00060). Many thanks to Dr. Naomi Stock at the Trent University Water Quality Centre for analysing the water samples, to Ridoy Uptal for assistance with data collection, and to Alain Filiatreault for technical assistance related to qPCR setup and instrumentation. The authors would also like to thank Drs. Jane Pappas and Jith Thomas for helpful comments during manuscript preparation and the internal review process by Health Canada.

2.8. Declaration on the use of artificial intelligence

During the preparation of this manuscript, the authors used Microsoft 365 Copilot (Microsoft Corporation) to improve clarity, grammar, and overall readability. All content was subsequently reviewed, revised as necessary and approved by the authors. The literature review, study design, data analysis, interpretation and conclusions remain the authors' authentic and original contributions and were not generated with AI tools. The

authors assume full responsibility for the integrity and accuracy of the content of the manuscript.

3. Chapter 3: Developmental exposures to fluoxetine, norfluoxetine, and sertraline cause divergent, stress-dependent transcriptomic responses in zebrafish larvae

3.1. Statement of contributions

Authors: Emmanuelle Monniez[1], John Stead[2], Errol M. Thomson[3, 4], Carole L. Yauk[1], Vance L. Trudeau[1]

Affiliations:

[1] Department of Biology, Faculty of Sciences, University of Ottawa, Ottawa, Canada

[2] Department of Neuroscience, Faculty of Science, Carleton University, Ottawa, Canada

[3] Environmental Health Science and Research Bureau, Healthy Environments and Consumer Safety Branch, Health Canada, Ottawa, Canada

[4] Department of Biochemistry, Microbiology, and Immunology, Faculty of Medicine, University of Ottawa, Ottawa, Canada

Emmanuelle Monniez designed the study, conducted the experiments, prepared the libraries for TempO-seq RNA sequencing, analysed the data and prepared the manuscript. Dr. John Stead helped with the sequencing design and conducted TempO-seq RNA data processing and downstream analyses of differentially expressed genes and gene set enrichment. Dr. Errol Thomson helped with the study design and obtained funding for the research. Dr. Carole L. Yauk and Dr. Vance L. Trudeau obtained funding for the research, helped with the study design, and assisted with manuscript review and editing.

3.2. Introduction

Pharmaceutical compounds contaminate diverse aquatic matrices, including wastewater effluent, surface water, groundwater and drinking water (aus der Beek et al., 2016; Fick et al., 2009; Kostich et al., 2014; Wilkinson et al., 2022). These bioactive contaminants enter aquatic ecosystems primarily due to incomplete municipal wastewater treatment following human consumption and excretion (Patel et al., 2019; Sanusi et al., 2023). Environmental persistence and continuous emissions raise concerns for aquatic organisms, potentially altering hormone-regulated processes and acting as endocrine disruptors (Vaudin et al., 2022). Among these, selective serotonin reuptake inhibitors (SSRIs) are frequently detected in global surface waters at concentrations ranging from nanograms to micrograms per litre (Mole & Brooks, 2019; Silva et al., 2012). SSRI metabolites also pose ecological risks; for example, the active fluoxetine metabolite norfluoxetine retains pharmacological potency and accumulates in teleost tissues at concentrations exceeding those of the parent compound (Arnnok et al., 2017).

Teleost fish are potentially susceptible to SSRI exposure because the primary pharmacological target, the teleost serotonin reuptake transporter (SERT), is evolutionarily conserved (McDonald, 2017; Mennigen et al., 2011). SERT inhibition elevates extracellular serotonin concentrations in the synaptic cleft, which can then drive downstream physiological cascades. Because serotonin modulates multiple physiological axes, SSRI exposure could thus disrupt feeding, locomotion, reproduction, or stress responses in teleosts (McDonald, 2017). For example, environmental SSRI concentrations (ranging from nanograms to low micrograms per litre) alter shelter-seeking behaviour, swimming activity, and predator avoidance (Henry, Bai, Kreuder, Saaristo, et al., 2022; Painter et al., 2009; Valenti et al., 2012), whereas higher, pharmacological concentrations (milligrams per litre) induce acute mortality, morphological deformities, and acetylcholinesterase inhibition (Duarte et al., 2019).

Among the targeted physiological systems, the teleost hypothalamic-pituitary-interrenal (HPI) axis is modulated by serotonergic signalling (Herculano & Maximino, 2014b; Winberg et al., 1997). Brain serotonergic signalling stimulates the release of corticotropin-releasing hormone (CRH), which triggers adrenocorticotropic hormone

(ACTH) secretion and subsequent cortisol production in the interrenal tissue. Developmental exposure to fluoxetine blunts stress-induced cortisol production in zebrafish (Nozari et al., 2021; Vera-Chang et al., 2018; Vera-Chang, Moon, et al., 2019; Vera-Chang, St-Jacques, et al., 2019). This suggests that an external, physiologically relevant stressor may be required to fully unmask SSRI-induced neuroendocrine disruption.

While SSRIs share a primary mechanism of action, they possess divergent secondary pharmacological targets, complicating toxicological predictions. For example, although fluoxetine and citalopram primarily inhibit the SERT, sertraline also acts as a dopamine transporter (DAT) inhibitor and a sigma-1 receptor antagonist (DeVane et al., 2002; Laux, 2022b). These varying receptor and transporter affinities dictate distinct human therapeutic and side-effect profiles (Laux, 2022b), yet their comparative molecular toxicology in non-target teleost species remains poorly characterised. Evaluating independent exposure of multiple SSRIs within a single experimental design is therefore necessary to distinguish class-wide from compound-specific adverse effects and toxicity.

Despite well-documented behavioural and endocrine effects, the molecular responses of teleosts to SSRI exposure remain poorly characterised. Traditional ecotoxicological assessments rely mostly on apical endpoints, leaving underlying molecular perturbations unresolved. High-throughput transcriptomic profiling in the zebrafish (*Danio rerio*) model offers a platform to bridge this gap by identifying molecular targets and perturbed pathways associated with chemical exposure (Bambino & Chu, 2017; Tanguay, 2018). However, comparative studies exploring the effects of multiple SSRIs on gene expression in teleosts remain rare. For example, 96 h exposures to fluoxetine or sertraline induce divergent transcriptional profiles in larval zebrafish, with only five genes differentially regulated by both compounds (Park et al., 2012). This indicates that a shared primary target does not predict a shared molecular response. This highlights the need to move beyond isolated, single-compound experiments and instead conduct parallel, independent assessments of different SSRIs within a unified experimental framework.

To address this gap, we used targeted high-throughput RNA sequencing (TempO-seq, Zebrafish S1500+ panel) to compare the transcriptomic responses of SR4G (Stress

Receptor 4-hour enhanced Green fluorescent protein) transgenic zebrafish larvae exposed to fluoxetine, norfluoxetine or sertraline (0.1 to 1000 nM). Our objectives were to (1) determine whether developmental exposure to these compounds alters transcriptional responses under basal conditions and following a standardized acute netting stress challenge, and (2) identify shared and compound-specific transcriptomic responses to these three SSRIs.

3.3. Material and Methods

3.3.1. Animal care and husbandry

Colony maintenance and experimental procedures were approved by the University of Ottawa Animal Care Protocol Review Committee and comply with the guidelines of the Canadian Council on Animal Care for the use of animals in research. The SR4G zebrafish line (Tg(6xGRE:EGFP,myl7:TagBFP)mn48) (Krug et al., 2014) was housed in the Aquatic Facility of the University of Ottawa and maintained on an automatic flow-through ZebTEC rack system (Tecniplast, Montréal, QC, Canada), with water at 27-29 °C, pH = 7.4-7.5, conductivity 290-300 µS, dissolved oxygen >7 mg/L, and in a 14:10h light/dark photoperiod. Adults were fed a commercial food daily (Gemma Micro 300, Skretting, NB, Canada).

Zebrafish embryos were obtained by breeding adults in 1.7 L sloped breeding tanks (Tecniplast, Montréal, QC, Canada), at a ratio of 3F:2M per breeding tank. Breeding tanks were set up in the late afternoon the day prior, and females and males were separated for the night. The next morning, traps were transferred to tanks with clean facility water, separations were lifted between 09:00 and 09:30 am, and fish were allowed to spawn for an hour. Adults were then returned to the system, and embryos were collected in Petri dishes. Embryos were kept for 24 hours in an incubator set at 28 ± 0.5 °C, and unfertilized and dead embryos were removed. Before starting exposure, the surfaces of viable embryos were sanitised to remove potential pathogens as follows: 10 min in diluted sodium hypochlorite (0.002%), 1 min in a sodium thiosulfate neutralisation solution, and three 2-min rinses in embryo medium (facility water, 0.00003% methylene blue).

3.3.2. Chemicals and solution preparations

Chemicals were purchased from Tocris (Toronto, ON, Canada) and TargetMol (Boston, MA, USA) as powder stocks (Table 3.1). Stock solutions were prepared in DMSO and diluted in 50 mL of embryo medium to obtain exposure solutions at 1000, 100, 10, 1, and 0.1 nM (nominal concentrations; final DMSO vehicle concentration 0.02% in all treatments). New stock solutions were prepared for each experimental replicate.

Table 3.1. List of test compounds.

Compound	Abbrev.	CAS#	Formula	Supplier	Purity[1]
Dexamethasone	DEX	50-02-2	C22H29FO5	Tocris	99.6%
Fluoxetine hydrochloride	FLX	56296-78-7	C17H19ClF3NO	TargetMol	99.98%
Norfluoxetine hydrochloride	NOR	57226-68-3	C16H17ClF3NO	TargetMol	99.71%
Sertraline hydrochloride	SER	79559-97-0	C17H18Cl3N	TargetMol	99.89%

[1] Reported in the supplier's certificate of analysis.

3.3.3. Exposure conditions and experimental design

Each biological replicate consisted of 50 embryos placed in 50 mL of exposure solution in glass Petri dishes, for each "concentration" x "stress" group. Embryos were exposed from 1 to 7 days post-fertilisation (dpf) in an incubator set at 28 ± 0.5 °C, under a 14:10 h light/dark photoperiod, with semi-static renewal of the exposure solutions. Exposures were performed in 3-4 independent biological replicates (separate experimental runs conducted on different spawning days) for each tested compound. Each replicate experiment included medium-only and vehicle controls (DMSO 0.02% v/v). Embryos were checked daily for malformations (oedema, trunk, tail) and survival under a microscope, and dead embryos were removed.

3.3.4. Standardised stress protocol, sample collection and RNA extractions

At 7 dpf, stressed groups underwent a standardised stress protocol as previously described (Nozari et al., 2021). Briefly, larvae were captured using a brine shrimp net, exposed to air for 1 min, given 3 min of rest in the medium, and netted again for another 1 min. Larvae were returned to Petri dishes filled with medium and placed back in the incubator before sampling. Within each experimental replicate, 20 larvae were sampled 60 min after the end of the stress protocol for RNA samples. Unstressed groups were euthanised directly, without undergoing the stress protocol, following the same sampling schedule as the stressed groups. Each pooled sample represented one biological replicate (see Box 3.1 for terminology). Sampling order was randomised for each experimental replicate to avoid sampling-time bias. Euthanasia was conducted in two steps: first, a rapid chilling in 4 °C facility water, then larvae were collected and pooled in a 1.5 mL tube and

kept on ice. Excess medium was removed and replaced with RNA*later* Stabilization Solution (Invitrogen, Thermo Fisher Scientific, Waltham, USA; Cat. No. AM7021). All samples were stored at -80 °C until further analysis.

Total RNA was extracted using the RNeasy Mini kit (Qiagen, Toronto, Canada; Cat. No. 74106) following the manufacturer's protocol. Samples were disrupted in 2 mL pre-filled bead tubes and homogenised using a 4-Place Mini Bead Mill Homogeniser (VWR International, Rendor, PA, USA). Total RNA was quantified with a Qubit 4 Fluorometer (Invitrogen, Thermo Fisher Scientific, Waltham, USA), and the RNA integrity number (RIN) was assessed using an Agilent 4150 TapeStation system (Agilent Technologies, Inc., Santa Clara, CA, USA). All samples included in this study had RIN ≥ 8.0.

3.3.5. TempO-Seq library preparation, sequencing, and data preprocessing

A portion of each RNA sample was diluted to 100 ng/µL for library preparation using the TempO-Seq S1500+Zebrafish Surrogate Assay panel (BioSpyder Technologies, Carlsbad, CA, USA), containing 3183 probes that detect 3112 different genes. Libraries included negative controls (RNA-free water), two reference RNAs (adult zebrafish liver and brain), and all samples. Sample positions across two 96-well plates were randomised to reduce bias in RNA library preparation. Each RNA sample was mixed with an equal volume of 2X Enhanced Lysis Buffer and underwent annealing, digestion, ligation and amplification steps according to BioSpyder's protocols. Following amplification, 5 µL of each sample library were pooled and purified using the NucleoSpin Gel and PCR Cleanup Kits (Macherey-Nagel, Düren, Germany). The purified pooled libraries were sequenced using an Illumina NextSeq 2000 using a P3 flow cell for 100 cycles (Illumina Inc., San Diego, USA).

Count data were generated using the omics data analysis framework for regulatory application (R-ODAF) pipeline available at https://github.com/R-ODAF/R-ODAF_Health_Canada/ (Verheijen et al., 2022). Briefly, sequences within fastq files were trimmed using *fastp* (v0.23.2) and aligned to a reference genome constructed from the 190820 Zebrafish S1500 (v1.0) probe manifest (BioSpyder Technologies, California, USA) using the *STAR aligner* (v2.7.10b), followed by count matrix generation with the

QuasR package (v1.44.0) run in R (v4.5.3). Sample quality assessment was performed following standard metrics of the R-ODAF pipeline: retained samples have a mean Spearman's correlation against all other samples of >0.85, a total of >100,000 aligned reads, >50% reads successfully mapped, and a Gini coefficient <0.95. All 124 samples passed these quality control filters. After preprocessing, principal component analysis (PCA) was used to identify batch effects, revealing a strong effect of the stressor, as well as a batch effect associated with the clutch identifier (nested within plate index) (Supplementary Figure B.2). Batch correction on the clutch identifier variable within each compound dataset was performed using "ComBat_seq" function from the *SVA* R package (Supplementary Figure B.3), and fitted models included clutch ID as a co-factor.

Box 3.1. Terminology.

Batch (clutch identifier): refers to embryos from a same experimental unit (same spawning date), exposed together; RNA extractions were performed for all samples of the same batch at a time.

Sample: biological unit. One sample is composed of 20 pooled larvae.

Sample size: number of samples used in a single group for statistical analysis.

Stress: refers to the stress condition, either unstressed larvae (uns), or stressed larvae sampled 60 min following the acute netting stress (str).

Concentration: refers to the SSRI concentration, vehicle control (c0), 0.1 nM (c1), 1 nM (c2), 10 nM (c3), 100 nM (c4), 1000 nM (c5).

Group: combination of stress and concentration conditions.

3.3.6. Differentially expressed genes and pathway analysis

Differentially expressed genes (DEGs) were identified using the *DESeq2* package (v1.50.2), with Benjamini-Hochberg correction for multiple testing (Love et al., 2014). To assess the effects of SSRI concentration in both stress states, each concentration group was compared to the vehicle group, separately for the unstressed and stressed samples. All DEGs were defined by adjusted p-value ≤ 0.05, and absolute linear fold change ≥ 1.2 following fold-change shrinkage using the *ashr* R package (Stephens, 2017). Gene set enrichment analysis (GSEA) was performed using the *clusterProfiler* R package (v4.18.4) on the Wikipathways database (release date 2023-06-10) (Martens et al., 2021). The DESeq2 test statistic was used as the ranking statistic for GSEA input, and statistically significant pathways were defined by a Benjamini-Hochberg adjusted p-value ≤ 0.05.

3.4. Results

3.4.1. Transcriptomic responses differ among SSRIs in unstressed larvae

3.4.1.1. Magnitude of basal transcriptomic disruption following developmental SSRI exposure

In the unstressed state, fluoxetine (FLX) and its active metabolite norfluoxetine (NOR) elicited limited basal transcriptomic responses across the tested concentration range. Applying an absolute linear fold-change threshold (FC) ≥ 1.2 ($p_{adj.} \leq 0.05$), FLX exposure induced 1 differentially expressed gene (DEG) at 10 nM and 2 DEGs at 1000 nM, with no overlap between concentrations (Figure 3.1). NOR exposure induced a broader response, yielding 14, 10, 2, and 12 DEGs at 1, 10, 100, and 1000 nM, respectively, sharing only 1 to 2 DEGs between concentration contrasts (Figure 3.1). The control dexamethasone (DEX) similarly altered the expression of only 2 genes in unstressed larvae (Supplementary Figure B.1). Sertraline (SER) exposure mirrored this restricted transcriptomic profile at lower concentrations (0.1 to 100 nM yielded 1 to 2 DEGs) but induced widespread transcriptional changes at 1000 nM, yielding 547 DEGs (Figure 3.1, Figure 3.2). DEG overlap across SER concentrations remained minimal (Figure 3.1).

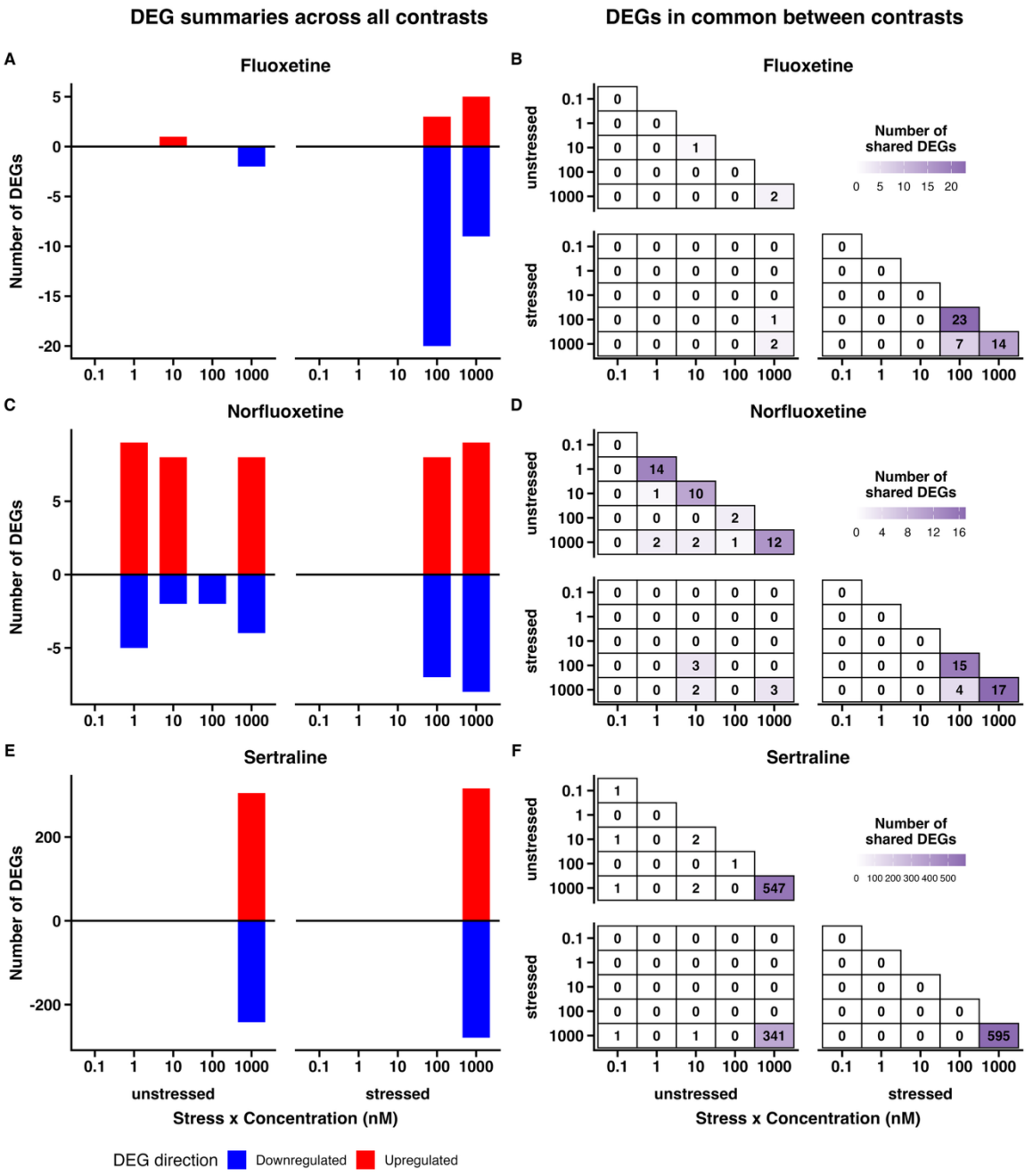

Figure 3.1. Differentially expressed genes (DEGs) summaries and overlaps across contrasts for fluoxetine, norfluoxetine, and sertraline exposure.

For each compound, DEG counts and pairwise DEG overlaps are shown across concentration contrasts relative to the vehicle condition. The left column shows the number of DEGs identified for each concentration, separated by stress condition. Positive bars (red) represent upregulated DEGs and negative bars (blue) represent downregulated DEGs. The right column shows pairwise overlaps between DEG lists from the different contrasts of each compound. Tile values and purple shading indicate the number of shared DEGs. Only the lower triangle of the overlap matrix is displayed to avoid redundant

pairwise comparisons. DEGs were defined using an absolute linear fold-change (FC) ≥ 1.2 and $p_{adj.} \leq 0.05$.

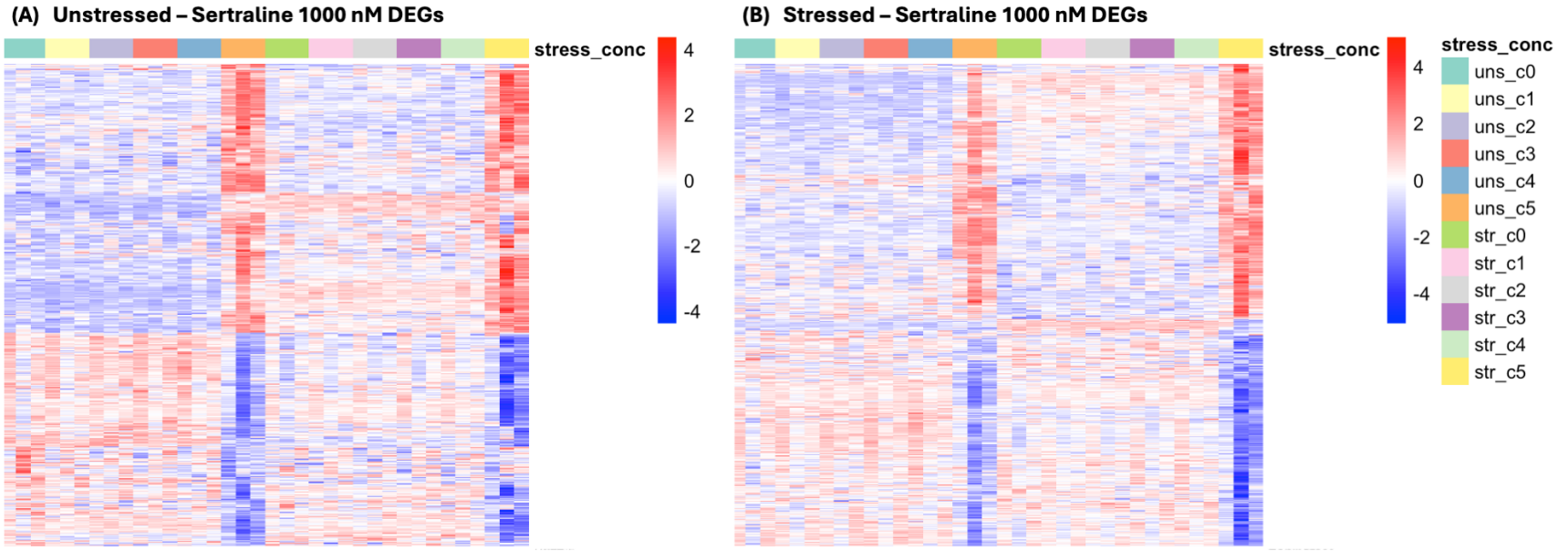

Figure 3.2. Effects of developmental exposure to sertraline on transcriptomic responses in 7 dpf unstressed and stressed SR4G larvae.

Panel (A) depicts the DEGs (differentially expressed genes) identified in the contrast comparing the unstressed larvae exposed to 1000 nM sertraline versus unstressed larvae exposed to the vehicle control. Panel (B) depicts the DEGs identified in the contrast comparing the stressed larvae exposed to 1000 nM sertraline versus stressed larvae exposed to the vehicle control. The transcriptional profiles of these DEGs across all samples is shown. Each heatmap shows the clustering by "stress x concentration" group (stress_conc), with the unstressed samples first, ordered by increasing concentration, followed by the stressed samples, ordered by increasing concentration (uns: unstressed, str: stressed; c0: vehicle, c1: 0.1, c2: 1, c3: 10, c4: 100, c5: 1000 nM). The y-axis consists of all DEGs with an absolute linear fold-change (FC) ≥ 1.2 and $p_{adj.} \leq 0.05$. Red: upregulation, and blue: downregulation.

3.4.1.2. FLX and NOR alter a small number of overlapping transcripts in unstressed larvae

Fluoxetine (FLX) and norfluoxetine (NOR) exposure altered the expression of a limited subset of genes in unstressed larvae, with shared targets varying by concentration (Supplementary Table B.1, Supplementary Table B.2). At 1000 nM, both FLX and NOR downregulated the expression of *agt* (angiotensinogen; FC = -2.0 and -1.5, respectively) (Figure 3.3). Additionally, *prg4b* (proteoglycan 4b) was downregulated by both 1000 nM FLX (FC = -1.5) and 100 nM NOR (FC = -1.4) (Figure 3.3). While FLX exposure induced very limited effects in unstressed larvae (Supplementary Table B.1), NOR exposure dysregulated transcripts associated with structural integrity and endocrine signalling (Supplementary Table B.2). Specifically, at 10 nM, NOR upregulated five collagen-associated genes, including *col1a1a* (FC = 1.8), *col11a1b* (FC = 1.5), and *col2a1b* (FC = 1.5). NOR exposure in unstressed larvae also disrupted glucocorticoid signalling, upregulating the glucocorticoid receptor *nr3c1* at both 10 nM (FC = 2.5) and 1000 nM (FC = 1.9). At 1000 nM, NOR also upregulated the lipid metabolism gene *fabp11b* (fatty acid binding protein 11b; FC = 3.6).

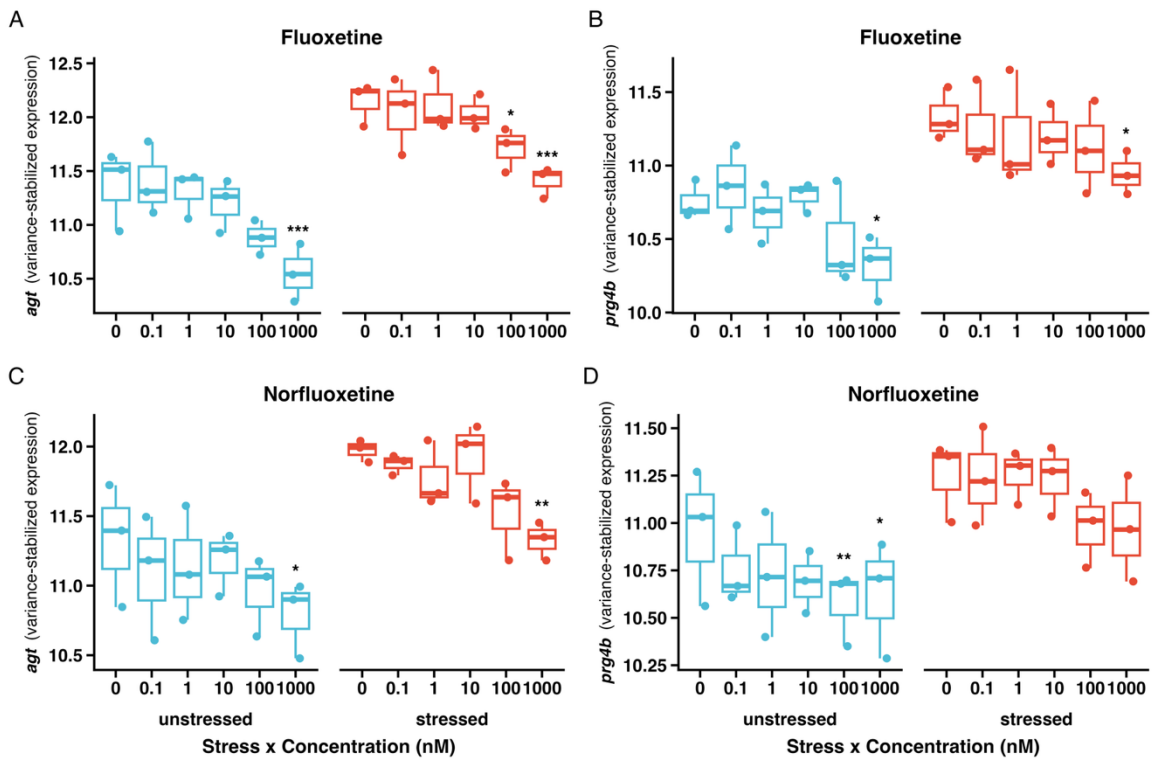

Figure 3.3. Similar effects of fluoxetine and norfluoxetine on the transcription of *agt* and *prg4b*. Panels on the left show *agt* expression, while panels on the right show *prg4b* expression, following fluoxetine (top) or norfluoxetine (bottom). Boxplots show the distribution of variance-stabilized expression values across biological replicates (N = 3 biological replicates; sampling unit = 20 larvae per sample), with individual observations overlaid (unstressed: cyan; stressed: coral). Asterisks indicate significantly differentially expressed genes (DEGs) relative to the corresponding vehicle control (0 nM) within each stress condition (fold-change ≥ 1.2 and adjusted *p*-value < 0.05; * $p_{adj.} < 0.05$, ** $p_{adj.} < 0.01$, *** $p_{adj.} < 0.001$).

3.4.2. Transcriptomic shifts following acute handling stress and SSRI exposure

3.4.2.1. Stress influences the magnitude of transcriptomic disruption

Following the acute handling stress, transcriptomic responses to FLX and NOR were observed exclusively at the two highest exposure concentrations (100 and 1000 nM), whereas SER only induced transcriptomic changes at the highest tested concentration. Stressed larvae exposed to 100 and 1000 nM FLX exhibited 23 and 14 DEGs, respectively, with 7 DEGs shared between these two concentrations (Figure 3.1, Figure 3.4). Similarly, under stress conditions, NOR exposure yielded 15 DEGs at 100 nM and 17 DEGs at 1000 nM, with 4 DEGs shared across these groups (Figure 3.1, Figure 3.5). DEX altered only 2 genes in stressed larvae (Supplementary Figure B.1). In contrast, SER exposure under stressed conditions mirrored the basal profile, inducing 0 to 2 DEGs at 0.1 to 100 nM but driving a pronounced transcriptional shift of 595 DEGs at 1000 nM (Figure 3.1, Figure 3.2). Comparison of the DEG lists from unstressed and stressed larvae exposed to 1000 nM SER revealed 341 common DEGs (Figure 3.1).

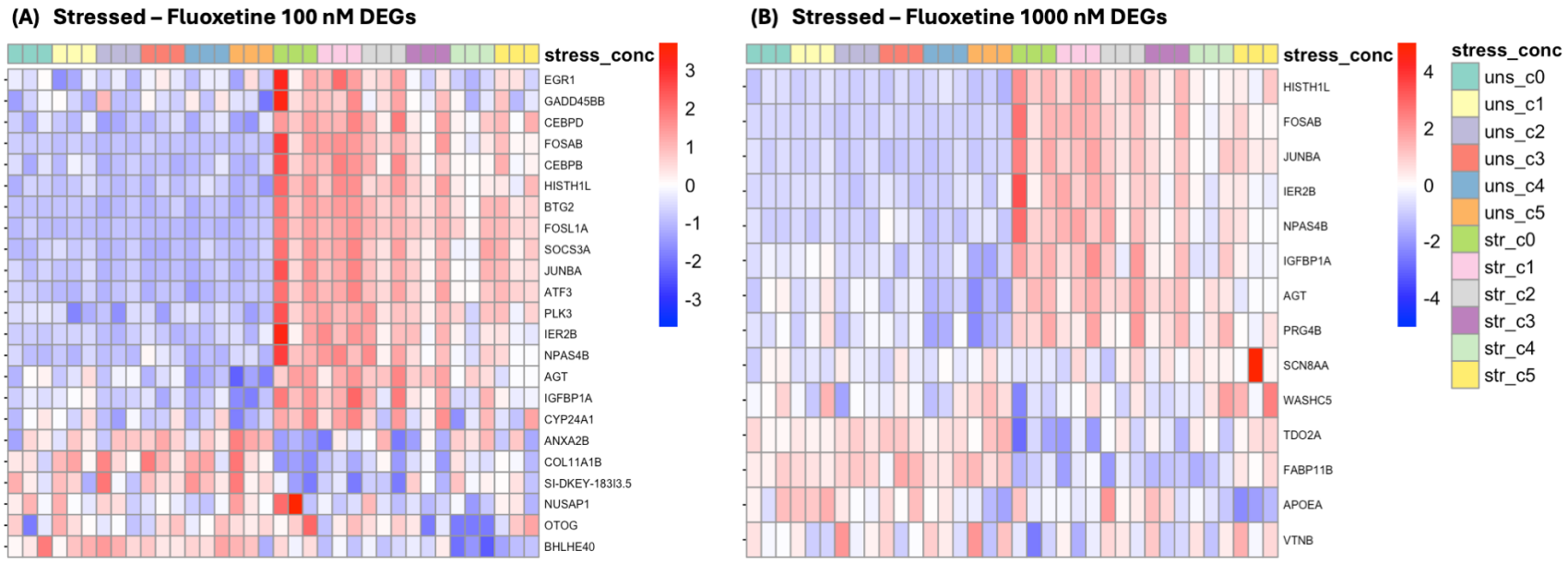

Figure 3.4. Effects of developmental exposure to fluoxetine on transcriptomic responses in 7 dpf unstressed and stressed SR4G larvae.

Panel (A) depicts the DEGs (differentially expressed genes) identified in the contrast comparing the stressed larvae exposed to 100 nM fluoxetine versus stressed larvae exposed to the vehicle control. Panel (B) depicts the DEGs identified in the contrast comparing the stressed larvae exposed to 1000 nM fluoxetine versus stressed larvae exposed to the vehicle control. The transcriptional profiles of these DEGs across all samples is shown. Each heatmap shows the clustering by "stress x concentration" group (stress_conc), with the unstressed samples first, ordered by increasing concentration, followed by the stressed samples, ordered by increasing concentration (uns: unstressed, str: stressed; c0: vehicle, c1: 0.1, c2: 1, c3: 10, c4: 100, c5: 1000 nM). The y-axis consists of all DEGs with an absolute linear fold-change (FC) ≥ 1.2 and $p_{adj.} \leq 0.05$. Red: upregulation, and blue: downregulation.

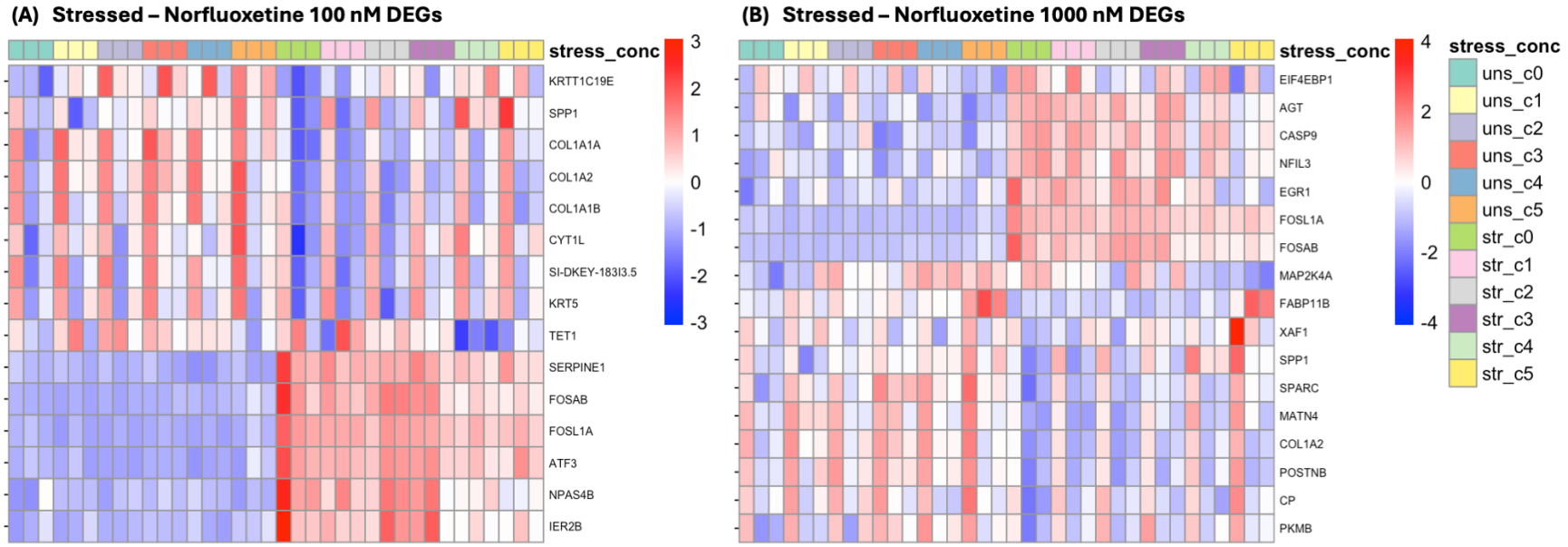

Figure 3.5. Effects of developmental exposure to norfluoxetine on transcriptomic responses in 7 dpf unstressed and stressed SR4G larvae.
Panel (A) depicts the DEGs (differentially expressed genes) identified in the contrast comparing the stressed larvae exposed to 100 nM norfluoxetine versus stressed larvae exposed to the vehicle control. Panel (B) depicts the DEGs identified in the contrast comparing the stressed larvae exposed to 1000 nM norfluoxetine versus stressed larvae exposed to the vehicle control. The transcriptional profiles of these DEGs across all samples is shown. Each heatmap shows the clustering by "stress x concentration" group (stress_conc), with the unstressed samples first, ordered by increasing concentration, followed by the stressed samples, ordered by increasing concentration (uns: unstressed, str: stressed; c0: vehicle, c1: 0.1, c2: 1, c3: 10, c4: 100, c5: 1000 nM). The y-axis consists of all DEGs with an absolute linear fold-change (FC) ≥ 1.2 and $p_{adj.} \leq 0.05$. Red: upregulation, and blue: downregulation.

3.4.2.2. FLX and NOR exposure in stressed larvae alters immediate-early genes and lipid metabolism transcripts

Following acute netting stress, FLX and NOR exposure elicited overlapping transcriptional changes at high concentrations, primarily altering the expression of immediate-early genes and lipid metabolism markers (Supplementary Table B.1, Supplementary Table B.2). Both compounds consistently downregulated the immediate-early gene *fosab* (v-fos FBJ murine osteosarcoma viral oncogene homolog Ab) at 100 and 1000 nM (FLX 100 nM: FC = -5.2; FLX 1000 nM: FC = -3.4; NOR 100 nM: FC = -3.2; NOR 1000 nM: FC = -3.2) (Figure 3.6). Furthermore, exposure to 1000 nM of either FLX or NOR upregulated the transcription of the fatty acid binding protein *fabp11b* (FC = 1.9 and 3.8, respectively) (Figure 3.6).

Beyond these shared targets between the parent and metabolite compound, FLX and NOR both induced specific transcriptional alterations across several concentrations in stressed larvae. FLX downregulated immediate-early and stress-response related genes at both 100 and 1000 nM, including *ier2b* (FC = -2.3 at both concentrations), *junba* (FC = -2.2 and -1.8), and *npas4* (FC = -2.1 and -2.0) (Supplementary Table B.1). Conversely, NOR exposure in stressed larvae at 100 and 1000 nM consistently upregulated *spp1* (secreted phosphoprotein 1; FC = 1.8 and 1.7, respectively) and downregulated additional immediate-early genes such as *fosl1a* (FC = -2.7 and -2.5, respectively) (Supplementary Table B.2).

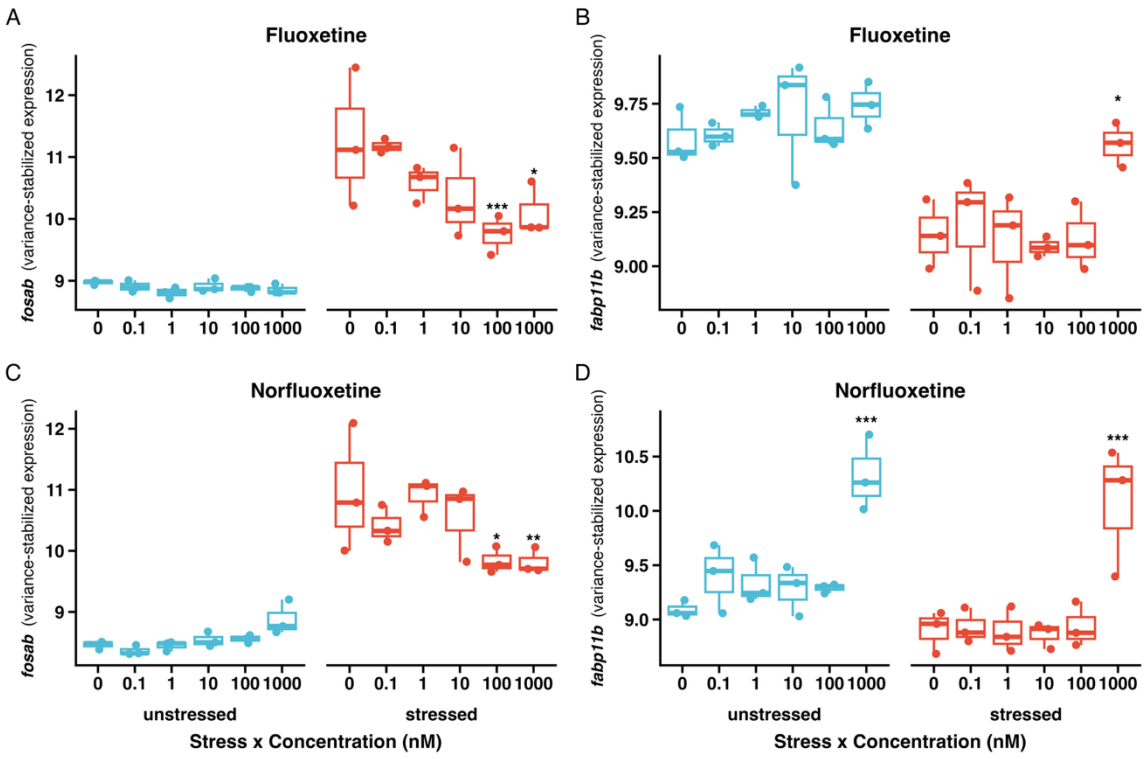

Figure 3.6. Similar effects of fluoxetine and norfluoxetine on the transcription of *fosab* and *fabp11b*.

Panels on the left show *fosab* expression, while panels on the right show *fabp11b* expression, following fluoxetine (top) or norfluoxetine (bottom). Boxplots show the distribution of variance-stabilized expression values across biological replicates (N = 3 biological replicates; sampling unit = 20 larvae per sample), with individual observations overlaid (unstressed: cyan; stressed: coral). Asterisks indicate significantly differentially expressed genes (DEGs) relative to the corresponding vehicle control (0 nM) within each stress condition (fold-change ≥ 1.2 and adjusted *p*-value < 0.05; * $p_{adj.} < 0.05$, ** $p_{adj.} < 0.01$, *** $p_{adj.} < 0.001$).

3.4.2.3. Core targets disrupted by FLX and NOR regardless of the stress status

Several targets were consistently disrupted regardless of the larvae's stress status. FLX and NOR both downregulated *agt* in both unstressed and stressed conditions at high concentration (uns-FLX 1000 nM: FC = -2.0; str-FLX 1000 nM: FC = -1.8; uns-NOR 1000 nM: FC = -1.5; str-NOR 1000 nM: FC = -1.6) (Figure 3.3, Supplementary Table B.1, Supplementary Table B.2). NOR exposure showed a distinct structural and metabolic signature in both unstressed and stressed larvae, upregulating multiple collagen-associated genes (*col1a1a*, *col1a1b*, and *col1a2*, in uns-NOR 10 and str-NOR 100 nM), *sparc* (uns-NOR 10 nM: FC = 1.5; uns-NOR 1000 nM: FC = 1.4; str-NOR 1000 nM: FC = 1.4), and *fabp11b* (uns-NOR 1000 nM: FC = 3.6; str-NOR 1000 nM: FC = 3.8) (Figure 3.6, Supplementary Table B.2).

3.4.3. High-concentration sertraline induces widespread proteotoxicity and divergent stress-responsive targets

3.4.3.1. Divergent and inverse transcriptomic profiles

In contrast to FLX and NOR, exposure to 1000 nM SER produced distinct, and frequently, inverse transcriptional responses (Supplementary Table B.3). In unstressed larvae, 1000 nM SER strongly downregulated the serotonin receptor *htr1b* (FC = -13.1), while upregulating the transcription factors *fosl1a* (FOS-like antigen 1a; FC = 16.9) and *atf3* (activating transcription factor 3; FC = 10.9) (Supplementary Table B.3). Following acute stress, SER elicited an opposite effect on specific immediate-early genes compared to FLX and NOR; while they repressed the transcription of *fosl1a* and *atf3*, 1000 nM SER upregulated both *fosl1a* (FC = 5.9) and *atf3* (FC = 5.7) (Figure 3.7, Supplementary Table B.3).

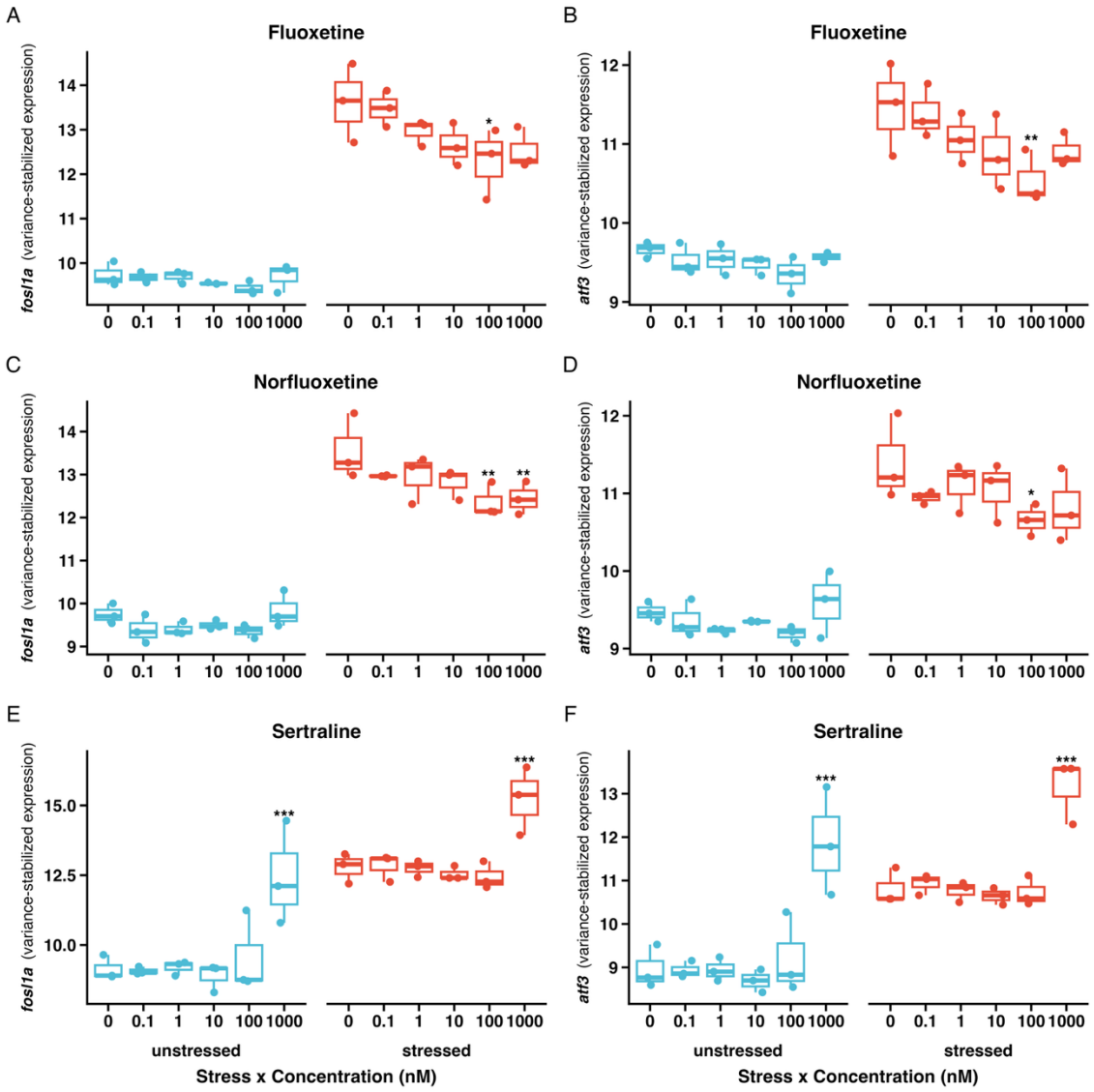

Figure 3.7. Fluoxetine and norfluoxetine repress, whereas sertraline induces *fosl1a* and *atf3* transcription in stressed larvae.

Panels on the left show *fosl1a* expression, while panels on the right show *atf3* expression, following fluoxetine, norfluoxetine or sertraline exposure (top to bottom). Boxplots show the distribution of variance-stabilized expression values across biological replicates (N = 3 biological replicates; sampling unit = 20 larvae per sample), with individual observations overlaid (unstressed: cyan; stressed: coral). Asterisks indicate significantly differentially expressed genes (DEGs) relative to the corresponding vehicle control (0 nM) within each stress condition (fold-change ≥ 1.2 and adjusted p-value < 0.05; * $p_{adj.} < 0.05$, ** $p_{adj.} < 0.01$, *** $p_{adj.} < 0.001$).

3.4.3.2. Widespread proteotoxicity and systemic physiological decline

The massive transcriptional shifts observed in larvae exposed to 1000 nM SER must be contextualised by the severe mortality previously observed at this concentration (Chapter 2). In both stressed and unstressed larvae, 1000 nM SER induced a pronounced cellular stress and protein degradation signature, upregulating 8 DEGs for heat shock proteins (HSP) and 13 proteasome-associated transcripts, including 20S and 26S activator subunits (Supplementary Table B.3). This high concentration also drove a massive suppression of metabolic and structural networks. SER 1000 nM downregulated 18 collagen-related genes (like *col9a1a*, collagen, type IX, alpha 1a; FC = -5.3), 10 cytochrome P450 (CYP450) enzymes, and 15 solute carrier (SLC) transporters across both unstressed and stressed conditions (Supplementary Table B.3). Additional structural targets, such as *mpz* (myelin protein zero; FC = -16.9) and *krt5* (keratin 5; FC = -7.8), were strongly downregulated, alongside upregulation of cellular defence mediators like *timp2b* (metallopeptidase inhibitor; FC = 17.9) and *isg15* (ISG15 ubiquitin-like modifier; FC = 12.6) (Supplementary Table B.3). This widespread induction of protein catabolism coupled with the repression of structural and transport machinery suggests that the transcriptional shift observed at 1000 nM SER is largely driven by systemic proteotoxicity and physiological collapse.

3.4.3.3. Sertraline disrupts specific monoaminergic and corticosteroidogenic regulators

Despite the overarching signature of cellular stress, 1000 nM SER exposure also disrupted specific targets associated with neurotransmitter metabolism and corticosteroid regulation. In unstressed larvae, SER downregulated the monoamine oxidase enzyme *mao* (FC = -2.7) and perturbed glucocorticoid receptor chaperone dynamics, downregulating *fkbp4* (FC = -1.6), while *fkbp5* was upregulated in stressed larvae (FC = 3.9) (Figure 3.8, Supplementary Table B.3). Additionally, 1000 nM SER downregulated the expression of key corticosteroidogenic enzymes, *hsd3b7* (FC = -1.7) at baseline, and the cortisol-inactivating enzyme *hsd11b2* (FC = -2.0) following acute stress (Figure 3.8, Supplementary Table B.3). Finally, SER also upregulated the dopamine β-hydroxylase transcript (*dbh;* FC = 2.3) in stressed larvae, but because this change occurred within a

profile dominated by protein damage and cellular stress responses, it cannot be attributed to a specific effect on catecholamine biosynthesis (Figure 3.8, Supplementary Table B.3).

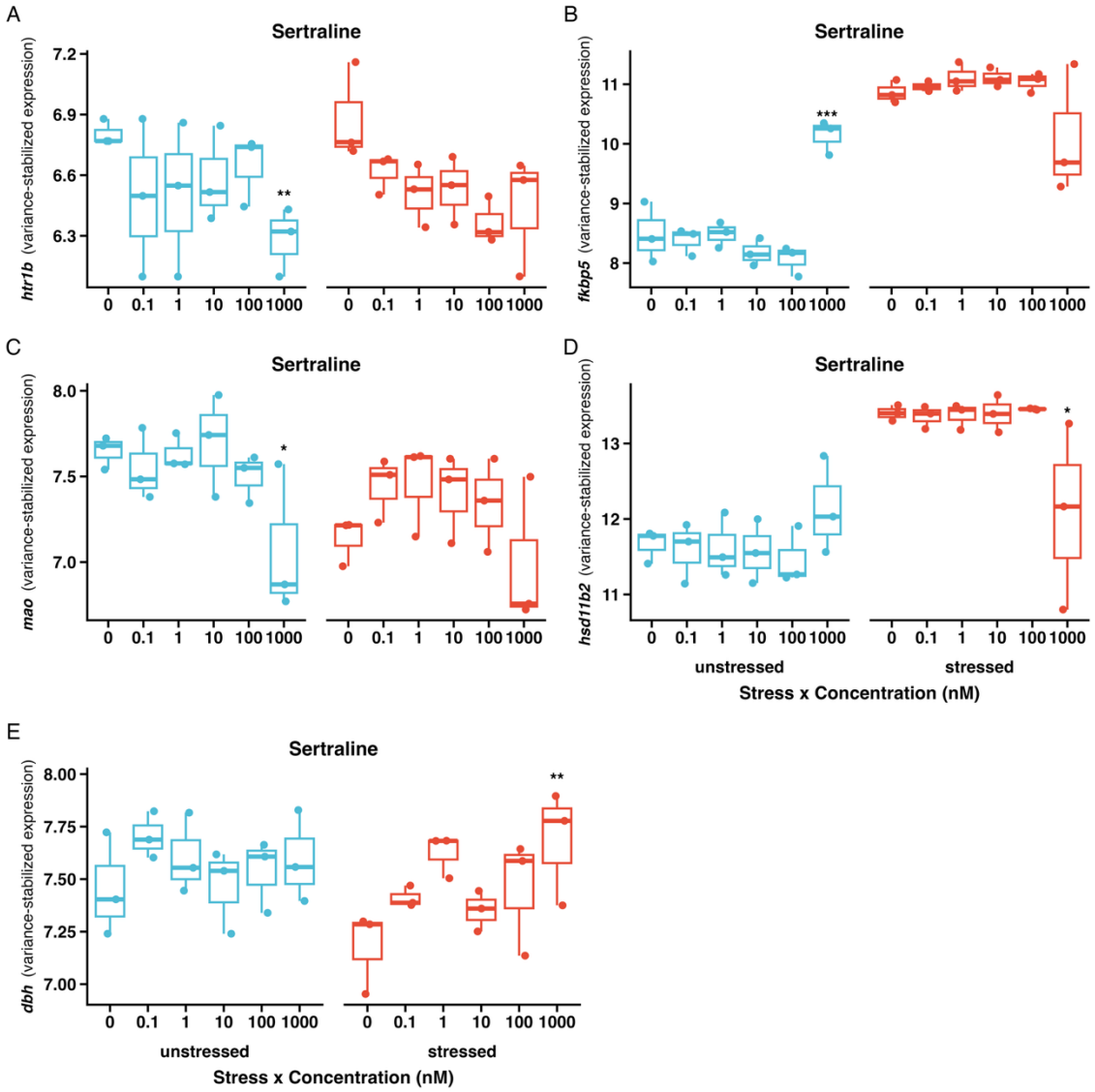

Figure 3.8. Sertraline at high concentration alters transcription of monoaminergic and corticosteroidogenic regulators.

Each panel represents the variance-stabilised expression of a different gene: (A) 5-hydroxytryptamine (serotonin) receptor 1B (*htr1b*), (B) FKBP prolyl isomerase 5 (*fkbp5*), (C) monoamine oxidase (*mao*), (D) 11β-hydroxysteroid dehydrogenase type 2 (*hsd11b2*), (E) dopamine β-hydroxylase (*dbh*). Boxplots show the distribution of variance-stabilised expression values across biological replicates (N = 3 biological replicates; sampling unit = 20 larvae per sample), with individual observations overlaid (unstressed: cyan; stressed: coral). Asterisks indicate significantly differentially expressed genes

(DEGs) relative to the corresponding vehicle control (0 nM) within each stress condition (fold-change ≥ 1.2 and adjusted p-value ≤ 0.05; * $p_{adj.} < 0.05$, ** $p_{adj.} < 0.01$, *** $p_{adj.} < 0.001$).

3.4.4. Pathway analysis

The Gene set enrichment analysis (GSEA) showed distinct concentration effects and divergent pathway enrichment among the compounds. In unstressed larvae, transcriptomic responses were specific to compounds. There were no significantly enriched pathways following NOR exposure (Table 3.2), while the cytoplasmic ribosomal proteins pathway was enriched in unstressed larvae exposed to FLX 1, 10, and 1000 nM (Table 3.2). SER induced broad pathway disruption in unstressed larvae exclusively at 1000 nM (Table 3.2). Immune-related pathways (IL-6 signalling, Toll-like receptor signalling), insulin signalling, hepatocyte growth factor receptor signalling, EGFR1 signalling and mRNA processing were positively enriched, whereas glycolysis and gluconeogenesis, PPAR signalling, nuclear receptors in lipid metabolism and toxicity, neural crest development and cytoplasmic ribosomal proteins were negatively enriched (Table 3.2).

GSEA revealed both shared and compound-specific pathway alterations across FLX, NOR, and SER treatments under stressed conditions. A conserved set of perturbed pathways emerged across FLX, NOR and SER, although the direction of enrichment differed between compounds Specifically, the ERK1/ERK2/MAPK cascade and FGF signalling were perturbed by all three compounds under stress, but at different concentrations and in opposite directions: negatively enriched following FLX (100 nM) and NOR (100 and 1000 nM), and positively enriched following SER (1000 nM) (Table 3.3). Exposure to 1000 nM of any of the three compounds consistently disrupted the pathway associated with cytoplasmic ribosomal proteins following the acute stressor (Table 3.3). The dysregulation of the neural crest development pathway was also shared between FLX and SER at the 1000 nM concentration under stressed conditions (Table 3.3).

In stressed larvae, NOR at 100 nM negatively enriched apoptosis, the TCA cycle, and the FAS pathway and stress induction of HSP regulation (Table 3.3). The last of these was also enriched following SER at 1000 nM, but with a positive score. In contrast, stressed larvae exposed to SER showed a broad disruption profile from 10 to 1000 nM, enriching metabolic and immune pathways, such as glycogen metabolism and Toll-like receptor signalling (Table 3.3), which were not significantly altered in the other treatments.

Table 3.2. Gene set enrichment analysis with WikiPathways, 7 dpf unstressed larvae exposed to fluoxetine, norfluoxetine, or sertraline.

		Fluoxetine				Norfluoxetine				Sertraline			
ID	**Enriched pathway and functions**	**1**	**10**	**100**	**1000**	**1**	**10**	**100**	**1000**	**1**	**10**	**100**	**1000**
WP1331	Adipogenesis	ns	ns	ns	ns	ns	ns	ns	ns	ns	ns	ns	0.55 (1.3^{E-02})
WP324	Cytoplasmic ribosomal proteins	-0.53 (1.1^{E-02})	-0.68 (2.8^{E-06})	ns	-0.75 (8.9^{E-10})	ns	ns	ns	ns	ns	ns	ns	-0.61 (1.1^{E-03})
WP1323	EGFR1 signaling pathway	ns	ns	ns	ns	ns	ns	ns	ns	ns	ns	ns	0.43 (4.8^{E-02})
WP402	ERK1 ERK2 MAPK cascade	ns	ns	ns	ns	ns	ns	ns	ns	ns	ns	ns	0.50 (2.2^{E-02})
WP511	FAS pathway and stress induction of HSP regulation	ns	ns	ns	ns	ns	ns	ns	ns	ns	ns	ns	0.60 (2.5^{E-02})
WP152	FGF signaling pathway	ns	ns	ns	ns	ns	ns	ns	ns	ns	ns	ns	0.53 (2.5^{E-02})
WP1356	Glycolysis and gluconeogenesis	ns	ns	ns	ns	ns	ns	ns	ns	ns	ns	ns	-0.57 (2.5^{E-02})
WP444	Hepatocyte growth factor receptor signaling	ns	ns	ns	ns	ns	ns	ns	ns	ns	ns	ns	0.71 (1.3^{E-02})
WP1322	IL 6 signaling pathway	ns	ns	ns	ns	ns	ns	ns	ns	ns	ns	ns	0.53 (2.1^{E-02})
WP1313	Insulin signaling	ns	ns	ns	ns	ns	ns	ns	ns	ns	ns	ns	0.52 (1.3^{E-02})
WP467	mRNA processing	ns	ns	ns	ns	ns	ns	ns	ns	ns	ns	ns	0.55 (4.8^{E-02})
WP548	Neural crest development	ns	ns	ns	ns	ns	ns	ns	ns	ns	ns	ns	-0.67 (8.1^{E-03})
WP1326	Nuclear receptors in lipid metabolism and toxicity	ns	ns	ns	ns	ns	ns	ns	ns	ns	ns	ns	-0.70 (2.2^{E-02})
WP4020	PPAR signaling pathway	ns	ns	ns	ns	ns	ns	ns	ns	ns	ns	ns	-0.60 (1.3^{E-02})
WP1384	Toll like receptor signaling pathway	ns	ns	ns	ns	ns	ns	ns	ns	ns	ns	ns	0.54 (4.3^{E-02})

Reported values are enrichment scores; a positive enrichment score (red background) indicates predicted activation, whereas a negative enrichment score (blue background) indicates a predicted inactivation of the enriched pathway. Values in parentheses are the associated adjusted *p*-values. Not significant (ns) is indicated when the pathway was not detected in this contrast. Lower concentrations for which no enriched pathways were identified have been removed for readability.

Table 3.3. Gene set enrichment analysis with WikiPathways, 7 dpf stressed larvae exposed to fluoxetine, norfluoxetine, or sertraline.

		Fluoxetine			Norfluoxetine			Sertraline		
ID	**Enriched pathway and functions**	**10**	**100**	**1000**	**10**	**100**	**1000**	**10**	**100**	**1000**
WP1331	Adipogenesis	-0.48 (4.8^{E-02})	-0.60 (7.0^{E-04})	ns	ns	-0.47 (1.8^{E-02})	-0.50 (1.3^{E-02})	ns	ns	ns
WP1351	Apoptosis	ns	ns	ns	ns	-0.52 (8.2^{E-03})	ns	ns	ns	ns
WP324	Cytoplasmic ribosomal proteins	ns	ns	-0.68 (4.0^{E-06})	0.53 (3.5^{E-02})	ns	-0.50 (1.3^{E-02})	0.67 (1.0^{E-06})	0.50 (3.9^{E-02})	-0.69 (6.6^{E-06})
WP1323	EGFR1 signaling pathway	-0.43 (4.8^{E-02})	ns	ns	ns	ns	ns	ns	ns	ns
WP402	ERK1 ERK2 MAPK cascade	ns	-0.52 (2.1^{E-02})	ns	ns	-0.50 (8.2^{E-03})	-0.53 (6.9^{E-03})	ns	ns	0.56 (8.6^{E-03})
WP511	FAS pathway and stress induction of HSP regulation	ns	ns	ns	ns	-0.64 (8.2^{E-03})	ns	ns	ns	0.67 (1.0^{E-02})
WP152	FGF signaling pathway	-0.49 (4.8^{E-02})	-0.55 (2.2^{E-02})	-0.53 (2.8^{E-02})	ns	-0.52 (8.2^{E-03})	-0.53 (9.4^{E-03})	ns	ns	0.58 (1.0^{E-02})
WP1388	Glycogen metabolism	ns	ns	ns	ns	ns	ns	ns	ns	-0.70 (2.2^{E-02})
WP444	Hepatocyte growth factor receptor signaling	-0.69 (4.8^{E-02})	ns	ns	ns	ns	ns	ns	ns	ns
WP1337	MAPK signaling pathway	ns	ns	ns	ns	-0.43 (8.2^{E-03})	ns	ns	ns	0.47 (8.6^{E-03})
WP548	Neural crest development	ns	ns	-0.67 (1.2^{E-02})	ns	ns	ns	ns	ns	-0.69 (7.7^{E-03})
WP1326	Nuclear receptors in lipid metabolism and toxicity	ns	ns	ns	ns	ns	ns	ns	ns	-0.71 (2.2^{E-02})
WP4020	PPAR signaling pathway	0.53 (4.8^{E-02})	ns	ns	ns	ns	ns	ns	ns	-0.61 (2.2^{E-02})
WP19	TCA cycle	ns	ns	ns	ns	-0.73 (8.2^{E-03})	ns	ns	ns	ns
WP1384	Toll like receptor signaling pathway	ns	ns	ns	ns	ns	ns	ns	ns	0.60 (1.1^{E-02})

Reported values are enrichment scores; a positive enrichment score (red background) indicates predicted activation, whereas a negative enrichment score (blue background) indicates a predicted inactivation of the enriched pathway. Values in parentheses are the associated adjusted *p*-values. Not significant

(ns) is indicated when the pathway was not detected in this contrast. Lower concentrations for which no enriched pathways were identified have been removed for readability.

3.5. Discussion

We compared the transcriptomic profiles of larval zebrafish exposed to fluoxetine (FLX), norfluoxetine (NOR) or sertraline (SER) under both basal conditions and following a standardized acute netting stress challenge. Early-life exposure to selective serotonin reuptake inhibitors (SSRIs) alters baseline and stress-induced transcriptional profiles in a compound- and context-dependent manner. NOR and SER elicited divergent transcriptomic responses, yet they share the serotonin reuptake transporter (SERT) as a primary pharmacological target. This divergence suggests that secondary mechanisms of action may drive the variety of physiological outcomes observed following SSRI exposure and cautions against using a single compound to derive class-wide ecotoxicological predictions.

Under basal (unstressed) conditions, FLX and NOR altered the expression of only a few genes. The single pathway reaching significance in these conditions, cytoplasmic ribosomal proteins following FLX exposure, is treated here as uninformative, because ribosomal gene sets recur as apparent false positives in zebrafish embryo datasets with few or no DEGs (Stead et al., 2025). NOR exposure elicited a concentration-dependent upregulation of *nr3c1*, which encodes the primary glucocorticoid receptor that mediates stress-response regulation and is critical for developmental transcription. In an NR3C1-overexpressing neuronal cell model, NR3C1 regulated the alternative splicing of genes involved in inflammatory response linked to the onset of post-traumatic stress disorders (L. Li et al., 2023). In zebrafish, loss-of-function *nr3c1* mutants exhibit elevated basal cortisol levels, reduced immune responses, and abnormal lipid deposition (Facchinello et al., 2017). FLX exposure in adult zebrafish blunts the cortisol response to physical stressors, altering *nr3c1*-mediated downstream signalling (Abreu et al., 2017). *In vitro* experiments with mammalian fibroblast cell models further demonstrate that FLX enhances GR-mediated transcription by inhibiting membrane steroid transporters, leading to intracellular accumulation of steroids like cortisol (Pariante et al., 2003). NOR upregulated *nr3c1* at 10 and 1000 nM in unstressed larvae. This is not readily explained as a compensatory response to disrupted baseline glucocorticoid signalling, because screening with the SR4G reporter detected no disruption of basal GRE-mediated transcription at these

concentrations (Chapter 2). Whether this transcript change has functional consequences for receptor abundance or activity remains to be determined.

Following acute netting stress, exposure to FLX and NOR suppressed the transcription of up to 13 immediate-early genes (IEGs), a category of genes transcribed rapidly and transiently in response to a stimulus, without requiring *de novo* protein synthesis (Morgan & Curran, 1989). FLX downregulated 13 IEGs at 100 nM and 4 at 1000 nM; NOR downregulated 4 IEGs at each concentration. Pooling across both compounds, five core IEGs (*fosab*, *fosl1a*, *ier2b*, *egr1*, and *npas4*) were downregulated. Among these, *fosab* (v-fos FBJ murine osteosarcoma viral oncogene homolog Ab) is a proto-oncogene that regulates central nervous system development and contributes to learning and spatial memory. Zebrafish *fosab* knockouts display reduced brain weight and impaired learning in spatial tasks compared to wild-type counterparts (Q. Wang et al., 2025). This target seems responsive to serotonergic modulation across vertebrates; acute FLX administration induces *c-fos* transcription in the rodent hypothalamus and the amygdala (Torres et al., 1998), while chronic FLX treatment induces FOS-family isoforms expression in the nucleus accumbens, prefrontal cortex, and hippocampus (Vialou et al., 2015). In zebrafish, developmental FLX exposure combined with an acute stressor upregulated *fosb* transcription in larval heads but downregulates it in the adult hypothalamus (Nozari et al., 2022). In rodents, however, FLX induces rather than represses FOS-family transcription (Torres et al., 1998; Vialou et al., 2015). The suppression observed here therefore differs in direction from the mammalian literature and may reflect the combination of developmental exposure with an acute stressor, the whole-body sampling design, or species differences. The downregulation of *fosab* and other IEGs observed here might indicate a maladaptive blunting of the neuronal immediate-early stress response when larvae face simultaneous chemical and physical challenges.

In addition to neurodevelopmental markers, FLX and NOR disrupted pathways governing lipid metabolism and systemic homeostasis under stressed conditions. Both compounds upregulated *fabp11b* (fatty acid binding protein 11b). The *fabp11b* gene regulates cellular lipid transport and early steps of adipogenesis, is induced during adipocyte differentiation in early larval stages, and is actively upregulated by peroxisome proliferator-activated receptors (PPARs) in response to lipid homeostatic changes (Flynn

et al., 2009; Venkatachalam et al., 2012). Recent evidence shows that Fluoxetine binds human FABP1 and alters both its own metabolism and cellular lipid transport (Yabut et al., 2024), whether fluoxetine interacts directly with teleost fabp11b is unknown. FLX and NOR also downregulated *agt* (angiotensinogen) and *prg4b* (proteoglycan 4b) under both basal and stressed states. Angiotensinogen is the precursor in the conserved renin-angiotensin system, which regulates blood pressure and fluid homeostasis. Genetic knockdown of the downstream angiotensin receptor 1 (*agtr1*) protects zebrafish dopaminergic neurons against mitochondrial dysfunction and cell loss (Kim et al., 2021); reduced *agt* transcription may represent a compensatory response that limits dopaminergic damage. The functional consequence of reduced *agt* transcription in whole larvae is unclear and was not assessed here but warrants further investigation. The *prg4b* gene encodes the proteoglycan 4b (or lubricin), a glycoprotein essential for articular joint maintenance, and its knockout produces age-related joint degeneration in zebrafish (Askary et al., 2016). Its downregulation here is consistent with a peripheral structural effect.

In contrast to the limited disruptions caused by FLX and NOR, exposure to 1000 nM SER induced widespread transcriptomic changes, in both unstressed (547 DEGs) and stressed (595 DEGs) states. This response coincided with severe larval morbidity and mortality (Chapter 2.4.1) and presented a generalised cellular stress and protein degradation signature rather than specific neuroendocrine disruption. Specifically, SER strongly upregulated heat shock proteins and proteasomal subunits, while downregulating collagen-associated genes, cytochrome P450 enzymes, and solute carrier transporters. This shift at high concentration toward proteotoxicity signatures and systemic toxicity aligns with transcriptomic points of departure (tPODs) in larval fathead minnows (*Pimephales promelas*), where sublethal FLX concentrations specifically disrupt neurotoxicity pathways, whereas higher concentrations additionally activate broad metabolic and cellular stress pathways (Alcaraz et al., 2022).

The severity of the 1000 nM SER exposure is further highlighted by the activation of tissue damage and regeneration pathways. Specifically, SER upregulated the transcription factors *fosl1a* and *atf3*, which remained unaffected by FLX and NOR in unstressed larvae and were downregulated following acute stress. The *fosl1a* gene mediates early-stage tissue regeneration by controlling dynamic chromatin accessibility and

epigenomic remodelling. Its mutation in zebrafish delays fin regeneration, demonstrating its necessity for normal tissue regrowth following an injury (H. J. Lee et al., 2020). Similarly, *atf3* is a conserved, pro-regenerative transcription factor rapidly induced by physiological stress and nerve injury. It is upregulated during optic nerve regeneration in adult zebrafish (Saul et al., 2010), and its genetic knockdown prevents axon regrowth (Katz et al., 2022). The upregulation of these targets by SER in this context suggests the activation of severe tissue-damage repair mechanisms preceding mortality.

Gene set enrichment analyses indicated that sublethal SSRI exposure modulates specific cellular signalling cascades in response to an acute stressor. At sublethal concentrations, FLX and NOR perturbed the ERK1/ERK2/MAPK cascade and FGF signalling; SER perturbed the same pathways only at 1000 nM, a concentration associated with mortality. In addition, FLX exposure was associated with enrichment of PPAR signalling (10 nM) and negative enrichment of neural crest development (1000 nM), and both FLX and NOR negatively enriched adipogenesis. The perturbation of adipogenesis and PPAR-associated pathways corroborates transcriptomic and proteomic profiles from other teleosts exposed to SSRIs (Colville et al., 2022; Rodrigues et al., 2020), and aligns with previous studies predicting lipid metabolism among the top networks affected by developmental FLX exposure in zebrafish (Nozari et al., 2022). Alterations in the neural crest development pathway align with evidence that serotonergic signalling and downstream effectors, including *rgs2* and *pparδ*, regulate early neural crest cell specification and migration (S.-J. Lin et al., 2017). Although exposure to 1000 nM of any of the three compounds was associated with enrichment of cytoplasmic ribosomal protein genes, this result should be interpreted cautiously because ribosomal gene sets have recently been shown to recur as apparent false positives in zebrafish embryo datasets with few or no DEGs (Stead et al., 2025).

A primary methodological limitation of this study is the use of whole-body, pooled embryo homogenates for RNA sequencing. This approach is likely to dilute localised, tissue-specific transcriptional responses, such as in the central nervous system (CNS) or in specific endocrine glands. Consequently, localised changes in serotonergic pathway genes or stress axis regulators may fall below the detection threshold in whole-body assays, explaining the absence of DEGs directly linked to serotonin synthesis or transport in our

study and in other omics analyses (Alcaraz et al., 2022). Future studies could benefit from spatial transcriptomics or single-cell RNA sequencing approaches to characterise tissue-specific responses. Additionally, using the SR4G transgenic reporter line can allow correlation between eGFP reporter transcript levels and transcriptional profiles in single cells, identifying which cell populations are responsive.

These transcriptional alterations suggest a plausible molecular basis for the apical phenotypes often observed in SSRI-exposed teleosts. The dysregulation of lipid metabolism (*fabp11b* transcription, adipogenesis and PPAR signalling pathways) and structural targets (*prg4b*, collagen-associated genes) is consistent with the reduced growth (H. Chen et al., 2021; de Farias et al., 2020; Nielsen et al., 2018; Ziegler et al., 2020), delayed development (Correia, Bellot, et al., 2023a; de Farias et al., 2019), and morphological deformities (Blahova et al., 2021; Nowakowska et al., 2020) frequently reported following early-life SSRI exposure. Concurrently, the disruption of immediate-early genes and neuronal stress markers provides directions for future research regarding the molecular mechanisms for the behavioural anomalies such as altered locomotor activity (Bachour et al., 2020; Henry, Bai, Kreuder, Mawdsley, et al., 2022; Kazi et al., 2024), blunted stress responses (Abreu et al., 2014, 2017; Vera-Chang et al., 2018; Vera-Chang, Moon, et al., 2019), and impaired predator avoidance (Painter et al., 2009; Saaristo et al., 2017) that characterize typical SSRI-induced behavioural phenotypes in fish.

3.6. Conclusion

Developmental SSRI exposure in larval zebrafish elicits context- and compound-dependent transcriptomic responses. While fluoxetine and norfluoxetine suppressed immediate-early genes and disrupted the transcription of genes involved in lipid homeostasis, specifically following an acute physical stressor, sertraline triggered a distinct proteotoxicity, cellular stress and tissue-damage signature. Consequently, environmental risk assessment for this drug class should not rely on a single “model SSRI”. The divergent profiles observed here suggest that secondary, off-target mechanisms may contribute to *in vivo* toxicity, although the sertraline signature was confined to 1000 nM, a concentration associated with mortality. Furthermore, because transcriptomic effects emerged when exposure was paired with an acute physical stressor, standard testing may underestimate

the disruptive potential of neuroactive pharmaceuticals. Finally, while the observed disruptions to neural pathways, structural tissue maintenance, and metabolic pathways provide mechanistic clues, future research must establish whether these specific transcriptomic alterations translate into the apical effects, such as delayed development, impaired growth, and maladaptive behaviours, frequently observed in SSRI-exposed fish.

3.7. Funding sources and acknowledgements

This research was supported by the Natural Sciences and Engineering Research Council of Canada (Vance L. Trudeau: RGPIN-2021-03174; Carole L. Yauk: RGPIN-2021-02806) and by Health Canada through the Chemicals Management Plan (Errol M. Thomson), with infrastructure funding to Carole L. Yauk from the Canada Foundation for Innovation John Evans Leaders Fund (#233109, #43247) and the Ontario Research Fund (#40569, #43247). Vance L. Trudeau was supported by the University of Ottawa Research Chairs program, and Carole L. Yauk was also supported by the Canada Research Chairs program (CRC-2020-00060).

3.8. Declaration on the use of artificial intelligence

Large language models (Gemini 3.1 Pro and Microsoft 365 Copilot) were used to assist with language editing and sentence structuring. The authors reviewed all suggestions for accuracy and maintained full editorial control over the final output. The AI tools were not used to generate scientific hypotheses, interpret data, or formulate conclusions. The underlying scientific concepts and interpretations originated from the authors. The authors are taking full responsibility for the data and conclusions presented in this study.

4. Chapter 4: Sertraline disrupts photomotor behaviour and glucocorticoid-responsive transcription in transgenic zebrafish larvae.

4.1. Statement of contributions

Authors: Emmanuelle Monniez[1], Shirley Zeng[1], John Stead[2], Errol M. Thomson[3, 4], Carole L. Yauk[1], Vance L. Trudeau[1]

Affiliations:

[1] Department of Biology, Faculty of Sciences, University of Ottawa, Ottawa, Canada

[2] Department of Neuroscience, Faculty of Science, Carleton University, Ottawa, Canada

[3] Environmental Health Science and Research Bureau, Healthy Environments and Consumer Safety Branch, Health Canada, Ottawa, Canada

[4] Department of Biochemistry, Microbiology, and Immunology, Faculty of Medicine, University of Ottawa, Ottawa, Canada

Emmanuelle Monniez designed the study, conducted the experiments, prepared the libraries for TempO-Seq RNA sequencing, analysed the data and prepared the manuscript. Shirley Zeng participated in the experiments and sample processing. Dr. John Stead helped with the sequencing design and conducted TempO-Seq RNA data processing and downstream analyses of differentially expressed genes and gene set enrichment. Dr. Errol Thomson helped with the study design and obtained funding for the research. Dr. Carole L. Yauk and Dr. Vance L. Trudeau obtained funding for the research, helped with the study design, and assisted with manuscript review and editing.

4.2. Introduction

Selective serotonin reuptake inhibitors (SSRIs), including sertraline, are the primary pharmacological treatments for major depressive, anxiety, and obsessive-compulsive disorders (Cipriani et al., 2010; Laux, 2022b). Their mechanism of action involves the inhibition of the presynaptic serotonin reuptake transporter (SERT), which elevates extracellular serotonin (5-HT) levels in the central nervous system (Hiemke & Härtter, 2000). Global antidepressant consumption has continuously increased over the past decade in OECD countries, driven in part by the rising prevalence of affective disorders following the COVID-19 pandemic (OECD, 2025; Peano et al., 2025; WHO, 2022). In the United States, sertraline was among the most prescribed psychiatric medications in 2020 based on the number of prescriptions purchased (Grohol & Wright, 2022). This high prescription volume and subsequent human consumption result in the continuous emission of SSRIs into wastewater systems and aquatic environments (Mole & Brooks, 2019).

Sertraline enters the environment primarily through human excretion, as conventional wastewater treatment plants (WWTPs) are not designed to eliminate these biologically active compounds (Diaz-Camal et al., 2022; Patel et al., 2019). Additional environmental loading occurs via psychiatric hospital effluents, pharmaceutical manufacturing discharges, improper disposal of unused medication, and runoff from sewage sludge application, although these are minor contributions (Castillo-Zacarías et al., 2021). In WWTP effluents, sertraline concentrations typically range from 5 to 100 ng/L (approximately 0.016 – 0.33 nM) but can reach up to 1,930 ng/L in highly impacted municipal locations and 17.1 µg/L in hospital wastewater (Arnnok et al., 2017; Davey et al., 2025; Mole & Brooks, 2019). In surface waters, sertraline concentrations are generally lower, often between 1 and 10 ng/L, but can reach up to 100 ng/L downstream of WWTP discharges in effluent-dominated streams (Conley et al., 2008; Mole & Brooks, 2019; Wu et al., 2023). The continuous discharge and environmental persistence of sertraline raise concerns regarding its biological activity and potential toxicity in non-target aquatic organisms (Silva et al., 2012).

The evolutionary conservation of the SERT renders non-target teleost fish susceptible to SSRI-induced physiological and behavioural disruptions (S. L. Gould et al., 2021; McDonald, 2017). SSRIs can bind to the teleost SERT in multiple fish taxa, providing evidence that sertraline can interact with its intended therapeutic target, with an affinity comparable to mammalian targets, directly inhibiting serotonin reuptake (G. G. Gould et al., 2007; S. L. Gould et al., 2021; Mennigen et al., 2011). At environmentally relevant concentrations, this disruption results in behavioural alterations across multiple teleost models. Specifically, sertraline exposure alters spontaneous swimming and visual-motor responses in larval zebrafish (*Danio rerio*) (Huang et al., 2019), suppresses C-start predator avoidance performance in larval fathead minnows (*Pimephales promelas*) (Painter et al., 2009), decreases swimming activity in Japanese medaka (*Oryzias latipes*) (Chiffre et al., 2016), and reduces shelter-seeking behaviour in adult fathead minnows (Valenti et al., 2012).

Beyond behaviour, early-life exposure to sertraline induces developmental and molecular impairments. Sertraline reduces food consumption and growth in juvenile yellow catfish (*Tachysurus fulvidraco*) (H. Chen et al., 2021) and inhibits feeding rates in fathead minnows (Valenti et al., 2009). Cardiovascular development is also affected by sertraline, altering the expression of genes involved in heart development in zebrafish larvae (Sehonova et al., 2019). At the transcriptomic level, sertraline dysregulates specific pathways associated with neurotransmission, energy metabolism, detoxification, and growth axis regulation, as well as feeding in yellow catfish (H. Chen et al., 2021), and genes linked to the serotonergic system and stress response in zebrafish (Park et al., 2012). These multi-level disruptions occur across several teleost species, although most reported effects arise above measured surface water concentrations. Their consequences for ecological fitness at environmental exposure levels remain undetermined.

One pathway through which such effects may occur is disruption of the teleost hypothalamic-pituitary-interrenal (HPI) axis, which coordinates the physiological and metabolic processes required to maintain homeostasis during adverse conditions (Wendelaar Bonga, 1997). Because this stress axis supports adaptive responses to environmental challenges, contaminant-induced disruption of cortisol or glucocorticoid

signalling can impair individual performance and, ultimately, population-level resilience (McDonald, 2017).

Serotonergic signalling directly regulates the HPI axis; serotonin stimulates corticotropin-releasing hormone release from the hypothalamus, which in turn triggers adrenocorticotropic hormone secretion from the pituitary, stimulating cortisol release from the interrenal tissue (McDonald, 2017). Previous studies demonstrated that developmental exposure to the SSRI fluoxetine disrupts cortisol production and stress-responsive gene expression across multiple generations in zebrafish, establishing that SSRIs can interfere with HPI axis function (Nozari et al., 2021, 2022; Vera-Chang et al., 2018; Vera-Chang, Moon, et al., 2019). While molecular and behavioural data suggest that sertraline similarly alters stress responsiveness, equivalent mechanistic data evaluating sertraline under ecologically relevant stress conditions is lacking.

The SR4G transgenic zebrafish line (Krug et al., 2014) offers a mechanistically anchored model to quantify stress disruption via glucocorticoid receptor-mediated transcriptional activity (Chapter 2) (Nozari et al., 2021). Expanding on established SR4G screening methods, this study integrates developmental, behavioural, and transcriptomic endpoints into a higher-throughput framework to assess stress-response disruption. Specifically, we determined whether developmental sertraline exposure (1) affects larval survival and development, (2) disrupts locomotor behaviour during a light/dark challenge, (3) alters the GRE-driven glucocorticoid reporter gene transcription following the light/dark challenge, and (4) perturbs transcriptional pathways associated with stress response and locomotion.

4.3. Material and Methods

4.3.1. Zebrafish maintenance and husbandry

Zebrafish colony maintenance and experimental procedures were approved by the University of Ottawa Animal Care Protocol Review Committee and comply with guidelines from the Canadian Council on Animal Care for the use of animals in research. The SR4G zebrafish line (Tg(6xGRE:EGFP,myl7:TagBFP)mn48) (Krug et al., 2014) was housed in the Aquatic Facility of the University of Ottawa and maintained on an automatic flow-through ZebTEC rack system (Tecniplast, Montréal, QC, Canada), with water at 27-29 °C, pH = 7.4-7.5, conductivity 290-300 µS, dissolved oxygen >7 mg/L, and in a 14:10h light/dark photoperiod. Adults were fed a commercial food daily (Gemma Micro 300, Skretting, NB, Canada).

Zebrafish embryos were obtained by breeding adults in 1.7 L sloped breeding tanks (Tecniplast, Montréal, QC, Canada), at a ratio of 2F:2M per breeding tank. Breeding tanks were set up in the late afternoon the day prior, and females and males were separated for the night. The next morning, traps were transferred to tanks with clean facility water, separations were lifted between 09:00 and 09:30 am, and fish were allowed to spawn for an hour. Adults were then returned to the system, and embryos were collected. Embryos were kept for 24 hours in an incubator set at 28 ± 0.5 °C, and unfertilized and dead embryos were removed. Before starting exposure, viable embryos were sanitised to remove potential pathogens as follows: 10 mins in diluted sodium hypochlorite (0.002%), 1 min in a sodium thiosulfate neutralisation solution, and 3 rinses for 2 mins in clean facility water.

4.3.2. Chemicals and solutions preparation

Sertraline hydrochloride was purchased from TargetMol as powder stocks (CAS# 79559-97-0, $C_{17}H_{18}Cl_3N$, purity 99.89%). Stock solutions were prepared in DMSO and diluted in 50 mL of facility water to obtain exposure solutions of 10, 50, 100, and 500 nM (nominal concentrations; final DMSO concentration of 0.02% in all treatments). New stock solutions were prepared for each experimental replicate, and exposure solutions were prepared each day before the medium was changed.

4.3.3. Experimental design and exposure conditions

Embryos were exposed from 24 to 120 hours post-fertilisation (hpf) in 96-well plates. For each experimental replicate, there were two identical exposure plates, one being used to measure larval behavioural response in a photomotor assay (stimulated larvae) to assess the combined effects of sertraline and external stimulus, the other one left undisturbed (unstimulated larvae) to assess the effect of sertraline alone (Figure 4.1). Twelve embryos per treatment were seeded in each of the two exposure plates, giving 24 individuals per treatment per experimental replicate (12 unstimulated, 12 stimulated), and six experimental replicates were performed. Embryos (one per well) were individually seeded at 24 hpf after surface sanitation and treated with 200 µL of the exposure solution. Semi-static renewal was performed daily, with half of the exposure solution exchanged (100 µL) until the end of the exposure period. Hatching, mortality and malformations were monitored daily until 120 hpf, and used to calculate hatching rate, cumulative mortality, and the frequency of malformed embryos.

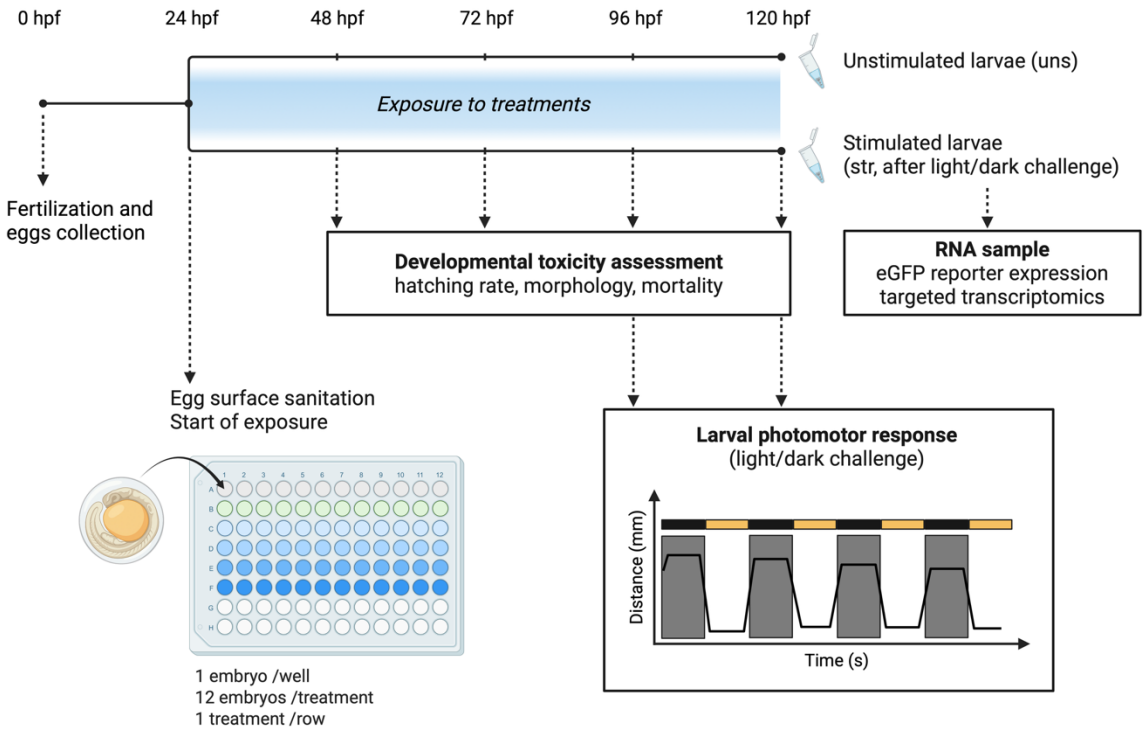

Figure 4.1. Overview of the experimental design.

SR4G transgenic zebrafish embryos were exposed from 24 to 120 hpf (hours post-fertilisation). Each exposure plate contained 1 embryo per well, exposed to medium only (internal control; grey wells), vehicle control (DMSO 0.02%; green wells), or 4 concentrations of sertraline (10, 50, 100, or 500 nM; shades of blue). From 48 to 120 hpf, embryos were assessed for hatching rate, malformations, and mortality. At 96 and 120 hpf, one plate was used to assess larval photomotor response to alternating light/dark cycles of 5 min, and 10 larvae per treatment were sampled 60 min after the light/dark challenge, constituting the stimulated larvae sample. A second exposure plate was raised in the same conditions, and 10 larvae per treatment were directly sampled at 120 hpf, constituting the unstimulated larvae samples.

4.3.4. Larval behaviour analysis

At 96 and 120 hpf, one of the two plates (later referred to as the stimulated plate) was used to measure behaviour using a larval photomotor response (LPR) assay with the ZebraBox video-tracking system (Viewpoint, Montréal, Canada). The movements of larval zebrafish were recorded during a repeated dark-light transition protocol, which included a 20-min acclimatization period under the light, followed by four cycles of 5 min dark and 5 min light. Movements were tracked in 1-min recording bins. For data analysis, dead or malformed larvae and the initial 20 min of acclimatization were excluded. More details on data processing and analysis are provided in section 4.3.5.2.

4.3.5. Data processing and statistical analysis for apical endpoints

4.3.5.1. Developmental endpoints

Hatching success was assessed as a binary response for each embryo (0: not hatched; 1: hatched) at 3, 4, and 5 dpf. The effect of the treatment on hatching success was tested using generalized linear mixed-effects models (GLMMs) with a binomial distribution and logit link function. Separate models were fitted for each time point, so time was not included as a predictor. Treatment was entered as a categorical fixed effect with the vehicle control as the reference level, and experimental replicate as a random intercept. The overall effect of treatment was tested with a Type-II Wald χ^2 test, and treatment-versus-control contrasts were computed from estimated marginal means on the response (probability) scale. Model-predicted probabilities reported in Supplementary Table C.2 are model-based estimates of hatching probability that account for replicate-level variation and unequal numbers of surviving embryos per replicate. Effect sizes are reported on the response scale, statistical inference is based on z-tests, and *p*-values were derived from these comparisons.

Similarly, mortality was recorded as a binary response (0: alive; 1: dead) at the end of the experiment. The effect of the treatment on cumulative mortality was tested with a GLMM with a binomial distribution. Treatment was entered as a categorical fixed effect with the vehicle control as the reference level, and experimental replicate as a random intercept. Overall effect of treatment was tested as described for hatching, and model-

predicted probabilities reported in Supplementary Table C.3 are model-based estimates of mortality probability.

Malformations were recorded as counts per embryo, by category (head, yolk sac, oedema, trunk, tail), and total malformation counts per embryo were calculated. Statistical analysis was performed using a GLMM with a negative binomial distribution, including treatment as a fixed effect and experimental replicate as a random effect. Due to the high proportion of zero counts, a negative binomial model provided a substantially better fit than a Poisson model (ΔAIC = 30.8), indicating overdispersion in the data.

4.3.5.2. Behavioural endpoints

The larval behaviour data at both time points were prepared by excluding the initial 20-min acclimatisation period and summing each variable for the duration of the dark or light phases. We first explored the datasets using principal component analysis (PCA), which indicated that amongst all the variables measured, the total distance moved and inactivity time contributed most to the observed variation. We thus focused on total distance moved and the sum of inactivity time during the dark or light phases per larva. To test the effect of the treatment on both variables, linear mixed-effect models were fitted to log-transformed data, with treatment, dark/light phase, and their interaction as fixed effects, and the animal ID (repeated measures on the same animals between the light and dark phases) and experimental replicate (animals within an experimental replicate are not independent) as random intercepts. Fixed effects were assessed using Type-III Wald χ^2 tests, and pairwise comparisons between treatments within each phase were calculated with the Holm adjustment to control for family-wise error rates. The estimated marginal means were back-transformed to the original scale for visualisation and interpretation.

4.3.6. Sample collection and preparation for gene expression analysis

At 120 hpf, larvae were euthanised by rapid chilling in 4 °C facility water, with samples maintained on ice to sustain the cold temperature until euthanasia was complete. 10 larvae per treatment were randomly selected and pooled into a 1.5 mL microtube, constituting one biological sample (Box 4.1). The cold water was replaced with RNA*later* Stabilization Solution (Invitrogen, Thermo Fisher Scientific, Waltham, USA; Cat. No. AM7021), and samples were stored at -80°C until extraction. Within each experimental

replicate, sample processing order was randomized. Total RNA was extracted using the RNeasy Mini kit (Qiagen, Toronto, Canada; Cat. No. 74106) following the manufacturer's protocol. Samples were disrupted in 2 mL pre-filled bead tubes and homogenized using a 4-Place Mini Bead Mill Homogenizer (VWR International, Rendor, PA, USA). Total RNA was quantified with a Qubit 4 Fluorometer (Invitrogen, Thermo Fisher Scientific, Waltham, USA), and the RNA integrity number (RIN) was assessed using an Agilent 4150 TapeStation system (Agilent Technologies, Inc., Santa Clara, CA, USA). All samples included in this study had RIN ≥ 9.0.

4.3.7. RT-qPCR analysis of eGFP reporter expression

For each sample, 500 ng of isolated total RNA was converted to cDNA using the QuantiTect® Reverse Transcription kit with gDNA elimination (Qiagen, Toronto, Canada; Cat. No. 205311). Forward and reverse primer sequences for *d4egfp* (eGFP, enhanced green fluorescent protein) and *eef1a1l1* (eukaryotic translation elongation factor 1 alpha 1, like 1; reference gene) were adopted from previously established sequences (Krug et al., 2014; Nozari et al., 2021) (Supplementary Table C.1). Real-time quantitative polymerase chain reaction (qPCR) was performed using the PowerUp™ SYBR™ Green Master Mix (Applied Biosystems, Thermo Fisher Scientific, Waltham, USA; Cat. No. A25742), with 10 ng of cDNA and 400 nM of each primer in a 10 µL reaction volume. Reactions were performed in technical duplicates in a spectrofluorometric thermal cycler following standard cycling parameters. Melt-curve analysis verified amplicon specificity and the absence of primer dimers. Negative "no reverse transcriptase" and "no template" controls were included on each plate.

The relative expression fold-change of the eGFP reporter was calculated using the $\Delta\Delta C_T$ method (Livak & Schmittgen, 2001) and the "tidyqpcr" R package (https://github.com/ewallace/tidyqpcr) (Wallace & Haynes, 2022), with the vehicle-unstimulated samples serving as the reference group. Raw C_T values for *eef1a1l1* averaged 17.1 ± 0.22 (mean ± standard deviation, n = 60 samples total), with mean C_T values in concentration and light/dark challenge groups differing by at most 0.4 cycles, supporting its use for normalisation. A two-way analysis of variance (ANOVA) was used to test the effects of sertraline concentration, light/dark challenge and their interaction. Pairwise

comparisons were carried out using Tukey's post-hoc test. Normality and homoscedasticity assumptions were assessed using the Shapiro-Wilk and Levene tests. For all analyses, the significance level was set at $p < 0.05$.

4.3.8. TempO-Seq library preparation, sequencing, and data preprocessing

A portion of each RNA sample was diluted to 100 ng/µL for library preparation using the TempO-Seq S1500+ Zebrafish Surrogate Assay Panel (BioSpyder Technologies, California, USA). Libraries included negative controls (RNA-free water), two reference RNAs (adult zebrafish liver and brain), and all samples. Sample positions across two 96-well plates were randomized to reduce bias in RNA library preparation. Each RNA sample was mixed with an equal volume of 2X Enhanced Lysis Buffer and underwent annealing, digestion, ligation and amplification steps according to BioSpyder's protocols. Following amplification, 5 µL of each sample library were pooled and purified using the NucleoSpin Gel and PCR Cleanup Kits (Macherey-Nagel, Düren, Germany). The purified pooled libraries were sequenced using an Illumina NextSeq 2000 using a P3 flow cell for 100 cycles (Illumina Inc., San Diego, USA).

Count data were generated using the omics data analysis framework for regulatory application (R-ODAF) pipeline (Verheijen et al., 2022), available at https://github.com/R-ODAF/R-ODAF_Health_Canada/. Briefly, sequences within fastq sequence files were trimmed using fastp v0.23.2 and aligned to a reference genome constructed from the 190820 Zebrafish S1500 (v1.0) probe manifest (BioSpyder Technologies, California, USA) using the *STAR* aligner (v2.7.10b), followed by count matrix generation with the *QuasR* package (v1.44.0) run in R (v4.4.1). Sample quality assessment was performed following standard metrics of the R-ODAF pipeline: each sample displays a mean Spearman's correlation against all other samples of >0.85, a total of >100,000 aligned reads, >50% reads successfully mapped, and a Gini coefficient <0.95. All 60 samples passed these quality control filters. After preprocessing, PCA was used to identify batch effects, revealing strong effects of the sequencing plate index and stimulus, as well as a batch effect associated with clutch ID (nested within plate index); thus, fitted models included clutch ID as a co-factor (Supplementary Figure C.1). Additionally, two samples

were identified as outliers after batch correction and were removed from downstream analysis (Supplementary Figure C.2).

Box 4.1. Terminology.

Batch: refers to embryos from a same experimental unit (same spawning date), exposed together, and RNA extractions were performed for all samples of the same batch at a time.
Sample: biological unit. One sample is composed of 10 pooled larvae.
Sample size: number of samples used in a single group for statistical analysis.
Stimulus: refers to the stress condition, either unstimulated larvae (uns), or stressed/stimulated larvae 60 min following the light/dark challenge (str).
Concentration: refers to the sertraline concentration, vehicle control (c0), 10 nM (c1), 50 nM (c2), 100 nM (c3), 500 nM (c4).
Group: combination of stimulus and concentration conditions.

4.3.9. Differentially expressed genes and pathway analysis

Differentially expressed genes (DEGs) were analysed using the *DESeq2* package, with Benjamini-Hochberg correction for multiple testing (Love et al., 2014). To determine the effect of the light/dark stimulus on gene expression, two approaches were used. First, a model testing the overall effect of the stimulus (stress in the models) using all samples combined (model design = ~clutch_id + concentration + stress) allowed us to compare unstimulated (uns) to stimulated (str) samples, and the concentration factor was used as an additional blocking factor (Figure 4.2.A). Second, a model testing the effect of the stimulus independently at each concentration (model design = ~clutch_id + group) allowed us to compare unstimulated to stimulated samples within each of the 5 concentration groups (c0: vehicle; c1: 10 nM; c2: 50 nM; c3: 100 nM; c4: 500 nM) (Figure 4.2.B). To assess the effects of sertraline concentration in both stress states, each concentration group was compared to the vehicle group, separately for the unstimulated and stimulated samples (Figure 4.2.C). All DEGs were defined by adjusted p-value ≤ 0.05, and absolute linear fold change ≥ 1.2. Fold-change shrinkage using the *ashr* R package (Stephens, 2017) was applied to the stimulus-effect contrasts (Figure 4.2.A and B), and sertraline concentration contrasts (Figure 4.2.C) are reported without fold-change shrinkage and without a fold-change threshold. Pathway enrichment analysis was run when there were enough DEGs ($\geq$ 5) using over-representation analyses (ORA) on the Gene Ontology Biological Processes

(GO-BP), Molecular Function (GO-MF), and Cellular Component (GO-CC) databases (release date 2023-06-11) (Ashburner et al., 2000). Statistically significant pathways were defined by a threshold of Benjamini-Hochberg adjusted $p \leq 0.05$.

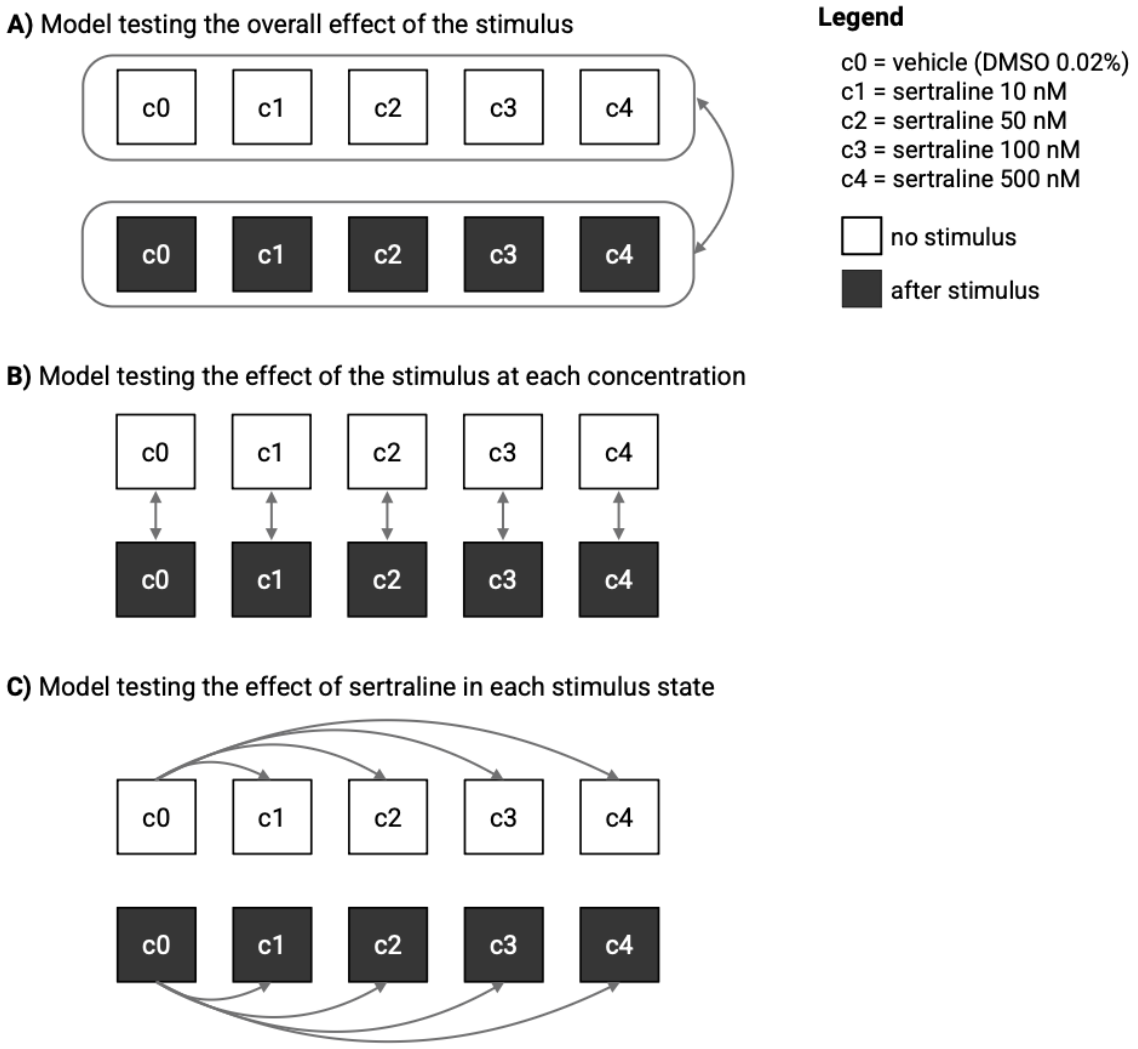

Figure 4.2. Schematic representation of the different comparisons performed for the differentially expressed genes analysis.

4.4. Results

4.4.1. Developmental effects

Sertraline exposure did not significantly alter hatching success at 3, 4, and 5 dpf, or survival at the end of exposures. Hatching success was high across all treatments and time points (3 dpf: 89.6 – 91.7%; 4 dpf: 97.9 – 100%; 5 dpf: 97.9 – 100%; Table 4.1), and did not differ between sertraline treatments and the vehicle control at any time point (GLMM, binomial, effect of treatment: 3 dpf $\chi^2_5 = 0.51$, $p = 0.99$; 4 dpf $\chi^2_5 = 2.03$, $p = 0.84$; 5 dpf $\chi^2_5 = 1.69$, $p = 0.89$). Cumulative mortality at 5 dpf was low across treatments (0.7 – 4.2%; Table 4.1), with no significant effect of treatment (GLMM, binomial $\chi^2_5 = 6.99$, $p = 0.22$). The malformations observed in 5 dpf larvae were rare across treatments, with only occasional low counts (≤ 3 malformations per embryo; 855 out of 864 observations were null; mean counts ranging from 0.00 ± 0.00 to 0.04 ± 0.03; Supplementary Table C.4). There was no significant effect of treatment on total malformation counts (GLMM, negative binomial: Wald $\chi^2_5 = 1.73$, $p = 0.88$).

Table 4.1. Effects of sertraline concentration on hatching success and mortality in larval SR4G zebrafish.

	Sertraline concentration (nM)				
	0 (vehicle)	**10**	**50**	**100**	**500**
Hatching success (%)					
3 dpf	91.0 ± 2.4	90.3 ± 2.5	91.7 ± 2.3	91.0 ± 2.4	89.6 ± 2.6
4 dpf	99.3 ± 0.7	100.0 ± 0.0	97.9 ± 1.2	97.9 ± 1.2	99.3 ± 0.7
5 dpf	100.0 ± 0.0	100.0 ± 0.0	97.9 ± 1.2	98.6 ± 1.0	99.3 ± 0.7
Cumulative mortality (%)					
5 dpf	4.2 ± 1.7	0.7 ± 0.7	3.5 ± 1.5	1.4 ± 1.0	1.4 ± 1.0

Hatching success (%) and cumulative mortality (%) of larvae exposed to sertraline from 24 hours post-fertilization to 5 days post-fertilization (dpf). Results are reported as mean ± SEM (N = 6 experimental replicates; n = 24 individuals per replicate).

4.4.2. Larval photomotor response (LPR)

At 4 dpf, larvae exhibited the characteristic photomotor response, with increased locomotion during dark phases relative to light phases (Figure 4.3A). The total distance moved was significantly affected by sertraline concentration, phase of the assay (light/dark), and their interaction (LMM: treatment $\chi^2_4 = 54.58$, $p < 0.0001$; light phase $\chi^2_1 = 87.74$, $p < 0.0001$; interaction $\chi^2_4 = 17.50$, $p = 0.0016$). The mean total distance travelled in the dark decreased from 1865 mm in vehicle-treated larvae to 1448, 1550, and 1311 mm in larvae exposed to 50, 100, and 500 nM sertraline, respectively (Figure 4.3B). The distance moved was not significantly different between vehicle and sertraline-treated larvae during light phases (Figure 4.3B). Concurrently, inactivity time was significantly altered by sertraline concentration and phase, but not their interaction (LMM: treatment $\chi^2_4 = 14.16$, $p = 0.0068$; light phase $\chi^2_1 = 12.19$, $p = 0.0005$; interaction $\chi^2_4 = 1.29$, $p = 0.863$; Figure 4.3C), pairwise comparisons showing increased inactivity time in the 500 nM sertraline group compared to the vehicle group in the dark phases. There were no significant differences between treatments during light phases.

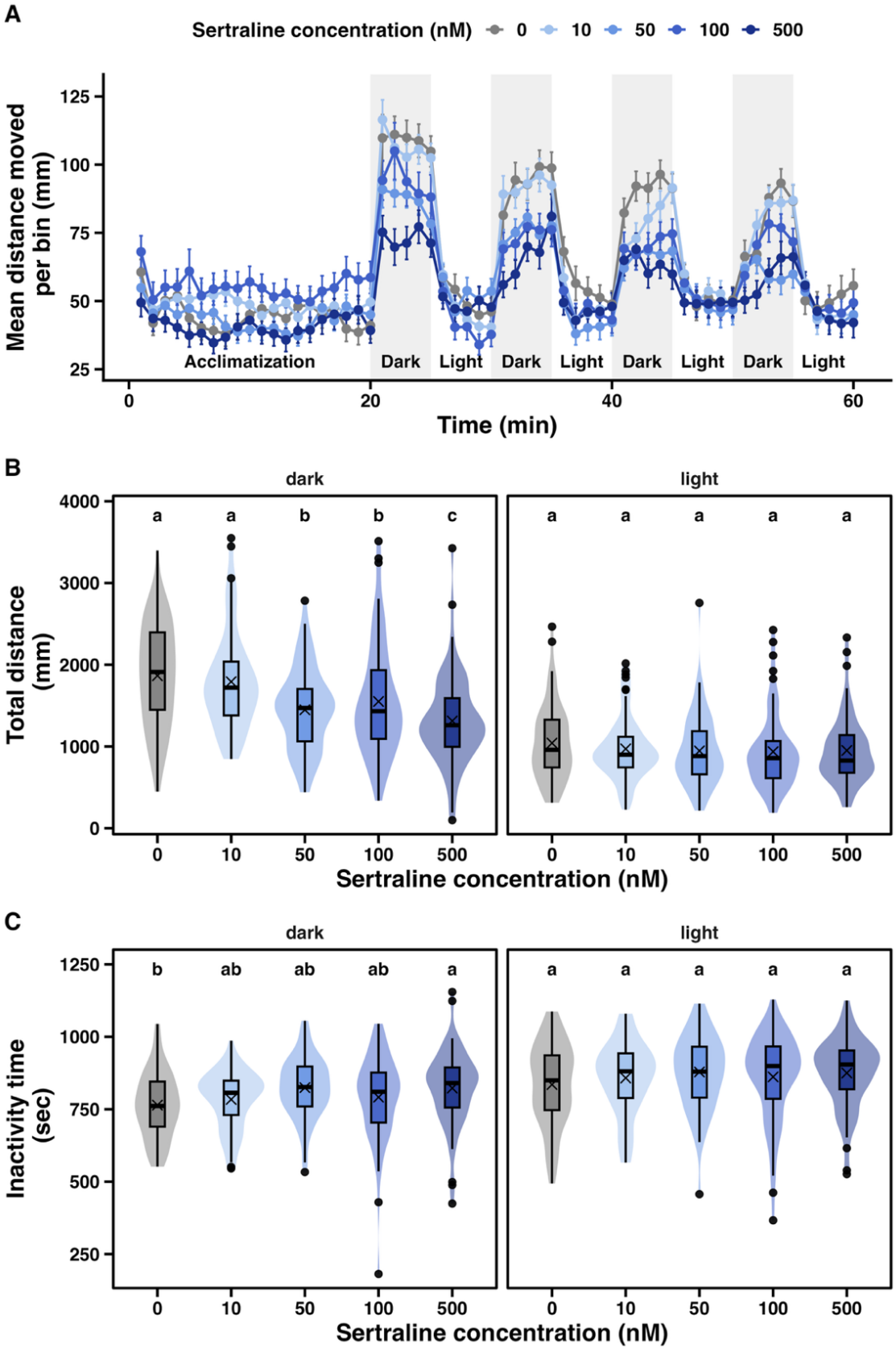

Figure 4.3. Effects of sertraline on 4 dpf SR4G zebrafish photomotor response.

(A) Mean distance moved per 1-min recording bin during a 20-min acclimatization period followed by four alternating 5-min dark and light phases. Grey shaded areas indicate dark phases. Data are shown as mean ± SEM for each concentration (0-500 nM). (B) Total distance moved per individual during dark and light phases. Violin plots represent the distribution density, and overlaid boxplots show the lower and upper quartiles with the mean (cross symbol), the median (bold line), the whiskers depict the minimum and maximum values, and outliers as single dots. (C) Total inactivity time per individual during dark and light phases, plotted as in (B). Statistical analyses were performed with linear mixed-effects models fitted on log-transformed data, with concentration, light condition, and their interaction as fixed effects, and experimental replicate and animal as random intercepts. Fixed effects were assessed using Type-III Wald χ^2 tests. Estimated marginal means (EMM) were back-transformed for interpretation, and pairwise comparisons between treatments were conducted within each light condition using Holm correction. Letter superscripts indicate statistically different groups within each lighting context (letter "a" was assigned to the highest EMM).

At 5 dpf, the photomotor response, with increased locomotion during dark phases relative to light phases, persisted (Figure 4.4A). The total distance moved was significantly affected by sertraline concentration, the phase, and their interaction (LMM: treatment $\chi^2_4 = 75.79$, $p < 0.0001$; light phase $\chi^2_1 = 209.81$, $p < 0.0001$; interaction $\chi^2_4 = 21.56$, $p = 0.0002$). Significant reductions in distance moved were observed at 100 and 500 nM, with values declining from 2073 mm in the vehicle group to 1695 and 1449 mm, respectively (Figure 4.4B). The distance moved during the light phases was not affected by the treatment. Inactivity time was significantly affected by both the sertraline concentration and phase of the assay, as well as their interaction (LMM: treatment $\chi^2_4 = 47.45$, $p < 0.0001$; light condition $\chi^2_1 = 53.88$, $p < 0.0001$; interaction $\chi^2_4 = 12.74$, $p = 0.0126$; Figure 4.4C): during dark phases, inactivity time significantly increased at 100 and 500 nM sertraline compared to the vehicle control, and there were no significant differences between treatments during light phases.

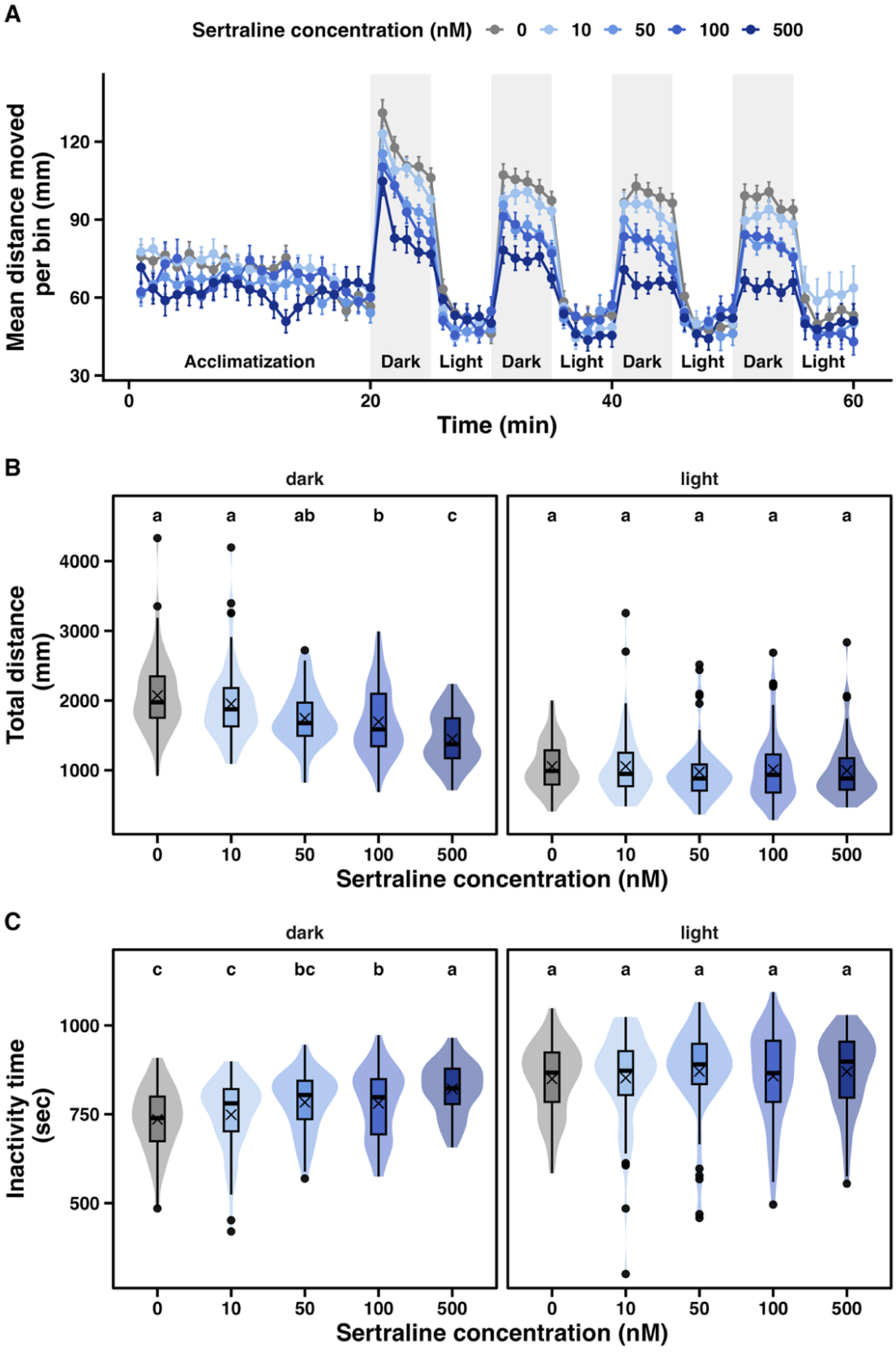

Figure 4.4. Effects of sertraline on 5 dpf SR4G zebrafish photomotor response.

(A) Mean distance moved per 1-min recording bin during a 20-min acclimatization period followed by four alternating 5-min dark and light phases. Grey shaded areas indicate dark phases. Data are shown as mean ± SEM for each concentration (0-500 nM). (B) Total distance moved per individual during dark and light phases. Violin plots represent the distribution density, and overlaid boxplots show the lower and upper quartiles with the mean (cross symbol), the median (bold line), the whiskers depict the minimum and maximum values, and outliers as single dots. (C) Total inactivity time per individual during dark and light phases, plotted as in (B). Statistical analyses were performed with linear mixed-effects models fitted on log-transformed data, with concentration, light condition, and their interaction as fixed effects, and experimental replicate and animal as random intercepts. Fixed effects were assessed using Type III Wald χ^2 tests. Estimated marginal means (EMM) were back-transformed for interpretation, and pairwise comparisons between treatments were conducted within each light condition using Holm correction. Letter superscripts indicate statistically different groups within each lighting context (letter "a" was assigned to the highest EMM).

4.4.3. GRE-driven eGFP expression

Sertraline exposure increased glucocorticoid receptor-mediated transcription of the eGFP reporter following a light/dark stimulus, without altering basal transcription levels. Relative eGFP expression was significantly affected by sertraline concentration ($F_{4,50}$ = 2.65, p = 0.044), the light/dark stimulus ($F_{1,50}$ = 59.77, $p < 0.001$), and their interaction ($F_{4,50}$ = 2.85, p = 0.033). First, in unstimulated larvae, sertraline did not significantly alter basal eGFP expression (0.9- to 1-fold relative to the unstimulated vehicle-treated larvae). In larvae submitted to the light/dark stimulus, sertraline induced a significant increase in transcription of the reporter at 100 nM (1.96-fold; $p_{adj.}$ = 0.03) and 500 nM (1.94-fold; $p_{adj.}$ = 0.04) when compared to the stimulated vehicle-treated larvae (Figure 4.5). The light/dark challenge alone did not significantly alter reporter transcription in vehicle-treated larvae (1.25-fold; $p_{adj.}$ = 0.96). A significant stimulus response was detected only in sertraline-exposed groups: 50 nM (1.6-fold; $p_{adj.}$ = 0.01), 100 nM (1.9-fold; $p_{adj.}$ = 0.003), and 500 nM (1.9-fold; $p_{adj.}$ = 0.003), compared to their unstimulated counterparts (0.9-fold, 1-fold, 0.9-fold, at 50, 100, and 500 nM respectively).

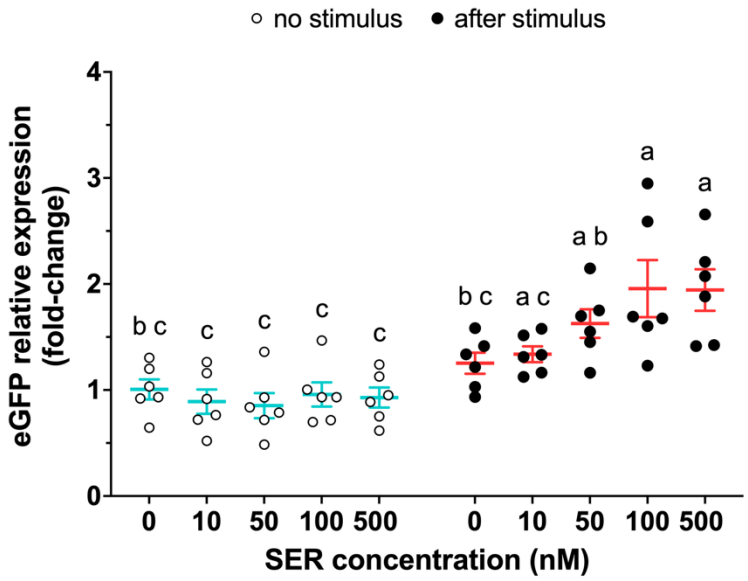

Figure 4.5. Effects of sertraline and light/dark challenge on eGFP relative expression in 5 dpf SR4G zebrafish.

Bars and intervals represent mean ± SEM (N = 6 biological replicates; sampling unit = 10 larvae/sample), with individual observations overlaid (no stimulus: white points, cyan bars; after light/dark stimulus: black points, coral bars). Two-way ANOVA, followed by Tukey's post-hoc test, were used to identify significant differences between groups. Letter superscripts indicate statistically different groups (letter "a" was assigned to the highest means).

4.4.4. Targeted transcriptomics

4.4.4.1. Effect of the light/dark challenge on transcriptomic responses

The light/dark challenge induced broad transcriptional changes in 5 dpf zebrafish larvae, yielding 472 differentially expressed genes (DEGs; $p_{adj.} < 0.05$). Applying an absolute linear fold-change (FC) threshold of ≥ 1.2 refined this profile to 179 DEGs (Supplementary Table C.5), comprising 157 upregulated and 22 downregulated genes. The light/dark challenge downregulated genes associated with the stress axis and cellular metabolism, including *fkbp5* (FKBP prolyl isomerase 5; FC = -1.7), *rrs1* (ribosome biogenesis regulator 1 homolog; FC = -1.4), *hif1al* (hypoxia inducible factor 1 subunit alpha, like; FC = -1.4), *blvra* (biliverdin reductase A; FC = -1.3), and *hsd11b2* (hydroxysteroid 11-beta dehydrogenase 2; FC = -1.3). The stimulus upregulated genes such as *adipoqb* (adiponectin, C1Q and collagen domain containing, b; FC = 2.28), *glod4* (glyoxalase domain containing 4; FC = 2.73), *cd79a* (CD79a molecule, immunoglobulin-associated alpha; FC = 2.91), *gnb3a* (guanine nucleotide binding protein, beta polypeptide 3a; FC = 2.86), and *vtg1* (vitellogenin 1; FC = 2.24). Overrepresentation analysis (ORA) revealed that this stimulus-driven transcriptional response was significantly enriched for biological processes mediating responses to chemical stimuli, hormone responses, cellular responses to hormone stimuli, and defence responses (Table 4.2).

Table 4.2. Enriched biological pathways (over-representation analysis) associated with the overall effect of the light/dark challenge.

Description (GO ID)	Gene ratio	Fold enrichment	*p*-adj	Genes symbol
Response to chemical (GO:0042221)	34/150	2.05	0.017	*adipor2, arnt, chrna2a, cpt1b, cxcl19, cxcl8b.1, cyp19a1b, cyp2aa3, cyp2aa8, duox, grb10b, grb14, hif1al, hmox1a, hsp90aa1.2, hsp90b1, il6, jak2b, slc47a2.2, nod1, nr1d1, nr1i2, nr5a1a, pora, pparab, samhd1, si:cabz01093077.1, slc40a1, socs1a, socs3a, vtg1, vtg2, vtg3, amy2al1*
Response to hormone (GO:0009725)	15/150	3.12	0.023	*adipor2, arnt, grb10b, grb14, jak2b, nr1d1, nr5a1a, pparab, vtg1, vtg2, vtg3, amy2al1*
Cellular response to hormone stimulus (GO:0032870)	12/150	3.46	0.032	*adipor2, arnt, grb10b, grb14, jak2b, nr1d1, nr5a1a, pparab, vtg1, vtg2, vtg3, amy2al1*
Defense response (GO:0006952)	18/150	2.55	0.033	*btr18, btr25, cxcl19, cxcl8b.1, duox, hmox1a, hsp90b1, il6, jak2b, nod1, pparab, rsad2, saa, samhd1, socs1a, tlr1, zgc:173581, zgc:194990*

All significant DEGs included in this comparison were defined by $p_{adj.} \leq 0.05$ and an absolute linear fold-change (FC) ≥ 1.2.

4.4.4.2. Effects of light/dark stimulus at each sertraline concentration

The magnitude of the transcriptional response to the light/dark challenge varied depending on sertraline concentration. Applying an |FC| threshold of ≥ 1.2 ($p_{adj.} \leq 0.05$), the stimulus induced a total of 22 DEGs in vehicle-treated larvae, compared to 8, 17, 27, and 49 DEGs in larvae exposed to 10, 50, 100, and 500 nM sertraline, respectively (Figure 4.6). Despite this variance in total DEG counts, five genes exhibited consistent stimulus responsiveness across all exposure conditions: *cdca7a* (cell division cycle associated 7a), *hsp90aa1.2* (heat shock protein 90, alpha (cytosolic), class A member 1, tandem duplicate 2), *loc108183819* (*si:ch211-22k7.9*), *rrs1* (ribosome biogenesis regulator 1 homolog), and *si:ch211-226o13.1* (Table 4.3). The complete list of concentration-specific DEGs induced by the light/dark challenge is provided in Supplementary Table C.6.

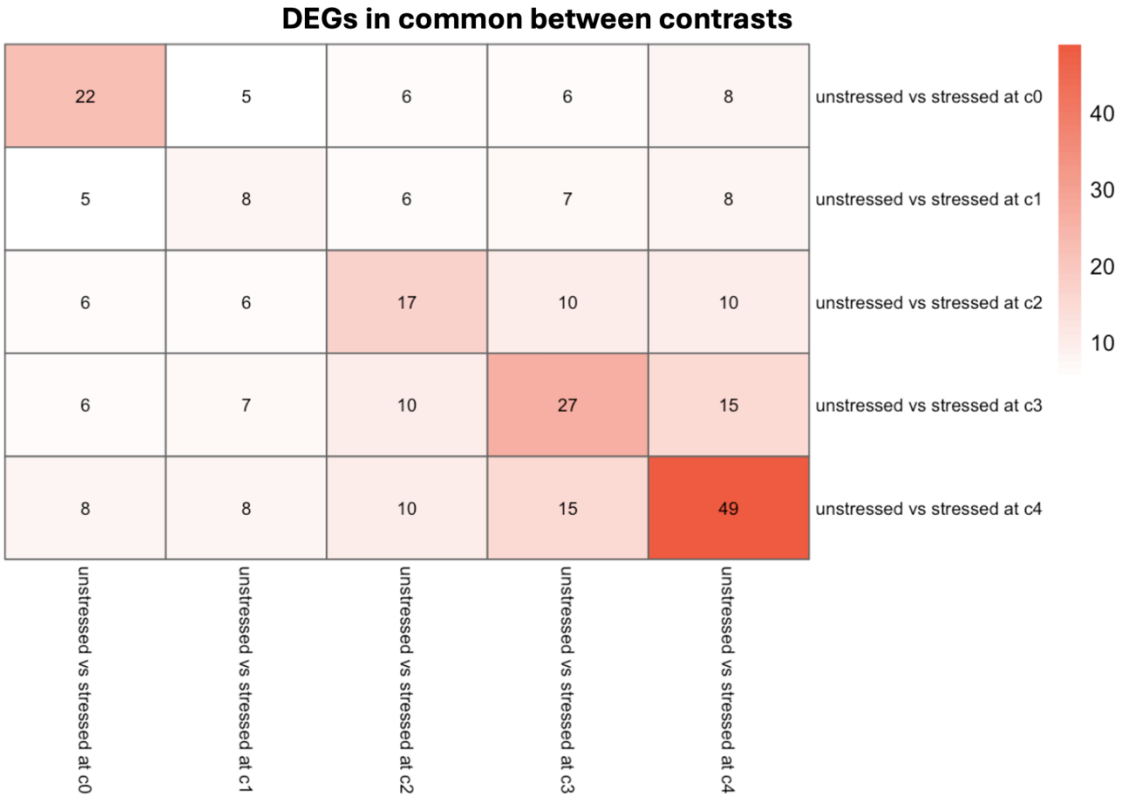

Figure 4.6. Differentially expressed genes (DEGs) overlap across contrasts testing the stimulus effect at each sertraline concentration.

For each concentration, contrasts are relative to the unstimulated condition. Tile values and red shading indicate the number of shared DEGs. Concentrations are as follows: c0: vehicle, c1: 10, c2: 50, c3: 100, c4: 500 nM. DEGs were defined using an absolute linear fold-change (FC) ≥ 1.2 and $p_{adj.} \leq 0.05$.

Table 4.3. Genes differentially expressed in response to the light/dark challenge across several concentration-specific contrasts.

Gene symbol	Description	Number of contrasts
cdca7a	cell division cycle associated 7a	5
hsp90aa1.2	heat shock protein 90, alpha (cytosolic), class A member 1, tandem duplicate 2	5
loc108183819	si:ch211-22k7.9 [Source:ZFIN;Acc:ZDB-GENE-070424-160]	5
rrs1	ribosome biogenesis regulator 1 homolog	5
si:ch211-226o13.1	si:ch211-226o13.1 [Source:ZFIN;Acc:ZDB-GENE-081104-491]	5
loc108184002	si:dkey-14o6.1 [Source:ZFIN;Acc:ZDB-GENE-081103-51]	4
nop58	NOP58 ribonucleoprotein homolog (yeast)	4
hif1al	hypoxia inducible factor 1 subunit alpha, like	3
hsd11b2	hydroxysteroid (11-beta) dehydrogenase 2	3
nr1i2	nuclear receptor subfamily 1, group I, member 2	3
pde4cb	phosphodiesterase 4C, cAMP-specific b	2
cyp2aa8	cytochrome P450, family 2, subfamily AA, polypeptide 8	2
e2f7	E2F transcription factor 7	2
g3bp1	GTPase activating protein (SH3 domain) binding protein 1	2
gnb3a	guanine nucleotide binding protein (G protein), beta polypeptide 3a	2
hist1h2a5	histone cluster 1 H2A family member 5	2
hmox1a	heme oxygenase 1a	2
si:ch211-113a14.22	si:ch211-113a14.22 [Source:ZFIN;Acc:ZDB-GENE-121214-203]	2
tert	telomerase reverse transcriptase	2
znf367	zinc finger protein 367	2

All significant DEGs included in this comparison were defined with $p_{adj.} \leq 0.05$ and an absolute linear fold-change (FC) ≥ 1.2.

4.4.4.3. Sertraline effects in unstimulated and stimulated larvae

Sertraline exposure did not substantially alter gene expression, with only five DEGs ($p_{adj.} \leq 0.05$, no FC threshold) relative to vehicle controls (Table 4.4). In unstimulated larvae, sertraline upregulated the transcript *si:dkey-183i3.5* at 10 nM and 100 nM, and downregulated *rgs2* at 50 nM and 100 nM. Following the light/dark stimulus, sertraline upregulated *plac8.2* at 100 nM, and upregulated both *hif1al* and *tdo2b* at 500 nM. The small number of DEGs and their concentration-specific expression patterns suggest that sertraline exposure induces relatively modest transcriptional changes under these test conditions, with effects depending on both concentration and stress condition.

Table 4.4. List of differentially expressed genes (DEGs) following sertraline exposure, in unstressed and stressed 5 dpf SR4G zebrafish.

Contrast	Gene symbol	Description	Linear FC	*p*-value	*p*-adj
Unstressed larvae					
c0 vs c1	*si-dkey-183i3.5*	si:dkey-183i3.5 [ZDB-GENE-030131-8568]	1.20	3.07E-06	8.75E-03
c0 vs c2	*rgs2*	regulator of G protein signalling 2	-2.34	1.37E-05	3.90E-02
c0 vs c3	*rgs2*	regulator of G protein signalling 2	-2.48	3.54E-06	1.01E-02
c0 vs c3	*si-dkey-183i3.5*	si:dkey-183i3.5 [ZDB-GENE-030131-8568]	1.18	2.29E-05	3.26E-02
Stressed larvae					
c0 vs c3	*plac8.2*	placenta associated 8, tandem duplicate 2	12.71	9.23E-06	2.53E-02
c0 vs c4	*hif1al*	hypoxia inducible factor 1 subunit alpha, like	1.39	3.52E-05	4.82E-02
c0 vs c4	*tdo2b*	tryptophan 2,3-dioxygenase b	1.33	2.75E-05	4.82E-02

Concentrations are as follows: c0: Vehicle; c1: SER 10 nM; c2: SER 50 nM; c3: SER 100 nM; c4: SER 500 nM. All significant DEGs included in this comparison were defined with $p_{adj.} < 0.05$ and no FC cut-off.

4.5. Discussion

Developmental exposure to sertraline induced behavioural and molecular changes without causing developmental toxicity in SR4G larvae. Sertraline disrupted locomotor activity in the photomotor assay, decreasing the distance moved and increasing inactivity time during the dark phases. At the molecular level, sertraline enhanced stimulus-induced transcription of the GR-mediated eGFP reporter, indicating modulation of glucocorticoid receptor signalling. Transcriptomic analysis using the Zebrafish S1500+ panel revealed that sertraline altered a small subset of assayed genes, rather than widespread transcriptional reprogramming.

Sertraline exposure did not significantly affect developmental endpoints in SR4G embryos, including survival, hatching success, and morphological abnormalities up to 5 dpf. This is consistent with the concentrations tested, the highest concentration evaluated here (500 nM) was well below the 72-hr LC50 of 841 μg/L (~2.45 μM) established in Japanese medaka (*Oryzias latipes*) larvae (Chiffre et al., 2016) and the 96-hr LC50 values (~0.41 to 1.10 μM) reported for other aquatic species (Minagh et al., 2009; Valenti et al., 2009). Consistent with these findings, sertraline concentrations up to 10 μM did not increase mortality or morphological abnormalities in zebrafish embryos (Richendrfer & Creton, 2018). The literature on hatching responses remains mixed; while some studies report no effects on hatching at sertraline concentrations up to 1000 μg/L (Sehonova et al., 2019), others found that 10 μg/L sertraline decreases the total hatching rate of zebrafish embryos at 96 hpf (Nowakowska et al., 2020).

The absence of lethality and morphological abnormalities indicates that the observed behavioural and molecular alterations reported below are unlikely to be secondary consequences of general developmental toxicity or delay. Selective serotonin reuptake inhibitors consistently induce behavioural or molecular alterations at sublethal concentrations across teleost models (Bachour et al., 2020; Correia, Bellot, et al., 2023b; Cunha et al., 2018; Rodrigues et al., 2020; Sehonova et al., 2019). Behavioural and transcriptomic endpoints can therefore detect sublethal SSRI-induced disruption that traditional apical toxicity assays do not capture (H. Lee et al., 2025). In the present study the behavioural endpoint proved the most sensitive, detecting effects at 50 nM, whereas

the targeted transcriptomic panel identified changes in only five genes across all concentrations.

Developmental exposure to sertraline reduced locomotor activity during the dark phases of the behavioural assay, decreasing the total distance moved and increasing inactivity time. These hypoactive effects occurred at both time points evaluated: at 4 dpf, sertraline decreased total distance moved at 50 nM (-22.4%), 100 nM (-16.9%) and 500 nM (-29.7%), while at 5 dpf, decreases occurred at 100 nM (-19.2%) and 500 nM (-30.1%). Consistent with these findings, sertraline concentrations between 100 and 1000 μg/L decrease swimming distance during dark conditions in larval zebrafish (Sehonova et al., 2019). Similarly, 1 to 10 μM sertraline decreases swim speed and increases resting behaviour in zebrafish larvae, independent of visual stimuli (Richendrfer & Creton, 2018). Long-term exposure to 100 μg/L sertraline, fluoxetine, or paroxetine from 5 dpf likewise reduces the total distance moved by adult zebrafish at 90 and 120 dpf in the novel tank test (Venkatachalam et al., 2023). In Japanese medaka larvae, 1000 μg/L sertraline reduces total distance moved, whereas concentrations as low as 10 μg/L induce significant hypoactivity specifically during dark phases (Chiffre et al., 2016). Repeated early developmental exposure to other SSRIs, including fluoxetine and paroxetine, decreases spontaneous swimming activity in zebrafish larvae by 25% to 40% (Huang et al., 2019). Beyond locomotion, 10 to 100 μg/L sertraline alters social behaviour by increasing shoaling and reducing food consumption in juvenile yellow catfish (H. Chen et al., 2021).

The differences in behavioural suppression at 5 dpf compared to 4 dpf suggest stage-dependent sensitivity to sertraline. Zebrafish larvae change developmentally over this 24h interval. Larvae inflate the swim bladder and transition to sustained free swimming at 5 dpf (Kimmel et al., 1995), and age at the time of testing is itself a recognised source of variation in larval locomotor assays (Hill et al., 2023). A one-day difference in age, therefore, corresponds to a marked change in motor competence, independent of any exposure. This observation aligns with other evidence that sertraline-induced decreases in swim speed and increases in resting behaviour are less prominent following exposures from 0 to 4 dpf than exposures maintained until 5 dpf (Richendrfer & Creton, 2018). These stage-dependent behavioural shifts coincide with the maturation of neuroendocrine systems. Indeed, the zebrafish serotonergic system develops between 1 and 4 dpf and is functionally

established by approximately 96 hours post-fertilisation (Kreke & Dietrich, 2008). Concurrently, the hypothalamic-pituitary-interrenal (HPI) axis initiates functional cortisol release in response to stress by 4 dpf and the glucocorticoid-mediated negative feedback is established by 5 dpf (Alsop & Vijayan, 2007, 2009b).

In the absence of stimuli, sertraline did not alter eGFP transcription, indicating that basal glucocorticoid receptor (GR)-mediated transcription remains unaffected under non-stressed conditions. Following a light/dark challenge, however, larvae exposed to 50 to 500 nM sertraline exhibited increased eGFP reporter expression relative to their unstimulated counterparts. Furthermore, stressed larvae at 100 and 500 nM sertraline showed greater reporter induction than vehicle-stressed controls. Therefore, sertraline does not alter GR signalling at baseline but amplifies the magnitude of GR-mediated transcription in response to a stimulus.

This stimulus-dependent amplification aligns with previous results, where developmental exposure to 1000 nM sertraline did not suppress stress axis responsiveness but instead enhanced stress-induced GRE-driven transcription in zebrafish larvae (Chapter 2). In these experiments, basal reporter activity remained unchanged at concentrations below 1000 nM, while acute stress handling (netting stress with brief removal from media) elicited significantly greater eGFP induction in larvae treated with 1000 nM sertraline and norfluoxetine compared to controls. These findings support the interpretation that serotonergic modulation by sertraline does not blunt the larval hypothalamic–pituitary–interrenal (HPI) axis activation but rather amplifies downstream GR-mediated transcriptional responses to stressors.

SSRIs alter cortisol signalling, though the direction of effect depends on the specific compound, exposure paradigm, and developmental stage. Fluoxetine exposure frequently attenuates cortisol responses to acute physical stressors in larval and adult zebrafish (Abreu et al., 2014, 2015, 2017; Marcon et al., 2016; Vera-Chang et al., 2018; Vera-Chang, Moon, et al., 2019), including blunted stress-induced eGFP expression in SR4G larvae (Nozari et al., 2021). In contrast, the enhanced reporter transcription observed following sertraline exposure here suggests a divergent, stimulatory modulation of stress response. Serotonergic signalling modulates the HPI axis at multiple levels, including the direct

stimulation of cortisol secretion from teleost interrenal tissue via specific serotonin receptors, such as 5-HT2 and 5-HT4 (McDonald, 2017). For example, 5-HT4 receptor activation directly stimulates cortisol production in the interrenal cells of rainbow trout (*Oncorhynchus mykiss*) (Tea et al., 2025). The specific increase in stimulus-induced GR activity by sertraline may reflect compound-specific differences in interrenal HPI axis modulation, alongside variation in exposure duration, endpoint selection and strain sensitivity (Abreu et al., 2021; Maximino et al., 2013). However, neither serotonin nor cortisol levels were measure in this study and remains to be investigated.

The light/dark challenge induced transcriptional changes, resulting in 179 DEGs across the Zebrafish S1500+ panel. These stimulus-responsive DEGs were associated with the enrichment of biological processes related to the response to chemical, response to hormone, cellular response to hormone stimulus and defence response. These results suggest that the light/dark stimulus elicits a coordinated response involving stress- and signalling-related pathways. Sertraline exposure was associated with 8 to 49 stimulus-responsive DEGs per concentration group, compared to the 22 in the vehicle-treated larvae. Five genes responded to the stimulus in every treatment group: *cdca7a* (cell division cycle associated 7a), *hsp90aa1.2* (heat shock protein 90, alpha (cytosolic), class A member 1, tandem duplicate 2), *rrs1* (ribosome biogenesis regulator 1 homolog), *loc108183819* (si:ch211-22k7.9), and *si:ch211-226o13.1*. Thus, while the light/dark challenge consistently alters gene expression, the extent of the response may be modulated by sertraline. With the eGFP reporter results, these data are consistent with sertraline modifying transcriptional responsiveness to the stimulus rather than inducing large-scale basal change.

Sertraline exposure altered the expression of only a small number of genes, with *rgs2* and *si-dkey-183i3.5* affected in unstimulated larvae, and *plac8.2*, *hif1a*l, and *tdo2b* affected following the light/dark challenge. This suggests interference with specific biological pathways, rather than widespread toxicity at the tested concentrations. The regulator of G protein signalling 2 (*rgs2*) modulates neural crest development through the Pparδ-Sox10 cascade in zebrafish embryos (S.-J. Lin et al., 2017). Similarly, functional disruption of the zebrafish paralog *rgs4* causes locomotion defects and aberrant axon development (Cheng et al., 2013). Hypoxia-inducible factor 1 subunit alpha (*hif1al*) is a

highly conserved transcription factor that mediates adaptations to stress and hypoxia tolerance in teleosts (Elbassiouny et al., 2024) and regulates macrophage-endothelial interactions during blood vessel and hemogenic endothelium development (Gerri et al., 2017, 2018). Tryptophan 2,3-dioxygenase b (*tdo2b*) encodes an enzyme involved in the first and rate-limiting step of tryptophan catabolism into kynurenine (Aslamkhan et al., 2020). Dysregulation of this kynurenine pathway in zebrafish impairs cellular bioenergetics and induces severe oedema (Bolanos-Palmieri et al., 2025). Additionally, *tdo2b* is differentially expressed in transcriptomic profiling studies in teleosts under physiological stress (H. Wang et al., 2022). Placenta-associated 8 family (*plac8*) regulates cellular proliferation and motility cascades, with targeted PLAC8 protein dysregulation driving epithelial-to-mesenchymal transition and aberrant cell migration (C. Li et al., 2014). The five sertraline-responsive genes identified here relate to neural, vascular and metabolic signalling, and no large-scale basal transcriptional reprogramming was detected at the concentrations tested. The modest number of DEGs observed under these sublethal conditions contrasts with broader transcriptomic disruptions reported at higher exposure concentrations. For example, a 14-day exposure to 100 µg/L sertraline elicits 405 and 1193 DEGs in the brain and liver, respectively, of juvenile yellow catfish, altering insulin signalling, growth hormone regulation, and immune pathways (H. Chen et al., 2021). Such widespread disruption indicates that prolonged, high-concentration exposures induce broader systemic toxicity, including inflammation. Furthermore, 96 h exposures to sertraline at 25 and 250 µg/L in zebrafish larvae resulted in 33 and 52 DEGs, respectively (Park et al., 2012). Among these, the *fkbp5* gene, a regulator of glucocorticoid receptor activity, was strongly downregulated at both concentrations and by both fluoxetine and sertraline, which is consistent with an effect on stress-axis regulation (Park et al., 2012).

Larval zebrafish provide a high-throughput, scalable, and cost-effective *in vivo* platform that bridges the gap between *in vitro* screens and mammalian models (Bailey et al., 2013; Tanguay, 2018). Because 5 days post-fertilization (dpf) larvae do not feed independently, they are excluded from protected animal regulations in many jurisdictions, aligning the model with the 3R (reduce, refine, replace) principles of animal welfare. The SR4G line provides a quantitative, mechanistically anchored readout of glucocorticoid receptor activation. Reporter transcription was measured here by RT-qPCR on pooled

larvae, but the optical transparency of early developmental stages also permits non-invasive, repeated fluorescence measurement in the same individuals (Krug et al., 2014; Nozari et al., 2021), which would allow longitudinal designs in future studies. Furthermore, integrating this mechanistically anchored reporter with a mild light/dark behavioural challenge resolves stimulus-dependent disruptions that are not apparent under basal conditions.

However, evaluating sertraline or other antidepressants in isolation limits ecological realism, as wild aquatic populations are continuously exposed to complex multi-stressor environments and pharmaceutical mixtures that exert interactive physiological effects (S. L. Gould et al., 2021; Maulvault et al., 2019). Sertraline contaminates surface waters at concentrations in the range of ng/L. Higher concentrations occur in wastewater effluents, particularly in psychiatric hospital effluents, reaching up to 17.1 µg/L (Arnnok et al., 2017; Davey et al., 2025). The concentrations evaluated in this study (10 to 500 nM; approximately 3 to 150 µg/L) therefore represent the upper end of environmental exposure scenarios, most relevant to effluent-contaminated aquatic systems. Nonetheless, antidepressants in the aquatic environment are present in mixtures, with cumulative maximum concentrations reaching 5 µg/L in the Laurentian Great Lake Basin in 2022 (Pappas et al., 2025). Disruption of the neuroendocrine stress response and predator-avoidance behaviours at these concentrations suggests that chronic antidepressant pollution could affect the ecological performance of teleost populations (Correia, Domingues, et al., 2023; S. L. Gould et al., 2021; McDonald, 2017).

Continuous waterborne exposure in larval zebrafish does not reflect the pharmacokinetic of oral ingestion and first-pass metabolism that determine internal doses in humans (Bambino & Chu, 2017). These findings are therefore most directly relevant to aquatic exposure scenarios and to the conserved biology of the glucocorticoid stress response, and extrapolation to human health effects should be made cautiously. The modest number of sertraline-responsive DEGs in this study should also be interpreted in the context of the pooled whole-larva sampling design. Whole-body homogenates provide an integrated measure of transcription across the organism but dilute localised, tissue-specific responses. Targeting specific tissues or cell populations would help resolve whether sertraline produces stronger transcriptional responses in neuroendocrine, vascular, or

metabolic compartments. Finally, larval zebrafish behavioural assays exhibit high intra- and inter-laboratory variability driven by subtle methodological discrepancies, such as light intensity, temperature fluctuations, and age at the time of testing (Hill et al., 2023). This inherent sensitivity necessitates rigorous protocol standardisation to ensure data reproducibility across toxicological studies.

4.6. Conclusions

Developmental exposure to sublethal concentrations of sertraline alters neuroendocrine stress axis responsiveness and locomotor behaviour in larval SR4G zebrafish. Sertraline concentrations up to 500 nM do not induce general developmental toxicity or morphological abnormalities, but reduced locomotion and increased GRE-driven reporter transcription following a light/dark challenge. Specifically, sertraline induced hypoactivity during dark phases at 4 and 5 dpf and increased the transcriptional response to a light/dark stimulus at 100 and 500 nM. Targeted transcriptomic profiling identified changes in only five genes, associated with neural, vascular and metabolic signalling, rather than widespread cellular toxicity or basal transcriptional reprogramming. The integration of the SR4G transgenic line with behavioural and transcriptomic assays provides a sensitive framework for detecting stress-axis disruption. Because these effects occurred at concentrations near the upper end of environmental levels, they suggest that chronic exposure to effluents highly polluted by pharmaceuticals may compromise the individuals in these locations, but do not indicate a risk for the general wild teleost populations exposed to current environmental sertraline concentrations. They do indicate that the framework detects neuroendocrine disruption that undisturbed, apical-endpoint testing would miss.

4.7. Funding sources and acknowledgment

Carole L. Yauk and Vance L. Trudeau are grateful for funding from the Natural Sciences and Engineering Research Council of Canada (Vance L. Trudeau: RGPIN-2021-03174; Carole L. Yauk: RGPIN-2021-02806), and Errol M. Thomson for funding from Health Canada through the Chemicals Management Plan. Carole L. Yauk acknowledges infrastructure support from the Canadian Foundation for Innovation (#233109, #43247) and the Ontario Research Fund (#40569, #43247). Vance L. Trudeau acknowledges

support from the University of Ottawa Research Chairs program, and Carole L. Yauk acknowledges that this project was conducted in part thanks to funding provided through the Canada Research Chairs program (CRC-2020-00060).

4.8. Declaration on the use of artificial intelligence

Large language models (Gemini 3.1 Pro and Microsoft 365 Copilot) were used to assist with language editing and sentence structuring. The authors reviewed all suggestions for accuracy and maintained full editorial control over the final output. The AI tools were not used to generate scientific hypotheses, interpret data, or formulate conclusions. The underlying scientific concepts and interpretations originated from the authors. The authors are taking full responsibility for the data and conclusions presented in this study.

5. Chapter 5: General discussion and future directions

5.1. Thesis summary and discussion

The goal of this thesis research was to evaluate whether developmental exposure to selective serotonin (and norepinephrine) reuptake inhibitors (SS(N)RIs) alters molecular, physiological and behavioural components of the stress response in larval zebrafish. The results provide partial support for this. Using the transgenic SR4G zebrafish larvae as an *in vivo* screening model, developmental SS(N)RIs exposure altered molecular and behavioural endpoints, but GRE-driven eGFP reporter transcription, used as a proxy for cortisol levels, was altered only at 1000 nM norfluoxetine and sertraline concentrations following an acute netting stress (Chapter 2), and from 100 nM sertraline following a light/dark stimulus (Chapter 4). Transcriptomic responses were compound- and context-dependent. With the exception of sertraline 1 μM and a small number of genes altered by norfluoxetine under basal conditions (Chapter 3), they emerged only when chemical exposure was paired with an acute netting stressor or light/dark stimulus, and not under undisturbed conditions used in standard testing (Chapter 3 and 4). Overall, these findings demonstrate that while environmentally relevant concentrations of these pharmaceuticals elicit minimal effects in undisturbed organisms, exposure can disrupt stress-induced glucocorticoid receptor (GR) signalling and alter transcriptomic profiles in a compound- and context-dependent way. The findings are summarised in Figure 5.1.

I first evaluated the utility of the SR4G transgenic zebrafish line as an *in vivo* screening tool for stress-disrupting compounds (Chapter 2). I found that GRE-driven eGFP reporter transcription closely tracks whole-body cortisol fluctuations following acute handling stress in 7-day post-fertilisation (dpf) larvae, confirming earlier studies (Nozari et al., 2021). Screening of six SS(N)RIs and one common metabolite revealed no effects on basal eGFP reporter transcription, except at the highest tested concentration of sertraline (1000 nM). Following a standardised handling stress, larvae exposed to the highest concentrations of norfluoxetine or sertraline exhibited significantly altered stress-induced eGFP reporter transcription (Chapter 2). The direction of this effect, however, is contrary to what was previously reported for fluoxetine.

These results contrast with the current literature dominated by studies showing that fluoxetine blunts the cortisol response. Acute exposure of adult zebrafish to 1 to 50 µg/L fluoxetine attenuates cortisol production following net chasing, air exposure or spatial restriction (Abreu et al., 2014, 2015, 2017), while previous evidence from our laboratory found that developmental exposure to 0.54 and 54 µg/L blunts cortisol increase after a swirling stress in 6 dpf AB larvae (Vera-Chang, Moon, et al., 2019), and 54 µg/L blunts both cortisol and GRE-driven eGFP reporter transcription in 7 dpf SR4G larvae following an acute netting stress (Nozari et al., 2021). In this thesis, effects were observed at the highest norfluoxetine and sertraline concentrations (1000 nM, ~295 and 306 µg/L, respectively), where stress-induced GRE-driven eGFP reporter transcription was instead amplified rather than suppressed.

Serotonin directly stimulates cortisol secretion at the interrenal level in goldfish through 5-HT1A and 5-HT4 receptors, and in rainbow trout through 5-HT4 (Lim et al., 2013; Tea et al., 2025), which offers a plausible explanation for the increased eGFP reporter transcription observed with norfluoxetine, although serotonin levels were not measured here. For sertraline at 1000 nM, the co-occurring mortality and the transcriptomic profiles described in Chapter 3 indicate that nonspecific toxicity and cellular stress cannot be separated from serotonergic overstimulation as the driver.

Following up on this screening, I investigated the molecular mechanisms underlying SSRI effects and toxicity using high-throughput TempO-Seq transcriptomics. Developmental exposure to fluoxetine, norfluoxetine, or sertraline altered baseline and stress-induced transcriptional profiles in a compound- and context-dependent manner (Chapter 3). Fluoxetine altered the expression of only two genes in unstressed larvae, consistent with the absence of an effect on reporter transcription in Chapter 2. Effects emerged predominantly in stressed larvae, where both fluoxetine and norfluoxetine suppressed the transcription of several immediate-early genes and disrupted transcriptomic pathways associated with lipid metabolism. In contrast, high concentrations of sertraline induced widespread transcriptomic changes in both unstressed and stressed states (547 and 595 differentially expressed genes, respectively). These changes were characterised by cellular stress and protein degradation signatures, concordant with severe larval morbidity observed in Chapter 2, rather than specific neuroendocrine disruption.

The suppression of immediate-early genes by both fluoxetine and norfluoxetine in stressed larvae is consistent with other studies reporting these genes responsive to serotonergic modulation across vertebrates, particularly the FOS family. For example, acute fluoxetine induces *c-fos* transcription in rodent hypothalamus and amygdala (Torres et al., 1998), and chronic fluoxetine treatment induces the FosB family of transcription factors across several regions of the brain in mice (Vialou et al., 2015). In zebrafish, developmental exposure to fluoxetine combined with an acute stressor upregulates *fosb* transcription in larval heads while downregulating it in the adult hypothalamus (Nozari et al., 2022).

The protein damage and cytotoxicity signature observed at 1000 nM sertraline aligns with another study in larval fathead minnows, where sublethal fluoxetine concentrations disrupt neurotoxicity pathways and higher concentrations activate broad metabolic and cellular stress pathways (Alcaraz et al., 2022). Studies in mammalian cell models have characterised similar mechanisms following sertraline exposure. In human hepatic cells (HepG2), sertraline induces endoplasmic reticulum stress and activates the unfolded protein response, upregulating the markers PERK, IRE1α and CHOP, and causes mitochondrial dysfunction and caspase-dependent apoptosis through the MAP4K4-JNK cascade (S. Chen et al., 2013, 2014). Further investigation found that sertraline toxicity causes DNA damage and topoisomerase inhibition, and cytochrome P450 metabolism contributes to decreasing DNA damage markers and attenuating sertraline toxicity (S. Chen et al., 2020), and the unfolded protein response has also been implicated in sertraline-induced apoptosis in pancreatic β-cells (Isaac et al., 2012). The upregulation of heat-shock proteins and proteasome subunits observed here (Chapter 3) is concordant with such protein damage and endoplasmic reticulum stress response. However, the whole-body transcriptomic data presented here cannot fully confirm that the same endoplasmic reticulum stress or mitochondrial pathways are engaged in zebrafish larvae; targeted measurement of unfolded-protein-response markers and mitochondrial endpoints would be required to establish this mechanism. Taken with the mortality reported in Chapter 2, these results place the transition from compound-specific modulation to general toxicity somewhere between 100 and 1000 nM sertraline, the two adjacent concentrations tested here.

Interestingly, although fluoxetine, norfluoxetine and sertraline share the serotonin transporter (SERT) as their primary pharmacological target, these three SSRIs produced different transcriptomic profiles. This divergence could be explained by divergent secondary pharmacological targets of these compounds. Sertraline inhibits the dopamine transporter (DAT) and antagonises the sigma-1 receptor in addition to SERT, whereas fluoxetine is comparatively SERT-selective (DeVane et al., 2002; Laux, 2022b). The dopaminergic activity of sertraline is also evident at a teleost transporter, where sertraline inhibited medaka DAT at lower concentrations than bupropion, a dedicated dopamine reuptake inhibitor (Honda et al., 2026). The broad cellular stress and protein degradation signature induced by 1000 nM sertraline suggests a combination of off-target pharmacological effects and emerging general toxicity, rather than a predominantly serotonergic or neuroendocrine response.

A second, untested explanation is differential action on the two zebrafish serotonin-transporter paralogues. Zebrafish express *slc6a4a* (*serta*) and *slc6a4b* (*sertb*), which differ in tissue distribution, with *serta* transcripts detected across central and peripheral tissues and *sertb* transcripts largely confined to the brain (Norton et al., 2008). In medaka, SERTa was inhibited by sertraline, fluoxetine and three other antidepressants at consistently lower concentrations than SERTb, a difference attributed to the substitution in SERTb of three residues of the inhibitor-binding site that are conserved between SERTa and human SERT (Honda et al., 2026). Loss of function of either paralogue in zebrafish alters the transcript abundance of multiple serotonergic-pathway components and produces opposing behavioural phenotypes, with increased aggression in *serta*-knockout males and reduced aggression in *sertb*-knockout fish of both sexes (Tea et al., 2024). These findings suggest that SSRI action in larvae is mediated predominantly through *serta*, but whether individual SSRIs differ in their relative potency at the two paralogues has not been tested, and the whole-body design used here cannot resolve paralogue-specific effects. Exposing the available *serta* and *sertb* knockout lines (Tea et al., 2024) to norfluoxetine and sertraline could test directly whether paralogue selectivity contributes to the compound-specific responses reported here.

In the last study, I integrated physiological, behavioural, and transcriptomic endpoints to evaluate the effect of sertraline within a new challenge framework, including

a light/dark stimulus. Developmental exposure to 500 nM of sertraline induced behavioural and molecular changes without developmental toxicity in SR4G larvae (5 dpf) (Chapter 4). During the light/dark assay, sertraline-exposed larvae exhibited decreased total distance moved and increased inactivity during the dark phases. The hypoactivity observed here during the dark phases is consistent with published effects of sertraline in other teleosts: 100 to 1000 µg/L decreases swimming distance in the dark in zebrafish larvae , and 10 µg/L induces hypoactivity during dark phases in Japanese medaka larvae (Chiffre et al., 2016).

At the molecular level, sertraline enhanced stimulus-induced transcription of the GRE-driven eGFP reporter, suggesting an effect on the modulation of glucocorticoid receptor signalling (Chapter 4). The direction of this effect on reporter transcription matches that observed in the screening (Chapter 2) and again opposes findings with fluoxetine. Sertraline did not alter eGFP reporter transcription at baseline but increased its induction by the light/dark stimulus at 100 and 500 nM, whereas fluoxetine attenuates cortisol responses to acute physical stressors in larval and adult zebrafish (Abreu et al., 2014, 2015, 2017; Vera-Chang, Moon, et al., 2019) and blunts stress-induced eGFP expression in the same SR4G line (Nozari et al., 2021). Finally, targeted transcriptomic analysis identified a small set of genes responsive to the light/dark challenge, and only five genes were altered by sublethal sertraline concentrations. This limited response most likely reflects the resolution of the approach, given the restricted gene coverage of the S1500+ panel and the dilution of localised signals in whole-body homogenates, rather than an absence of molecular effect.

To place the concentrations tested in this thesis on the same scale as environmental and clinical measurements, nominal molar concentrations were converted to mass units using each compound's free-base molecular weight, the appropriate basis for a compound dissolved in water and the basis on which environmental monitoring reports parent-compound mass (Figure 5.1). On this scale, the effective concentrations identified in Chapters 2 and 3 are approximately three to four orders of magnitude above the maximum concentrations reported in surface freshwater, which range from 75 ng/L (~0.25 nM) for sertraline up to 426 ng/L for citalopram (Mole & Brooks, 2019), and above the mean measured concentrations of 18.1 ng/L (~0.05 nM) for fluoxetine to 58.3 ng/L (~0.20 nM)

for norfluoxetine in the Laurentian Great Lakes Basin (Pappas et al., 2025). The lowest concentration at which any effect was detected, 50 nM sertraline (~15 µg/L) in Chapter 4, is instead comparable to concentrations measured in psychiatric hospital effluent, reaching ~17.1 µg/L for (Arnnok et al., 2017; Davey et al., 2025), whereas the 1000 nM concentrations that altered reporter transcription (~295 µg/L norfluoxetine and ~306 µg/L sertraline) fall within the human therapeutic plasma range summarised in Figure 5.1.

Under the conditions tested, single SS(N)RIs at environmentally relevant concentrations are therefore unlikely to alter stress-axis responsiveness in developing teleost fish. However, that conclusion does not extend to mixtures and to effluent-dominated environments, where cumulative antidepressant concentrations in the Laurentian Great Lakes Basin reached up to 5 µg/L in 2022 (Pappas et al., 2025). Exposure of juvenile zebrafish to fluoxetine, paroxetine, sertraline, or a mixture of the three reduces the novel-tank stress response and impairs fecundity and fertility (Venkatachalam et al., 2023), indicating that chronic exposure to these compounds, alone or combined, can affect endpoints not assessed here.

The exposure windows analyzed in this thesis differed across chapters, ranging from 1 to 7 dpf in the screening and transcriptomic studies (Chapters 2 and 3) to 1 to 5 dpf in the integrative behavioural study (Chapter 4). The 1 to 7 dpf window was chosen to encompass the full functional maturation of the HPI axis, so that the netting-stress response at 7 dpf could be assayed once both stressor-induced cortisol secretion and negative feedback are established (Alsop & Vijayan, 2007, 2009b). The shorter 1 to 5 dpf exposure window in Chapter 4 was chosen to make this method compliant with the 3Rs of animal research (Reduction, Refinement and Replacement), as zebrafish larvae until 5 dpf (until the onset of independent feeding) remain outside protected-animal regulations. Additionally, maturation of sustained swimming and swim-bladder inflation at 5 dpf makes locomotor endpoints interpretable (Hill et al., 2023; Kimmel et al., 1995). Measuring behaviour at both 4 and 5 dpf was deliberate, because motor competence changes markedly over this one-day interval and age at testing has been identified as a source of variation in larval locomotor assays (Hill et al., 2023). Reporting both time points allowed us to distinguish developmental effects from exposure effects. A limitation of the different exposure windows and designs is that endpoints were not all collected after an identical

exposure duration, so cross-chapter comparisons of effect thresholds should account for the shorter exposure and earlier sampling in Chapter 4.

Both transcriptomic analyses used a pooled whole-larva sampling design. While this approach provides an integrated measure of organismal response, it may dilute localised or tissue-specific effects. Future work targeting specific tissues or cell populations could resolve whether sertraline produces stronger localised transcriptional responses in neuroendocrine, vascular, or metabolic compartments. Extrapolating these developmental impacts to human health risks requires careful consideration of exposure routes, early developmental pharmacokinetics and pharmacodynamics, and zebrafish-to-human modelling. Models using zygotic microinjection may approximate human maternal-fetal transfer scenarios and early developmental effects more closely than waterborne exposure scenarios.

5.2. Significance and contribution to scientific knowledge

This thesis contributes to the development of an integrative *in vivo* testing platform to evaluate neuroactive contaminants that act as stress-response disruptors. A major contribution of this research is demonstrating the need for an external stressor or challenge to reveal neuroendocrine disruption, which is absent in traditional testing paradigms. By establishing the divergent transcriptomic effects of three compounds within the same pharmacological class, this research highlights the limitations of focusing studies on a single "model" SSRI (such as fluoxetine). Future studies comparing multiple SS(N)RIs within a standardised framework are required to unravel compound-specific effects and provide a stronger foundation for testing the effects of environmental mixtures. Under the conditions tested, low, environmentally relevant concentrations of individual SS(N)RIs are unlikely to impair basal HPI axis function or its stress-induced activation in zebrafish larvae. This adds an important perspective to the current ecotoxicological evidence, with the caveats that internal concentrations were not measured, that a single species and life stage were examined, and that mixtures remain to be tested. At pharmacological concentrations overlapping the human therapeutic plasma range, sertraline amplified stimulus-induced GR-mediated transcription, suppressed locomotor activity, and altered the transcription of genes associated with neural, vascular and metabolic signalling.

Because the organisation of the glucocorticoid stress axis and of the serotonergic system is conserved across vertebrates (Alsop & Vijayan, 2009a, 2009b; Schaaf et al., 2009), the SR4G zebrafish larva can be relevant beyond environmental risk assessment, and may serve as a model for screening the neuroendocrine effects of serotonergic drugs at patient-relevant concentrations.

5.3. Future perspectives

There are several important directions for future research. In addition to what has been outlined in the individual chapters, the following main lines of investigation should be considered:

1) Improvement of the integrative methodology described in Chapter 4 by testing diverse stimuli in combination with chemical exposure to screen potential stress-response-disrupting compounds.
2) Characterisation of tissue-level alterations following developmental exposure to SSRIs and SNRIs in larvae using spatial transcriptomics and proteomics to overcome the signal-dilution limitations of whole-body homogenates.
3) Correlation of eGFP reporter expression with single-cell transcriptional profiles to identify responsive cell populations.
4) Identification of the neural circuits affected by developmental exposure to SSRIs and SNRIs using *in situ* hybridisation and immunochemistry.
5) Extension of the integrative methodology described in Chapter 4 to questions beyond toxicology, for example, stress-behaviour interactions and the effects of environmental factors, such as temperature, osmotic change, light stimuli, and disrupted photoperiods.

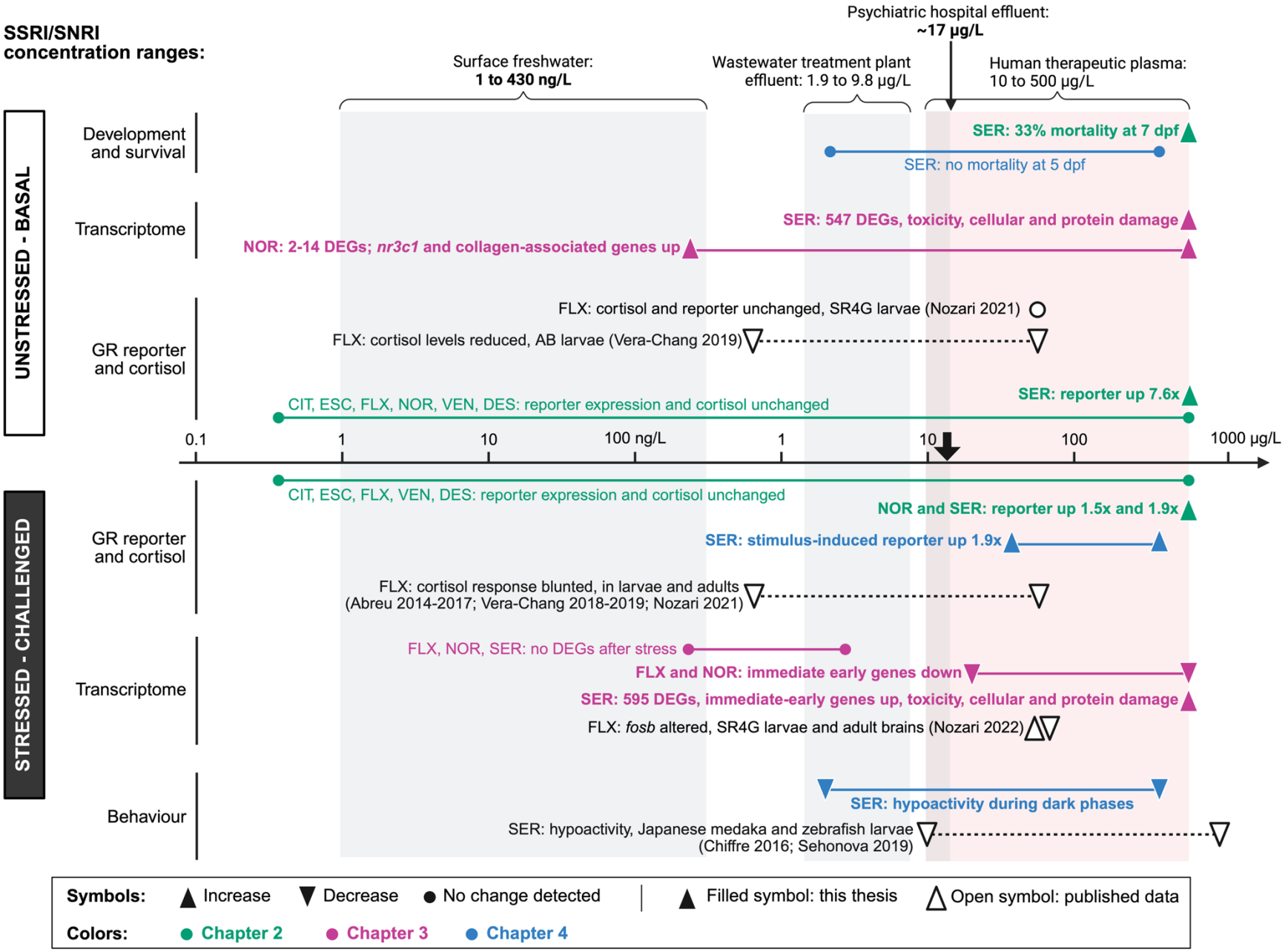
SSRI/SNRI
concentration ranges:
Surface freshwater:
1 to 430 ng/L
Wastewater treatment plant
effluent: 1.9 to 9.8 µg/L
Psychiatric hospital effluent:
~17 µg/L
Human therapeutic plasma:
10 to 500 µg/L
UNSTRESSED - BASAL
Development
and survival
SER: 33% mortality at 7 dpf
SER: no mortality at 5 dpf
Transcriptome
SER: 547 DEGs, toxicity, cellular and protein damage
NOR: 2-14 DEGs; nr3c1 and collagen-associated genes up
GR reporter
and cortisol
FLX: cortisol and reporter unchanged, SR4G larvae (Nozari 2021)
FLX: cortisol levels reduced, AB larvae (Vera-Chang 2019)
SER: reporter up 7.6x
CIT, ESC, FLX, NOR, VEN, DES: reporter expression and cortisol unchanged
0.1
1
10
100 ng/L
1
10
100
1000 µg/L
STRESSED - CHALLENGED
CIT, ESC, FLX, VEN, DES: reporter expression and cortisol unchanged
GR reporter
and cortisol
NOR and SER: reporter up 1.5x and 1.9x
SER: stimulus-induced reporter up 1.9x
FLX: cortisol response blunted, in larvae and adults
(Abreu 2014-2017; Vera-Chang 2018-2019; Nozari 2021)
Transcriptome
FLX, NOR, SER: no DEGs after stress
FLX and NOR: immediate early genes down
SER: 595 DEGs, immediate-early genes up, toxicity, cellular and protein damage
FLX: fosb altered, SR4G larvae and adult brains (Nozari 2022)
Behaviour
SER: hypoactivity during dark phases
SER: hypoactivity, Japanese medaka and zebrafish larvae
(Chiffre 2016; Sehonova 2019)
Symbols:
Increase
Decrease
No change detected
Filled symbol: this thesis
Open symbol: published data
Colors:
Chapter 2
Chapter 3
Chapter 4

Figure 5.1. SS(N)RI effects on the modulation of zebrafish stress responses across environmentally and pharmacologically relevant concentrations.
Test concentrations reported as nominal molar concentrations in the present studies were converted to mass concentrations for this figure using each compound's free-base molecular weight, to allow comparison with environmental and clinical measurements reported in ng/L and µg/L. Grey-shaded background bands highlight reported environmental concentrations of SS(N)RIs in different aquatic matrices: surface freshwater (1 to 430 ng/L; Mole & Brooks, 2019; Pappas et al., 2025), maximum measured concentrations in wastewater treatment plant effluent (1.9 to 9.8 µg/L; Mole & Brooks, 2019) and psychiatric hospital effluent (up to 17 µg/L; Arnnok et al., 2017; Davey et al., 2025). The red shaded background band highlights the human therapeutic reference range measured in plasma and is included for pharmacological context (Hiemke et al., 2018). The bold arrow marks approximately 15 µg/L, the lowest concentration at which any effect was detected in the current studies (50 nM sertraline). Entries above the axis summarise unstressed, basal conditions; entries below the axis summarise conditions following an acute netting stress or a light/dark stimulus. Symbol shape indicates the direction of the reported effect (increase or decrease) and symbol fill indicates the source (filled: this thesis; open: published data). Results from Chapters 2 to 4 are colour coded (teal: Chapter 2; magenta: Chapter 3; blue: Chapter 4). Individual symbols represent effects at one concentration; Horizontal bars represent a tested concentration range; Paired symbols joined by a dashed line represent two separate tested concentrations. Created with BioRender.com.

List of References

Abreu, M. S. de, Demin, K. A., Giacomini, A. C. V. V., Amstislavskaya, T. G., Strekalova, T., Maslov, G. O., Kositsin, Y., Petersen, E. V., & Kalueff, A. V. (2021). Understanding how stress responses and stress-related behaviors have evolved in zebrafish and mammals. *Neurobiology of Stress*, *15*(100405), 100405. https://doi.org/10.1016/j.ynstr.2021.100405

Abreu, M. S. de, Koakoski, G., Ferreira, D., Oliveira, T. A., Rosa, J. G. S., Gusso, D., Giacomini, A. C. V. V., Piato, A. L., & Barcellos, L. J. G. (2014). Diazepam and Fluoxetine Decrease the Stress Response in Zebrafish. *PLoS ONE*, *9*(7), 103232. https://doi.org/10.1371/journal.pone.0103232

Abreu, M. S., Giacomini, A. C. V. V., Koakoski, G., Oliveira, T. A., Gusso, D., Baldisserotto, B., & Barcellos, L. J. G. (2015). Effects of waterborne fluoxetine on stress response and osmoregulation in zebrafish. *Environmental Toxicology and Pharmacology*, *40*(3), 704–707. https://doi.org/10.1016/j.etap.2015.09.001

Abreu, M. S., Giacomini, A. C. V. V., Koakoski, G., Piato, A. L. S., & Barcellos, L. J. G. (2017). Divergent effect of fluoxetine on the response to physical or chemical stressors in zebrafish. *PeerJ*, *2017*(5), e3330. https://doi.org/10.7717/peerj.3330

Albert, P. R., Benkelfat, C., & Descarries, L. (2012). The neurobiology of depression—Revisiting the serotonin hypothesis. I. Cellular and molecular mechanisms. *Philosophical Transactions of the Royal Society B: Biological Sciences*, *367*(1601), 2378–2381. https://doi.org/10.1098/rstb.2012.0190

Alcaraz, A. J. G., Baraniuk, S., Mikulášek, K., Park, B., Lane, T., Burbridge, C., Ewald, J., Potěšil, D., Xia, J., Zdráhal, Z., Schneider, D., Crump, D., Basu, N., Hogan, N., Brinkmann, M., & Hecker, M. (2022). Comparative analysis of transcriptomic points-of-departure (tPODs) and apical responses in embryo-larval fathead minnows exposed to fluoxetine. *Environmental Pollution*, *295*, 118667. https://doi.org/10.1016/j.envpol.2021.118667

Alsop, D., & Vijayan, M. (2009a). The zebrafish stress axis: Molecular fallout from the teleost-specific genome duplication event. *General and Comparative Endocrinology*, *161*(1), 62–66. https://doi.org/10.1016/j.ygcen.2008.09.011

Alsop, D., & Vijayan, M. M. (2007). Development of the corticosteroid stress axis and receptor expression in zebrafish. *American Journal of Physiology - Regulatory Integrative and Comparative Physiology*, *294*(3), 711–719. https://doi.org/10.1152/ajpregu.00671.2007

Alsop, D., & Vijayan, M. M. (2009b). Molecular programming of the corticosteroid stress axis during zebrafish development. *Comparative Biochemistry and Physiology, Part A*, *153*(1), 49–54. https://doi.org/10.1016/j.cbpa.2008.12.008

Arnnok, P., Singh, R. R., Burakham, R., Pérez-Fuentetaja, A., & Aga, D. S. (2017). Selective Uptake and Bioaccumulation of Antidepressants in Fish from Effluent-Impacted Niagara River. *Environmental Science and Technology*, *51*(18), 10652–10662. https://doi.org/10.1021/acs.est.7b02912

Aryal, B., Aryal, D., Kim, E.-J., & Kim, H.-G. (2012). Pharmacokinetics of venlafaxine and its major metabolite o-desmethylvenlafaxine in freely moving mice using automated dosing/sampling system. *Indian Journal of Pharmacology*, *44*(1). https://doi.org/10.4103/0253-7613.91861

Ashburner, M., Ball, C. A., Blake, J. A., Botstein, D., Butler, H., Cherry, J. M., Davis, A. P., Dolinski, K., Dwight, S. S., Eppig, J. T., Harris, M. A., Hill, D. P., Issel-Tarver, L., Kasarskis, A., Lewis, S., Matese, J. C., Richardson, J. E., Ringwald, M., Rubin, G. M., & Sherlock, G. (2000). Gene Ontology: Tool for the unification of biology. *Nature Genetics*, *25*(1), 25–29. https://doi.org/10.1038/75556

Askary, A., Smeeton, J., Paul, S., Schindler, S., Braasch, I., Ellis, N. A., Postlethwait, J., Miller, C. T., & Crump, J. G. (2016). Ancient origin of lubricated joints in bony vertebrates. *eLife*, *5*, e16415. https://doi.org/10.7554/eLife.16415

Aslamkhan, A. G., Xu, Q., Loughlin, A., Vu, H., Pacchione, S., Bhatt, B., Garfinkel, I., Styring, T. G., LaFranco-Scheuch, L., Pearson, K., Reynolds, S., Li, N., Zhou, H., Miller, J. R., Solban, N., Bass, A., & Glaab, W. E. (2020). Characterization of indoleamine-2,3-dioxygenase 1, tryptophan-2,3-dioxygenase, and *Ido1/Tdo2* knockout mice. *Toxicology and Applied Pharmacology*, *406*, 115216. https://doi.org/10.1016/j.taap.2020.115216

aus der Beek, T., Weber, F.-A., Bergmann, A., Hickmann, S., Ebert, I., Hein, A., & Küster, A. (2016). Pharmaceuticals in the environment—Global occurrences and perspectives. *Environmental Toxicology and Chemistry*, *35*(4), 823–835. https://doi.org/10.1002/etc.3339

Bachour, R.-L., Golovko, O., Kellner, M., & Pohl, J. (2020). Behavioral effects of citalopram, tramadol, and binary mixture in zebrafish (*Danio rerio*) larvae. *Chemosphere*, *238*. https://doi.org/10.1016/j.chemosphere.2019.124587

Bailey, J., Oliveri, A., & Levin, E. D. (2013). Zebrafish model systems for developmental neurobehavioral toxicology. *Birth Defects Research (Part C)*, *99*, 14–23. https://doi.org/10.1002/bdrc.21027

Bambino, K., & Chu, J. (2017). Zebrafish in Toxicology and Environmental Health. In *Current Topics in Developmental Biology* (Vol. 124, pp. 331–367). Academic Press Inc. https://doi.org/10.1016/bs.ctdb.2016.10.007

Barton, B. A. (2002). Stress in Fishes: A Diversity of Responses with Particular Reference to Changes in Circulating Corticosteroids. *Integrative and Comparative Biology*, *42*(3), 517–525. https://doi.org/10.1093/icb/42.3.517

Bernier, N. J., Flik, G., & Klaren, P. H. M. (2009). Regulation and contribution of the corticotropic, melanotropic and thyrotropic axes to the stress response in fishes. In *Fish Neuroendocrinology* (Vol. 28, pp. 235–311). Academic Press. https://doi.org/10.1016/S1546-5098(09)28006-X

Blahova, J., Doubkova, V., Plhalova, L., Lakdawala, P., Medkova, D., Vecerek, V., Svobodova, Z., & Faggio, C. (2021). Embryotoxicity of Selective Serotonin Reuptake Inhibitors—Comparative Sensitivity of Zebrafish (*Danio rerio*) and

African Clawed Frog (*Xenopus laevis*) Embryos. *Applied Sciences*, *11*, 10015. https://doi.org/10.3390/app112110015

Bolanos-Palmieri, P., Schenk, H., Bähre, H., Schroder, P., Staggs, L., Haller, H., & Schiffer, M. (2025). Kynurenine Pathway Dysregulation Impairs Podocyte Morphology and Bioenergetics In Vitro and Leads to Glomerular Dysfunction. *The FASEB Journal*, *39*(22), e71228. https://doi.org/10.1096/fj.202502175R

Cannon, W. B. (1939). The Wisdom of the Body. *The American Journal of the Medical Sciences*, *198*(1), 113. https://doi.org/10.1097/00000441-193907000-00031

Castillo-Zacarías, C., Barocio, M. E., Hidalgo-Vázquez, E., Sosa-Hernández, J. E., Parra-Arroyo, L., López-Pacheco, I. Y., Barceló, D., Iqbal, H. N. M., & Parra-Saldívar, R. (2021). Antidepressant drugs as emerging contaminants: Occurrence in urban and non-urban waters and analytical methods for their detection. *Science of the Total Environment*, *757*(143722). https://doi.org/10.1016/j.scitotenv.2020.143722

Castro, M. E., Diaz, A., del Olmo, E., & Pazos, A. (2003). Chronic fluoxetine induces opposite changes in G protein coupling at pre and postsynaptic 5-HT1A receptors in rat brain. *Neuropharmacology*, *44*(1), 93–101. https://doi.org/10.1016/S0028-3908(02)00340-4

Chakravarthy, S., Sadagopan, S., Nair, A., & Sukumaran, S. K. (2014). Zebrafish as an In Vivo High-Throughput Model for Genotoxicity. *Zebrafish*, *11*(2), 154–166. https://doi.org/10.1089/zeb.2013.0924

Chatzopoulou, A., Roy, U., Meijer, A. H., Alia, A., Spaink, H. P., & Schaaf, M. J. M. (2015). Transcriptional and Metabolic Effects of Glucocorticoid Receptor α and β Signaling in Zebrafish. *Endocrinology*, *156*(5), 1757–1769. https://doi.org/10.1210/en.2014-1941

Chatzopoulou, A., Schoonheim, P. J., Torraca, V., Meijer, A. H., Spaink, H. P., & Schaaf, M. J. M. (2017). Functional analysis reveals no transcriptional role for the glucocorticoid receptor β-isoform in zebrafish. *Molecular and Cellular Endocrinology*, *447*, 61–70. https://doi.org/10.1016/j.mce.2017.02.036

ChemSpider: Search and Share Chemistry. (2026). https://www.chemspider.com/

Chen, H., Liang, X., Gu, X., Zeng, Q., Mao, Z., & Martyniuk, C. J. (2021). Environmentally relevant concentrations of sertraline disrupts behavior and the brain and liver transcriptome of juvenile yellow catfish (*Tachysurus fulvidraco*): Implications for the feeding and growth axis. *Journal of Hazardous Materials*, *409*. https://doi.org/10.1016/j.jhazmat.2020.124974

Chen, S., Wu, Q., Li, X., Li, D., Fan, M., Ren, Z., Bryant, M., Mei, N., Ning, B., & Guo, L. (2020). The role of hepatic cytochrome P450s in the cytotoxicity of sertraline. *Archives of Toxicology*, *94*(7), 2401–2411. https://doi.org/10.1007/s00204-020-02753-y

Chen, S., Xuan, J., Couch, L., Iyer, A., Wu, Y., Li, Q.-Z., & Guo, L. (2014). Sertraline induces endoplasmic reticulum stress in hepatic cells. *Toxicology*, *322*, 78–88. https://doi.org/10.1016/j.tox.2014.05.007

Chen, S., Xuan, J., Wan, L., Lin, H., Couch, L., Mei, N., Dobrovolsky, V. N., & Guo, L. (2013, November 5). Sertraline, an Antidepressant, Induces Apoptosis in Hepatic Cells Through the Mitogen-Activated Protein Kinase Pathway. *Toxicological Sciences*, *137*(2), 404–415. https://doi.org/10.1093/toxsci/kft254

Cheng, Y.-C., Scotting, P. J., Hsu, L.-S., Lin, S.-J., Shih, H.-Y., Hsieh, F.-Y., Wu, H.-L., Tsao, C.-L., & Shen, C.-J. (2013). Zebrafish *rgs4* is essential for motility and axonogenesis mediated by Akt signaling. *Cellular and Molecular Life Sciences*, *70*(5), 935–950. https://doi.org/10.1007/s00018-012-1178-z

Chiffre, A., Clérandeau, C., Dwoinikoff, C., Le Bihanic, F., Budzinski, H., Geret, F., & Cachot, J. (2016). Psychotropic drugs in mixture alter swimming behaviour of Japanese medaka (Oryzias latipes) larvae above environmental concentrations. *Environmental Science and Pollution Research*, *23*(6), 4964–4977. https://doi.org/10.1007/s11356-014-3477-4

Cipriani, A., Ferla, T. L., Furukawa, T. A., Signoretti, A., Nakagawa, A., Churchill, R., McGuire, H., & Barbui, C. (2010). Sertraline versus other antidepressive agents for depression. *The Cochrane Database of Systematic Reviews*, (4), CD006117. https://doi.org/10.1002/14651858.CD006117.pub4

Cipriani, A., Furukawa, T. A., Salanti, G., Chaimani, A., Atkinson, L. Z., Ogawa, Y., Leucht, S., Ruhe, H. G., Turner, E. H., Higgins, J. P. T., Egger, M., Takeshima, N., Hayasaka, Y., Imai, H., Shinohara, K., Tajika, A., Ioannidis, J. P. A., & Geddes, J. R. (2018). Comparative efficacy and acceptability of 21 antidepressant drugs for the acute treatment of adults with major depressive disorder: A systematic review and network meta-analysis. *The Lancet*, *391*(10128), 1357–1366. https://doi.org/10.1016/S0140-6736(17)32802-7

Colville, C., Alcaraz, A. J., Green, D., Park, B., Xia, J., Soufan, O., Hruška, P., Potěšil, D., Zdráhal, Z., Crump, D., Basu, N., Hogan, N., & Hecker, M. (2022). Characterizing toxicity pathways of fluoxetine to predict adverse outcomes in adult fathead minnows (*Pimephales promelas*). *Science of The Total Environment*, *817*, 152747. https://doi.org/10.1016/j.scitotenv.2021.152747

Conley, J. M., Symes, S. J., Schorr, M. S., & Richards, S. M. (2008). Spatial and temporal analysis of pharmaceutical concentrations in the upper Tennessee River basin. *Chemosphere*, *73*(8), 1178–1187. https://doi.org/10.1016/j.chemosphere.2008.07.062

Coppen, A. (1967). The Biochemistry of Affective Disorders. *The British Journal of Psychiatry*, *113*(504), 1237–1264. https://doi.org/10.1192/bjp.113.504.1237

Correia, D., Bellot, M., Prats, E., Gómez-Canela, C., Moro, H., Raldúa, D., Domingues, I., Oliveira, M., & Faria, M. (2023a). Impact of environmentally relevant concentrations of fluoxetine on zebrafish larvae: From gene to behavior. *Chemosphere*, *345*, 140468. https://doi.org/10.1016/j.chemosphere.2023.140468

Correia, D., Bellot, M., Prats, E., Gómez-Canela, C., Moro, H., Raldúa, D., Domingues, I., Oliveira, M., & Faria, M. (2023b). Impact of environmentally relevant concentrations of fluoxetine on zebrafish larvae: From gene to behavior. *Chemosphere*, *345*, 140468. https://doi.org/10.1016/j.chemosphere.2023.140468

Correia, D., Domingues, I., Faria, M., & Oliveira, M. (2023). Effects of fluoxetine on fish: What do we know and where should we focus our efforts in the future? *Science of The Total Environment*, *857*, 159486. https://doi.org/10.1016/j.scitotenv.2022.159486

Cunha, V., Rodrigues, P., Santos, M. M., Moradas-ferreira, P., & Ferreira, M. (2016). Danio rerio embryos on Prozac – Effects on the detoxification mechanism and embryo development. *Aquatic Toxicology*, *178*, 182–189. https://doi.org/10.1016/j.aquatox.2016.08.003

Cunha, V., Rodrigues, P., Santos, M. M., Moradas-ferreira, P., & Ferreira, M. (2018). Fluoxetine modulates the transcription of genes involved in serotonin, dopamine and adrenergic signalling in zebrafish embryos. *Chemosphere*, *191*, 954–961. https://doi.org/10.1016/j.chemosphere.2017.10.100

Davey, C. J. E., Hartelust, A. K., Helmus, R., Praetorius, A., Van Wezel, A. P., & Ter Laak, T. L. (2025). Presence, removal, and risks of psychopharmaceuticals in wastewater streams. *Environmental Toxicology and Chemistry*, *44*(2), 375–385. https://doi.org/10.1093/etojnl/vgae042

de Farias, N. O., Oliveira, R., Moretti, P. N. S., e Pinto, J. M., Oliveira, A. C., Santos, V. L., Rocha, P. S., Andrade, T. S., & Grisolia, C. K. (2020). Fluoxetine chronic exposure affects growth, behavior and tissue structure of zebrafish. *Comparative Biochemistry and Physiology, Part C*, *237*. https://doi.org/10.1016/j.cbpc.2020.108836

de Farias, N. O., Oliveira, R., Sousa-Moura, D., de Oliveira, R. C. S., Rodrigues, M. A. C., Andrade, T. S., Domingues, I., Camargo, N. S., Muehlmann, L. A., & Grisolia, C. K. (2019). Exposure to low concentration of fluoxetine affects development, behaviour and acetylcholinesterase activity of zebrafish embryos. *Comparative Biochemistry and Physiology, Part C*, *215*, 1–8. https://doi.org/10.1016/j.cbpc.2018.08.009

Demin, K. A., Kolesnikova, T. O., Galstyan, D. S., Krotova, N. A., Ilyin, N. P., Derzhavina, K. A., Levchenko, N. A., Strekalova, T., de Abreu, M. S., Petersen, E. V., Seredinskaya, M., Cherneyko, Y. V., Kositsyn, Y. M., Sorokin, D. V., Zabegalov, K. N., Mor, M. S., Efimova, E. V., & Kalueff, A. V. (2021). Modulation of behavioral and neurochemical responses of adult zebrafish by fluoxetine, eicosapentaenoic acid and lipopolysaccharide in the prolonged chronic unpredictable stress model. *Scientific Reports*, *11*(1). https://doi.org/10.1038/S41598-021-92422-6

DeVane, C. L., Liston, H. L., & Markowitz, J. S. (2002). Clinical Pharmacokinetics of Sertraline. *Clinical Pharmacokinetics*, *41*(15), 1247–1266. https://doi.org/10.2165/00003088-200241150-00002

Diaz-Camal, N., Cardoso-Vera, J. D., Islas-Flores, H., Gómez-Oliván, L. M., & Mejía-García, A. (2022). Consumption and ocurrence of antidepressants (SSRIs) in pre- and post-COVID-19 pandemic, their environmental impact and innovative removal methods: A review. *Science of the Total Environment*, *829*(154656). https://doi.org/10.1016/j.scitotenv.2022.154656

Dinan, T. G. (1996). Serotonin and the Regulation of Hypothalamic-Pituitary-Adrenal Axis Function. *Life Sciences*, *58*(20), 1683–1694.

Duarte, I. A., Fick, J., Cabral, H. N., & Fonseca, V. F. (2022). Bioconcentration of neuroactive pharmaceuticals in fish: Relation to lipophilicity, experimental design and toxicity in the aquatic environment. *Science of the Total Environment*, *812*. https://doi.org/10.1016/j.scitotenv.2021.152543

Duarte, I. A., Pais, M. P., Reis-Santos, P., Cabral, H. N., & Fonseca, V. F. (2019). Biomarker and behavioural responses of an estuarine fish following acute exposure to fluoxetine. *Marine Environmental Research*, *147*, 24–31. https://doi.org/10.1016/j.marenvres.2019.04.002

Duarte, I. A., Reis-Santos, P., Fick, J., Cabral, H. N., Duarte, B., & Fonseca, V. F. (2023). Neuroactive pharmaceuticals in estuaries: Occurrence and tissue-specific bioaccumulation in multiple fish species. *Environmental Pollution*, *316*. https://doi.org/10.1016/j.envpol.2022.120531

Egan, R. J., Bergner, C. L., Hart, P. C., Cachat, J. M., Canavello, P. R., Elegante, M. F., Elkhayat, S. I., Bartels, B. K., Tien, A. K., Tien, D. H., Mohnot, S., Beeson, E., Glasgow, E., Amri, H., Zukowska, Z., & Kalueff, A. V. (2009). Understanding behavioral and physiological phenotypes of stress and anxiety in zebrafish. *Behavioural Brain Research*, *205*, 38–44. https://doi.org/10.1016/j.bbr.2009.06.022

Elbassiouny, A. A., Buck, L. T., Abatti, L. E., Mitchell, J. A., Crampton, W. G. R., Lovejoy, N. R., & Chang, B. S. W. (2024). Evolution of a novel regulatory mechanism of hypoxia inducible factor in hypoxia-tolerant electric fishes. *Journal of Biological Chemistry*, *300*(3). https://doi.org/10.1016/j.jbc.2024.105727

El-Farhan, N., Rees, D. A., & Evans, C. (2017). Measuring cortisol in serum, urine and saliva – are our assays good enough? *Annals of Clinical Biochemistry*, *54*(3), 308–322. https://doi.org/10.1177/0004563216687335

Facchinello, N., Skobo, T., Meneghetti, G., Colletti, E., Dinarello, A., Tiso, N., Costa, R., Gioacchini, G., Carnevali, O., Argenton, F., Colombo, L., & Dalla Valle, L. (2017). *Nr3c1* null mutant zebrafish are viable and reveal DNA-binding-independent activities of the glucocorticoid receptor. *Scientific Reports*, *7*(1), 4371. https://doi.org/10.1038/s41598-017-04535-6

Fernandes, M. J., Paíga, P., Silva, A., Llaguno, C. P., Carvalho, M., Vázquez, F. M., & Delerue-Matos, C. (2020). Antibiotics and antidepressants occurrence in surface waters and sediments collected in the north of Portugal. *Chemosphere*, *239*, 124729. https://doi.org/10.1016/j.chemosphere.2019.124729

Ferreira, C. S. S., Soares, S. C., Kille, P., & Oliveira, M. (2023). Identifying knowledge gaps in understanding the effects of selective serotonin reuptake inhibitors (SSRIs) on fish behaviour. *Chemosphere*, *335*, 139124. https://doi.org/10.1016/J.CHEMOSPHERE.2023.139124

Fick, J., Söderström, H., Lindberg, R. H., Phan, C., Tysklind, M., & Larsson, D. G. J. (2009). Contamination of surface, ground, and drinking water from pharmaceutical

production. *Environmental Toxicology and Chemistry*, *28*(12), 2522–2527. https://doi.org/10.1897/09-073.1

Fitzgerald, J. A., Könemann, S., Krümpelmann, L., Županič, A., & vom Berg, C. (2020). Approaches to Test the Neurotoxicity of Environmental Contaminants in the Zebrafish Model: From Behavior to Molecular Mechanisms. *Environmental Toxicology and Chemistry*, *40*(4), 989–1006. https://doi.org/10.1002/etc.4951

Flynn, E. J., Trent, C. M., & Rawls, J. F. (2009). Ontogeny and nutritional control of adipogenesis in zebrafish (*Danio rerio*). *Journal of Lipid Research*, *50*(8), 1641–1652. https://doi.org/10.1194/jlr.M800590-JLR200

Gallo-Payet, N., Martinez, A., & Lacroix, A. (2017). Editorial: ACTH Action in the Adrenal Cortex: From Molecular Biology to Pathophysiology. *Frontiers in Endocrinology*, *8*(101), 12. https://doi.org/10.3389/fendo.2017.00101

Gerri, C., Marass, M., Rossi, A., & Stainier, D. Y. R. (2018). Hif-1α and Hif-2α regulate hemogenic endothelium and hematopoietic stem cell formation in zebrafish. *Blood*, *131*(9), 963–973. https://doi.org/10.1182/blood-2017-07-797795

Gerri, C., Marín-Juez, R., Marass, M., Marks, A., Maischein, H.-M., & Stainier, D. Y. R. (2017). Hif-1α regulates macrophage-endothelial interactions during blood vessel development in zebrafish. *Nature Communications*, *8*(1), 15492. https://doi.org/10.1038/ncomms15492

Gesto, M., López-Patïo, M. A., Hernández, J., Soengas, J. L., & Míguez, J. M. (2013). The response of brain serotonergic and dopaminergic systems to an acute stressor in rainbow trout: A time course study. *Journal of Experimental Biology*, *216*(23), 4435–4442. https://doi.org/10.1242/jeb.091751

Godoy, L. D., Rossignoli, M. T., Delfino-Pereira, P., Garcia-Cairasco, N., & Umeoka, E. H. de L. (2018). A comprehensive overview on stress neurobiology: Basic concepts and clinical implications. *Frontiers in Behavioral Neuroscience*, *12*, 127. https://doi.org/10.3389/fnbeh.2018.00127

Gould, G. G., Brooks, B. W., & Frazer, A. (2007). [3H] Citalopram Binding to Serotonin Transporter Sites in Minnow Brains. *Basic & Clinical Pharmacology & Toxicology*, *101*(3), 203–210. https://doi.org/10.1111/j.1742-7843.2007.00100.x

Gould, S. L., Winter, M. J., Norton, W. H. J., & Tyler, C. R. (2021). The potential for adverse effects in fish exposed to antidepressants in the aquatic environment. *Environmental Science & Technology*, *55*(24), 16299–16312. https://doi.org/10.1021/acs.est.1c04724

Grohol, J. M., & Wright, S. A. (2022, November 1). *Top 25 Psychiatric Medications for 2020*. Psych Central. https://psychcentral.com/blog/top-25-psychiatric-medications-for-2020

Gunnarsson, L., Jauhiainen, A., Kristiansson, E., Nerman, O., & Larsson, D. G. J. (2008). Evolutionary Conservation of Human Drug Targets in Organisms used for Environmental Risk Assessments. *Environmental Science & Technology*, *42*(15), 5807–5813. https://doi.org/10.1021/es8005173

Harris, B. N., & Carr, J. A. (2016). The role of the hypothalamus-pituitary-adrenal/interrenal axis in mediating predator-avoidance trade-offs. *General and Comparative Endocrinology*, *230–231*, 110–142. https://doi.org/10.1016/j.ygcen.2016.04.006

Heitzer, M. D., Wolf, I. M., Sanchez, E. R., Witchel, S. F., & DeFranco, D. B. (2007). Glucocorticoid receptor physiology. *Reviews in Endocrine and Metabolic Disorders*, *8*(4), 321–330. https://doi.org/10.1007/s11154-007-9059-8

Henry, J., Bai, Y., Kreuder, F., Mawdsley, D., Kaslin, J., & Wlodkowic, D. (2022). Accelerating Chemobehavioral Phenotypic Screening in Neurotoxicology Using a Living Embryo Array System. *Zebrafish*, *19*(1), 32–35. https://doi.org/10.1089/zeb.2021.0072

Henry, J., Bai, Y., Kreuder, F., Saaristo, M., Kaslin, J., & Wlodkowic, D. (2022). Sensory-Motor Perturbations in Larval Zebrafish (*Danio rerio*) Induced by Exposure to Low Levels of Neuroactive Micropollutants during Development. *International Journal of Molecular Sciences*, *23*(16), 8990. https://doi.org/10.3390/ijms23168990

Herculano, A. M., & Maximino, C. (2014a). Serotonergic modulation of zebrafish behavior: Towards a paradox. *Progress in Neuro-Psychopharmacology and Biological Psychiatry*, *55*, 50–66. https://doi.org/10.1016/j.pnpbp.2014.03.008

Herculano, A. M., & Maximino, C. (2014b). Serotonergic modulation of zebrafish behavior: Towards a paradox. *Progress in Neuro-Psychopharmacology and Biological Psychiatry, Special Issue: Zebrafish Models of Brain Disorders*, *55*, 50–66. https://doi.org/10.1016/j.pnpbp.2014.03.008

Hiemke, C., Bergemann, N., Clement, H. W., Conca, A., Deckert, J., Domschke, K., Eckermann, G., Egberts, K., Gerlach, M., Greiner, C., Gründer, G., Haen, E., Havemann-Reinecke, U., Hefner, G., Helmer, R., Janssen, G., Jaquenoud, E., Laux, G., Messer, T., … Baumann, P. (2018). Consensus Guidelines for Therapeutic Drug Monitoring in Neuropsychopharmacology: Update 2017. *Pharmacopsychiatry*, *51*(1/2), 9–62. https://doi.org/10.1055/s-0043-116492

Hiemke, C., & Härtter, S. (2000). Pharmacokinetics of selective serotonin reuptake inhibitors. *Pharmacology & Therapeutics*, *85*, 11–28.

Hill, B. N., Britton, K. N., Hunter, D. L., Olin, J. K., Lowery, M., Hedge, J. M., Knapp, B. R., Jarema, K. A., Rowson, Z., & Padilla, S. (2023). Inconsistencies in variable reporting and methods in larval zebrafish behavioral assays. *Neurotoxicology and Teratology*, *96*. https://doi.org/10.1016/j.ntt.2023.107163

Höglund, E., Balm, P. H. M., & Winberg, S. (2002). Stimulatory and inhibitory effects of 5-HT1A receptors on adrenocorticotropic hormone and cortisol secretion in a teleost fish, the Arctic charr (*Salvelinus alpinus*). *Neuroscience Letters*, *324*(3), 193–196. https://doi.org/10.1016/S0304-3940(02)00200-8

Honda, K., Han, M., Mori, F., Morinaga, A., Nishimura, Y., Kaneko, R., Oizumi, K., Kajiyama, H., Ihara, M. O., Zhang, H., Kato, D., Toyota, K., Lange, A., Tyler, C. R., Iguchi, T., Mushirobira, Y., Nagae, M., Soyano, K., Ihara, M., & Miyagawa, S. (2026). Characterizationof Fish Serotonin, Dopamine and

NorepinephrineTransporters as a Potential Target for Environmental Pharmaceuticals. *Environmental Science & Technology*, *60*(35), 24580–24590. https://doi.org/10.1021/acs.est.6c04982

Horzmann, K. A., & Freeman, J. L. (2018). Making Waves: New Developments in Toxicology With the Zebrafish. *Toxicological Sciences*, *163*(1), 5–12. https://doi.org/10.1093/toxsci/kfy044

Howe, K., Clark, M. D., Torroja, C. F., Torrance, J., Berthelot, C., Muffato, M., Collins, J. E., Humphray, S., Mclaren, K., Matthews, L., Mclaren, S., Sealy, I., Caccamo, M., White, S., Chow, W., Kilian, B., Churcher, C., Scott, C., Barrett, J. C., … Stemple, D. L. (2013). The zebrafish reference genome sequence and its relationship to the human genome. *Nature*, *496*, 498–503. https://doi.org/10.1038/nature12111

Huang, I. J., Sirotkin, H. I., & McElroy, A. E. (2019). Varying the exposure period and duration of neuroactive pharmaceuticals and their metabolites modulates effects on the visual motor response in zebrafish (*Danio rerio*) larvae. *Neurotoxicology and Teratology*, *72*, 39–48. https://doi.org/10.1016/j.ntt.2019.01.006

Isaac, R., Boura-Halfon, S., Gurevitch, D., Shainskaya, A., Levkovitz, Y., & Zick, Y. (2012). Selective Serotonin Reuptake Inhibitors (SSRIs) Inhibit Insulin Secretion and Action in Pancreatic β Cells. *Journal of Biological Chemistry*, *288*(8), 5682–5693. https://doi.org/10.1074/jbc.M112.408641

Jensen, M. A., Mortier, L., Koh, E., Keevil, B., Hyttinen, S., & Hansen, Å. M. (2014). An interlaboratory comparison between similar methods for determination of melatonin, cortisol and testosterone in saliva. *Scandinavian Journal of Clinical and Laboratory Investigation*, *74*(5), 454–461. https://doi.org/10.3109/00365513.2014.900693

Jørgensen, H., Kjær, A., Knigge, U., Møller, M., & Warberg, J. (2003). Serotonin stimulates hypothalamic mRNA expression and local release of neurohypophysial peptides. *Journal of Neuroendocrinology*, *15*(6), 564–571. https://doi.org/10.1046/j.1365-2826.2003.01032.x

Jørgensen, H., Knigge, U., Kjær, A., Møller, M., & Warberg, J. (2002). Serotonergic stimulation of corticotropin-releasing hormone and pro-opiomelanocortin gene expression. *Journal of Neuroendocrinology*, *14*(10), 788–795. https://doi.org/10.1046/j.1365-2826.2002.00839.x

Katz, H. R., Arcese, A. A., Bloom, O., & Morgan, J. R. (2022). Activating Transcription Factor 3 (ATF3) is a Highly Conserved Pro-regenerative Transcription Factor in the Vertebrate Nervous System. *Frontiers in Cell and Developmental Biology*, *10*. https://doi.org/10.3389/fcell.2022.824036

Kazi, K. J., English, C. D., Ivantsova, E., Souders II, C. L., & Martyniuk, C. J. (2024). Transcriptome networks and physiology related to cardiac function and motor activity are perturbed in larval zebrafish (*Danio rerio*) following exposure to the antidepressant citalopram. *Environmental Pollution*, *361*, 124767. https://doi.org/10.1016/j.envpol.2024.124767

Kellner, M., Porseryd, T., Porsch-Hällström, I., Borg, B., Roufidou, C., & Olsén, K. H. (2018). Developmental exposure to the SSRI citalopram causes long-lasting behavioural effects in the three-spined stickleback (*Gasterosteus aculeatus*). *Ecotoxicology*, *27*(1), 12–22. https://doi.org/10.1007/S10646-017-1866-4

Kimmel, C. B., Ballard, W. W., Kimmel, S. R., Ullmann, B., & Schilling, T. F. (1995). Stages of embryonic development of the zebrafish. *Developmental Dynamics*, *203*(3), 253–310. https://doi.org/10.1002/aja.1002030302

Knigge, T. (2024). Antidepressants – The new endocrine disruptors? The case of crustaceans. *Molecular and Cellular Endocrinology*, *583*. https://doi.org/10.1016/j.mce.2024.112155

Kostich, M. S., Batt, A. L., & Lazorchak, J. M. (2014). Concentrations of prioritized pharmaceuticals in effluents from 50 large wastewater treatment plants in the US and implications for risk estimation. *Environmental Pollution*, *184*, 354–359. https://doi.org/10.1016/j.envpol.2013.09.013

Kreke, N., & Dietrich, D. R. (2008). Physiological endpoints for potential SSRI interactions in fish. *Critical Reviews in Toxicology*, *38*(3), 215–247. https://doi.org/10.1080/10408440801891057

Krug, R. G., Poshusta, T. L., Skuster, K. J., Berg, M. R., Gardner, S. L., & Clark, K. J. (2014). A transgenic zebrafish model for monitoring glucocorticoid receptor activity. *Genes, Brain, and Behavior*, *13*(5), 478–487. https://doi.org/10.1111/gbb.12135

Lambert, O., & Bourin, M. (2002). SNRIs: Mechanism of action and clinical features. *Expert Review of Neurotherapeutics*, *2*(6), 849–858. https://doi.org/10.1586/14737175.2.6.849

Laux, G. (2022a). Antidepressants: Definition, Classification, Guidelines. In *NeuroPsychopharmacotherapy* (pp. 1101–1108). Springer, Cham. https://doi.org/10.1007/978-3-030-62059-2_24

Laux, G. (2022b). Serotonin Reuptake Inhibitors: Citalopram, Escitalopram, Fluoxetine, Fluvoxamine, Paroxetine, and Sertraline. In *NeuroPsychopharmacotherapy* (pp. 1257–1269). Springer, Cham. https://doi.org/10.1007/978-3-030-62059-2_413

Le Moal, M. (2007). Historical approach and evolution of the stress concept: A personal account. *Psychoneuroendocrinology, Integrative Approaches to Neural Plasticity (Lille Summer School, 2006)*, *32*, S3–S9. https://doi.org/10.1016/j.psyneuen.2007.03.019

Lee, H., Curry, J., Stead, J. D. H., Williams, A., Atlas, E., Eccles, K. M., Mennigen, J. A., Yauk, C., & O'Brien, J. M. (2025). Acute toxicity, behaviour, metabolism, and transcriptomic points of departure in embryo-larval zebrafish exposed to nine different PFAS. *Journal of Hazardous Materials*, *500*, 140599. https://doi.org/10.1016/j.jhazmat.2025.140599

Lee, H. J., Hou, Y., Chen, Y., Dailey, Z. Z., Riddihough, A., Jang, H. S., Wang, T., & Johnson, S. L. (2020). Regenerating zebrafish fin epigenome is characterized by

stable lineage-specific DNA methylation and dynamic chromatin accessibility. *Genome Biology*, *21*(1), 52. https://doi.org/10.1186/s13059-020-1948-0

León-Olea, M., Martyniuk, C. J., Orlando, E. F., Ottinger, M. A., Rosenfeld, C. S., Wolstenholme, J. T., & Trudeau, V. L. (2014). Current concepts in neuroendocrine disruption. *General and Comparative Endocrinology*, *203*, 158–173. https://doi.org/10.1016/j.ygcen.2014.02.005

Li, C., Ma, H., Wang, Y., Cao, Z., Graves-Deal, R., Powell, A. E., Starchenko, A., Ayers, G. D., Washington, M. K., Kamath, V., Desai, K., Gerdes, M. J., Solnica-Krezel, L., & Coffey, R. J. (2014). Excess PLAC8 promotes an unconventional ERK2-dependent EMT in colon cancer. *The Journal of Clinical Investigation*, *124*(5), 2172–2187. https://doi.org/10.1172/JCI71103

Li, L., Xing, W., Jiang, L., Chen, D., & Zhang, G. (2023). NR3C1 overexpression regulates the expression and alternative splicing of inflammation-associated genes involved in PTSD. *Gene*, *859*, 147199. https://doi.org/10.1016/j.gene.2023.147199

Lillesaar, C. (2011). The serotonergic system in fish. *Journal of Chemical Neuroanatomy*, *41*(4), 294–308. https://doi.org/10.1016/j.jchemneu.2011.05.009

Lim, J. E., Porteus, C. S., & Bernier, N. J. (2013). Serotonin directly stimulates cortisol secretion from the interrenals in goldfish. *General and Comparative Endocrinology*, *192*, 246–255. https://doi.org/10.1016/j.ygcen.2013.08.008

Lin, J.-C., Hu, S., Ho, P.-H., Hsu, H.-J., Postlethwait, J. H., & Chung, B. (2015). Two Zebrafish *hsd3b* Genes Are Distinct in Function, Expression, and Evolution. *Endocrinology*, *156*(8), 2854–2862. https://doi.org/10.1210/en.2014-1584

Lin, S.-J., Chiang, M.-C., Shih, H.-Y., Hsu, L.-S., Yeh, T.-H., Huang, Y.-C., Lin, C.-Y., & Cheng, Y.-C. (2017). Regulator of G protein signaling 2 (Rgs2) regulates neural crest development through Pparδ-Sox10 cascade. *Biochimica et Biophysica Acta (BBA) - Molecular Cell Research*, *1864*(3), 463–474. https://doi.org/10.1016/j.bbamcr.2016.12.013

Livak, K. J., & Schmittgen, T. D. (2001). Analysis of Relative Gene Expression Data Using Real-Time Quantitative PCR and the 2−ΔΔCT Method. *Methods*, *25*(4), 402–408. https://doi.org/10.1006/meth.2001.1262

Locher, C., Koechlin, H., Zion, S. R., Werner, C., Pine, D. S., Kirsch, I., Kessler, R. C., & Kossowsky, J. (2017). Efficacy and Safety of Selective Serotonin Reuptake Inhibitors, Serotonin-Norepinephrine Reuptake Inhibitors, and Placebo for Common Psychiatric Disorders Among Children and Adolescents: A Systematic Review and Meta-analysis. *JAMA Psychiatry*, *74*(10), 1011–1020. https://doi.org/10.1001/jamapsychiatry.2017.2432

Loomer, H. P., Saunders, J. C., & Kline, N. S. (1957). A clinical and pharmacodynamic evaluation of iproniazid as a psychic energizer. *Psychiatric Research Reports*, *8*, 129–141.

López-Muñoz, F., & Álamo, C. (2016). History of the Discovery of Antidepressant Drugs. In F. López-Muñoz, V. Srinivasan, D. De Berardis, C. Álamo, & T. A. Kato (Eds),

Melatonin, Neuroprotective Agents and Antidepressant Therapy (pp. 365–383). Springer India. https://doi.org/10.1007/978-81-322-2803-5_26

Love, M. I., Huber, W., & Anders, S. (2014). Moderated estimation of fold change and dispersion for RNA-seq data with DESeq2. *Genome Biology*, *15*(12), 1–21. https://doi.org/10.1186/s13059-014-0550-8

Lowry, C. A., & Lowry, C. A. (2002). Functional Subsets of Serotonergic Neurones: Implications for Control of the Hypothalamic-Pituitary-Adrenal Axis. *Journal of Neuroendocrinology*, *14*(11), 911–923. https://doi.org/10.1046/j.1365-2826.2002.00861.x

Lu, C., Peng, D., Erandani, W. C. K. U., Mitchell, K., Martyniuk, C. J., & Trudeau, V. L. (2023). Simultaneous extraction and detection of peptides, steroids, and proteins in small tissue samples. *Frontiers in Endocrinology*, *14*, 1266985. https://doi.org/10.3389/fendo.2023.1266985

Marcon, M., Herrmann, A. P., Mocelin, R., Rambo, C. L., Koakoski, G., Abreu, M. S., Conterato, G. M. M., Kist, L. W., Bogo, M. R., Zanatta, L., Barcellos, L. J. G., & Piato, A. L. (2016). Prevention of unpredictable chronic stress-related phenomena in zebrafish exposed to bromazepam, fluoxetine and nortriptyline. *Psychopharmacology*, *233*(21–22), 3815–3824. https://doi.org/10.1007/s00213-016-4408-5

Martens, M., Ammar, A., Riutta, A., Waagmeester, A., Slenter, D. N., Hanspers, K., A. Miller, R., Digles, D., Lopes, E. N., Ehrhart, F., Dupuis, L. J., Winckers, L. A., Coort, S. L., Willighagen, E. L., Evelo, C. T., Pico, A. R., & Kutmon, M. (2021). WikiPathways: Connecting communities. *Nucleic Acids Research*, *49*(D1), D613–D621. https://doi.org/10.1093/nar/gkaa1024

Martinez, R., Vera-Chang, M. N., Haddad, M., Zon, J., Navarro-Martin, L., Trudeau, V. L., & Mennigen, J. A. (2019). Developmental fluoxetine exposure in zebrafish reduces offspring basal cortisol concentration via life stage-dependent maternal transmission. *PLoS ONE*, *14*(2), e0212577. https://doi.org/10.1371/journal.pone.0212577

Maulvault, A. L., Camacho, C., Barbosa, V., Alves, R., Anacleto, P., Pousão-Ferreira, P., Rosa, R., Marques, A., & Diniz, M. S. (2019). Living in a multi-stressors environment: An integrated biomarker approach to assess the ecotoxicological response of meagre (*Argyrosomus regius*) to venlafaxine, warming and acidification. *Environmental Research*, *169*, 7–25. https://doi.org/10.1016/j.envres.2018.10.021

Maximino, C., Puty, B., Matos Oliveira, K. R., & Herculano, A. M. (2013). Behavioral and neurochemical changes in the zebrafish leopard strain. *Genes, Brain and Behavior*, *12*(5), 576–582. https://doi.org/10.1111/gbb.12047

McDonald, M. D. (2017). An AOP analysis of selective serotonin reuptake inhibitors (SSRIs) for fish. *Comparative Biochemistry and Physiology Part C: Toxicology & Pharmacology*, *197*, 19–31. https://doi.org/10.1016/j.cbpc.2017.03.007

McEwen, B. S., & Wingfield, J. C. (2003). The concept of allostasis in biology and biomedicine. *Hormones and Behavior*, *43*(1), 2–15. https://doi.org/10.1016/S0018-506X(02)00024-7

McGrath, P., & Li, C.-Q. (2008). Zebrafish: A predictive model for assessing drug-induced toxicity. *Drug Discovery Today*, *13*(9–10), 394–401. https://doi.org/10.1016/j.drudis.2008.03.002

McLean, D. L., & Fetcho, J. R. (2004). Ontogeny and innervation patterns of dopaminergic, noradrenergic, and serotonergic neurons in larval zebrafish. *Journal of Comparative Neurology*, *480*(1), 38–56. https://doi.org/10.1002/cne.20280

Medeiros, L. R., Mager, E. M., Grosell, M., & McDonald, M. D. (2010). The serotonin subtype 1A receptor regulates cortisol secretion in the Gulf toadfish, *Opsanus beta*. *General and Comparative Endocrinology*, *168*(3), 377–387. https://doi.org/10.1016/j.ygcen.2010.05.004

Mennigen, J. A., Harris, E. A., Chang, J. P., Moon, T. W., & Trudeau, V. L. (2009). Fluoxetine affects weight gain and expression of feeding peptides in the female goldfish brain. *Regulatory Peptides*, *155*(1–3), 99–104. https://doi.org/10.1016/j.regpep.2009.01.001

Mennigen, J. A., Lado, W. E., Zamora, J. M., Duarte-Guterman, P., Langlois, V. S., Metcalfe, C. D., Chang, J. P., Moon, T. W., & Trudeau, V. L. (2010). Waterborne fluoxetine disrupts the reproductive axis in sexually mature male goldfish, *Carassius auratus*. *Aquatic Toxicology*, *100*(4), 354–364. https://doi.org/10.1016/j.aquatox.2010.08.016

Mennigen, J. A., Martyniuk, C. J., Crump, K., Xiong, H., Zhao, E., Popesku, J., Anisman, H., Cossins, A. R., Xia, X., & Trudeau, V. L. (2008). Effects of fluoxetine on the reproductive axis of female goldfish (*Carassius auratus*). *Physiological Genomics*, *35*(3), 273–282. https://doi.org/10.1152/physiolgenomics.90263.2008

Mennigen, J. A., Stroud, P., Zamora, J. M., Moon, T. W., & Trudeau, V. L. (2011). Pharmaceuticals as Neuroendocrine Disruptors: Lessons Learned from Fish on Prozac. *Journal of Toxicology and Environmental Health, Part B*, *14*(5–7), 387–412. https://doi.org/10.1080/10937404.2011.578559

Miller, W. L. (2013). Steroid hormone synthesis in mitochondria. *Molecular and Cellular Endocrinology, Mitochondrial Endocrinology – Mitochondria as Key to Hormones and Metabolism*, *379*(1), 62–73. https://doi.org/10.1016/j.mce.2013.04.014

Minagh, E., Hernan, R., O'Rourke, K., Lyng, F. M., & Davoren, M. (2009). Aquatic ecotoxicity of the selective serotonin reuptake inhibitor sertraline hydrochloride in a battery of freshwater test species. *Ecotoxicology and Environmental Safety*, *72*(2), 434–440. https://doi.org/10.1016/j.ecoenv.2008.05.002

Mole, R. A., & Brooks, B. W. (2019). Global scanning of selective serotonin reuptake inhibitors: Occurrence, wastewater treatment and hazards in aquatic systems. *Environmental Pollution*, *250*, 1019–1031. https://doi.org/10.1016/j.envpol.2019.04.118

Mommsen, T. P., Vijayan, M. M., & Moon, T. W. (1999). Cortisol in teleosts: Dynamics, mechanisms of action, and metabolic regulation. *Reviews in Fish Biology and Fisheries*, *9*, 211–268. https://doi.org/10.1023/A:1008924418720

Morgan, J. I., & Curran, T. (1989). Stimulus-transcription coupling in neurons: Role of cellular immediate-early genes. *Trends in Neurosciences*, *12*(11), 459–462. https://doi.org/10.1016/0166-2236(89)90096-9

Muir, D., Simmons, D., Wang, X., Peart, T., Villella, M., Miller, J., & Sherry, J. (2017). Bioaccumulation of pharmaceuticals and personal care product chemicals in fish exposed to wastewater effluent in an urban wetland. *Scientific Reports*, *7*(16999), 1–11. https://doi.org/10.1038/s41598-017-15462-x

Nielsen, S. V., Kellner, M., Henriksen, P. G., Olsén, H., Hansen, S. H., & Baatrup, E. (2018). The psychoactive drug Escitalopram affects swimming behaviour and increases boldness in zebrafish (*Danio rerio*). *Ecotoxicology*, *27*(4), 485–497. https://doi.org/10.1007/s10646-018-1920-x

Norton, W. H. J., Folchert, A., & Bally-Cuif, L. (2008). Comparative analysis of serotonin receptor (HTR1A/HTR1B families) and transporter (slc6a4a/b) gene expression in the zebrafish brain. *Journal of Comparative Neurology*, *511*(4), 521–542. https://doi.org/10.1002/cne.21831

Nowakowska, K., Giebułtowicz, J., Kamaszewski, M., Adamski, A., Szudrowicz, H., Ostaszewska, T., Solarska-Dzięciołowska, U., Nałęcz-Jawecki, G., Wroczyński, P., & Drobniewska, A. (2020). Acute exposure of zebrafish (*Danio rerio*) larvae to environmental concentrations of selected antidepressants: Bioaccumulation, physiological and histological changes. *Comparative Biochemistry and Physiology Part - C: Toxicology and Pharmacology*, *229*. https://doi.org/10.1016/j.cbpc.2019.108670

Nozari, A., Do, S., & Trudeau, V. L. (2021). Applications of the SR4G Transgenic Zebrafish Line for Biomonitoring of Stress-Disrupting Compounds: A Proof-of-Concept Study. *Frontiers in Endocrinology*, *12*, 1–12. https://doi.org/10.3389/fendo.2021.727777

Nozari, A., Gagné, R., Lu, C., Yauk, C., & Trudeau, V. L. (2022). Brief Developmental Exposure to Fluoxetine Causes Life-Long Alteration of the Brain Transcriptome in Zebrafish. *Frontiers in Endocrinology*, *13*, 1–15. https://doi.org/10.3389/fendo.2022.847322

Oakley, R. H., & Cidlowski, J. A. (2013). The biology of the glucocorticoid receptor: New signaling mechanisms in health and disease. *Journal of Allergy and Clinical Immunology*, *132*(5), 1033–1044. https://doi.org/10.1016/j.jaci.2013.09.007

OECD. (2025). *Health at a Glance 2025: OECD Indicators*. OECD Publishing. https://doi.org/10.1787/8f9e3f98-en

Painter, M. M., Buerkley, M. A., Julius, M. L., Vajda, A. M., Norris, D. O., Barber, L. B., Furlong, E. T., Schultz, M. M., & Schoenfuss, H. L. (2009). Antidepressants at environmentally relevant concentrations affect predator avoidance behavior of

larval fathead minnows (*Pimephales promelas*). *Environmental Toxicology and Chemistry*, *28*(12), 2677–2684. https://doi.org/10.1897/08-556.1

Pallan, P. S., Nagy, L. D., Lei, L., Gonzalez, E., Kramlinger, V. M., Azumaya, C. M., Wawrzak, Z., Waterman, M. R., Guengerich, F. P., & Egli, M. (2015). Structural and Kinetic Basis of Steroid 17α,20-Lyase Activity in Teleost Fish Cytochrome P450 17A1 and Its Absence in Cytochrome P450 17A2*. *Journal of Biological Chemistry*, *290*(6), 3248–3268. https://doi.org/10.1074/jbc.M114.627265

Pappas, J. J., DesRochers, N., Tuteja, B., Hughes, D., McLaughlin, A., Sabourin, L., Renaud, J. B., Littlejohn, C., Parrott, J., Lapen, D. R., & Sumarah, M. W. (2025). Ecotoxicological implications of increased antidepressant concentrations in the Laurentian Great Lakes Basin, 2018–2023. *Science of The Total Environment*, *981*, 179331. https://doi.org/10.1016/j.scitotenv.2025.179331

Parajes, S., Griffin, A., Taylor, A. E., Rose, I. T., Miguel-Escalada, I., Hadzhiev, Y., Arlt, W., Shackleton, C., Müller, F., & Krone, N. (2013). Redefining the Initiation and Maintenance of Zebrafish Interrenal Steroidogenesis by Characterizing the Key Enzyme Cyp11a2. *Endocrinology*, *154*(8), 2702–2711. https://doi.org/10.1210/en.2013-1145

Pariante, C. M., Kim, R. B., Makoff, A., & Kerwin, R. W. (2003). Antidepressant fluoxetine enhances glucocorticoid receptor function in vitro by modulating membrane steroid transporters. *British Journal of Pharmacology*, *139*(6), 1111–1118. https://doi.org/10.1038/sj.bjp.0705357

Park, J. W., Heah, T. P., Gouffon, J. S., Henry, T. B., & Sayler, G. S. (2012). Global gene expression in larval zebrafish (*Danio rerio*) exposed to selective serotonin reuptake inhibitors (fluoxetine and sertraline) reveals unique expression profiles and potential biomarkers of exposure. *Environmental Pollution*, *167*, 163–170. https://doi.org/10.1016/j.envpol.2012.03.039

Patel, M., Kumar, R., Kishor, K., Mlsna, T., Pittman, C. U., & Mohan, D. (2019). Pharmaceuticals of emerging concern in aquatic systems: Chemistry, occurrence, effects, and removal methods. *Chemical Reviews*, *119*(6), 3510–3673. https://doi.org/10.1021/acs.chemrev.8b00299

Payne, A. H., & Hales, D. B. (2004). Overview of Steroidogenic Enzymes in the Pathway from Cholesterol to Active Steroid Hormones. *Endocrine Reviews*, *25*(6), 947–970. https://doi.org/10.1210/er.2003-0030

Peano, A., Calabrese, F., Pechlivanidis, K., Mimmo, R., Politano, G., Martella, M., & Gianino, M. M. (2025). International Trends in Antidepressant Consumption: A 10-year Comparative Analysis (2010–2020). *Psychiatric Quarterly*, *96*(2), 241–255. https://doi.org/10.1007/s11126-025-10122-0

Piñeyro, G., & Blier, P. (1999). Autoregulation of Serotonin Neurons: Role in Antidepressant Drug Action. *Pharmacological Reviews*, *51*(3), 533–591. https://doi.org/10.1016/S0031-6997(24)01417-0

Preskorn, S. H. (2012). Clinically Relevant Pharmacology of Selective Serotonin Reuptake Inhibitors. *Clinical Pharmacokinetics 1997 32:1*, *32*(1), 1–21. https://doi.org/10.2165/00003088-199700321-00003

Rao, N. (2007). The clinical pharmacokinetics of escitalopram. *Clinical Pharmacokinetics*, *46*(4), 281–290. https://doi.org/10.2165/00003088-200746040-00002

Richendrfer, H., & Creton, R. (2018). Cluster analysis profiling of behaviors in zebrafish larvae treated with antidepressants and pesticides. *Neurotoxicology and Teratology*, *69*, 54. https://doi.org/10.1016/j.ntt.2017.10.009

Rochat, B., Baumann, P., & Audus, K. L. (1999). Transport mechanisms for the antidepressant citalopram in brain microvessel endothelium. *Brain Research*, *831*, 229–236. https://doi.org/10.1016/S0006-8993(99)01461-4

Rodrigues, P., Cunha, V., Oliva-Teles, L., Ferreira, M., & Guimarães, L. (2020). Norfluoxetine and venlafaxine in zebrafish larvae: Single and combined toxicity of two pharmaceutical products relevant for risk assessment. *Journal of Hazardous Materials*, *400*, 123171. https://doi.org/10.1016/j.jhazmat.2020.123171

Romero, L. M. (2004). Physiological stress in ecology: Lessons from biomedical research. *Trends in Ecology & Evolution*, *19*(5), 249–255. https://doi.org/10.1016/j.tree.2004.03.008

Romero, L. M., Dickens, M. J., & Cyr, N. E. (2009). The reactive scope model—A new model integrating homeostasis, allostasis, and stress. *Hormones and Behavior*, *55*(3), 375–389. https://doi.org/10.1016/j.yhbeh.2008.12.009

Rudorfer, M. V., & Potter, W. Z. (1997). The Role of Metabolites of Antidepressants in the Treatment of Depression. *CNS Drugs*, *7*(4), 273–312. https://doi.org/10.2165/00023210-199707040-00003

Rzymski, P., Drewek, A., & Klimaszyk, P. (2017). Pharmaceutical pollution of aquatic environment: An emerging and enormous challenge. *Limnological Review*, *17*(2), 97–107. https://doi.org/10.1515/limre-2017-0010

Saaristo, M., Brodin, T., Balshine, S., Bertram, M. G., Brooks, B. W., Ehlman, S. M., McCallum, E. S., Sih, A., Sundin, J., Wong, B. B. M., & Arnold, K. E. (2018). Direct and indirect effects of chemical contaminants on the behaviour, ecology and evolution of wildlife. *Proceedings of the Royal Society B*, *285*(20181297). https://doi.org/10.1098/rspb.2018.1297

Saaristo, M., McLennan, A., Johnstone, C. P., Clarke, B. O., & Wong, B. B. M. (2017). Impacts of the antidepressant fluoxetine on the anti-predator behaviours of wild guppies (*Poecilia reticulata*). *Aquatic Toxicology*, *183*, 38–45. https://doi.org/10.1016/j.aquatox.2016.12.007

Sallinen, V., Sundvik, M., Reenilä, I., Peitsaro, N., Khrustalyov, D., Anichtchik, O., Toleikyte, G., Kaslin, J., & Panula, P. (2009). Hyperserotonergic phenotype after monoamine oxidase inhibition in larval zebrafish. *Journal of Neurochemistry*, *109*(2), 403–415. https://doi.org/10.1111/j.1471-4159.2009.05986.x

Sanusi, I. O., Olutona, G. O., Wawata, I. G., & Onohuean, H. (2023). Occurrence, environmental impact and fate of pharmaceuticals in groundwater and surface water: A critical review. *Environmental Science and Pollution Research 2023 30:39*, *30*(39), 90595–90614. https://doi.org/10.1007/s11356-023-28802-4

Sapolsky, R. M., Romero, L. M., & Munck, A. U. (2000). How do glucocorticoids influence stress responses? Integrating permissive, suppressive, stimulatory, and preparative actions. *Endocrine Reviews*, *21*(1), 55–89. https://doi.org/10.1210/edrv.21.1.0389

Saul, K. E., Koke, J. R., & García, D. M. (2010). Activating transcription factor 3 (ATF3) expression in the neural retina and optic nerve of zebrafish during optic nerve regeneration. *Comparative Biochemistry and Physiology Part A: Molecular & Integrative Physiology*, *155*(2), 172–182. https://doi.org/10.1016/j.cbpa.2009.10.042

Schaaf, M. J. M., Champagne, D., van Laanen, I. H. C., van Wijk, D. C. W. A., Meijer, A. H., Meijer, O. C., Spaink, H. P., & Richardson, M. K. (2008). Discovery of a Functional Glucocorticoid Receptor β-Isoform in Zebrafish. *Endocrinology*, *149*(4), 1591–1599. https://doi.org/10.1210/en.2007-1364

Schaaf, M. J. M., Chatzopoulou, A., & Spaink, H. P. (2009). The zebrafish as a model system for glucocorticoid receptor research. *Comparative Biochemistry and Physiology Part A: Molecular & Integrative Physiology*, *153*(1), 75–82. https://doi.org/10.1016/j.cbpa.2008.12.014

Schildkraut, J. J. (1965). The catecholamine hypothesis of affective disorders: A review of supporting evidence. *American Journal of Psychiatry*, *122*, 509–522. https://doi.org/10.1176/ajp.122.5.509

Schoonheim, P. J., Chatzopoulou, A., & Schaaf, M. J. M. (2010). The zebrafish as an *in vivo* model system for glucocorticoid resistance. *Steroids*, *75*(12), 918–925. https://doi.org/10.1016/j.steroids.2010.05.010

Sehonova, P., Hodkovicova, N., Urbanova, M., Örn, S., Blahova, J., Svobodova, Z., Faldyna, M., Chloupek, P., Briedikova, K., & Carlsson, G. (2019). Effects of antidepressants with different modes of action on early life stages of fish and amphibians. *Environmental Pollution*, *254*, 112999. https://doi.org/10.1016/j.envpol.2019.112999

Sehonova, P., Plhalova, L., Blahova, J., Doubkova, V., Marsalek, P., Prokes, M., Tichy, F., Skladana, M., Fiorino, E., Mikula, P., Vecerek, V., Faggio, C., & Svobodova, Z. (2017). Effects of selected tricyclic antidepressants on early-life stages of common carp (*Cyprinus carpio*). *Chemosphere*, *185*, 1072–1080. https://doi.org/10.1016/j.chemosphere.2017.07.092

Sehonova, P., Svobodova, Z., Dolezelova, P., Vosmerova, P., & Faggio, C. (2018). Effects of waterborne antidepressants on non-target animals living in the aquatic environment: A review. *Science of The Total Environment*, *631–632*, 789–794. https://doi.org/10.1016/j.scitotenv.2018.03.076

Selye, H. (1946). The General Adaptation Syndrome and the Diseases of Adaptation. *The Journal of Clinical Endocrinology & Metabolism*, *6*(2), 117–230. https://doi.org/10.1210/jcem-6-2-117

Silva, L. J. G., Lino, C. M., Meisel, L. M., & Pena, A. (2012). Selective serotonin re-uptake inhibitors (SSRIs) in the aquatic environment: An ecopharmacovigilance approach. *Science of The Total Environment*, *437*, 185–195. https://doi.org/10.1016/j.scitotenv.2012.08.021

Stahl, S. M. (1998). Mechanism of action of serotonin selective reuptake inhibitors: Serotonin receptors and pathways mediate therapeutic effects and side effects. *Journal of Affective Disorders*, *51*, 215–235.

Stead, J. D. H., Lee, H., Williams, A., Ramírez, S. A. C., Atlas, E., Mennigen, J. A., O'Brien, J. M., & Yauk, C. (2025). Gene Set Enrichment Analysis in Zebrafish Embryos Is Susceptible to False-Positive Results in the Absence of Differentially Expressed Genes. *Bioinformatics and Biology Insights*, *19*. https://doi.org/10.1177/11779322251321071

Stephens, M. (2017). False discovery rates: A new deal. *Biostatistics*, *18*(2), 275–294. https://doi.org/10.1093/biostatistics/kxw041

Sullivan, P. F., Neale, M. C., & Kendler, K. S. (2000). Genetic Epidemiology of Major Depression: Review and Meta-Analysis. *American Journal of Psychiatry*, *157*, 1552–1562. https://doi.org/10.1176/appi.ajp.157.10.1552

Suwała, J., Machowska, M., & Wiela-Hojeńska, A. (2019). Venlafaxine pharmacogenetics: A comprehensive review. *Pharmacogenomics*, *20*(11), 829–845. https://doi.org/10.2217/pgs-2019-0031

Takahashi, A., & Mizusawa, K. (2013). Posttranslational Modifications of Proopiomelanocortin in Vertebrates and Their Biological Significance. *Frontiers in Endocrinology*, *4*. https://doi.org/10.3389/fendo.2013.00143

Tang, Y., Mi, P., Li, M., Zhang, S., Li, J., & Feng, X. (2021). Environmental level of the antidepressant venlafaxine induces behavioral disorders through cortisol in zebrafish larvae (*Danio rerio*). *Neurotoxicology and Teratology*, *83*, 106942. https://doi.org/10.1016/j.ntt.2020.106942

Tanguay, R. L. (2018). The Rise of Zebrafish as a Model for Toxicology. *Toxicological Sciences*, *163*(1), 3–4. https://doi.org/10.1093/toxsci/kfx295

Tanguay, R. L. (2025). ToxPoint: The indispensable role of zebrafish as a new approach methodology (NAM) in toxicology. *Toxicological Sciences*, *208*(1), 40–41. https://doi.org/10.1093/toxsci/kfaf121

Tea, M., Dionne-Wilson, L. E., Bélair-Bambrick, M. È., & Gilmour, K. M. (2025). Cortisol production by interrenal cells in rainbow trout (Oncorhynchus mykiss) is stimulated by 5-HT4 receptor activation. *General and Comparative Endocrinology*, *364*. https://doi.org/10.1016/j.ygcen.2025.114694

Tea, M., Pan, Y. K., Lister, J. G. R., Perry, S. F., & Gilmour, K. M. (2024). Effects of serta and sertb knockout on aggression in zebrafish (Danio rerio). *Journal of*

Comparative Physiology A, *210*(5), 785–799. https://doi.org/10.1007/s00359-024-01693-7

Thompson, W. A., Arnold, V. I., & Vijayan, M. M. (2017). Venlafaxine in Embryos Stimulates Neurogenesis and Disrupts Larval Behavior in Zebrafish. *Environmental Science & Technology*, *51*(21), 12889–12897. https://doi.org/10.1021/acs.est.7b04099

Thompson, W. A., Shvartsburd, Z., & Vijayan, M. M. (2022). Sex-Specific and Long-Term Impacts of Early-Life Venlafaxine Exposure in Zebrafish. *Biology*, *11*(250). https://doi.org/10.3390/biology11020250

Thompson, W. A., & Vijayan, M. M. (2020a). Environmental levels of venlafaxine impact larval behavioural performance in fathead minnows. *Chemosphere*, *259*. https://doi.org/10.1016/j.chemosphere.2020.127437

Thompson, W. A., & Vijayan, M. M. (2020b). Zygotic Venlafaxine Exposure Impacts Behavioral Programming by Disrupting Brain Serotonin in Zebrafish. *Environmental Science and Technology*, *54*(22), 14578–14588. https://doi.org/10.1021/acs.est.0c06032

Thompson, W. A., & Vijayan, M. M. (2022). Antidepressants as Endocrine Disrupting Compounds in Fish. *Frontiers in Endocrinology*, *13*, 895064. https://doi.org/10.3389/fendo.2022.895064

Thunga, P., Truong, L., Tanguay, R. L., & Reif, D. M. (2021). Concurrent Evaluation of Mortality and Behavioral Responses: A Fast and Efficient Testing Approach for High-Throughput Chemical Hazard Identification. *Frontiers in Toxicology*, *3*(June), 1–8. https://doi.org/10.3389/ftox.2021.670496

Torres, G., Horowitz, J. M., Laflamme, N., & Rivest, S. (1998). Fluoxetine induces the transcription of genes encoding c-fos, corticotropin-releasing factor and its type 1 receptor in rat brain. *Neuroscience*, *87*(2), 463–477. https://doi.org/10.1016/S0306-4522(98)00147-X

Trudeau, V. L., & Somoza, G. M. (2020). Multimodal hypothalamo-hypophysial communication in the vertebrates. *General and Comparative Endocrinology*, *293*(March), 113475. https://doi.org/10.1016/j.ygcen.2020.113475

Tsachaki, M., Meyer, A., Weger, B., Kratschmar, D. V., Tokarz, J., Adamski, J., Belting, H.-G., Affolter, M., Dickmeis, T., & Odermatt, A. (2017). Absence of 11-keto reduction of cortisone and 11-ketotestosterone in the model organism zebrafish. *Journal of Endocrinology*, *232*(2), 323–335. https://doi.org/10.1530/JOE-16-0495

Valenti, T. W., Gould, G. G., Berninger, J. P., Connors, K. A., Keele, N. B., Prosser, K. N., & Brooks, B. W. (2012). Human Therapeutic Plasma Levels of the Selective Serotonin Reuptake Inhibitor (SSRI) Sertraline Decrease Serotonin Reuptake Transporter Binding and Shelter-Seeking Behavior in Adult Male Fathead Minnows. *Environmental Science & Technology*, *46*(4), 2427–2435. https://doi.org/10.1021/es204164b

Valenti, T. W., Perez-Hurtado, P., Chambliss, C. K., & Brooks, B. W. (2009). Aquatic toxicity of Sertraline to <i>Pimephales promelas<i/> at environmentally relevant

surface water pH. *Environmental Toxicology and Chemistry*, *28*(12), 2685–2694. https://doi.org/10.1897/08-546.1

Vaudin, P., Augé, C., Just, N., Mhaouty-Kodja, S., Mortaud, S., & Pillon, D. (2022). When pharmaceutical drugs become environmental pollutants: Potential neural effects and underlying mechanisms. *Environmental Research*, *205*, 112495. https://doi.org/10.1016/j.envres.2021.112495

Venkatachalam, A. B., Lall, S. P., Denovan-Wright, E. M., & Wright, J. M. (2012). Tissue-specific differential induction of duplicated fatty acid-binding protein genes by the peroxisome proliferator, clofibrate, in zebrafish (*Danio rerio*). *BMC Evolutionary Biology*, *12*(1), 112. https://doi.org/10.1186/1471-2148-12-112

Venkatachalam, A. B., Levesque, B., Achenbach, J. C., Pappas, J. J., & Ellis, L. D. (2023). Long and Short Duration Exposures to the Selective Serotonin Reuptake Inhibitors (SSRIs) Fluoxetine, Paroxetine and Sertraline at Environmentally Relevant Concentrations Lead to Adverse Effects on Zebrafish Behaviour and Reproduction. *Toxics*, *151*(11). https://doi.org/10.3390/toxics11020151

Vera-Chang, M. N., Moon, T. W., & Trudeau, V. L. (2019). Cortisol disruption and transgenerational alteration in the expression of stress-related genes in zebrafish larvae following fluoxetine exposure. *Toxicology and Applied Pharmacology*, *382*(April), 114742. https://doi.org/10.1016/j.taap.2019.114742

Vera-Chang, M. N., St-Jacques, A. D., Gagné, R., Martyniuk, C. J., Yauk, C. L., Moon, T. W., & Trudeau, V. L. (2018). Transgenerational hypocortisolism and behavioral disruption are induced by the antidepressant fluoxetine in male zebrafish *Danio rerio*. *Proceedings of the National Academy of Sciences*, *115*(52), E12435–E12442. https://doi.org/10.1073/pnas.1811695115

Vera-Chang, M. N., St-Jacques, A. D., Lu, C., Moon, T. W., & Trudeau, V. L. (2019). Fluoxetine Exposure During Sexual Development Disrupts the Stress Axis and Results in Sex- and Time- Dependent Effects on the Exploratory Behavior in Adult Zebrafish *Danio rerio*. *Frontiers in Neuroscience*, *13*. https://doi.org/10.3389/fnins.2019.01015

Verheijen, M. CT., Meier, M. J., Asensio, J. O., Gant, T. W., Tong, W., Yauk, C. L., & Caiment, F. (2022). R-ODAF: Omics data analysis framework for regulatory application. *Regulatory Toxicology and Pharmacology*, *131*, 105143. https://doi.org/10.1016/j.yrtph.2022.105143

Vialou, V., Thibault, M., Kaska, S., Cooper, S., Gajewski, P., Eagle, A., Mazei-Robison, M., Nestler, E. J., & Robison, A. J. (2015). Differential induction of FosB isoforms throughout the brain by fluoxetine and chronic stress. *Neuropharmacology*, *99*, 28–37. https://doi.org/10.1016/j.neuropharm.2015.07.005

von Hellfeld, R., Brotzmann, K., Baumann, L., Strecker, R., & Braunbeck, T. (2020). Adverse effects in the fish embryo acute toxicity (FET) test: A catalogue of unspecific morphological changes versus more specific effects in zebrafish (*Danio rerio*) embryos. *Environmental Sciences Europe*, *32*(1), 122. https://doi.org/10.1186/s12302-020-00398-3

Wallace, E. W. J., & Haynes, S. J. (2022). tidyqpcr: Quantitative PCR analysis in the tidyverse. *Journal of Open Source Software*, *7*(74), 4507. https://doi.org/10.21105/joss.04507

Wang, H., Montague, H. R., Hess, H. N., Zhang, Y., Aguilar, G. L., Dunham, R. A., Butts, I. A. E., & Wang, X. (2022). Transcriptome Analysis Reveals Key Gene Expression Changes in Blue Catfish Sperm in Response to Cryopreservation. *International Journal of Molecular Sciences*, *23*(14), 7618. https://doi.org/10.3390/ijms23147618

Wang, Q., Zhang, L., Zhu, C., Lu, K., Wu, J., & Liang, X.-F. (2025). *Fosab*, but not *fosaa*, plays important role in learning and memory in fish—Insights from zebrafish gene knockout study. *Frontiers in Cell and Developmental Biology*, *13*. https://doi.org/10.3389/fcell.2025.1503066

Weikum, E. R., Knuesel, M. T., Ortlund, E. A., & Yamamoto, K. R. (2017). Glucocorticoid receptor control of transcription: Precision and plasticity via allostery. *Nature Reviews Molecular Cell Biology*, *18*(3), 159–174. https://doi.org/10.1038/nrm.2016.152

Wendelaar Bonga, S. E. (1997). The Stress Response in Fish. *Physiological Reviews*, *77*(3). https://doi.org/10.1152/physrev.1997.77.3.591

WHO. (2022). *Mental Health and COVID-19: Early evidence of the pandemic's impact*. World Health Organization. https://www.who.int/publications/i/item/WHO-2019-nCoV-Sci_Brief-Mental_health-2022.1

Wilkinson, J. L., Boxall, A. B. A., Kolpin, D. W., Leung, K. M. Y., Lai, R. W. S., Galbán-Malagón, C., Adell, A. D., Mondon, J., Metian, M., Marchant, R. A., Bouzas-Monroy, A., Cuni-Sanchez, A., Coors, A., Carriquiriborde, P., Rojo, M., Gordon, C., Cara, M., Moermond, M., Luarte, T., … Teta, C. (2022). Pharmaceutical pollution of the world's rivers. *Proceedings of the National Academy of Sciences*, *119*(8), e2113947119. https://doi.org/10.1073/pnas.2113947119

Wilson, K. S., Matrone, G., Livingstone, D. E. W., Al-Dujaili, E. A. S., Mullins, J. J., Tucker, C. S., Hadoke, P. W. F., Kenyon, C. J., & Denvir, M. A. (2013). Physiological roles of glucocorticoids during early embryonic development of the zebrafish (*Danio rerio)*. *The Journal of Physiology*, *591*(24), 6209–6220. https://doi.org/10.1113/jphysiol.2013.256826

Winberg, S., & Lepage, O. (1998). Elevation of brain 5-HT activity, POMC expression, and plasma cortisol in socially subordinate rainbow trout. *American Journal of Physiology-Regulatory, Integrative and Comparative Physiology*, *274*(3), R645–R654. https://doi.org/10.1152/ajpregu.1998.274.3.R645

Winberg, S., Nilsson, A., Hylland, P., Söderstöm, V., & Nilsson, G. E. (1997). Serotonin as a regulator of hypothalamic-pituitary-interrenal activity in teleost fish. *Neuroscience Letters*, *230*, 113–116.

Winberg, S., & Nilsson, G. E. (1993). Roles of brain monoamine neurotransmitters in agonistic behaviour and stress reactions, with particular reference to fish.

Comparative Biochemistry and Physiology Part C: Pharmacology, Toxicology and Endocrinology, *106*(3), 597–614. https://doi.org/10.1016/0742-8413(93)90216-8

Winberg, S., & Thörnqvist, P. O. (2016). Role of brain serotonin in modulating fish behavior. *Current Zoology*, *62*(3), 317–323. https://doi.org/10.1093/cz/zow037

Wong, D. T., Bymaster, F. P., & Engleman, E. A. (1995). Prozac (fluoxetine, lilly 110140), the first selective serotonin uptake inhibitor and an antidepressant drug: Twenty years since its first publication. *Life Sciences*, *57*(5), 411–441. https://doi.org/10.1016/0024-3205(95)00209-O

Wu, G., Wang, X., Zhang, X., Ren, H., Wang, Y., Yu, Q., Wei, S., & Geng, J. (2023). Nontarget screening based on molecular networking strategy to identify transformation products of citalopram and sertraline in wastewater. *Water Research*, *232*, 119509. https://doi.org/10.1016/j.watres.2022.119509

Yabut, K. C. B., Martynova, A., Nath, A., Zercher, B. P., Bush, M. F., & Isoherranen, N. (2024). Drugs Form Ternary Complexes with Human Liver Fatty Acid Binding Protein 1 (FABP1) and FABP1 Binding Alters Drug Metabolism. *Molecular Pharmacology*, *105*(6), 395–410. https://doi.org/10.1124/molpharm.124.000878

Zhou, Z., Zhen, J., Karpowich, N. K., Law, C. J., Reith, M. E. A., & Wang, D. N. (2009). Antidepressant specificity of serotonin transporter suggested by three LeuT–SSRI structures. *Nature Structural & Molecular Biology 2009 16:6*, *16*(6), 652–657. https://doi.org/10.1038/nsmb.1602

Ziegler, M., Knoll, S., Köhler, H. R., Tisler, S., Huhn, C., Zwiener, C., & Triebskorn, R. (2020). Impact of the antidepressant citalopram on the behaviour of two different life stages of brown trout. *PeerJ*, (3). https://doi.org/10.7717/peerj.8765

Zindler, F., Stoll, S., Baumann, L., Knoll, S., Huhn, C., & Braunbeck, T. (2020). Do environmentally relevant concentrations of fluoxetine and citalopram impair stress-related behavior in zebrafish (Danio rerio) embryos? *Chemosphere*, *261*. https://doi.org/10.1016/j.chemosphere.2020.127753

Appendix

A. Supplementary materials of Chapter 2

Supplementary Table A.1. Water sample analysis results of vehicle control and SS(N)RIs solutions.

Sample description	Nominal concentration (µg/L)	Measured concentration (µg/L)	Mean ± SEM (µg/L)
Vehicle control – 1	0	< LOQ	N/A
Vehicle control – 2	0	< LOQ	
Vehicle control – 3	0	< LOQ	
Fluoxetine HCl 1 µM – 1	346	275	263.7 ± 16.59
Fluoxetine HCl 1 µM – 2	346	285	
Fluoxetine HCl 1 µM – 3	346	231	
Norfluoxetine HCl 1 µM – 1	332	368	379.3 ± 6.64
Norfluoxetine HCL 1 µM – 2	332	391	
Norfluoxetine HCl 1 µM – 3	332	379	
Citalopram HBr 1 µM – 1	405	424	406.7 ± 8.97
Citalopram HBr 1 µM – 2	405	394	
Citalopram HBr 1 µM – 3	405	402	
Escitalopram oxalate 1 µM – 1	414	409	406.7 ± 7.88
Escitalopram oxalate 1 µM – 2	414	419	
Escitalopram oxalate 1 µM – 3	414	392	
Sertraline HCl 1 µM – 1	342	345	341.7 ± 4.37
Sertraline HCl 1 µM – 2	342	333	
Sertraline HCl 1 µM – 3	342	347	
Venlafaxine HCl 1 µM – 1	313	341	353.0 ± 6.66
Venlafaxine HCl 1 µM – 2	313	354	
Venlafaxine HCl 1 µM – 3	313	364	
Desvenlafaxine 1 µM – 1	263	404	392.7 ± 18.22
Desvenlafaxine 1 µM – 2	263	417	
Desvenlafaxine 1 µM – 3	263	357	

The limit of quantification for all molecules was 0.25 µg/L. Nominal concentrations are expressed based on the salt form weighed to prepare the stock solutions. Expressed on a free-base basis, a nominal 1 µM corresponds to 309 µg/L fluoxetine, 295 µg/L norfluoxetine, 324 µg/L citalopram, 324 µg/L escitalopram, 306 µg/L sertraline, and 277 µg/L venlafaxine. Measured concentrations are the values reported by the analytical laboratory. Nominal molar concentrations in the main text and in Figure 5.1 are reported with free-base mass equivalents to allow comparison to measured environmental concentrations.

Supplementary Table A.2. List of primers used for real-time qPCR on samples from 7 dpf SR4G larvae.

Gene symbol	ZFIN ID	Primer sequence
eef1a1l1	ZDB-GENE-990415-52	F: CCGTCTGCCACTTCAGGATGTGT R: TTGAGGACACCAGTCTCCACACGA
d4egfp	ZDB-EFG-070117-1	F: CGAGCAACTGAGGATCCCATTCTCT R: CACCCCGGTGAACAGCTCCT

Supplementary Table A.3. Raw C_T values of the reference gene eef1a1l1 in 7 dpf SR4G larvae, per compound series.

Exposure series	Groups (n)	Samples (n)	C_T (mean ± SD)	Group means, min–max	Range of group means (cycles)
Fluoxetine	16	48	16.9 ± 0.67	16.1–17.7	1.57
Norfluoxetine	16	48	18.2 ± 0.93	17.7–18.6	0.84
Citalopram	16	48	17.4 ± 0.75	17.2–18.4	1.27
Escitalopram	16	48	17.9 ± 0.89	17.2–18.2	1.02
Sertraline	16	48	17.8 ± 1.02	17.4–18.2	0.76
Venlafaxine	16	48	18.0 ± 0.62	17.6–18.3	0.64
Desvenlafaxine	16	44	18.0 ± 0.58	17.3–18.3	0.95
Cortisol	16	46	17.3 ± 0.34	17.1–18.3	1.24
Dexamethasone	16	44	18.1 ± 0.47	17.3–18.7	1.38
Cortisol overnight	4	12	17.7 ± 0.61	17.4–18.1	0.70
Dexamethasone overnight	4	12	17.7 ± 0.61	17.4–18.1	0.73
All series		440	17.7 ± 0.83		

Each C_T value is the mean of technical duplicates for one biological sample (sampling unit = 20 larvae/sample). Groups are concentration × stress combinations, including the vehicle control (0.02% DMSO). Group means are averaged over the three experimental replicates. Range = highest minus lowest group mean within a series. The two overnight series share the same vehicle-control samples, which are counted once in the total. The higher SD for sertraline reflects differences between experimental replicates, which cancel out in the within-sample ΔC_T normalisation before fold-change calculations.

Supplementary Table A.4. Summary table of the number and percentage of larvae affected by any malformation, and malformation counts per category, for each treatment.

				Malformation counts			
Compound	**Concentration (nM)**	**Larvae affected (%)**	**Larvae affected (count)**	**Edema**	**Trunk**	**Tail**	**Exp. Rep.**
Citalopram							
	0	0.0 ± 0.0	0.0 ± 0.0	0.0 ± 0.0	0.0 ± 0.0	0.0 ± 0.0	6
	0.001	0.0 ± 0.0	0.0 ± 0.0	0.0 ± 0.0	0.0 ± 0.0	0.0 ± 0.0	6
	0.01	0.0 ± 0.0	0.0 ± 0.0	0.0 ± 0.0	0.0 ± 0.0	0.0 ± 0.0	6
	0.1	0.0 ± 0.0	0.0 ± 0.0	0.0 ± 0.0	0.0 ± 0.0	0.0 ± 0.0	6
	1	0.0 ± 0.0	0.0 ± 0.0	0.0 ± 0.0	0.0 ± 0.0	0.0 ± 0.0	6
	10	0.0 ± 0.0	0.0 ± 0.0	0.0 ± 0.0	0.0 ± 0.0	0.0 ± 0.0	6
	100	0.0 ± 0.0	0.0 ± 0.0	0.0 ± 0.0	0.0 ± 0.0	0.0 ± 0.0	6
	1000	0.0 ± 0.0	0.0 ± 0.0	0.0 ± 0.0	0.0 ± 0.0	0.0 ± 0.0	6
Cortisol							
	0	1.0 ± 1.5	0.5 ± 0.8	0.5 ± 0.8	0.4 ± 0.7	0.0 ± 0.0	8
	0.001	0.8 ± 1.0	0.4 ± 0.5	0.6 ± 0.9	0.1 ± 0.4	0.0 ± 0.0	8
	0.01	1.0 ± 2.1	0.5 ± 1.1	1.0 ± 2.1	0.4 ± 1.1	0.0 ± 0.0	8
	0.1	0.0 ± 0.0	0.0 ± 0.0	0.0 ± 0.0	0.0 ± 0.0	0.0 ± 0.0	8
	1	0.8 ± 1.5	0.4 ± 0.7	0.5 ± 0.9	0.0 ± 0.0	0.0 ± 0.0	8
	10	0.0 ± 0.0	0.0 ± 0.0	0.0 ± 0.0	0.0 ± 0.0	0.0 ± 0.0	8
	100	0.5 ± 0.9	0.2 ± 0.5	0.0 ± 0.0	0.2 ± 0.5	0.0 ± 0.0	8
Desvenlafaxine							
	0	1.0 ± 1.5	0.5 ± 0.8	0.5 ± 0.8	0.2 ± 0.5	0.0 ± 0.0	6
	0.001	0.0 ± 0.0	0.0 ± 0.0	0.0 ± 0.0	0.0 ± 0.0	0.0 ± 0.0	6
	0.01	0.5 ± 1.0	0.2 ± 0.5	0.0 ± 0.0	0.0 ± 0.0	0.0 ± 0.0	4
	0.1	0.0 ± 0.0	0.0 ± 0.0	0.0 ± 0.0	0.0 ± 0.0	0.0 ± 0.0	6
	1	1.5 ± 3.0	0.8 ± 1.5	0.8 ± 1.5	0.2 ± 0.5	0.0 ± 0.0	4
	10	0.3 ± 0.8	0.2 ± 0.4	0.0 ± 0.0	0.2 ± 0.4	0.0 ± 0.0	6

	100	0.0 ± 0.0	0.0 ± 0.0	0.0 ± 0.0	0.0 ± 0.0	0.0 ± 0.0	6
	1000	0.3 ± 0.8	0.2 ± 0.4	0.2 ± 0.4	0.0 ± 0.0	0.0 ± 0.0	6
Dexamethasone							
	0	1.0 ± 1.5	0.5 ± 0.8	0.5 ± 0.8	0.2 ± 0.5	0.0 ± 0.0	8
	0.001	0.2 ± 0.7	0.1 ± 0.4	0.1 ± 0.4	0.1 ± 0.4	0.0 ± 0.0	8
	0.01	1.0 ± 2.1	0.5 ± 1.1	0.8 ± 2.1	0.5 ± 1.1	0.0 ± 0.0	8
	0.1	0.5 ± 1.4	0.2 ± 0.7	0.2 ± 0.7	0.0 ± 0.0	0.0 ± 0.0	8
	1	1.5 ± 2.3	0.8 ± 1.2	0.6 ± 1.2	0.5 ± 0.8	0.0 ± 0.0	8
	10	1.2 ± 2.1	0.6 ± 1.1	0.4 ± 1.1	0.4 ± 0.5	0.0 ± 0.0	8
	100	0.8 ± 1.0	0.4 ± 0.5	0.5 ± 0.8	0.1 ± 0.4	0.0 ± 0.0	8
Escitalopram							
	0	0.0 ± 0.0	0.0 ± 0.0	0.0 ± 0.0	0.0 ± 0.0	0.0 ± 0.0	6
	0.001	0.7 ± 1.6	0.3 ± 0.8	0.3 ± 0.8	0.2 ± 0.4	0.0 ± 0.0	6
	0.01	1.0 ± 1.7	0.5 ± 0.8	0.5 ± 0.8	0.0 ± 0.0	0.0 ± 0.0	6
	0.1	0.3 ± 0.8	0.2 ± 0.4	0.2 ± 0.4	0.0 ± 0.0	0.0 ± 0.0	6
	1	0.3 ± 0.8	0.2 ± 0.4	0.2 ± 0.4	0.0 ± 0.0	0.0 ± 0.0	6
	10	0.0 ± 0.0	0.0 ± 0.0	0.0 ± 0.0	0.0 ± 0.0	0.0 ± 0.0	6
	100	0.3 ± 0.8	0.2 ± 0.4	0.2 ± 0.4	0.0 ± 0.0	0.0 ± 0.0	6
	1000	0.0 ± 0.0	0.0 ± 0.0	0.0 ± 0.0	0.0 ± 0.0	0.0 ± 0.0	6
Fluoxetine							
	0	0.3 ± 0.8	0.2 ± 0.4	0.3 ± 0.8	0.0 ± 0.0	0.0 ± 0.0	6
	0.001	0.3 ± 0.8	0.2 ± 0.4	0.2 ± 0.4	0.0 ± 0.0	0.0 ± 0.0	6
	0.01	1.7 ± 1.5	0.8 ± 0.8	1.3 ± 1.2	0.2 ± 0.4	0.0 ± 0.0	6
	0.1	1.0 ± 1.7	0.5 ± 0.8	0.7 ± 1.0	0.2 ± 0.4	0.0 ± 0.0	6
	1	0.7 ± 1.0	0.3 ± 0.5	0.0 ± 0.0	0.3 ± 0.5	0.0 ± 0.0	6
	10	0.3 ± 0.8	0.2 ± 0.4	0.2 ± 0.4	0.2 ± 0.4	0.0 ± 0.0	6
	100	0.0 ± 0.0	0.0 ± 0.0	0.0 ± 0.0	0.0 ± 0.0	0.0 ± 0.0	6
	1000	0.3 ± 0.8	0.2 ± 0.4	0.3 ± 0.8	0.0 ± 0.0	0.0 ± 0.0	6

Norfluoxetine							
	0	0.3 ± 0.8	0.2 ± 0.4	0.3 ± 0.8	0.0 ± 0.0	0.0 ± 0.0	6
	0.001	0.7 ± 1.0	0.3 ± 0.5	0.0 ± 0.0	0.3 ± 0.5	0.0 ± 0.0	6
	0.01	1.3 ± 1.0	0.7 ± 0.5	0.7 ± 1.0	0.5 ± 0.5	0.0 ± 0.0	6
	0.1	1.3 ± 1.6	0.7 ± 0.8	0.7 ± 1.6	0.5 ± 0.5	0.0 ± 0.0	6
	1	1.7 ± 2.0	0.8 ± 1.0	1.0 ± 1.1	0.5 ± 0.8	0.2 ± 0.4	6
	10	2.3 ± 1.5	1.2 ± 0.8	0.8 ± 1.0	0.7 ± 0.8	0.2 ± 0.4	6
	100	1.7 ± 1.5	0.8 ± 0.8	1.2 ± 1.0	0.5 ± 0.5	0.0 ± 0.0	6
	1000	2.3 ± 2.7	1.2 ± 1.3	1.3 ± 1.6	0.5 ± 0.8	0.0 ± 0.0	6
Sertraline							
	0	1.7 ± 2.0	0.8 ± 1.0	1.7 ± 2.0	0.0 ± 0.0	0.7 ± 1.0	6
	0.001	1.7 ± 0.8	0.8 ± 0.4	1.0 ± 1.1	0.2 ± 0.4	0.2 ± 0.4	6
	0.01	1.3 ± 1.6	0.7 ± 0.8	0.8 ± 1.0	0.2 ± 0.4	0.0 ± 0.0	6
	0.1	0.7 ± 1.0	0.3 ± 0.5	0.5 ± 0.8	0.0 ± 0.0	0.2 ± 0.4	6
	1	1.7 ± 1.5	0.8 ± 0.8	0.5 ± 1.2	0.5 ± 0.5	0.0 ± 0.0	6
	10	1.7 ± 1.5	0.8 ± 0.8	1.2 ± 1.6	0.2 ± 0.4	0.2 ± 0.4	6
	100	0.7 ± 1.0	0.3 ± 0.5	0.0 ± 0.0	0.3 ± 0.5	0.0 ± 0.0	6
	1000	1.0 ± 1.7	0.5 ± 0.8	0.5 ± 0.8	0.2 ± 0.4	0.0 ± 0.0	6
Venlafaxine							
	0	0.0 ± 0.0	0.0 ± 0.0	0.0 ± 0.0	0.0 ± 0.0	0.0 ± 0.0	6
	0.001	0.0 ± 0.0	0.0 ± 0.0	0.0 ± 0.0	0.0 ± 0.0	0.0 ± 0.0	6
	0.01	0.3 ± 0.8	0.2 ± 0.4	0.3 ± 0.8	0.0 ± 0.0	0.0 ± 0.0	6
	0.1	0.0 ± 0.0	0.0 ± 0.0	0.0 ± 0.0	0.0 ± 0.0	0.0 ± 0.0	6
	1	0.0 ± 0.0	0.0 ± 0.0	0.0 ± 0.0	0.0 ± 0.0	0.0 ± 0.0	6
	10	0.0 ± 0.0	0.0 ± 0.0	0.0 ± 0.0	0.0 ± 0.0	0.0 ± 0.0	6
	100	0.3 ± 0.8	0.2 ± 0.4	0.2 ± 0.4	0.0 ± 0.0	0.0 ± 0.0	6
	1000	0.0 ± 0.0	0.0 ± 0.0	0.0 ± 0.0	0.0 ± 0.0	0.0 ± 0.0	6

Values are presented as mean ± SD.

Supplementary Table A.5. Survival rates of control groups, in both unstressed (uns) and stressed (str) conditions, across all experimental batches.

Treatment	Stress	N	Mean ± SEM	95% Confidence Interval
Medium	uns	25	92.15 ± 0.94	90.20 – 94.10
Medium	str	25	92.72 ± 1.23	90.18 – 95.26
Vehicle	uns	29	92.34 ± 1.09	90.12 – 94.57
Vehicle	str	29	92.22 ± 0.90	90.37 – 94.07

Supplementary Table A.6. Effects of treatment concentration and acute stress on the cumulative survival of SR4G larvae.

Compound	Term	Mean sq.	df	F statistic	*p*-value
Citalopram					
	Concentration	6.38	7	0.16	0.99
	Stress	0.41	1	0.01	0.92
	Residuals	38.96	39		
Cortisol					
	Concentration	11.48	6	1.43	0.22
	Stress	1.14	1	0.14	0.71
	Residuals	8.02	48		
Desvenlafaxine					
	Concentration	10.16	7	0.23	0.98
	Stress	4.74	1	0.11	0.75
	Residuals	45.04	35		
Dexamethasone					
	Concentration	9.18	6	0.81	0.57
	Stress	0.67	1	0.06	0.81
	Residuals	11.39	46		
Escitalopram					
	Concentration	8.88	7	0.21	0.98
	Stress	1.58	1	0.04	0.85
	Residuals	42.27	39		
Fluoxetine					
	Concentration	15.42	7	0.33	0.94
	Stress	6.75	1	0.14	0.71
	Residuals	46.65	39		
Norfluoxetine					
	Concentration	16.90	7	0.33	0.93
	Stress	0.33	1	0.01	0.94
	Residuals	50.49	39		
Sertraline					
	Concentration	1592	7	9.80	**<0.0001*** **
	Stress	192	1	1.18	0.28
	Residuals	162	41		
Venlafaxine					
	Concentration	14.18	7	0.38	0.91
	Stress	0.05	1	0.00	0.97
	Residuals	37.66	39		

Results from the two-way ANOVA models. As interactions were not significant in all models, models were simplified to test the main effects of treatment concentration and stress factors only. Significant main effects are shown in bold (***$p < 0.0001$).

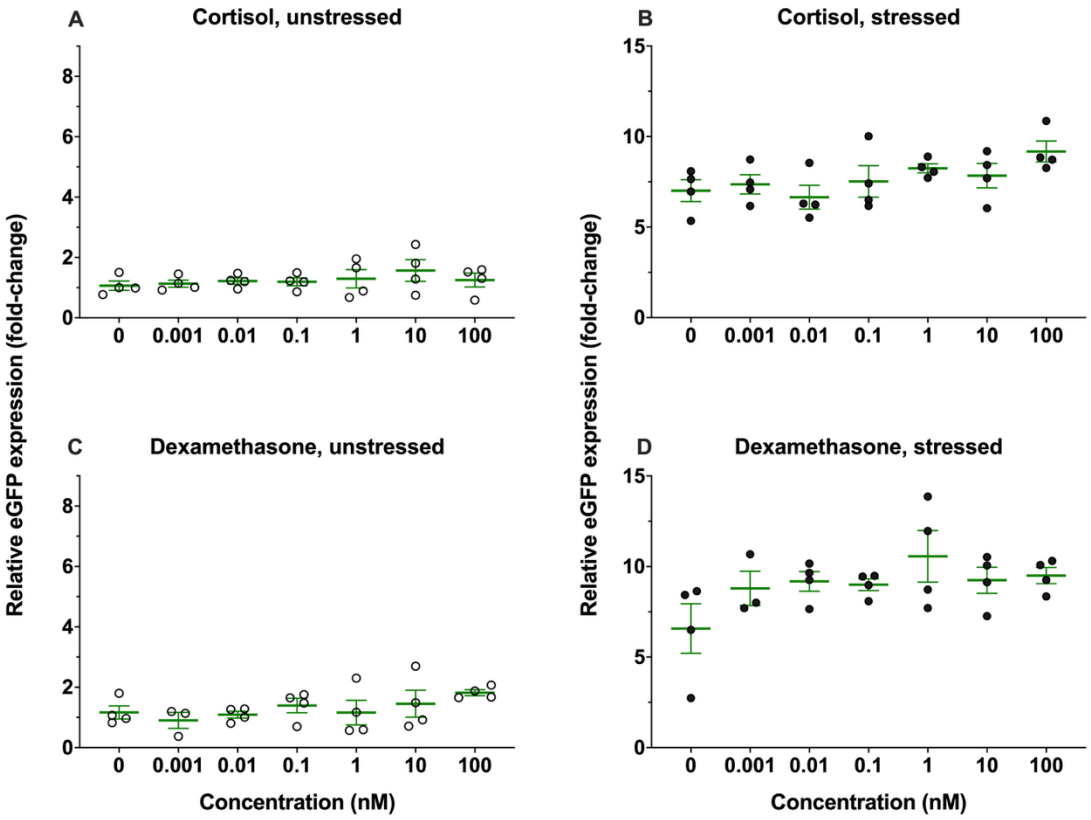

Supplementary Figure A.1. Relative eGFP expression fold-change in response to glucocorticoid treatment for 6 days in SR4G larvae.

Panels on the left show unstressed larvae (direct euthanasia; white dots) and panels on the right show stressed larvae (60 mins after handling stress; black dots). Green bars and intervals represent mean ± SEM (N = 4 biological replicates; sampling unit = 20 larvae/sample). One-way ANOVA, followed by Dunnett's post hoc test, were used to identify significant differences relative to the vehicle groups. Significant differences are represented by asterisks (*p-value$_{adj.}$ < 0.05, **p-value$_{adj.}$ < 0.01).

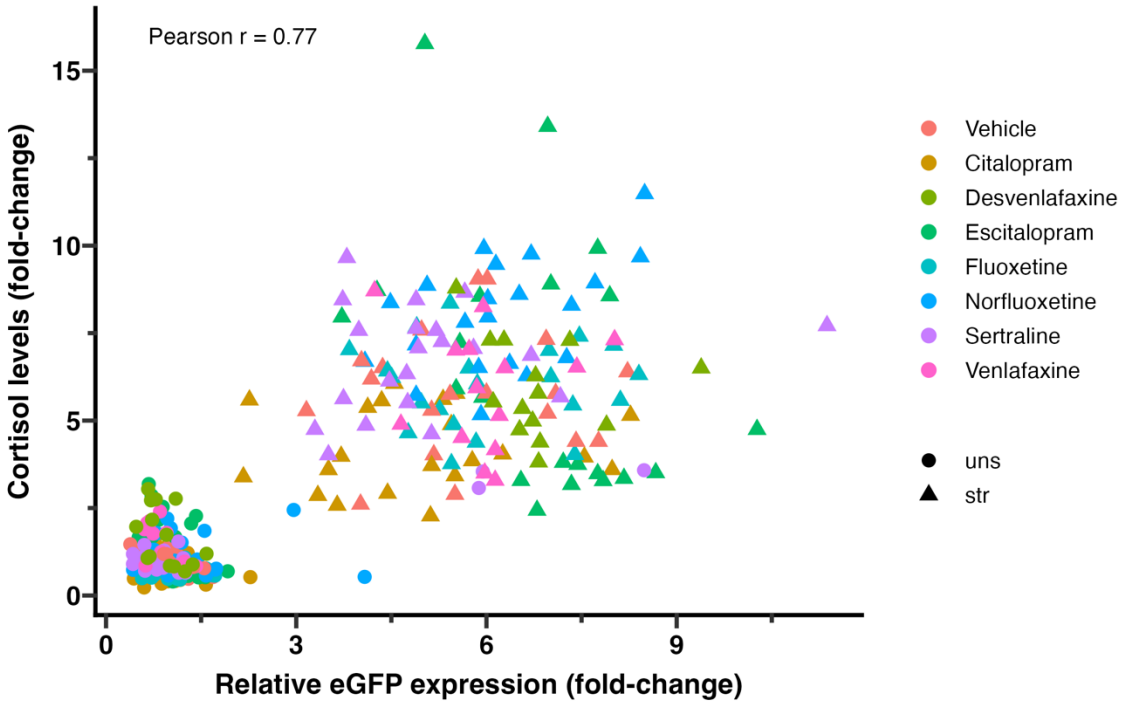

Supplementary Figure A.2. Correlation between whole-body cortisol and relative eGFP expression levels in 7 dpf SR4G larvae across all complete pairs of samples.

Each treatment group is represented by a different colour, while shapes represent the stress condition (unstressed: rounds; stressed: triangles) (n = 305 pairs; sampling unit = 20 larvae/sample). The correlation between both endpoints was evaluated with the Pearson test (all samples pooled, regardless of treatment or stress condition).

B. Supplementary materials for Chapter 3

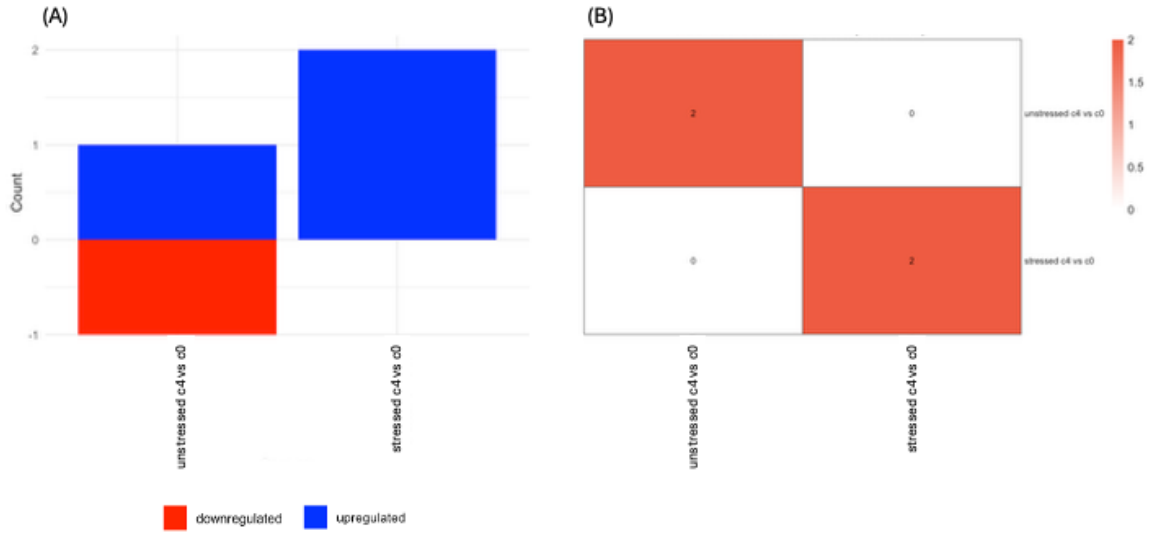

Supplementary Figure B.1. Differentially expressed genes summary following dexamethasone exposure.

Panel (A) shows the number of up- (blue) and down-regulated (red) DEGs in each contrast. Panel (B) shows the number of DEGs overlapping between contrasts.

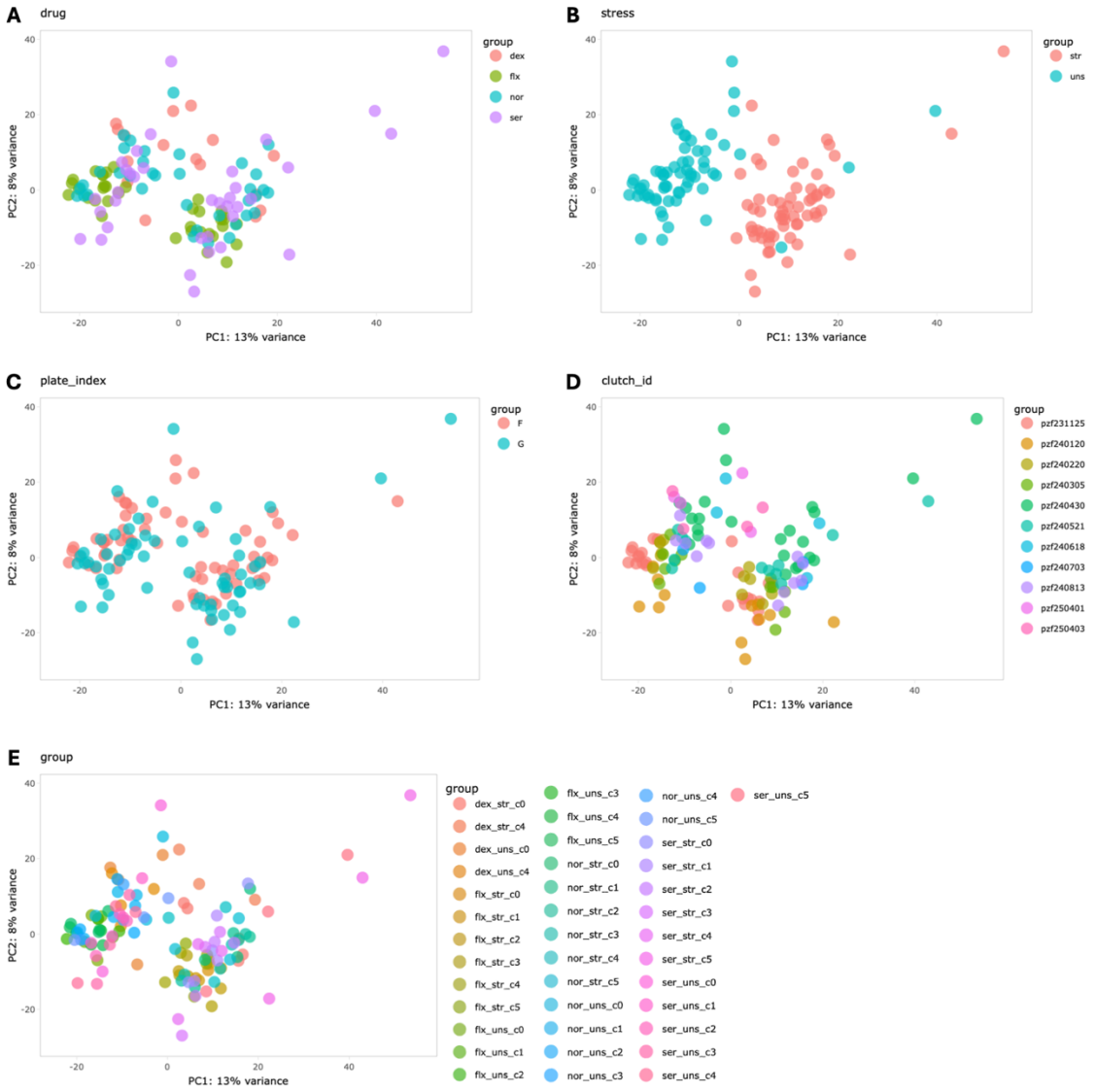

Supplementary Figure B.2. Variation between samples before batch effect normalization. Principal components analysis shows samples clustered by compound (A), stress condition (B), library preparation plate index (C), clutch identifier (D), and group (compound, concentration, and stress; E).

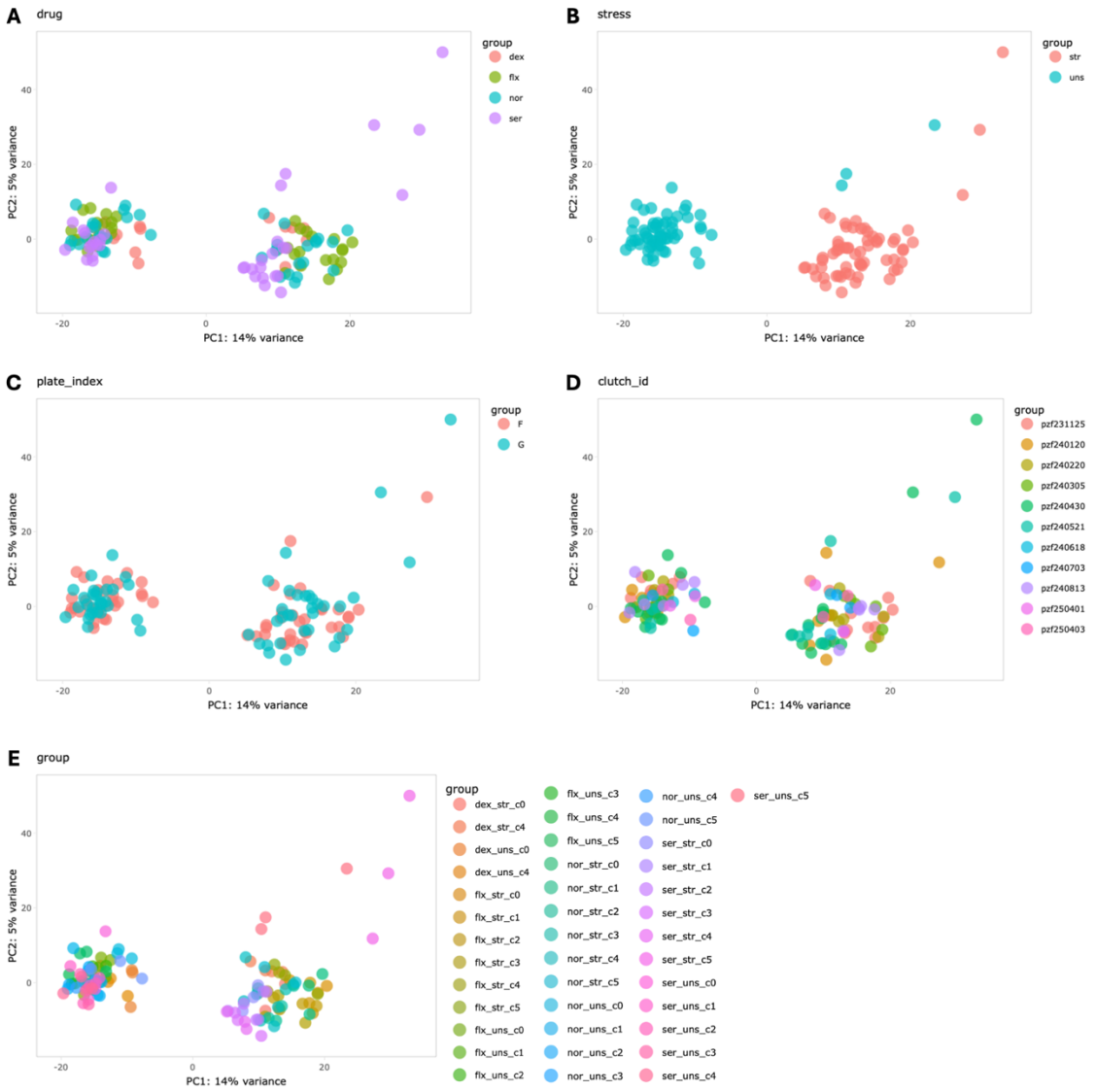

Supplementary Figure B.3. Variation between samples after batch effect normalization.
Principal components analysis shows samples clustered by compound (A), stress condition (B), library preparation plate index (C), clutch identifier (D), and group (compound, concentration, and stress; E).

Supplementary Table B.1. List of differentially expressed genes following fluoxetine exposure, in unstressed and stressed 7 dpf SR4G zebrafish.

Contrast	Gene symbol	Description	FC	*p*-adj
Unstressed larvae				
10 nM	*fbxo22*	F-box protein 22	8.53	2.7E-02
1000 nM	*agt*	angiotensinogen	-2.04	1.8E-12
	prg4b	proteoglycan 4b	-1.52	2.0E-02
Stressed larvae				
100 nM	*otog*	otogelin	-103.83	3.7E-03
	fosab	v-fos FBJ murine osteosarcoma viral oncogene homolog Ab	-5.18	5.4E-04
	nusap1	nucleolar and spindle associated protein 1	-4.40	8.0E-03
	fosl1a	FOS-like antigen 1a	-2.79	4.1E-02
	cebpb	CCAAT enhancer binding protein beta	-2.74	3.8E-02
	atf3	activating transcription factor 3	-2.38	6.8E-03
	ier2b	immediate early response 2b	-2.31	5.4E-04
	socs3a	suppressor of cytokine signaling 3a	-2.23	4.4E-02
	btg2	B-cell translocation gene 2	-2.22	1.1E-02
	junba	JunB proto-oncogene, AP-1 transcription factor subunit a	-2.15	5.1E-03
	npas4b	neuronal PAS domain protein 4b	-2.12	7.4E-03
	egr1	early growth response 1	-2.03	2.4E-03
	igfbp1a	insulin-like growth factor binding protein 1a	-1.67	6.9E-03
	gadd45bb	growth arrest and DNA-damage-inducible, beta b	-1.65	4.1E-02
	histh1l	histone H1 like	-1.54	3.7E-03
	bhlhe40	basic helix-loop-helix family, member e40	-1.50	4.7E-03
	cebpd	CCAAT enhancer binding protein delta	-1.46	3.8E-02
	agt	angiotensinogen	-1.39	2.1E-02
	plk3	polo-like kinase 3 (Drosophila)	-1.37	1.1E-02
	cyp24a1	cytochrome P450, family 24, subfamily A, polypeptide 1	-1.31	3.1E-02
	col11a1b	collagen, type XI, alpha 1b	1.30	2.1E-02
	si-dkey-183i3.5	si:dkey-183i3.5 [Source:ZFIN;Acc:ZDB-GENE-030131-8568]	1.42	2.4E-02
	anxa2b	annexin A2b	1.50	3.8E-02
1000 nM	*fosab*	v-fos FBJ murine osteosarcoma viral oncogene homolog Ab	-3.40	1.7E-02
	ier2b	immediate early response 2b	-2.28	4.2E-04
	npas4b	neuronal PAS domain protein 4b	-2.02	1.4E-02
	junba	JunB proto-oncogene, AP-1 transcription factor subunit a	-1.82	4.9E-02
	agt	angiotensinogen	-1.78	2.7E-08
	igfbp1a	insulin-like growth factor binding protein 1a	-1.71	2.7E-03
	apoea	apolipoprotein Ea	-1.68	2.7E-03
	histh1l	histone H1 like	-1.44	1.7E-02
	prg4b	proteoglycan 4b	-1.39	3.9E-02
	tdo2a	tryptophan 2,3-dioxygenase a	1.37	1.8E-03
	vtnb	vitronectin b	1.38	9.7E-03
	washc5	WASH complex subunit 5	1.63	6.3E-03

1000 nM	*fabp11b*	fatty acid binding protein 11b	1.87	1.6E-02
	scn8aa	sodium channel, voltage gated, type VIII, alpha subunit a	2.68	1.2E-02

All significant DEGs were defined with FC > |1.2| and *p*-adj < 0.05.

Supplementary Table B.2. List of differentially expressed genes following norfluoxetine exposure, in unstressed and stressed 7 dpf SR4G zebrafish.

Contrast	Gene symbol	Description	FC	*p*-adj
Unstressed larvae				
1 nM	*strbp*	spermatid perinuclear RNA binding protein	2.14	1.0E-02
	ascl1b	achaete-scute family bHLH transcription factor 1b	1.89	2.2E-02
	bcl2l1	BCL2 like 1	1.84	1.5E-02
	camk2b1	calcium/calmodulin-dependent protein kinase (CaM kinase) II beta 1	1.78	3.5E-02
	thrb	thyroid hormone receptor beta	1.77	4.7E-02
	zgc-113436	zgc:113436 [Source:ZFIN;Acc:ZDB-GENE-050220-6]	1.71	3.5E-02
	c5	complement component 5	1.44	2.2E-02
	coq8aa	coenzyme Q8A, genome duplicate a	1.35	3.5E-02
	si-ch211-14c7.2	periaxin [Source:ZFIN;Acc:ZDB-GENE-030131-5790]	1.31	2.9E-02
	ctsla	cathepsin La	-1.34	1.5E-02
	oclnb	occludin b	-1.35	3.5E-02
	yipf5	Yip1 domain family, member 5	-1.49	3.5E-02
	lipf	lipase, gastric	-1.54	4.3E-02
	abcf1	ATP-binding cassette, sub-family F (GCN20), member 1	-1.65	1.5E-02
10 nM	*nr3c1*	nuclear receptor subfamily 3, group C, member 1 (glucocorticoid receptor)	2.52	6.5E-04
	col1a1a	collagen, type I, alpha 1a	1.82	2.0E-02
	col11a1b	collagen, type XI, alpha 1b	1.54	1.6E-03
	col2a1b	collagen, type II, alpha 1b	1.51	4.9E-02
	col1a2	collagen, type I, alpha 2	1.47	1.0E-02
	sparc	secreted protein, acidic, cysteine-rich (osteonectin)	1.47	1.7E-05
	col1a1b	collagen, type I, alpha 1b	1.44	4.9E-02
	scn8ab	sodium channel, voltage gated, type VIII, alpha subunit b	1.39	4.5E-02
	nucb2a	nucleobindin 2a	-1.42	4.5E-02
	abcf1	ATP-binding cassette, sub-family F (GCN20), member 1	-1.67	1.0E-02
100 nM	*eif2s2*	eukaryotic translation initiation factor 2, subunit 2 beta	-1.26	7.7E-04
	prg4b	proteoglycan 4b [Source:ZFIN;Acc:ZDB-GENE-041014-324]	-1.37	4.4E-03
1000 nM	*fabp11b*	fatty acid binding protein 11b	3.58	2.3E-08
	nr3c1	nuclear receptor subfamily 3, group C, member 1 (glucocorticoid receptor)	1.99	4.8E-02
	strbp	spermatid perinuclear RNA binding protein	1.95	2.6E-02
	rlbp1b	retinaldehyde binding protein 1b	1.75	5.0E-02
	c5	complement component 5	1.53	3.3E-03
	clu	clusterin	1.51	4.5E-03
	stat3	signal transducer and activator of transcription 3 (acute-phase response factor)	1.46	4.8E-02
	sparc	secreted protein, acidic, cysteine-rich (osteonectin)	1.38	2.0E-03
	prg4b	proteoglycan 4b	-1.31	3.0E-02
	agt	angiotensinogen	-1.54	2.6E-02
	apoea	apolipoprotein Ea	-1.88	4.0E-03
	rpl22	ribosomal protein L22	-2.11	4.8E-02

Stressed larvae

100 nM	*fosab*	v-fos FBJ murine osteosarcoma viral oncogene homolog Ab	-3.17	1.7E-02
	fosl1a	FOS-like antigen 1a	-2.65	2.5E-03
	atf3	activating transcription factor 3	-1.98	4.9E-02
	npas4b	neuronal PAS domain protein 4b	-1.93	4.9E-02
	ier2b	immediate early response 2b	-1.92	4.9E-02
	serpine1	serpin peptidase inhibitor, clade E (nexin, plasminogen activator inhibitor type 1), member 1	-1.66	2.5E-02
	tet1	tet methylcytosine dioxygenase 1	-1.60	4.9E-02
	cyt1l	type I cytokeratin, enveloping layer	1.29	1.7E-02
	col1a1b	collagen, type I, alpha 1b	1.42	4.9E-02
	col1a2	collagen, type I, alpha 2	1.43	2.5E-02
	krt5	keratin 5	1.44	4.9E-02
	si-dkey-183i3.5	si:dkey-183i3.5 [Source:ZFIN;Acc:ZDB-GENE-030131-8568]	1.59	4.9E-02
	spp1	secreted phosphoprotein 1	1.82	7.5E-05
	col1a1a	collagen, type I, alpha 1a	1.83	2.5E-02
	krtt1c19e	keratin type 1 c19e	1.91	3.1E-02
1000 nM	*fosab*	v-fos FBJ murine osteosarcoma viral oncogene homolog Ab	-3.24	4.5E-03
	fosl1a	FOS-like antigen 1a	-2.51	2.2E-03
	egr1	early growth response 1	-1.90	5.6E-03
	agt	angiotensinogen	-1.64	1.5E-03
	eif4ebp1	eukaryotic translation initiation factor 4E binding protein 1	-1.61	3.9E-02
	casp9	caspase 9, apoptosis-related cysteine peptidase	-1.58	3.6E-02
	map2k4a	mitogen-activated protein kinase kinase 4a	-1.46	3.6E-02
	nfil3	nuclear factor, interleukin 3 regulated	-1.40	3.6E-02
	sparc	secreted protein, acidic, cysteine-rich (osteonectin)	1.36	1.5E-03
	matn4	matrilin 4	1.39	1.5E-02
	postnb	periostin, osteoblast specific factor b	1.40	3.6E-02
	col1a2	collagen, type I, alpha 2	1.43	1.3E-02
	pkmb	pyruvate kinase M1/2b	1.45	3.6E-02
	cp	ceruloplasmin	1.51	1.5E-03
	spp1	secreted phosphoprotein 1	1.72	5.0E-04
	xaf1	XIAP associated factor 1	1.75	1.9E-02
	fabp11b	fatty acid binding protein 11b	3.80	1.5E-09

All significant DEGs were defined with FC > |1.2| and *p*-adj < 0.05.

Supplementary Table B.3. List of differentially expressed genes following sertraline exposure, in unstressed and stressed 7 dpf SR4G zebrafish.

Concentration	Gene symbol	Description	FC	*p*-adj
Unstressed				
0.1 nM	*gria4a*	glutamate receptor, ionotropic, AMPA 4a	2.25	1.8E-03
10 nM	*gria4a*	glutamate receptor, ionotropic, AMPA 4a	2.20	4.1E-03
	slc2a1b	solute carrier family 2 member 1b	6.01	2.8E-02
100 nM	*ggt1a*	gamma-glutamyltransferase 1a	-2.84	4.4E-02
1000 nM	*aars1*	alanyl-tRNA synthetase 1	2.26	3.0E-03
	abcb11b	ATP-binding cassette, sub-family B (MDR/TAP), member 11b	-2.65	2.8E-03
	abcf1	ATP-binding cassette, sub-family F (GCN20), member 1	2.01	4.5E-04
	abcg1	ATP-binding cassette, sub-family G (WHITE), member 1	-3.58	2.0E-02
	acadm	acyl-CoA dehydrogenase medium chain	-1.29	1.7E-02
	acbd3	acyl-Coenzyme A binding domain containing 3	1.70	5.1E-03
	acp1	acid phosphatase 1	1.63	5.0E-02
	acta1a	actin alpha 1, skeletal muscle a	-2.12	1.3E-02
	adam10a	ADAM metallopeptidase domain 10a	1.24	1.4E-02
	adam8a	ADAM metallopeptidase domain 8a	2.62	6.5E-05
	adgra2	adhesion G protein-coupled receptor A2	-1.83	4.7E-02
	adh5	alcohol dehydrogenase 5	-2.41	6.6E-04
	adh8a	alcohol dehydrogenase 8a	-3.53	1.7E-02
	adi1	acireductone dioxygenase 1	1.90	4.4E-07
	adipor2	adiponectin receptor 2	1.71	5.0E-05
	agtrap	angiotensin II receptor-associated protein	3.37	4.7E-06
	agtrap	angiotensin II receptor-associated protein	2.60	5.7E-16
	ahcy	adenosylhomocysteinase	-1.52	1.7E-03
	aldh1l1	aldehyde dehydrogenase 1 family, member L1	-1.72	1.4E-02
	aldh9a1a.1	aldehyde dehydrogenase 9 family, member A1a, tandem duplicate 1	-2.24	1.9E-07
	aldoca	aldolase C, fructose-bisphosphate, a	-1.41	4.1E-02
	amdhd2	amidohydrolase domain containing 2	1.82	6.8E-03
	amy2a	amylase alpha 2A	-2.91	5.0E-04
	angptl4	angiopoietin-like 4	-1.73	1.0E-03
	ano9a	anoctamin 9a	-1.94	4.4E-02
	apoc1	apolipoprotein C-I	-1.54	4.3E-05
	apoea	apolipoprotein Ea	-2.00	6.6E-04
	arid5b	AT-rich interaction domain 5B	-1.54	3.6E-02
	arpc3	actin related protein 2/3 complex, subunit 3	1.30	6.6E-03
	arr3a	arrestin 3a, retinal (X-arrestin)	-2.08	4.6E-02
	atf3	activating transcription factor 3	10.88	1.3E-16
	atf4a	activating transcription factor 4a	1.43	2.6E-04
	atf5a	activating transcription factor 5a	2.38	3.9E-02
	atf6	activating transcription factor 6	1.87	3.3E-06
	atg12	ATG12 autophagy related 12 homolog (*S. cerevisiae*)	1.57	1.2E-05

Unstressed	*atg3*	autophagy related 3	1.42	7.9E-03
1000 nM	*atp1a1a.1*	ATPase Na+/K+ transporting subunit alpha 1a, tandem duplicate 1	1.28	4.4E-02
	atp6v0a1a	ATPase H+ transporting V0 subunit a1a	1.29	3.7E-02
	atp6v1d	ATPase H+ transporting V1 subunit D	1.88	6.4E-14
	atp6v1f	ATPase H+ transporting V1 subunit F	1.71	5.9E-15
	atraid	all-trans retinoic acid-induced differentiation factor	2.46	4.2E-12
	bag3	BCL2 associated athanogene 3	2.14	1.2E-02
	bambia	BMP and activin membrane-bound inhibitor (*Xenopus laevis*) homolog a	-1.47	1.4E-02
	banf1	barrier to autointegration factor 1	1.66	4.6E-07
	bard1	BRCA1 associated RING domain 1	-4.06	6.7E-03
	baxa	BCL2 associated X, apoptosis regulator a	2.18	1.4E-03
	bcl6aa	BCL6A transcription repressor a	-1.38	4.4E-02
	bdh1	3-hydroxybutyrate dehydrogenase, type 1	-1.77	4.6E-04
	bin2a	bridging integrator 2a	-1.36	4.0E-02
	birc6	baculoviral IAP repeat containing 6	1.43	1.6E-03
	blmh	bleomycin hydrolase	1.66	4.6E-07
	bloc1s2	biogenesis of lysosomal organelles complex-1, subunit 2	2.18	1.9E-07
	blvra	biliverdin reductase A	-1.67	1.2E-02
	bmp3	bone morphogenetic protein 3	-1.44	6.1E-03
	bnip4	BCL2 interacting protein 4	-1.52	3.7E-02
	bphl	biphenyl hydrolase like	-3.11	5.3E-04
	btg2	B-cell translocation gene 2	2.05	5.6E-06
	btr04	bloodthirsty-related gene family, member 4	1.60	5.0E-02
	btr05	bloodthirsty-related gene family, member 5	-3.77	3.0E-02
	btr22	bloodthirsty-related gene family, member 22	-2.40	4.6E-02
	c5ar1	C5a anaphylatoxin chemotactic receptor	2.40	3.8E-04
	ca9	carbonic anhydrase IX	-1.63	1.4E-03
	cahz	carbonic anhydrase	-2.59	7.9E-03
	camk1gb	calcium/calmodulin-dependent protein kinase IGb	-1.75	2.0E-03
	canx	calnexin	2.58	1.1E-12
	casp10	caspase 10, apoptosis-related cysteine peptidase	1.97	3.9E-02
	cat	catalase	-1.99	1.3E-02
	cav1	caveolin 1	-1.23	4.9E-02
	cavin2b	caveolae associated protein 2b	-1.54	1.4E-02
	cbr1	carbonyl reductase 1	-1.51	1.0E-03
	ccdc85b	coiled-coil domain containing 85B	1.38	7.5E-03
	cd36	CD36 molecule (thrombospondin receptor)	-1.78	4.8E-05
	cd4-1	CD4-1 molecule	-2.73	3.2E-02
	cd40	CD40 molecule, TNF receptor superfamily member 5	2.01	1.4E-02
	cd9b	CD9 molecule b	1.50	1.0E-02
	cd9b	CD9 molecule b	1.31	4.4E-02
	cdh1	cadherin 1, type 1, E-cadherin (epithelial)	1.39	4.3E-02
	cdkn1a	cyclin-dependent kinase inhibitor 1A	5.01	2.5E-02
	cdx1b	caudal type homeobox 1 b	-1.54	2.8E-06

Unstressed 1000 nM	*cebpa*	CCAAT enhancer binding protein alpha	1.83	1.3E-05
	cebpb	CCAAT enhancer binding protein beta	5.62	1.0E-10
	cebpd	CCAAT enhancer binding protein delta	1.69	1.2E-03
	cebpz	CCAAT enhancer binding protein zeta	1.38	2.2E-03
	cel.2	carboxyl ester lipase, tandem duplicate 2	-4.28	9.2E-07
	cert1b	ceramide transporter 1b	1.68	4.7E-05
	cflara	CASP8 and FADD-like apoptosis regulator a	1.33	4.3E-03
	chac1	ChaC, cation transport regulator homolog 1 (*E. coli*)	2.55	5.3E-05
	ciao2a	cytosolic iron-sulfur assembly component 2A	2.14	6.0E-11
	ciapin1	cytokine induced apoptosis inhibitor 1	2.66	3.6E-07
	cirbpb	cold inducible RNA binding protein b	-1.24	1.2E-02
	ckmt2a	creatine kinase, mitochondrial 2a (sarcomeric)	-2.45	6.4E-07
	clu	clusterin	2.48	2.5E-29
	cmpk2	cytidine monophosphate (UMP-CMP) kinase 2, mitochondrial	3.17	5.0E-02
	cnmd	chondromodulin	-2.19	1.7E-04
	cog7	component of oligomeric golgi complex 7	1.37	2.1E-02
	col11a1a	collagen, type XI, alpha 1a	-2.73	5.0E-04
	col11a1b	collagen, type XI, alpha 1b	-1.97	1.0E-03
	col16a1	collagen, type XVI, alpha 1	-2.32	2.0E-06
	col1a1a	collagen, type I, alpha 1a	-2.61	2.1E-04
	col1a1b	collagen, type I, alpha 1b	-2.62	1.7E-04
	col1a2	collagen, type I, alpha 2	-2.20	4.0E-05
	col2a1a	collagen, type II, alpha 1a	-2.78	5.5E-03
	col2a1b	collagen, type II, alpha 1b	-2.27	1.0E-03
	col4a2	collagen, type IV, alpha 2	-1.26	4.5E-02
	col5a3b	collagen, type V, alpha 3b	-2.72	2.6E-02
	col8a2	collagen, type VIII, alpha 2	-1.89	2.4E-02
	col9a1a	collagen, type IX, alpha 1a	-2.94	3.4E-02
	col9a2	procollagen, type IX, alpha 2	-2.29	2.3E-02
	col9a3	collagen, type IX, alpha 3	-2.95	7.8E-05
	copa	coatomer protein complex, subunit alpha	1.77	4.1E-03
	coq8aa	coenzyme Q8A, genome duplicate a	-1.56	3.7E-03
	cox4i2	cytochrome c oxidase subunit 4I2	-1.69	4.2E-02
	cox8a	cytochrome c oxidase subunit 8A	1.30	4.5E-02
	creb1b	cAMP responsive element binding protein 1b	-2.49	1.4E-02
	creld2	cysteine-rich with EGF-like domains 2	3.57	3.1E-02
	crhb	corticotropin releasing hormone b	-2.56	4.3E-05
	crot	carnitine O-octanoyltransferase	-2.79	1.6E-02
	csf3r	colony stimulating factor 3 receptor (granulocyte)	2.15	1.1E-05
	ctnna1	catenin (cadherin-associated protein), alpha 1	1.36	3.7E-02
	ctps1a	CTP synthase 1a	2.17	3.9E-10
	ctsc	cathepsin C	1.69	2.4E-02
	ctsd	cathepsin D	2.45	1.3E-08
	ctsla	cathepsin La	3.34	1.2E-21

Unstressed	*ctss2.1*	cathepsin S, ortholog2, tandem duplicate 1	2.67	3.6E-02
1000 nM	*cttn*	cortactin	1.34	2.1E-03
	cyp1d1	cytochrome P450, family 1, subfamily D, polypeptide 1	-1.48	1.2E-03
	cyp2aa11	cytochrome P450, family 2, subfamily AA, polypeptide 7	1.72	1.2E-02
	cyp2aa3	cytochrome P450, family 2, subfamily AA, polypeptide 3	-2.47	3.6E-02
	cyp2aa8	cytochrome P450, family 2, subfamily AA, polypeptide 8	-4.53	1.2E-03
	cyp2k8	cytochrome P450, family 2, subfamily K, polypeptide 8	2.13	3.0E-02
	cyp2y3	cytochrome P450, family 2, subfamily Y, polypeptide 3	-2.24	8.4E-08
	cyp3a65	cytochrome P450, family 3, subfamily A, polypeptide 65	-2.89	2.5E-09
	cyp4t8	cytochrome P450, family 4, subfamily T, polypeptide 8	-1.45	2.4E-02
	cyp4v7	cytochrome P450, family 4, subfamily V, polypeptide 7	-2.34	1.7E-05
	cyt1l	type I cytokeratin, enveloping layer	-3.61	8.2E-08
	cyt1l	type I cytokeratin, enveloping layer, like	-3.59	2.0E-04
	dad1	defender against cell death 1	2.12	3.3E-03
	daxx	death-domain associated protein	1.83	5.7E-05
	dcn	decorin	-1.77	7.4E-03
	dcun1d4	DCN1, defective in cullin neddylation 1, domain containing 4 (*S. cerevisiae)*	-1.34	4.0E-02
	ddb2	damage-specific DNA binding protein 2	-1.51	3.1E-02
	ddit3	DNA-damage-inducible transcript 3	2.95	2.7E-12
	decr1	2,4-dienoyl CoA reductase 1, mitochondrial	-1.71	4.1E-02
	dhcr7	7-dehydrocholesterol reductase	-6.72	2.1E-02
	dhdds	dehydrodolichyl diphosphate synthase	2.32	1.6E-05
	dio1	iodothyronine deiodinase 1	-1.65	2.4E-02
	dna2	DNA replication helicase/nuclease 2	4.78	3.5E-03
	dusp1	dual specificity phosphatase 1	1.63	7.4E-03
	dusp11	dual specificity phosphatase 11 (RNA/RNP complex 1-interacting)	1.60	3.8E-02
	dusp22b	dual specificity phosphatase 22b	2.43	3.2E-04
	dusp3b	dual specificity phosphatase 3b	-2.49	1.2E-02
	dync1h1	dynein, cytoplasmic 1, heavy chain 1	1.68	1.4E-06
	ebna1bp2	EBNA1 binding protein 2	1.44	7.0E-06
	eif1axa	eukaryotic translation initiation factor 1A X-linked a	1.37	2.4E-02
	eif2s2	eukaryotic translation initiation factor 2, subunit 2 beta	1.22	1.3E-02
	eif4ba	eukaryotic translation initiation factor 4Ba	-1.35	1.6E-02
	eif4g2a	eukaryotic translation initiation factor 4, gamma 2a	2.12	3.8E-06
	elavl1a	ELAV like RNA binding protein 1a	1.56	2.1E-02
	elocb	elongin C paralog b	1.48	9.2E-05
	ephx1	epoxide hydrolase 1, microsomal (xenobiotic)	-1.92	1.1E-02
	etf1b	eukaryotic translation termination factor 1b	2.33	2.5E-13
	exosc5	exosome component 5	1.64	2.1E-03
	fabp10a	fatty acid binding protein 10a, liver basic	-4.53	2.1E-25
	fabp11a	fatty acid binding protein 11a	8.97	1.3E-02
	fabp11b	fatty acid binding protein 11b	2.23	1.2E-05
	fabp1a	fatty acid binding protein 1a, liver	-3.90	6.4E-05
	fas	Fas cell surface death receptor	3.54	1.1E-06

Unstressed	*fasn*	fatty acid synthase	2.46	4.9E-05
1000 nM	*fgb*	fibrinogen beta chain	1.80	1.1E-02
	fgf3	fibroblast growth factor 3	-5.47	2.6E-02
	fgg	fibrinogen gamma chain	1.35	2.0E-02
	fhl3a	four and a half LIM domains 3a	1.46	1.4E-02
	fis1	fission, mitochondrial 1	1.76	1.2E-05
	fkbp4	FKBP prolyl isomerase 4	-1.57	3.9E-04
	fkbp5	FKBP prolyl isomerase 5	3.93	1.8E-05
	fmo5	flavin containing dimethylaniline monoxygenase 5	-2.20	2.8E-03
	fosab	v-fos FBJ murine osteosarcoma viral oncogene homolog Ab	4.20	1.1E-09
	fosl1a	FOS-like antigen 1a	16.85	1.5E-09
	foxb1a	forkhead box B1a	-1.49	4.6E-02
	fstl1b	follistatin-like 1b	1.76	1.6E-02
	g3bp1	GTPase activating protein (SH3 domain) binding protein 1	1.84	1.4E-06
	gabrb3	gamma-aminobutyric acid type A receptor beta3 subunit	-1.54	2.1E-02
	gabrd	gamma-aminobutyric acid (GABA) A receptor, delta	-1.30	4.6E-02
	gadd45bb	growth arrest and DNA-damage-inducible, beta b	1.98	4.5E-04
	gadd45ga	growth arrest and DNA-damage-inducible, gamma a	2.28	6.9E-04
	gapdh	glyceraldehyde-3-phosphate dehydrogenase	-2.23	2.1E-02
	gata4	GATA binding protein 4	-2.91	1.2E-03
	gbf1	golgi brefeldin A resistant guanine nucleotide exchange factor 1	1.72	2.0E-02
	gclm	glutamate-cysteine ligase, modifier subunit	2.18	1.4E-06
	gdpd3a	glycerophosphodiester phosphodiesterase domain containing 3a	-1.68	4.6E-02
	gemin5	gem (nuclear organelle) associated protein 5	2.22	1.4E-04
	ggt5a	gamma-glutamyltransferase 5a	1.71	4.3E-02
	glb1	galactosidase, beta 1	2.39	2.5E-06
	gli2a	GLI family zinc finger 2a	-1.51	6.1E-03
	glud1a	glutamate dehydrogenase 1a	-1.71	2.7E-02
	glulb	glutamate-ammonia ligase (glutamine synthase) b	1.44	4.0E-06
	gnb3a	guanine nucleotide binding protein (G protein), beta polypeptide 3a	-5.08	4.1E-03
	gngt1	guanine nucleotide binding protein (G protein), gamma transducing activity polypeptide 1	-2.03	1.4E-02
	gnpda1	glucosamine-6-phosphate deaminase 1	1.63	8.0E-03
	gria4a	glutamate receptor, ionotropic, AMPA 4a	1.67	1.3E-02
	grwd1	glutamate-rich WD repeat containing 1	1.50	7.7E-03
	gstk1	glutathione S-transferase kappa 1	-1.63	7.0E-03
	hadh	hydroxyacyl-CoA dehydrogenase	1.56	4.3E-03
	havcr1	hepatitis A virus cellular receptor 1	2.46	8.5E-03
	heatr1	HEAT repeat containing 1	1.50	1.2E-03
	hells	helicase, lymphoid specific	-1.89	1.1E-02
	herpud1	homocysteine-inducible, endoplasmic reticulum stress-inducible, ubiquitin-like domain member 1	1.72	1.0E-03
	hexb	hexosaminidase B (beta polypeptide)	1.79	6.8E-03
	hif1ab	hypoxia inducible factor 1 subunit alpha b	1.41	4.1E-04
	hif1al	hypoxia inducible factor 1 subunit alpha, like	3.19	1.1E-12

Unstressed 1000 nM	*hnf4a*	hepatocyte nuclear factor 4, alpha	-1.62	1.1E-02
	homer2	homer scaffold protein 2	-1.77	1.2E-03
	hprt1	hypoxanthine phosphoribosyltransferase 1	1.32	6.8E-03
	hsd3b7	hydroxy-delta-5-steroid dehydrogenase, 3 beta- and steroid delta-isomerase	-1.66	3.6E-02
	hsp70.3	heat shock cognate 70-kd protein, tandem duplicate 3	4.06	3.9E-04
	hsp70l	heat shock cognate 70-kd protein, like	3.72	5.6E-06
	hsp90b1	heat shock protein 90, beta (grp94), member 1	2.82	8.5E-15
	hspa5	heat shock protein 5	4.41	1.7E-20
	hspb8	heat shock protein b8	2.80	2.5E-13
	hspd1	heat shock 60 protein 1	1.46	3.7E-02
	htr1b	5-hydroxytryptamine (serotonin) receptor 1B	-13.08	7.4E-03
	iars1	isoleucyl-tRNA synthetase 1	1.69	6.5E-04
	icn	ictacalcin	-1.54	3.5E-04
	id1	inhibitor of DNA binding 1, HLH protein	-1.39	2.0E-02
	ide	insulin-degrading enzyme	1.69	1.2E-05
	idi1	isopentenyl-diphosphate delta isomerase 1	1.52	2.8E-03
	ifi45	interferon alpha inducible protein 45	2.62	3.3E-03
	igfbp1a	insulin-like growth factor binding protein 1a	1.80	5.2E-04
	ikbkg	inhibitor of nuclear factor kappa B kinase regulatory subunit gamma	1.31	7.5E-03
	il7r	interleukin 7 receptor	-2.04	3.1E-02
	impdh2	IMP (inosine 5'-monophosphate) dehydrogenase 2	1.62	5.3E-03
	ins	preproinsulin	-1.73	9.2E-03
	irf7	interferon regulatory factor 7	2.57	1.7E-04
	isg15	ISG15 ubiquitin like modifier	9.18	7.1E-10
	isg20	interferon stimulated exonuclease gene	2.66	8.6E-18
	itih3a	inter-alpha-trypsin inhibitor heavy chain 3a	-1.77	2.2E-02
	itpkcb	inositol-trisphosphate 3-kinase Cb	2.08	2.3E-07
	jak1	Janus kinase 1	1.85	3.3E-03
	jam3b	junctional adhesion molecule 3b	1.35	4.7E-02
	jun	Jun proto-oncogene, AP-1 transcription factor subunit	2.71	6.5E-05
	junba	JunB proto-oncogene, AP-1 transcription factor subunit a	3.30	3.7E-10
	kdm5c	lysine (K)-specific demethylase 5C	1.42	7.8E-03
	kdr	kinase insert domain receptor (a type III receptor tyrosine kinase)	1.61	7.8E-03
	kif13a	kinesin family member 13A	-5.26	6.4E-03
	kif23	kinesin family member 23	2.14	8.9E-03
	klf6a	Kruppel-like factor 6a	1.44	1.7E-04
	klhl21	kelch-like family member 21	1.68	1.0E-03
	krt18a.1	keratin 18a, tandem duplicate 1	1.65	9.8E-05
	krt5	keratin 5	-5.16	1.4E-03
	krt94	keratin 94	-2.37	9.0E-06
	krtt1c19e	keratin type 1 c19e	-5.12	4.5E-06
	lamb2	laminin, beta 2 (laminin S)	-1.45	1.6E-02
	lamb4	laminin, beta 4	-5.71	1.2E-05
	lamc2	laminin, gamma 2	7.98	3.3E-21

Unstressed 1000 nM	*lamp1b*	lysosomal associated membrane protein 1b	1.32	2.1E-02
	lap3	leucine aminopeptidase 3	1.68	3.6E-08
	ldlra	low density lipoprotein receptor a	1.37	9.9E-03
	leg1.2	liver-enriched gene 1, tandem duplicate 2	-2.85	1.1E-04
	lgi1b	leucine-rich, glioma inactivated 1b	-2.10	1.4E-02
	lgmn	legumain	2.23	1.5E-09
	lipf	lipase, gastric	1.50	9.9E-03
	litaf	lipopolysaccharide-induced TNF factor	1.68	1.3E-06
	loc100151049	lysosomal protein transmembrane 5	1.68	1.1E-02
	loc100331467	steroidogenic acute regulatory protein, mitochondrial-like	-5.85	2.9E-02
	loc101885363	si:ch211-235i11.3 [Source:ZFIN;Acc:ZDB-GENE-131125-9]	-2.09	4.8E-02
	loc101886435	inactive dipeptidyl peptidase 10-like	-1.47	4.4E-02
	loc108183819	si:ch211-22k7.9 [Source:ZFIN;Acc:ZDB-GENE-070424-160]	-1.73	1.3E-02
	loc110437775	phosphodiesterase 6H, cGMP-specific, cone, gamma, paralog a	-2.95	3.0E-03
	lpar2b	lysophosphatidic acid receptor 2b	-4.02	2.0E-02
	lrrfip2	leucine rich repeat (in FLII) interacting protein 2	1.56	1.3E-04
	lss	lanosterol synthase (2,3-oxidosqualene-lanosterol cyclase)	5.74	1.2E-02
	lum	lumican	-3.18	5.3E-08
	maff	v-maf avian musculoaponeurotic fibrosarcoma oncogene homolog F	2.39	1.4E-02
	mag	myelin associated glycoprotein	-1.87	8.0E-09
	mao	monoamine oxidase	-2.68	1.9E-02
	mapkapk2a	MAPK activated protein kinase 2a	1.70	1.4E-06
	mapkapk2a	MAPK activated protein kinase 2a	1.64	2.2E-03
	matn1	matrilin 1	-1.83	1.2E-02
	matn4	matrilin 4	-2.19	9.5E-08
	mbpa	myelin basic protein a	-1.66	2.4E-02
	mbpa	myelin basic protein a	-2.79	1.9E-13
	mcl1a	MCL1 apoptosis regulator, BCL2 family member a	1.48	3.2E-05
	mcm4	minichromosome maintenance complex component 4	2.12	4.1E-05
	mdh1ab	malate dehydrogenase 1Ab, NAD (soluble)	-1.43	1.5E-02
	me2	malic enzyme 2, NAD(+)-dependent, mitochondrial	1.58	2.0E-02
	meis3	myeloid ecotropic viral integration site 3	-1.42	5.3E-03
	mex3b	mex-3 RNA binding family member B	-2.66	2.0E-04
	mfap2	microfibril associated protein 2	-1.95	1.2E-02
	mfsd2ab	major facilitator superfamily domain containing 2ab	2.70	2.6E-04
	mgst1.2	microsomal glutathione S-transferase 1.2	-1.31	3.1E-02
	mia	MIA SH3 domain containing	-3.40	8.2E-03
	mindy1	MINDY lysine 48 deubiquitinase 1	1.43	4.4E-02
	mlec	malectin	1.91	4.9E-05
	mms22l	MMS22-like, DNA repair protein	-5.78	3.7E-02
	mnd1	meiotic nuclear divisions 1 homolog (*S. cerevisiae*)	-1.50	4.7E-02
	mpz	myelin protein zero	-5.01	3.0E-16
	mrpl14	mitochondrial ribosomal protein L14	2.04	1.8E-08
	mrpl40	mitochondrial ribosomal protein L40	-2.32	4.4E-02

Unstressed	*msra*	methionine sulfoxide reductase A	-1.66	1.9E-02
1000 nM	*mthfs*	5,10-methenyltetrahydrofolate synthetase (5-formyltetrahydrofolate cyclo-ligase)	-1.89	1.2E-03
	mtor	mechanistic target of rapamycin kinase	1.41	3.9E-02
	mvp	major vault protein	2.59	3.4E-08
	myca	MYC proto-oncogene, bHLH transcription factor a	-1.47	2.8E-03
	myom2a	myomesin 2a	-2.02	6.1E-08
	myorg	myogenesis regulating glycosidase (putative)	-1.42	7.4E-03
	naalad2	N-acetylated alpha-linked acidic dipeptidase 2	-1.64	4.4E-02
	ndrg1a	N-myc downstream regulated 1a	1.67	2.0E-02
	nefla	neurofilament, light polypeptide a	-1.93	4.1E-05
	nefmb	neurofilament, medium polypeptide b	-1.61	2.2E-02
	nes	nestin	3.10	2.3E-06
	nfe2	nuclear factor, erythroid 2	-1.48	2.6E-02
	nfe2l2b	nuclear factor, erythroid 2-like 2b	1.97	3.7E-02
	nfkb2	nuclear factor of kappa light polypeptide gene enhancer in B-cells 2 (p49/p100)	1.56	8.9E-03
	nfkb2	nuclear factor of kappa light polypeptide gene enhancer in B-cells 2 (p49/p100)	1.52	4.6E-03
	nfkb2	nuclear factor of kappa light polypeptide gene enhancer in B-cells 2 (p49/p100)	1.51	3.0E-02
	nhp2	NHP2 ribonucleoprotein homolog (yeast)	1.40	1.0E-04
	nkd1	NKD inhibitor of WNT signaling pathway 1	-1.44	2.1E-02
	noc3l	NOC3-like DNA replication regulator	1.38	1.6E-04
	nolc1	nucleolar and coiled-body phosphoprotein 1	1.42	1.2E-02
	nop58	NOP58 ribonucleoprotein homolog (yeast)	1.67	4.5E-05
	npc1	Niemann-Pick disease, type C1	2.00	1.9E-06
	nsa2	NSA2 ribosome biogenesis homolog (S. cerevisiae)	-2.32	2.4E-02
	nudt5	nudix (nucleoside diphosphate linked moiety X)-type motif 5	2.56	7.9E-05
	nup62l	nucleoporin 62 like	1.33	6.7E-04
	nus1	NUS1 dehydrodolichyl diphosphate synthase subunit	2.38	2.5E-04
	opn1lw1	opsin 1 (cone pigments), long-wave-sensitive, 1	-2.73	9.7E-03
	opn1lw2	opsin 1 (cone pigments), long-wave-sensitive, 2	-3.38	5.5E-04
	opn1mw1	opsin 1 (cone pigments), medium-wave-sensitive, 1	-3.95	3.4E-08
	opn1mw2	opsin 1 (cone pigments), medium-wave-sensitive, 2	-2.94	3.0E-03
	opn1mw4	opsin 1 (cone pigments), medium-wave-sensitive, 4	-10.92	1.4E-02
	opn1sw1	opsin 1 (cone pigments), short-wave-sensitive 1	-3.22	1.9E-04
	opn1sw2	opsin 1 (cone pigments), short-wave-sensitive 2	-1.63	2.1E-02
	ostc	oligosaccharyltransferase complex subunit	2.28	1.9E-06
	otos	otospiralin	-2.76	1.3E-03
	oxct1a	3-oxoacid CoA transferase 1a	1.37	1.2E-02
	pacsin3	protein kinase C and casein kinase substrate in neurons 3	-1.54	9.9E-03
	paf1	PAF1 homolog, Paf1/RNA polymerase II complex component	1.23	2.9E-02
	pafah1b1a	platelet-activating factor acetylhydrolase 1b, regulatory subunit 1a	1.27	4.3E-02
	pcmt	protein-L-isoaspartate (D-aspartate) O-methyltransferase	-1.43	2.1E-02
	pde6c	phosphodiesterase 6C, cGMP-specific, cone, alpha prime	-2.35	3.4E-02

Unstressed	*pebp1*	phosphatidylethanolamine binding protein 1	-1.84	9.0E-06
1000 nM	*pfn1*	profilin 1	-1.71	6.4E-07
	phf5a	PHD finger protein 5A	1.64	6.9E-04
	pik3ca	phosphatidylinositol-4,5-bisphosphate 3-kinase, catalytic subunit alpha	1.84	2.9E-02
	pim1	Pim-1 proto-oncogene, serine/threonine kinase	1.68	3.5E-03
	pklr	pyruvate kinase L/R	-3.86	9.1E-17
	pkmb	pyruvate kinase M1/2b	-2.59	1.2E-05
	pla2g15	phospholipase A2, group XV	1.65	5.1E-08
	pla2g4aa	phospholipase A2, group IVAa (cytosolic, calcium-dependent)	1.86	9.9E-03
	plac8.1	placenta associated 8, tandem duplicate 1	1.67	9.9E-05
	plekhh1	pleckstrin homology domain containing, family H (with MyTH4 domain) member 1	2.25	6.1E-03
	plekhm1	pleckstrin homology domain containing, family M (with RUN domain) member 1	1.67	2.7E-03
	plk3	polo-like kinase 3 (*Drosophila*)	1.51	1.6E-04
	plp1a	proteolipid protein 1a	-2.11	3.5E-02
	pnp5b	purine nucleoside phosphorylase 5b	1.89	5.9E-04
	polr2eb	polymerase (RNA) II (DNA directed) polypeptide E, b	1.43	5.6E-03
	polr2i	polymerase (RNA) II (DNA directed) polypeptide I	2.04	1.1E-02
	pop4	POP4 homolog, ribonuclease P/MRP subunit	1.58	1.3E-02
	postnb	periostin, osteoblast specific factor b	-2.05	3.1E-05
	pou3f1	POU class 3 homeobox 1	-1.38	3.2E-02
	ppil1	peptidylprolyl isomerase (cyclophilin)-like 1	-1.83	5.0E-08
	ppp2r5a	protein phosphatase 2, regulatory subunit B', alpha isoform	-2.08	4.3E-02
	prcp	prolylcarboxypeptidase (angiotensinase C)	1.95	6.7E-03
	prdx2	peroxiredoxin 2	-1.83	2.9E-02
	prg4b	proteoglycan 4b	1.40	7.0E-03
	prkag2b	protein kinase, AMP-activated, gamma 2 non-catalytic subunit b	-1.60	4.6E-03
	prkcz	protein kinase C, zeta	1.40	1.2E-02
	prmt5	protein arginine methyltransferase 5	1.77	2.0E-03
	prr15la	proline rich 15 like a	-1.41	3.8E-02
	prrx1a	paired related homeobox 1a	-2.26	3.4E-02
	prss1	serine protease 1	-2.38	9.5E-07
	prss59.1	serine protease 59, tandem duplicate 1	-3.61	7.9E-06
	psap	prosaposin	1.70	1.5E-03
	psen2	presenilin 2	1.80	9.0E-04
	psma4	proteasome 20S subunit alpha 4	2.01	1.5E-04
	psmb3	proteasome 20S subunit beta 3	2.16	3.0E-13
	psmb6	proteasome 20S subunit beta 6	1.80	2.2E-08
	psmc1a	proteasome 26S subunit, ATPase 1a	1.95	8.6E-04
	psmc3	proteasome 26S subunit, ATPase 3	2.65	9.3E-14
	psmc6	proteasome 26S subunit, ATPase 6	2.63	9.0E-07
	psmd10	proteasome 26S subunit, non-ATPase 10	2.23	1.7E-04
	psmd12	proteasome 26S subunit, non-ATPase 12	2.53	2.9E-18
	psmd14	proteasome 26S subunit, non-ATPase 14	1.86	1.9E-06

Unstressed	*psmd4a*	proteasome 26S subunit, non-ATPase 4a	2.51	3.0E-10
1000 nM	*psme1*	proteasome activator subunit 1	2.01	6.1E-04
	psme3	proteasome activator subunit 3	1.88	2.3E-15
	psmg1	proteasome (prosome, macropain) assembly chaperone 1	1.52	7.1E-03
	ptch2	patched 2	-1.56	5.2E-05
	ptk2ba	protein tyrosine kinase 2 beta, a	-12.64	1.8E-02
	ptpn1	protein tyrosine phosphatase non-receptor type 1	1.33	1.1E-02
	ptprc	protein tyrosine phosphatase receptor type C	1.70	2.3E-02
	pus1	pseudouridine synthase 1	1.36	3.7E-02
	pvalb4	parvalbumin 4	-2.06	8.4E-05
	pwp1	PWP1 homolog, endonuclein	1.65	4.6E-04
	pxk	PX domain containing serine/threonine kinase	1.50	2.9E-02
	pxnb	paxillin b	-1.51	5.6E-03
	pygl	phosphorylase, glycogen, liver	-2.92	1.4E-18
	rac1a	Rac family small GTPase 1a	1.52	2.4E-02
	rac1l	Rac family small GTPase 1, like	1.82	4.1E-03
	rac2	Rac family small GTPase 2	1.33	1.2E-02
	rad51c	RAD51 paralog C	-4.25	2.3E-02
	ralab	v-ral simian leukemia viral oncogene homolog Ab (ras related)	1.80	1.1E-06
	rbms2a	RNA binding motif, single stranded interacting protein 2a	1.50	2.0E-06
	rbp2b	retinol binding protein 2b, cellular	-1.77	2.0E-02
	rca2.2	regulator of complement activation group 2 gene 2	-2.83	4.7E-02
	ret	ret proto-oncogene receptor tyrosine kinase	-1.78	2.5E-02
	rgra	retinal G protein coupled receptor a	-2.11	3.4E-02
	rgs2	regulator of G protein signaling 2	3.84	4.9E-06
	rhoab	ras homolog gene family, member Ab	2.02	4.6E-14
	rpl36	ribosomal protein L36	-1.28	2.4E-03
	rpl7l1	ribosomal protein L7-like 1	1.57	2.0E-02
	rraga	Ras-related GTP binding A	1.77	1.6E-06
	rrp12	ribosomal RNA processing 12 homolog	1.46	9.9E-09
	rrs1	ribosome biogenesis regulator 1 homolog	2.00	3.7E-09
	rsl24d1	ribosomal L24 domain containing 1	-1.28	4.4E-02
	rtn2a	reticulon 2a	-1.93	1.5E-02
	rxrab	retinoid x receptor, alpha b	1.54	3.7E-02
	sat1a.1	spermidine/spermine N1-acetyltransferase 1a, duplicate 1	-1.71	2.3E-03
	satb2	SATB homeobox 2	-1.37	2.6E-02
	scn4ab	sodium channel, voltage-gated, type IV, alpha, b	1.47	3.2E-02
	scn4ba	sodium channel, voltage-gated, type IV, beta a	-1.51	1.1E-02
	scn4bb	sodium channel, voltage-gated, type IV, beta b	-1.86	8.9E-03
	scn4bb	sodium channel, voltage-gated, type IV, beta b	-2.35	1.7E-05
	scp2a	sterol carrier protein 2a	-1.89	2.7E-09
	sdf4	stromal cell derived factor 4	1.64	2.9E-09
	sec63	SEC63 homolog, protein translocation regulator	1.63	4.2E-06
	selenow1	selenoprotein W, 1	-1.55	5.0E-04

Unstressed	*sema4ba*	sema domain, immunoglobulin domain (Ig), transmembrane domain (TM) and short cytoplasmic domain, (semaphorin) 4Ba	1.42	1.2E-02
1000 nM	*sema7a*	semaphorin 7A	-1.56	4.7E-02
	serhl	serine hydrolase like	1.70	1.3E-03
	serpine1	serpin peptidase inhibitor, clade E (nexin, plasminogen activator inhibitor type 1), member 1	3.15	6.3E-03
	serpinf1	serpin peptidase inhibitor, clade F (alpha-2 antiplasmin, pigment epithelium derived factor), member 1	-3.53	1.6E-11
	sesn2	sestrin 2	3.27	2.2E-04
	sfrp1a	secreted frizzled-related protein 1a	-1.55	1.6E-03
	sgcb	sarcoglycan, beta (dystrophin-associated glycoprotein)	-1.33	3.0E-02
	sgk2a	serum/glucocorticoid regulated kinase 2a	-1.70	2.3E-02
	shhb	sonic hedgehog signaling molecule b	-1.83	1.7E-02
	si-ch1073-153i20.4	si:ch1073-153i20.4 [Source:ZFIN;Acc:ZDB-GENE-160113-41]	1.66	4.6E-02
	si-ch211-113a14.22	si:ch211-113a14.22 [Source:ZFIN;Acc:ZDB-GENE-121214-203]	-2.37	5.5E-04
	si-ch211-14c7.2	periaxin [Source:ZFIN;Acc:ZDB-GENE-030131-5790]	-1.69	6.1E-06
	si-ch211-207n23.2	si:ch211-207n23.2 [Source:ZFIN;Acc:ZDB-GENE-131121-310]	1.64	4.4E-02
	si-ch211-226o13.1	si:ch211-226o13.1 [Source:ZFIN;Acc:ZDB-GENE-081104-491]	-1.85	7.1E-03
	si-ch211-236h17.3	si:ch211-236h17.3 [Source:ZFIN;Acc:ZDB-GENE-030131-738]	2.40	1.3E-02
	si-ch211-251j10.3	si:ch211-251j10.3 [Source:ZFIN;Acc:ZDB-GENE-081105-110]	1.79	1.8E-03
	si-ch73-158p21.3	si:ch73-158p21.3 [Source:ZFIN;Acc:ZDB-GENE-030131-4747]	-6.19	2.1E-03
	si-ch73-364h19.2	si:ch73-364h19.2 [Source:ZFIN;Acc:ZDB-GENE-131119-21]	-1.52	1.2E-02
	si-dkey-183i3.5	si:dkey-183i3.5 [Source:ZFIN;Acc:ZDB-GENE-030131-8568]	-4.36	4.5E-04
	si-dkey-219e21.2	si:dkey-219e21.2 [Source:ZFIN;Acc:ZDB-GENE-141215-26]	-2.12	1.9E-06
	si-dkey-28b4.7	si:dkey-28b4.7 [Source:ZFIN;Acc:ZDB-GENE-050506-118]	-1.44	1.2E-02
	si-dkeyp-51b9.3	si:dkeyp-51b9.3 [Source:ZFIN;Acc:ZDB-GENE-081104-469]	1.87	9.9E-03
	sla1a	Src like adaptor 1a	1.73	1.3E-02
	slc1a2b	solute carrier family 1 member 2b	-2.14	1.6E-03
	slc25a4	solute carrier family 25 member 4	-2.53	9.0E-03
	slc2a1b	solute carrier family 2 member 1b	5.32	8.6E-04
	slc39a4	solute carrier family 39 member 4	-2.00	4.4E-02
	slc3a2b	solute carrier family 3 member 2b	2.18	2.2E-05
	slc4a1a	solute carrier family 4 member 1a (Diego blood group)	-2.70	3.6E-02
	slc5a1	solute carrier family 5 member 1	-1.93	2.8E-02
	slc6a19b	solute carrier family 6 member 19b	-1.47	4.0E-02
	slc6a8	solute carrier family 6 member 8	1.72	1.4E-02
	slc7a3a	solute carrier family 7 member 3a	1.95	5.0E-05
	slc7a7	solute carrier family 7 member 7	1.48	1.6E-02
	smpdl3a	sphingomyelin phosphodiesterase acid like 3A	1.95	1.6E-06
	snrpb	small nuclear ribonucleoprotein polypeptides B and B1	1.40	1.7E-04
	snrpg	small nuclear ribonucleoprotein polypeptide G	2.80	5.0E-10

Unstressed	*snx22*	sorting nexin 22	1.95	3.5E-02
1000 nM	*socs3a*	suppressor of cytokine signaling 3a	5.01	4.8E-15
	sod3b	superoxide dismutase 3, extracellular b	-2.84	1.6E-05
	sparc	secreted protein, acidic, cysteine-rich (osteonectin)	-1.82	5.6E-05
	spcs2	signal peptidase complex subunit 2	1.42	1.4E-02
	sptlc2a	serine palmitoyltransferase, long chain base subunit 2a	1.68	4.0E-02
	sqstm1	sequestosome 1	3.80	2.1E-04
	srgn	serglycin	1.82	3.3E-03
	srm	spermidine synthase	5.03	4.5E-05
	srp72	signal recognition particle 72	1.78	1.6E-03
	srsf2a	serine and arginine rich splicing factor 2a	1.27	7.2E-03
	sst1.1	somatostatin 1, tandem duplicate 1	-1.53	3.6E-02
	stam2	signal transducing adaptor molecule (SH3 domain and ITAM motif) 2	1.49	2.0E-06
	star	steroidogenic acute regulatory protein	-1.74	4.6E-02
	stat3	signal transducer and activator of transcription 3 (acute-phase response factor)	2.73	2.7E-12
	stat5a	signal transducer and activator of transcription 5a	2.06	7.9E-03
	stmn1a	stathmin 1a	-1.48	3.8E-02
	stxbp1a	syntaxin binding protein 1a	-1.30	6.1E-03
	tagln2	transgelin 2	1.42	1.3E-03
	tbx2b	T-box transcription factor 2b	-1.35	1.5E-02
	tcap	titin-cap (telethonin)	4.16	3.4E-15
	tcn2	transcobalamin II	-1.57	3.1E-02
	tgfb1a	transforming growth factor, beta 1a	-9.07	4.0E-02
	thrb	thyroid hormone receptor beta	-1.76	1.9E-02
	thy1	Thy-1 cell surface antigen	-1.65	1.7E-02
	timp2b	TIMP metallopeptidase inhibitor 2b	6.30	1.9E-02
	tlcd3a	TLC domain containing 3A	1.49	9.9E-03
	tm7sf3	transmembrane 7 superfamily member 3	1.47	3.5E-03
	tm9sf2	transmembrane 9 superfamily member 2	1.34	2.9E-02
	tmbim1a	transmembrane BAX inhibitor motif containing 1a	1.47	1.0E-02
	tmco1	transmembrane and coiled-coil domains 1	1.67	2.5E-08
	tmed10	transmembrane p24 trafficking protein 10	1.62	3.8E-08
	tmed2	transmembrane p24 trafficking protein 2	1.60	8.3E-06
	tmem167a	transmembrane protein 167A	1.69	2.2E-08
	tnfrsf19	tumor necrosis factor receptor superfamily, member 19	-1.87	6.0E-05
	tnfrsf1b	tumor necrosis factor receptor superfamily, member 1B	1.44	1.2E-02
	tnfrsfa	tumor necrosis factor receptor superfamily, member a	2.55	1.2E-02
	tnfsf10	TNF superfamily member 10	-4.01	8.2E-21
	tnip1	TNFAIP3 interacting protein 1	1.41	2.4E-02
	tp53	tumor protein p53	1.67	1.3E-03
	traf6	TNF receptor-associated factor 6	1.57	2.7E-02
	trap1	TNF receptor-associated protein 1	1.47	3.3E-02
	trappc3	trafficking protein particle complex 3	1.85	9.3E-14

Unstressed	*trib3*	tribbles pseudokinase 3	2.91	7.7E-20
1000 nM	*trim13*	tripartite motif containing 13	-1.57	3.5E-03
	ttr	transthyretin (prealbumin, amyloidosis type I)	-2.87	1.3E-06
	tubb2	tubulin, beta 2A class IIa	-1.57	7.8E-03
	twf2	twinfilin actin binding protein 2	2.07	1.4E-02
	ubb	ubiquitin B	1.60	1.7E-02
	ube2a	ubiquitin-conjugating enzyme E2A (RAD6 homolog)	1.60	5.0E-04
	ube2g1a	ubiquitin-conjugating enzyme E2G 1a (UBC7 homolog, yeast)	1.86	2.8E-02
	ube2j1	ubiquitin-conjugating enzyme E2, J1	1.68	9.7E-04
	ube2ka	ubiquitin-conjugating enzyme E2Ka (UBC1 homolog, yeast)	-1.51	4.1E-02
	ufm1	ubiquitin-fold modifier 1	1.99	4.0E-07
	ugdh	UDP-glucose 6-dehydrogenase	1.90	1.0E-02
	ugt1a2	UDP glucuronosyltransferase 1 family, polypeptide A1	-1.61	2.1E-02
	ugt1b4	UDP glucuronosyltransferase 1 family, polypeptide B4	-4.15	1.4E-02
	usp14	ubiquitin specific peptidase 14 (tRNA-guanine transglycosylase)	2.98	1.1E-23
	usp9	ubiquitin specific peptidase 9	1.36	3.5E-02
	utp25	UTP25 small subunit processor component	1.42	2.9E-02
	vamp1	vesicle-associated membrane protein 1	-1.40	9.9E-03
	vim	vimentin	-1.59	3.0E-02
	vps4b	vacuolar protein sorting 4 homolog B	1.83	1.0E-08
	vsig10	V-set and immunoglobulin domain containing 10	1.51	7.5E-03
	vsx1	visual system homeobox 1 homolog, chx10-like	-1.33	3.4E-02
	wars	tryptophanyl-tRNA synthetase 1	2.47	6.3E-10
	washc4	WASH complex subunit 4	1.97	1.0E-02
	washc5	WASH complex subunit 5	1.98	1.4E-05
	wu-fi04e12	desmoplakin b	-1.77	8.6E-05
	xaf1	XIAP associated factor 1	1.73	3.0E-02
	xbp1	X-box binding protein 1	2.16	2.3E-08
	xiap	X-linked inhibitor of apoptosis	1.35	2.2E-02
	yipf5	Yip1 domain family, member 5	1.43	9.9E-03
	ykt6	YKT6 v-SNARE homolog (*S. cerevisiae*)	1.38	1.7E-02
	zcchc24	zinc finger, CCHC domain containing 24	-1.58	3.2E-03
	zgc-100868	zgc:100868 [Source:ZFIN;Acc:ZDB-GENE-040801-33]	2.51	8.4E-06
	zgc-103586	zgc:103586 [Source:ZFIN;Acc:ZDB-GENE-041114-88]	-1.36	3.2E-02
	zgc-136930	zgc:136930 [Source:ZFIN;Acc:ZDB-GENE-060312-16]	-7.42	7.9E-07
	zgc-162730	zgc:162730 [Source:ZFIN;Acc:ZDB-GENE-030131-6366]	2.33	1.3E-08
	zgc-165532	zgc:165532 [Source:ZFIN;Acc:ZDB-GENE-050417-213]	1.57	1.0E-02
	zgc-92137	zgc:92137 [Source:ZFIN;Acc:ZDB-GENE-040801-179]	-3.39	1.8E-04
	zic2a	zic family member 2 (odd-paired homolog, *Drosophila*), a	-1.75	9.9E-03
Stressed larvae				
1000 nM	*aars1*	alanyl-tRNA synthetase 1	3.05	1.3E-05
	abcf1	ATP-binding cassette, sub-family F (GCN20), member 1	2.84	2.8E-08
	abcf3	ATP-binding cassette, sub-family F (GCN20), member 3	2.53	4.4E-02
	acadm	acyl-CoA dehydrogenase medium chain	-1.28	2.0E-02

Stressed	*acat2*	acetyl-CoA acetyltransferase 2	-1.61	3.1E-02
1000 nM	*ace2*	angiotensin I converting enzyme 2	-1.83	1.5E-04
	acta1a	actin alpha 1, skeletal muscle a	-2.19	6.7E-03
	acta2	actin alpha 2, smooth muscle	-1.62	2.2E-02
	actl6a	actin-like 6A	1.46	3.8E-02
	adam10a	ADAM metallopeptidase domain 10a	1.27	3.4E-03
	adam8a	ADAM metallopeptidase domain 8a	2.90	5.7E-06
	adh5	alcohol dehydrogenase 5	-2.21	2.2E-03
	adh8a	alcohol dehydrogenase 8a	-3.07	3.9E-02
	adi1	acireductone dioxygenase 1	2.18	4.7E-10
	adma	adrenomedullin a	2.49	5.4E-04
	agt	angiotensinogen	1.39	4.9E-02
	agtrap	angiotensin II receptor-associated protein	2.19	4.5E-03
	agtrap	angiotensin II receptor-associated protein	2.82	3.7E-18
	ahcy	adenosylhomocysteinase	-1.82	1.4E-06
	ahr1b	aryl hydrocarbon receptor 1b	-1.68	8.9E-03
	ahr2	aryl hydrocarbon receptor 2	1.42	2.1E-02
	aldh1l1	aldehyde dehydrogenase 1 family, member L1	-2.30	3.3E-05
	aldh9a1a.1	aldehyde dehydrogenase 9 family, member A1a, tandem duplicate 1	-2.10	2.0E-06
	alpi.2	alkaline phosphatase, intestinal, tandem duplicate 2	-1.62	4.5E-02
	amdhd2	amidohydrolase domain containing 2	1.61	3.6E-02
	amy2a	amylase alpha 2A	-3.63	1.3E-05
	angpt1	angiopoietin 1	-1.54	4.7E-02
	angptl2a	angiopoietin-like 2a	1.57	8.8E-03
	apoa2	apolipoprotein A-II	-2.51	2.2E-03
	apoc1	apolipoprotein C-I	-1.40	1.8E-03
	apoea	apolipoprotein Ea	-1.69	1.3E-02
	appb	amyloid beta (A4) precursor protein b	-1.92	1.9E-02
	aqp9b	aquaporin 9b	-2.00	6.4E-03
	arhgap45a	Rho GTPase activating protein 45a	2.28	2.6E-02
	arid4b	translocase of outer mitochondrial membrane 20	1.72	2.7E-03
	arpc3	actin related protein 2/3 complex, subunit 3	1.32	2.2E-03
	arpp19a	cAMP-regulated phosphoprotein 19a	1.30	8.7E-03
	arr3a	arrestin 3a, retinal (X-arrestin)	-2.74	2.5E-03
	ascc3	activating signal cointegrator 1 complex subunit 3	1.44	3.2E-02
	ascl1b	achaete-scute family bHLH transcription factor 1b	-1.93	1.5E-02
	aspn	asporin (LRR class 1)	-1.60	3.1E-02
	atf1	activating transcription factor 1	1.45	1.6E-05
	atf3	activating transcription factor 3	5.68	5.7E-09
	atf4a	activating transcription factor 4a	1.41	3.9E-04
	atf5a	activating transcription factor 5a	2.35	3.5E-02
	atf6	activating transcription factor 6	1.90	1.5E-06
	atg12	ATG12 autophagy related 12 homolog (*S. cerevisiae*)	1.36	4.9E-03
	atp11c	ATPase phospholipid transporting 11C	-2.21	1.1E-02

Stressed larvae	*atp1a1a.1*	ATPase Na+/K+ transporting subunit alpha 1a, tandem duplicate 1	1.35	8.8E-03
1000 nM	*atp6v0a1a*	ATPase H+ transporting V0 subunit a1a	1.43	1.4E-03
	atp6v1d	ATPase H+ transporting V1 subunit D	1.87	2.4E-13
	atp6v1f	ATPase H+ transporting V1 subunit F	1.54	1.9E-09
	atraid	all-trans retinoic acid-induced differentiation factor	1.84	5.5E-06
	b4galt1	UDP-Gal:betaGlcNAc beta 1,4- galactosyltransferase, polypeptide 1	-1.68	2.6E-04
	bag3	BCL2 associated athanogene 3	2.13	8.0E-03
	bambia	BMP and activin membrane-bound inhibitor (*Xenopus laevis*) homolog a	-2.86	6.2E-03
	bambia	BMP and activin membrane-bound inhibitor (*Xenopus laevis*) homolog a	-1.59	1.8E-03
	banf1	barrier to autointegration factor 1	1.56	1.2E-05
	bdh1	3-hydroxybutyrate dehydrogenase, type 1	-1.54	1.1E-02
	bhlhe40	basic helix-loop-helix family, member e40	1.53	4.1E-03
	bin2a	bridging integrator 2a	-1.41	1.6E-02
	birc6	baculoviral IAP repeat containing 6	1.41	1.9E-03
	blmh	bleomycin hydrolase	1.75	1.7E-08
	bloc1s2	biogenesis of lysosomal organelles complex-1, subunit 2	1.92	1.7E-05
	bmp3	bone morphogenetic protein 3	-1.52	1.1E-03
	btr04	bloodthirsty-related gene family, member 4	1.73	1.4E-02
	c1qbp	complement component 1, q subcomponent binding protein	1.26	4.9E-02
	c2cd2l	c2cd2 like	-1.79	7.5E-04
	c5ar1	C5a anaphylatoxin chemotactic receptor	3.52	1.8E-07
	calm1a	calmodulin 1a	-1.27	5.3E-03
	calm3a	calmodulin 3a (phosphorylase kinase, delta)	-1.61	9.5E-03
	calr	calreticulin	1.96	2.5E-02
	camk1gb	calcium/calmodulin-dependent protein kinase IGb	-1.51	2.7E-02
	camk2b1	calcium/calmodulin-dependent protein kinase (CaM kinase) II beta 1	-1.82	7.3E-03
	camsap2a	calmodulin regulated spectrin-associated protein family, member 2a	-1.40	8.8E-03
	canx	calnexin	2.93	6.6E-16
	casp3b	caspase 3, apoptosis-related cysteine peptidase b	2.27	3.5E-07
	casp7	caspase 7, apoptosis-related cysteine peptidase	1.76	2.6E-04
	casp8	caspase 8, apoptosis-related cysteine peptidase	1.49	3.3E-02
	cat	catalase	-1.94	1.6E-02
	cav1	caveolin 1	-1.37	6.5E-04
	cavin2b	caveolae associated protein 2b	-1.67	1.8E-03
	ccdc80l1	coiled-coil domain containing 80 like 1	-2.26	4.0E-02
	ccl35.2	chemokine (C-C motif) ligand 35, duplicate 2	2.38	3.2E-02
	ccnc	cyclin C	1.77	4.4E-02
	cct5	chaperonin containing TCP1, subunit 5 (epsilon)	1.29	2.9E-02
	cct7	chaperonin containing TCP1, subunit 7 (eta)	1.64	1.9E-02
	cd36	CD36 molecule (thrombospondin receptor)	-2.08	1.8E-07
	cd40	CD40 molecule, TNF receptor superfamily member 5	2.93	4.3E-05
	cd9b	CD9 molecule b	1.34	1.9E-02
	cd9b	CD9 molecule b	1.54	4.6E-03
	cdh1	cadherin 1, type 1, E-cadherin (epithelial)	1.54	3.4E-03

Stressed larvae	*cdkn1ca*	cyclin-dependent kinase inhibitor 1Ca	1.44	4.2E-02
1000 nM	*cebpa*	CCAAT enhancer binding protein alpha	1.80	1.6E-05
	cebpb	CCAAT enhancer binding protein beta	2.52	3.6E-04
	cebpz	CCAAT enhancer binding protein zeta	1.26	3.8E-02
	cecr2	CECR2 histone acetyl-lysine reader	1.49	2.2E-02
	cel.2	carboxyl ester lipase, tandem duplicate 2	-2.76	8.9E-04
	ces2	carboxylesterase 2a	-1.86	4.6E-02
	cga	glycoprotein hormones, alpha polypeptide	-1.67	3.2E-02
	cgrrf1	cell growth regulator with ring finger domain 1	1.68	1.8E-02
	chmp4c	charged multivesicular body protein 4C	-1.51	4.0E-02
	chn1	chimerin 1	-1.27	4.4E-02
	chrna4b	cholinergic receptor, nicotinic, alpha 4b	-3.59	5.0E-02
	ciao2a	cytosolic iron-sulfur assembly component 2A	2.04	1.7E-09
	ciapin1	cytokine induced apoptosis inhibitor 1	2.75	1.1E-07
	cirbpb	cold inducible RNA binding protein b	-1.38	4.1E-05
	clk4a	CDC-like kinase 4a	-2.22	1.2E-03
	clocka	clock circadian regulator a	-2.06	2.8E-03
	cltcl1	clathrin, heavy chain-like 1	-2.55	2.4E-02
	clu	clusterin	2.01	1.3E-17
	cnmd	chondromodulin	-1.87	4.5E-03
	cog7	component of oligomeric golgi complex 7	1.49	1.6E-03
	coil	coilin p80	2.11	1.5E-02
	col11a1a	collagen, type XI, alpha 1a	-3.19	6.5E-05
	col11a1b	collagen, type XI, alpha 1b	-2.11	1.8E-04
	col15a1b	collagen, type XV, alpha 1b	-2.12	9.2E-06
	col16a1	collagen, type XVI, alpha 1	-2.69	1.6E-08
	col1a1a	collagen, type I, alpha 1a	-3.42	1.5E-06
	col1a1b	collagen, type I, alpha 1b	-3.25	2.0E-06
	col1a2	collagen, type I, alpha 2	-2.52	8.3E-07
	col2a1a	collagen, type II, alpha 1a	-3.68	1.5E-04
	col2a1b	collagen, type II, alpha 1b	-2.59	8.5E-05
	col4a1	collagen, type IV, alpha 1	-2.11	4.4E-02
	col5a2a	collagen, type V, alpha 2a	-1.63	1.7E-02
	col9a1a	collagen, type IX, alpha 1a	-5.32	1.8E-04
	col9a2	procollagen, type IX, alpha 2	-3.95	2.8E-05
	col9a3	collagen, type IX, alpha 3	-2.54	1.3E-03
	copa	coatomer protein complex, subunit alpha	1.84	1.4E-03
	coq8aa	coenzyme Q8A, genome duplicate a	-1.54	4.5E-03
	cox6b1	cytochrome c oxidase subunit 6B1	1.47	4.5E-02
	csf3r	colony stimulating factor 3 receptor (granulocyte)	2.28	1.7E-06
	csk	C-terminal Src kinase	-2.45	1.4E-03
	ctcf	CCCTC-binding factor (zinc finger protein)	1.48	4.9E-02
	ctnna1	catenin (cadherin-associated protein), alpha 1	1.44	8.8E-03
	ctps1a	CTP synthase 1a	1.43	8.7E-03

Stressed larvae	*ctsc*	cathepsin C	1.60	4.5E-02
1000 nM	*ctsd*	cathepsin D	1.69	1.7E-03
	ctsla	cathepsin La	3.40	2.8E-22
	ctss2.1	cathepsin S, ortholog2, tandem duplicate 1	3.80	1.7E-03
	cttn	cortactin	1.27	1.3E-02
	cx43	connexin 43	-1.61	4.5E-04
	cybb	cytochrome b-245, beta polypeptide (chronic granulomatous disease)	2.89	6.4E-03
	cyp1c1	cytochrome P450, family 1, subfamily C, polypeptide 1	-1.89	5.6E-03
	cyp2aa1	cytochrome P450, family 2, subfamily AA, polypeptide 1	-2.46	6.4E-04
	cyp2aa4	cytochrome P450, family 2, subfamily AA, polypeptide 4	2.35	4.1E-02
	cyp2aa8	cytochrome P450, family 2, subfamily AA, polypeptide 8	-3.63	3.6E-03
	cyp2k17	cytochrome P450, family 2, subfamily K, polypeptide17	-2.58	4.6E-02
	cyp2k8	cytochrome P450, family 2, subfamily K, polypeptide 8	2.12	2.5E-02
	cyp2y3	cytochrome P450, family 2, subfamily Y, polypeptide 3	-2.17	4.1E-07
	cyp3a65	cytochrome P450, family 3, subfamily A, polypeptide 65	-1.89	7.5E-04
	cyp4t8	cytochrome P450, family 4, subfamily T, polypeptide 8	-1.82	4.8E-05
	cyt1l	type I cytokeratin, enveloping layer	-4.59	1.3E-10
	cyt1l	type I cytokeratin, enveloping layer, like	-2.88	2.5E-03
	dad1	defender against cell death 1	2.02	5.9E-03
	dbh	dopamine beta-hydroxylase (dopamine beta-monooxygenase)	2.27	4.6E-03
	dcn	decorin	-2.39	8.5E-06
	dcun1d4	DCN1, defective in cullin neddylation 1, domain containing 4 (*S. cerevisiae*)	-1.31	4.8E-02
	ddb2	damage-specific DNA binding protein 2	-1.48	3.7E-02
	ddit3	DNA-damage-inducible transcript 3	2.49	7.9E-09
	dera	deoxyribose-phosphate aldolase (putative)	1.78	1.0E-02
	desma	desmin a	1.55	4.1E-02
	dhdds	dehydrodolichyl diphosphate synthase	2.10	1.5E-04
	dio1	iodothyronine deiodinase 1	-1.84	3.6E-03
	dio3b	iodothyronine deiodinase 3b	-2.51	4.3E-02
	dkk1b	dickkopf WNT signaling pathway inhibitor 1b	-2.58	9.0E-03
	dldh	dihydrolipoamide dehydrogenase	-1.45	6.8E-03
	dlx3b	distal-less homeobox 3b	-1.72	1.4E-02
	dlx5a	distal-less homeobox 5a	-1.98	1.7E-02
	dsc2l	desmocollin 2 like	-2.08	8.7E-07
	dusp1	dual specificity phosphatase 1	1.86	2.2E-04
	dusp11	dual specificity phosphatase 11 (RNA/RNP complex 1-interacting)	1.69	1.5E-02
	dusp22b	dual specificity phosphatase 22b	2.17	1.8E-03
	dync1h1	dynein, cytoplasmic 1, heavy chain 1	1.57	4.0E-05
	dynlt3	dynein, light chain, Tctex-type 3	1.67	2.3E-07
	edem1	ER degradation enhancer, mannosidase alpha-like 1	2.02	1.3E-03
	egr1	early growth response 1	1.55	3.9E-02
	eif2b1	eukaryotic translation initiation factor 2B, subunit 1 alpha	2.00	2.7E-03
	eif2s2	eukaryotic translation initiation factor 2, subunit 2 beta	1.25	2.6E-03
	eif3s10	eukaryotic translation initiation factor 3, subunit 10 (theta)	-1.29	4.4E-02

Stressed larvae	*eif4g2a*	eukaryotic translation initiation factor 4, gamma 2a	1.49	2.5E-02
1000 nM	*elocb*	elongin C paralog b	1.45	1.8E-04
	eml3	EMAP like 3	1.57	3.0E-02
	eml3	EMAP like 3	1.60	2.1E-03
	emx2	empty spiracles homeobox 2	-1.95	5.9E-04
	enosf1	enolase superfamily member 1	1.97	2.5E-04
	ephx1	epoxide hydrolase 1, microsomal (xenobiotic)	-2.04	3.9E-03
	erbb3a	erb-b2 receptor tyrosine kinase 3a	-1.58	2.5E-03
	etf1b	eukaryotic translation termination factor 1b	1.61	9.2E-05
	exorh	extra-ocular rhodopsin	-2.97	5.7E-03
	f3a	coagulation factor IIIa	2.41	2.7E-05
	fabp10a	fatty acid binding protein 10a, liver basic	-5.45	3.9E-32
	fabp11b	fatty acid binding protein 11b	2.30	6.2E-06
	fabp1a	fatty acid binding protein 1a, liver	-3.80	8.5E-05
	fas	Fas cell surface death receptor	4.41	5.1E-09
	fbxo21	F-box protein 21	-1.53	3.1E-02
	fcer1gl	Fc receptor, IgE, high affinity I, gamma polypeptide like	2.90	2.8E-03
	fgb	fibrinogen beta chain	1.63	3.6E-02
	fgg	fibrinogen gamma chain	1.35	1.9E-02
	fignl1	fidgetin-like 1	2.79	1.9E-02
	fis1	fission, mitochondrial 1	1.96	1.2E-07
	flna	filamin A, alpha (actin binding protein 280)	1.86	1.9E-02
	fosab	v-fos FBJ murine osteosarcoma viral oncogene homolog Ab	3.20	6.9E-07
	fosl1a	FOS-like antigen 1a	5.97	2.6E-04
	foxo3b	forkhead box O3b	-1.23	3.0E-02
	fpgs	folylpolyglutamate synthase	1.25	4.0E-02
	gabrb3	gamma-aminobutyric acid type A receptor beta3 subunit	-1.66	5.4E-03
	gabrd	gamma-aminobutyric acid (GABA) A receptor, delta	-1.32	2.8E-02
	gadd45aa	growth arrest and DNA-damage-inducible, alpha, a	2.36	4.0E-02
	gadd45bb	growth arrest and DNA-damage-inducible, beta b	2.11	7.0E-05
	gadd45ga	growth arrest and DNA-damage-inducible, gamma a	2.77	1.2E-05
	gap43	growth associated protein 43	1.79	1.1E-03
	gbf1	golgi brefeldin A resistant guanine nucleotide exchange factor 1	2.40	2.8E-05
	gclm	glutamate-cysteine ligase, modifier subunit	1.57	8.8E-03
	gfap	glial fibrillary acidic protein	-1.47	3.8E-02
	ggcx	gamma-glutamyl carboxylase	1.35	1.5E-02
	glb1	galactosidase, beta 1	1.49	5.0E-02
	gli2a	GLI family zinc finger 2a	-1.37	3.9E-02
	gnaq	guanine nucleotide binding protein (G protein), q polypeptide	-2.01	4.0E-02
	gngt1	guanine nucleotide binding protein (G protein), gamma transducing activity polypeptide 1	-3.33	4.0E-06
	gria4a	glutamate receptor, ionotropic, AMPA 4a	1.63	1.5E-02
	grin1a	glutamate receptor, ionotropic, N-methyl D-aspartate 1a	-1.46	2.8E-03
	grwd1	glutamate-rich WD repeat containing 1	1.57	1.7E-03

Stressed larvae	*gstz1*	glutathione S-transferase zeta 1	-1.92	9.8E-03
1000 nM	*hadh*	hydroxyacyl-CoA dehydrogenase	2.05	5.2E-07
	hcls1	hematopoietic cell-specific Lyn substrate 1	1.63	1.3E-03
	heatr1	HEAT repeat containing 1	1.36	1.9E-02
	her6	hairy-related 6	-1.88	2.1E-04
	herpud1	homocysteine-inducible, endoplasmic reticulum stress-inducible, ubiquitin-like domain member 1	1.54	1.3E-02
	hexb	hexosaminidase B (beta polypeptide)	1.68	1.5E-02
	hif1ab	hypoxia inducible factor 1 subunit alpha b	1.55	3.2E-06
	histh1l	histone H1 like	1.94	1.7E-04
	hk1	hexokinase 1	2.20	1.7E-04
	hmgcs1	3-hydroxy-3-methylglutaryl-CoA synthase 1 (soluble)	2.08	1.0E-02
	hnf4a	hepatocyte nuclear factor 4, alpha	-2.21	4.2E-06
	homer2	homer scaffold protein 2	-1.64	5.0E-03
	hsd11b2	hydroxysteroid (11-beta) dehydrogenase 2	-2.00	2.3E-02
	hsp70.3	heat shock cognate 70-kd protein, tandem duplicate 3	4.81	4.6E-05
	hsp70l	heat shock cognate 70-kd protein, like	4.13	1.0E-06
	hsp90aa1.2	heat shock protein 90, alpha (cytosolic), class A member 1, tandem duplicate 2	2.19	2.6E-05
	hsp90ab1	heat shock protein 90, alpha (cytosolic), class A member 1, tandem duplicate 2	-1.30	9.6E-03
	hsp90b1	heat shock protein 90, beta (grp94), member 1	3.56	1.1E-21
	hspa5	heat shock protein 5	6.25	4.6E-31
	hspb8	heat shock protein b8	2.38	1.5E-09
	hspd1	heat shock 60 protein 1	1.81	2.9E-04
	iars1	isoleucyl-tRNA synthetase 1	1.97	3.7E-06
	icn	ictacalcin	-1.40	6.7E-03
	id1	inhibitor of DNA binding 1, HLH protein	-1.73	1.3E-05
	idi1	isopentenyl-diphosphate delta isomerase 1	1.65	1.6E-04
	ier2b	immediate early response 2b	2.03	1.5E-04
	ifi45	interferon alpha inducible protein 45	3.33	9.0E-05
	ifi46	interferon alpha inducible protein 46	2.69	1.1E-02
	igfbp1a	insulin-like growth factor binding protein 1a	1.99	2.5E-05
	ikbkg	inhibitor of nuclear factor kappa B kinase regulatory subunit gamma	1.23	4.3E-02
	il11a	interleukin 11a	3.56	1.7E-02
	il13ra1	interleukin 13 receptor, alpha 1	1.62	9.2E-03
	ins	preproinsulin	-1.77	4.9E-03
	insl3	insulin-like 3 (Leydig cell)	-2.58	1.3E-02
	ints3	integrator complex subunit 3	1.78	3.8E-02
	ipo13	importin 13	1.81	3.2E-02
	irf7	interferon regulatory factor 7	2.93	9.2E-06
	irf8	interferon regulatory factor 8	2.09	1.5E-04
	isg15	ISG15 ubiquitin like modifier	12.59	1.5E-12
	isg20	interferon stimulated exonuclease gene	1.45	3.1E-03
	isl2b	ISL LIM homeobox 2b	-1.71	5.6E-04

Stressed larvae	*itih3a*	inter-alpha-trypsin inhibitor heavy chain 3a	-1.92	9.2E-03
1000 nM	*jak1*	Janus kinase 1	2.03	3.1E-04
	jun	Jun proto-oncogene, AP-1 transcription factor subunit	3.18	1.3E-06
	junba	JunB proto-oncogene, AP-1 transcription factor subunit a	2.87	5.0E-08
	kcnj12a	potassium inwardly rectifying channel subfamily J member 12a	-1.88	7.6E-03
	kdm5c	lysine (K)-specific demethylase 5C	1.31	4.6E-02
	kdr	kinase insert domain receptor (a type III receptor tyrosine kinase)	2.10	6.0E-06
	khdrbs3	KH domain containing, RNA binding, signal transduction associated 3	-1.32	1.3E-02
	klf6a	Kruppel-like factor 6a	1.35	2.3E-03
	klf9	Kruppel-like factor 9	-2.22	1.1E-02
	krt18a.1	keratin 18a, tandem duplicate 1	1.50	1.8E-03
	krt5	keratin 5	-7.68	3.1E-05
	krt8	keratin 8	-1.48	5.4E-03
	krt94	keratin 94	-1.59	3.1E-02
	krtt1c19e	keratin type 1 c19e	-3.77	2.5E-04
	lamb2	laminin, beta 2 (laminin S)	-1.44	1.8E-02
	lamc2	laminin, gamma 2	2.26	3.0E-04
	lap3	leucine aminopeptidase 3	1.58	1.6E-06
	leg1.2	liver-enriched gene 1, tandem duplicate 2	-2.78	1.6E-04
	lgi1a	leucine-rich, glioma inactivated 1a	-1.53	4.9E-02
	lgmn	legumain	2.08	5.5E-08
	lingo1b	leucine rich repeat and Ig domain containing 1b	-1.41	1.2E-02
	litaf	lipopolysaccharide-induced TNF factor	1.46	5.5E-04
	loc100000034	chemokine (C-C motif) ligand 35, duplicate 1	2.93	1.9E-02
	loc100151049	lysosomal protein transmembrane 5	1.75	4.8E-03
	loc100536500	cysteine-rich venom protein natrin-1-like	-1.63	1.6E-02
	loc108179064	exostosin-1c	-3.31	1.2E-02
	loc110437775	phosphodiesterase 6H, cGMP-specific, cone, gamma, paralog a	-3.51	3.0E-04
	lpgat1	lysophosphatidylglycerol acyltransferase 1	1.42	1.1E-03
	lrrc58b	leucine rich repeat containing 58b	1.45	4.0E-02
	lrrfip2	leucine rich repeat (in FLII) interacting protein 2	1.33	1.9E-02
	lsm1	LSM1, U6 small nuclear RNA associated	1.53	4.0E-02
	lum	lumican	-4.12	4.7E-11
	mag	myelin associated glycoprotein	-1.57	6.6E-05
	map7a	microtubule-associated protein 7a	1.93	6.1E-03
	mapkapk2a	MAPK activated protein kinase 2a	1.53	1.4E-04
	mapkapk2a	MAPK activated protein kinase 2a	1.63	1.8E-03
	mapta	microtubule-associated protein tau a	-1.42	2.0E-02
	matn1	matrilin 1	-2.94	8.1E-07
	matn4	matrilin 4	-2.06	1.4E-06
	mbnl2	muscleblind-like splicing regulator 2	1.68	3.1E-03
	mbpa	myelin basic protein a	-2.52	8.7E-11
	mbpa	myelin basic protein a	-1.85	3.6E-03
	mcl1a	MCL1 apoptosis regulator, BCL2 family member a	1.25	3.0E-02

Stressed larvae	*mcm3*	minichromosome maintenance complex component 3	1.57	4.6E-02
1000 nM	*mcm4*	minichromosome maintenance complex component 4	1.87	6.2E-04
	mdh1ab	malate dehydrogenase 1Ab, NAD (soluble)	-1.35	4.3E-02
	mdh2	malate dehydrogenase 2, NAD (mitochondrial)	-1.62	6.1E-03
	mex3b	mex-3 RNA binding family member B	-2.55	4.5E-04
	mfap2	microfibril associated protein 2	-1.94	1.2E-02
	mfsd2ab	major facilitator superfamily domain containing 2ab	2.39	8.9E-04
	mia	MIA SH3 domain containing	-4.72	4.6E-04
	mindy1	MINDY lysine 48 deubiquitinase 1	1.62	3.0E-03
	mlec	malectin	2.41	1.1E-08
	mpx	myeloid-specific peroxidase	2.09	3.0E-02
	mpz	myelin protein zero	-16.94	5.5E-05
	mpz	myelin protein zero	-4.66	3.1E-15
	mrpl14	mitochondrial ribosomal protein L14	1.82	3.3E-06
	mrps6	mitochondrial ribosomal protein S6	1.90	2.7E-02
	ms4a17a.17	membrane-spanning 4-domains, subfamily A, member 17A.17	-1.90	3.6E-03
	msra	methionine sulfoxide reductase A	-2.16	7.3E-05
	mthfs	5,10-methenyltetrahydrofolate synthetase (5-formyltetrahydrofolate cyclo-ligase)	-2.10	9.1E-05
	mvp	major vault protein	1.90	3.6E-04
	myca	MYC proto-oncogene, bHLH transcription factor a	-1.60	1.5E-04
	myd88	MYD88 innate immune signal transduction adaptor	1.53	1.6E-02
	myl1	myosin, light chain 1, alkali; skeletal, fast	-1.42	5.0E-03
	myl12.1	myosin, light chain 12, genome duplicate 1	1.35	1.7E-03
	myom2a	myomesin 2a	-2.26	2.5E-10
	myorg	myogenesis regulating glycosidase (putative)	-1.48	1.4E-03
	narfl	nuclear prelamin A recognition factor-like	1.49	3.3E-03
	ndufb3	NADH:ubiquinone oxidoreductase subunit B3	-1.36	8.8E-03
	ndufv2	NADH:ubiquinone oxidoreductase core subunit V2	-1.44	6.9E-03
	nefla	neurofilament, light polypeptide a	-2.21	5.7E-07
	nefmb	neurofilament, medium polypeptide b	-2.08	9.8E-05
	nes	nestin	3.63	5.8E-08
	net1	neuroepithelial cell transforming 1	-1.31	5.0E-02
	neurod1	neuronal differentiation 1	-2.57	1.9E-03
	nfkb2	nuclear factor of kappa light polypeptide gene enhancer in B-cells 2 (p49/p100)	1.71	9.5E-05
	nfkb2	nuclear factor of kappa light polypeptide gene enhancer in B-cells 2 (p49/p100)	2.37	1.0E-08
	nfkb2	nuclear factor of kappa light polypeptide gene enhancer in B-cells 2 (p49/p100)	2.55	1.6E-08
	nhp2	NHP2 ribonucleoprotein homolog (yeast)	1.32	2.0E-03
	nipsnap1	nipsnap homolog 1 (*C. elegans*)	-2.11	1.7E-03
	nkd1	NKD inhibitor of WNT signaling pathway 1	-1.83	3.3E-05
	notch3	notch receptor 3	-1.52	2.6E-02
	nt5dc2	5'-nucleotidase domain containing 2	-1.57	2.1E-02
	nucb2a	nucleobindin 2a	1.55	1.1E-03

Stressed larvae 1000 nM	*nudt5*	nudix (nucleoside diphosphate linked moiety X)-type motif 5	2.08	2.9E-03
	nuf2	UF2 component of NDC80 kinetochore complex	2.32	3.2E-02
	nup37	nucleoporin 37	2.08	1.5E-02
	nus1	NUS1 dehydrodolichyl diphosphate synthase subunit	1.80	1.9E-02
	opn1lw1	opsin 1 (cone pigments), long-wave-sensitive, 1	-4.41	2.7E-05
	opn1lw2	opsin 1 (cone pigments), long-wave-sensitive, 2	-4.50	6.4E-06
	opn1mw1	opsin 1 (cone pigments), medium-wave-sensitive, 1	-4.53	3.8E-10
	opn1mw2	opsin 1 (cone pigments), medium-wave-sensitive, 2	-3.77	9.0E-05
	opn1sw1	opsin 1 (cone pigments), short-wave-sensitive 1	-4.78	2.4E-07
	opn1sw2	opsin 1 (cone pigments), short-wave-sensitive 2	-2.50	1.4E-06
	ostc	oligosaccharyltransferase complex subunit	2.08	3.1E-05
	ovol1a	ovo-like zinc finger 1a	-3.31	7.8E-03
	pacsin3	protein kinase C and casein kinase substrate in neurons 3	-1.45	2.5E-02
	pafah1b1a	platelet-activating factor acetylhydrolase 1b, regulatory subunit 1a	1.30	2.1E-02
	pax6a	paired box 6a	-1.45	8.1E-03
	pcdhb	protocadherin b	-2.09	1.4E-02
	pcolcea	procollagen C-endopeptidase enhancer a	-1.91	4.9E-02
	pdcd6ip	programmed cell death 6 interacting protein	1.68	3.6E-02
	pde6c	phosphodiesterase 6C, cGMP-specific, cone, alpha prime	-2.30	3.4E-02
	pde6gb	phosphodiesterase 6G, cGMP-specific, rod, gamma, paralog b	-2.07	4.3E-05
	pdgfab	platelet-derived growth factor alpha polypeptide b	-2.44	8.6E-03
	pdgfbb	platelet-derived growth factor beta polypeptide b	-2.27	4.5E-05
	pdia6	protein disulfide isomerase family A, member 6	3.09	3.1E-03
	pebp1	phosphatidylethanolamine binding protein 1	-1.49	5.6E-03
	pfkpa	phosphofructokinase, platelet a	2.19	1.4E-03
	pfn1	profilin 1	-1.62	8.2E-06
	pgm1	phosphoglucomutase 1	-2.04	1.5E-02
	phgdh	phosphoglycerate dehydrogenase	1.76	5.0E-02
	phkg2	phosphorylase kinase, gamma 2 (testis)	-5.00	1.1E-02
	phlda3	pleckstrin homology-like domain, family A, member 3	1.77	4.1E-02
	piezo1	piezo-type mechanosensitive ion channel component 1	1.85	3.0E-02
	pik3r1	phosphoinositide-3-kinase, regulatory subunit 1 (alpha)	-1.42	8.5E-03
	pim1	Pim-1 proto-oncogene, serine/threonine kinase	1.44	4.7E-02
	pink1	PTEN induced kinase 1	-1.34	4.6E-02
	pklr	pyruvate kinase L/R	-3.46	4.3E-14
	pkmb	pyruvate kinase M1/2b	-3.39	8.9E-09
	pla2g15	phospholipase A2, group XV	1.23	4.6E-02
	pla2g4aa	phospholipase A2, group IVAa (cytosolic, calcium-dependent)	2.23	2.6E-04
	plac8.2	placenta associated 8, tandem duplicate 2	3.50	3.1E-02
	plce1	phospholipase C, epsilon 1	-2.51	4.9E-02
	plekhg4	pleckstrin homology domain containing, family G (with RhoGef domain) member 4	-1.75	1.7E-02
	plekhh1	pleckstrin homology domain containing, family H (with MyTH4 domain) member 1	2.17	5.7E-03

Stressed larvae	*plekhm1*	pleckstrin homology domain containing, family M (with RUN domain) member 1	1.44	3.0E-02
1000 nM	*plk3*	polo-like kinase 3 (*Drosophila*)	1.26	4.9E-02
	pnkp	polynucleotide kinase 3'-phosphatase	2.13	3.6E-02
	pnp5b	purine nucleoside phosphorylase 5b	1.71	3.8E-03
	polr2eb	polymerase (RNA) II (DNA directed) polypeptide E, b	1.38	1.2E-02
	polr2i	polymerase (RNA) II (DNA directed) polypeptide I	2.70	1.6E-04
	pora	P450 (cytochrome) oxidoreductase a	1.50	4.2E-02
	postnb	periostin, osteoblast specific factor b	-2.21	3.5E-06
	pou3f1	POU class 3 homeobox 1	-1.71	7.5E-05
	ppil1	peptidylprolyl isomerase (cyclophilin)-like 1	-1.88	1.3E-08
	ppp1r14aa	protein phosphatase 1, regulatory (inhibitor) subunit 14Aa	-1.84	2.4E-02
	prdx2	peroxiredoxin 2	-1.80	3.1E-02
	preb	prolactin regulatory element binding	1.60	2.6E-03
	prkab1a	protein kinase, AMP-activated, beta 1 non-catalytic subunit, a	-1.36	7.0E-03
	prkag2b	protein kinase, AMP-activated, gamma 2 non-catalytic subunit b	-1.68	1.6E-03
	prkcha	protein kinase C, eta, a	-2.82	1.3E-02
	prmt5	protein arginine methyltransferase 5	2.00	7.1E-05
	prss1	serine protease 1	-2.61	4.7E-08
	prss59.1	serine protease 59, tandem duplicate 1	-3.73	4.2E-06
	psma4	proteasome 20S subunit alpha 4	2.12	3.0E-05
	psmb3	proteasome 20S subunit beta 3	1.94	1.1E-09
	psmb6	proteasome 20S subunit beta 6	1.56	3.8E-05
	psmc1a	proteasome 26S subunit, ATPase 1a	1.88	1.4E-03
	psmc3	proteasome 26S subunit, ATPase 3	1.98	6.1E-07
	psmc6	proteasome 26S subunit, ATPase 6	2.70	3.4E-07
	psmd10	proteasome 26S subunit, non-ATPase 10	2.50	1.2E-05
	psmd12	proteasome 26S subunit, non-ATPase 12	2.36	1.0E-15
	psmd14	proteasome 26S subunit, non-ATPase 14	1.60	4.4E-04
	psmd4a	proteasome 26S subunit, non-ATPase 4a	1.98	6.0E-06
	psme1	proteasome activator subunit 1	2.80	2.0E-07
	psme3	proteasome activator subunit 3	1.77	2.0E-12
	psmg1	proteasome (prosome, macropain) assembly chaperone 1	1.70	2.0E-04
	ptch2	patched 2	-1.56	5.5E-05
	ptgs2b	prostaglandin-endoperoxide synthase 2b	1.93	3.6E-02
	ptprc	protein tyrosine phosphatase receptor type C	1.80	8.5E-03
	pvalb4	parvalbumin 4	-2.50	2.6E-07
	pxnb	paxillin b	-1.36	4.4E-02
	pygl	phosphorylase, glycogen, liver	-2.38	3.5E-12
	pygma	phosphorylase, glycogen, muscle A	-2.89	1.0E-03
	rabggtb	Rab geranylgeranyltransferase subunit beta	1.97	2.5E-06
	rac1a	Rac family small GTPase 1a	1.67	2.8E-03
	rac2	Rac family small GTPase 2	1.82	3.1E-09
	rac3b	Rac family small GTPase 3b	-1.76	2.4E-03

Stressed larvae	*rai14*	retinoic acid induced 14	2.68	2.4E-03
1000 nM	*ralab*	v-ral simian leukemia viral oncogene homolog Ab (ras related)	1.69	1.3E-05
	rb1	retinoblastoma 1	1.64	2.3E-02
	rbms2a	RNA binding motif, single stranded interacting protein 2a	1.46	1.0E-05
	rca2.2	regulator of complement activation group 2 gene 2	-3.17	2.6E-02
	rhoab	ras homolog gene family, member Ab	1.75	5.1E-09
	rmi1	RMI1, RecQ mediated genome instability 1, homolog (*S. cerevisiae*)	1.80	1.4E-02
	rpl19	ribosomal protein L19	-1.39	4.6E-03
	rpl32	ribosomal protein L32	-1.26	1.4E-02
	rpl35	ribosomal protein L35	-1.29	2.3E-02
	rpl36	ribosomal protein L36	-1.29	1.4E-03
	rpl39	ribosomal protein L39	-1.30	2.6E-02
	rpl6	ribosomal protein L6	-1.40	7.6E-03
	rpl7a	ribosomal protein L7a	-1.27	2.3E-03
	rps2	ribosomal protein S2	-1.34	2.1E-02
	rps20	ribosomal protein S20	-1.32	1.1E-03
	rps27.2	ribosomal protein S27, isoform 2	-1.24	4.6E-03
	rraga	Ras-related GTP binding A	1.35	2.2E-02
	rrp1	ribosomal RNA processing 1	-2.26	1.9E-02
	rrp12	ribosomal RNA processing 12 homolog	1.39	1.0E-06
	rsrc1	arginine/serine-rich coiled-coil 1	1.40	1.9E-02
	saa	serum amyloid A	1.84	5.0E-02
	sat1a.1	spermidine/spermine N1-acetyltransferase 1a, duplicate 1	-1.75	1.1E-03
	satb2	SATB homeobox 2	-1.46	4.3E-03
	sbspon	somatomedin B and thrombospondin type 1 domain containing	-2.72	1.1E-03
	scn3b	sodium channel, voltage-gated, type III, beta	-1.57	4.5E-02
	scn4ab	sodium channel, voltage-gated, type IV, alpha, b	1.68	1.4E-03
	scn4ba	sodium channel, voltage-gated, type IV, beta a	-1.44	2.6E-02
	scn4bb	sodium channel, voltage-gated, type IV, beta b	-2.05	4.0E-04
	scp2a	sterol carrier protein 2a	-2.39	9.1E-17
	sdf4	stromal cell derived factor 4	1.47	6.4E-06
	sec63	SEC63 homolog, protein translocation regulator	1.47	4.5E-04
	selenbp1	selenium binding protein 1	1.55	3.5E-02
	selenow1	selenoprotein W, 1	-1.69	1.9E-05
	sept5b	septin 5b	-1.56	7.5E-04
	serhl	serine hydrolase like	1.82	1.6E-04
	serpina1	serpin peptidase inhibitor, clade A (alpha-1 antiproteinase, antitrypsin), member 1	-1.79	2.2E-03
	serpine1	serpin peptidase inhibitor, clade E (nexin, plasminogen activator inhibitor type 1), member 1	4.57	9.1E-05
	serpinf1	serpin peptidase inhibitor, clade F (alpha-2 antiplasmin, pigment epithelium derived factor), member 1	-2.68	4.1E-07
	sesn2	sestrin 2	3.49	5.3E-05
	sfrp1a	secreted frizzled-related protein 1a	-1.57	1.0E-03
	sfrp1b	secreted frizzled-related protein 1b	-1.51	2.5E-03

Stressed larvae	*shhb*	sonic hedgehog signaling molecule b	-1.96	6.1E-03
1000 nM	*si-ch1073-153i20.4*	si:ch1073-153i20.4 [Source:ZFIN;Acc:ZDB-GENE-160113-41]	2.21	4.2E-04
	si-ch1073-159d7.7	si:ch1073-159d7.7 [Source:ZFIN;Acc:ZDB-GENE-160113-58]	2.00	2.0E-04
	si-ch1073-55a19.2	si:ch1073-55a19.2 [Source:ZFIN;Acc:ZDB-GENE-081104-93]	1.75	2.4E-03
	si-ch211-14c7.2	periaxin [Source:ZFIN;Acc:ZDB-GENE-030131-5790]	-1.46	1.9E-03
	si-ch211-199f5.1	si:ch211-199f5.1 [Source:ZFIN;Acc:ZDB-GENE-120215-215]	-1.59	1.5E-02
	si-ch73-248e21.1	si:ch73-248e21.1 [Source:ZFIN;Acc:ZDB-GENE-120215-198]	1.86	9.2E-03
	si-ch73-364h19.2	si:ch73-364h19.2 [Source:ZFIN;Acc:ZDB-GENE-131119-21]	-2.05	1.4E-06
	si-dkey-183i3.5	si:dkey-183i3.5 [Source:ZFIN;Acc:ZDB-GENE-030131-8568]	-5.44	3.1E-05
	si-dkey-219e21.2	si:dkey-219e21.2 [Source:ZFIN;Acc:ZDB-GENE-141215-26]	-1.48	2.8E-02
	si-dkey-21h14.3	si:dkey-21h14.3 [Source:ZFIN;Acc:ZDB-GENE-041210-92]	-3.81	1.3E-02
	si-dkey-251i10.3	si:dkey-251i10.3 [Source:ZFIN;Acc:ZDB-GENE-060526-271]	2.02	7.6E-03
	si-dkey-28b4.7	si:dkey-28b4.7 [Source:ZFIN;Acc:ZDB-GENE-050506-118]	-1.58	8.4E-04
	si-dkey-46i9.6	si:dkey-46i9.6 [Source:ZFIN;Acc:ZDB-GENE-160114-63]	-1.84	2.6E-04
	si-dkeyp-113d7.1	si:dkeyp-113d7.1 [Source:ZFIN;Acc:ZDB-GENE-030131-755]	-1.59	1.0E-02
	sinhcaf	SIN3-HDAC complex associated factor	1.53	3.6E-03
	sirt3	sirtuin 3	-1.55	5.6E-04
	sla1a	Src like adaptor 1a	2.61	2.5E-06
	slc1a2b	solute carrier family 1 member 2b	-2.49	9.8E-05
	slc1a3a	solute carrier family 1 member 3a	-1.45	4.7E-03
	slc22a6l	solute carrier family 22 member 6, like	-2.06	5.7E-03
	slc25a4	solute carrier family 25 member 4	-3.48	1.6E-04
	slc3a2a	solute carrier family 3 member 2a	-1.87	1.2E-02
	slc51a	solute carrier family 51 alpha subunit	-1.97	1.2E-05
	slc6a8	solute carrier family 6 member 8	1.77	5.9E-03
	slc7a3a	solute carrier family 7 member 3a	1.60	5.8E-03
	smoc1	SPARC related modular calcium binding 1	-1.76	2.3E-02
	smpdl3a	sphingomyelin phosphodiesterase acid like 3A	1.66	3.6E-04
	snap25a	synaptosome associated protein 25a	-1.48	8.7E-03
	snrpb	small nuclear ribonucleoprotein polypeptides B and B1	1.25	2.1E-02
	snrpg	small nuclear ribonucleoprotein polypeptide G	1.97	7.7E-05
	socs3a	suppressor of cytokine signaling 3a	2.48	2.8E-05
	sod3b	superoxide dismutase 3, extracellular b	-2.56	1.4E-04
	sox4a	SRY-box transcription factor 4a	-1.39	1.5E-05
	sparc	secreted protein, acidic, cysteine-rich (osteonectin)	-1.43	2.6E-02
	sptlc2a	serine palmitoyltransferase, long chain base subunit 2a	1.65	4.1E-02
	sqstm1	sequestosome 1	4.42	2.6E-05
	srgn	serglycin	1.99	3.5E-04
	sst1.1	somatostatin 1, tandem duplicate 1	-1.80	1.7E-03
	stam2	signal transducing adaptor molecule (SH3 domain and ITAM motif) 2	1.30	3.6E-03

Stressed larvae	*stambpa*	STAM binding protein a	2.10	3.6E-03
1000 nM	*stat1a*	signal transducer and activator of transcription 1a	1.32	8.9E-03
	stat3	signal transducer and activator of transcription 3 (acute-phase response factor)	2.49	3.8E-10
	stk10	serine/threonine kinase 10	1.71	3.6E-03
	sult1st3	sulfotransferase family 1, cytosolic sulfotransferase 3	-1.69	2.0E-04
	sys1	SYS1 golgi trafficking protein	2.72	1.7E-03
	tagln2	transgelin 2	1.44	6.2E-04
	tbx1	T-box transcription factor 1	-1.73	1.2E-02
	tcap	titin-cap (telethonin)	1.51	4.8E-02
	tcf12	transcription factor 12	-1.51	2.1E-02
	tdo2a	tryptophan 2,3-dioxygenase a	-1.62	1.6E-03
	tfap2a	transcription factor AP-2 alpha	-1.56	6.2E-03
	thrb	thyroid hormone receptor beta	-2.16	5.6E-04
	timm17b	translocase of inner mitochondrial membrane 17 homolog B (yeast)	-1.40	2.0E-02
	timp2b	TIMP metallopeptidase inhibitor 2b	17.94	5.4E-05
	timp4.1	TIMP metallopeptidase inhibitor 4, tandem duplicate 1	-3.29	1.2E-04
	tiparp	TCDD-inducible poly(ADP-ribose) polymerase	-1.77	4.2E-02
	tm7sf3	transmembrane 7 superfamily member 3	1.39	1.3E-02
	tmbim1a	transmembrane BAX inhibitor motif containing 1a	1.74	5.8E-05
	tmco1	transmembrane and coiled-coil domains 1	1.83	2.9E-11
	tmed10	transmembrane p24 trafficking protein 10	1.57	3.7E-07
	tmed2	transmembrane p24 trafficking protein 2	1.49	1.9E-04
	tmem14ca	transmembrane protein 14Ca	1.52	1.4E-03
	tmem167a	transmembrane protein 167A	1.69	2.7E-08
	tmem30c	cms1 ribosomal small subunit homolog	-1.63	5.0E-02
	tnfaip3	tumor necrosis factor, alpha-induced protein 3	2.43	4.5E-05
	tnfrsf19	tumor necrosis factor receptor superfamily, member 19	-1.53	1.1E-02
	tnfrsf1b	tumor necrosis factor receptor superfamily, member 1B	1.58	7.4E-04
	tnfsf10	TNF superfamily member 10	-2.55	6.3E-09
	tnip1	TNFAIP3 interacting protein 1	1.62	6.3E-04
	tnnt3b	troponin T type 3b (skeletal, fast)	-1.98	1.2E-02
	tp53	tumor protein p53	1.84	6.2E-05
	tpm1	tropomyosin 1 (alpha)	-1.71	6.1E-03
	tprkb	Tp53rk binding protein	1.89	5.2E-03
	trap1	TNF receptor-associated protein 1	1.49	2.2E-02
	trappc3	trafficking protein particle complex 3	1.65	5.0E-09
	trib3	tribbles pseudokinase 3	1.70	2.2E-05
	tsg101a	tumor susceptibility 101a	1.32	2.8E-02
	tsta3	tissue specific transplantation antigen P35B	1.54	3.6E-02
	ttr	transthyretin (prealbumin, amyloidosis type I)	-2.86	1.6E-06
	tubb2	tubulin, beta 2A class IIa	-1.59	6.2E-03
	tubb6	tubulin, beta 6 class V	-3.42	1.4E-02
	uba3	ubiquitin-like modifier activating enzyme 3	1.51	4.1E-03

Stressed larvae	*ubb*	ubiquitin B	1.67	6.6E-03
1000 nM	*ube2a*	ubiquitin-conjugating enzyme E2A (RAD6 homolog)	1.82	4.2E-06
	ube2j1	ubiquitin-conjugating enzyme E2, J1	1.63	1.7E-03
	ube2ka	ubiquitin-conjugating enzyme E2Ka (UBC1 homolog, yeast)	-1.65	8.1E-03
	ube3c	ubiquitin protein ligase E3C	1.58	3.0E-02
	ufm1	ubiquitin-fold modifier 1	1.92	1.8E-06
	ugdh	UDP-glucose 6-dehydrogenase	1.89	8.2E-03
	ugt1a2	UDP glucuronosyltransferase 1 family, polypeptide A1	-2.09	9.4E-05
	ugt1b1	UDP glucuronosyltransferase 1 family, polypeptide B1	-2.90	9.1E-05
	usp14	ubiquitin specific peptidase 14 (tRNA-guanine transglycosylase)	2.60	3.0E-18
	usp6nl	USP6 N-terminal like	-1.56	5.0E-02
	usp9	ubiquitin specific peptidase 9	1.34	4.1E-02
	vamp1	vesicle-associated membrane protein 1	-1.52	6.3E-04
	vav3b	vav 3 guanine nucleotide exchange factor b	-3.22	3.3E-05
	vbp1	von Hippel-Lindau binding protein 1	1.76	3.6E-04
	vcam1b	vascular cell adhesion molecule 1b	-1.83	3.1E-02
	veph1	ventricular zone expressed PH domain-containing 1	-2.36	5.5E-03
	vim	vimentin	-1.67	1.1E-02
	vps4b	vacuolar protein sorting 4 homolog B	1.55	6.0E-05
	wars	tryptophanyl-tRNA synthetase 1	3.19	6.6E-16
	washc5	WASH complex subunit 5	2.22	2.9E-07
	wdr62	WD repeat domain 62	1.90	1.9E-02
	xaf1	XIAP associated factor 1	2.42	9.2E-05
	xbp1	X-box binding protein 1	1.98	1.1E-06
	xpnpep1	X-prolyl aminopeptidase (aminopeptidase P) 1, soluble	1.47	4.9E-02
	xrcc5	X-ray repair complementing defective repair in Chinese hamster cells 5	1.76	2.2E-03
	yipf5	Yip1 domain family, member 5	1.58	3.4E-04
	yrk	Yes-related kinase	1.65	6.9E-03
	zeb2b	zinc finger E-box binding homeobox 2b	-1.49	3.1E-04
	zgc-103697	zgc:103697 [Source:NCBI gene;Acc:447921]	1.32	6.6E-03
	zgc-136930	zgc:136930 [Source:ZFIN;Acc:ZDB-GENE-060312-16]	-7.75	4.3E-07
	zgc-162730	zgc:162730 [Source:ZFIN;Acc:ZDB-GENE-030131-6366]	1.49	1.1E-02
	zgc-92137	zgc:92137 [Source:ZFIN;Acc:ZDB-GENE-040801-179]	-3.43	1.4E-04
	zic2a	zic family member 2 (odd-paired homolog, *Drosophila*), a	-1.68	1.5E-02

All significant DEGs were defined with FC > |1.2| and *p*-adj < 0.05.

C. Supplementary materials for Chapter 4

Supplementary Table C.1. List of primers used for real-time qPCR on samples from 5 dpf SR4G larvae.

Gene symbol	ZFIN ID	Primer sequence
eef1a1l1	ZDB-GENE-990415-52	F: CCGTCTGCCACTTCAGGATGTGT R: TTGAGGACACCAGTCTCCACACGA
d4egfp	ZDB-EFG-070117-1	F: CGAGCAACTGAGGATCCCATTCTCT R: CACCCCGGTGAACAGCTCCT

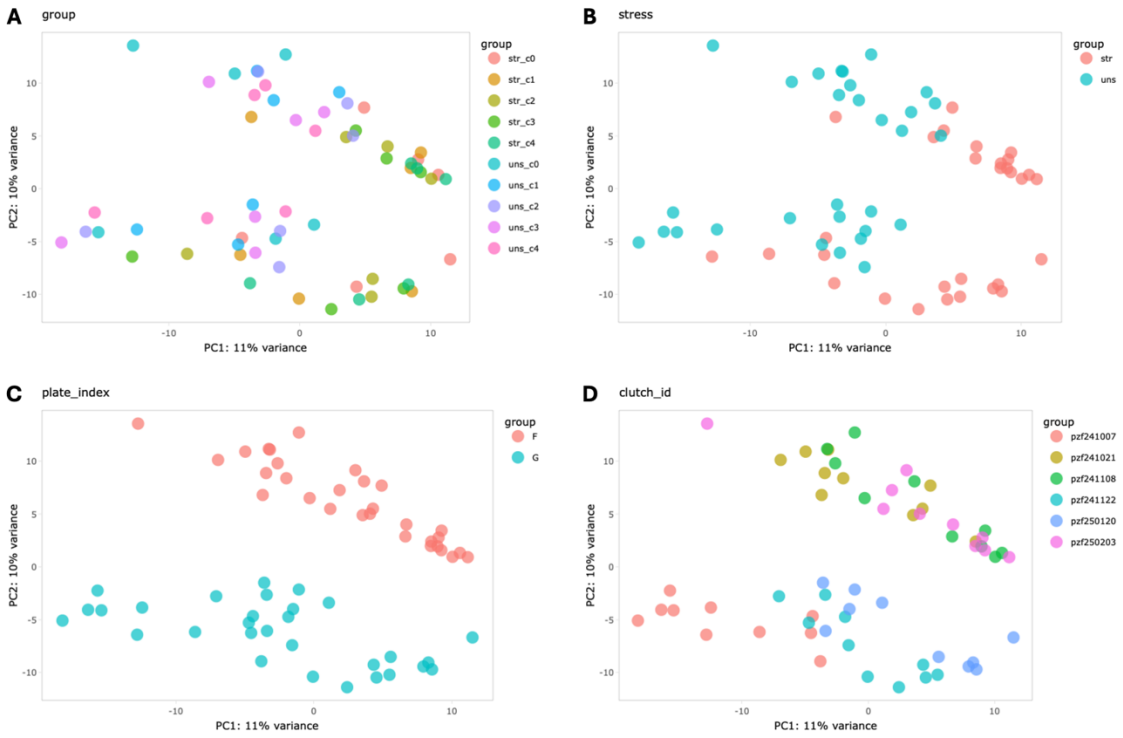

Supplementary Figure C.1. Variation between samples before batch effect normalisation. Principal components analysis shows samples clustered by stress and concentration group (A), stress condition (B), library preparation plate index (C), and clutch identifier (D).

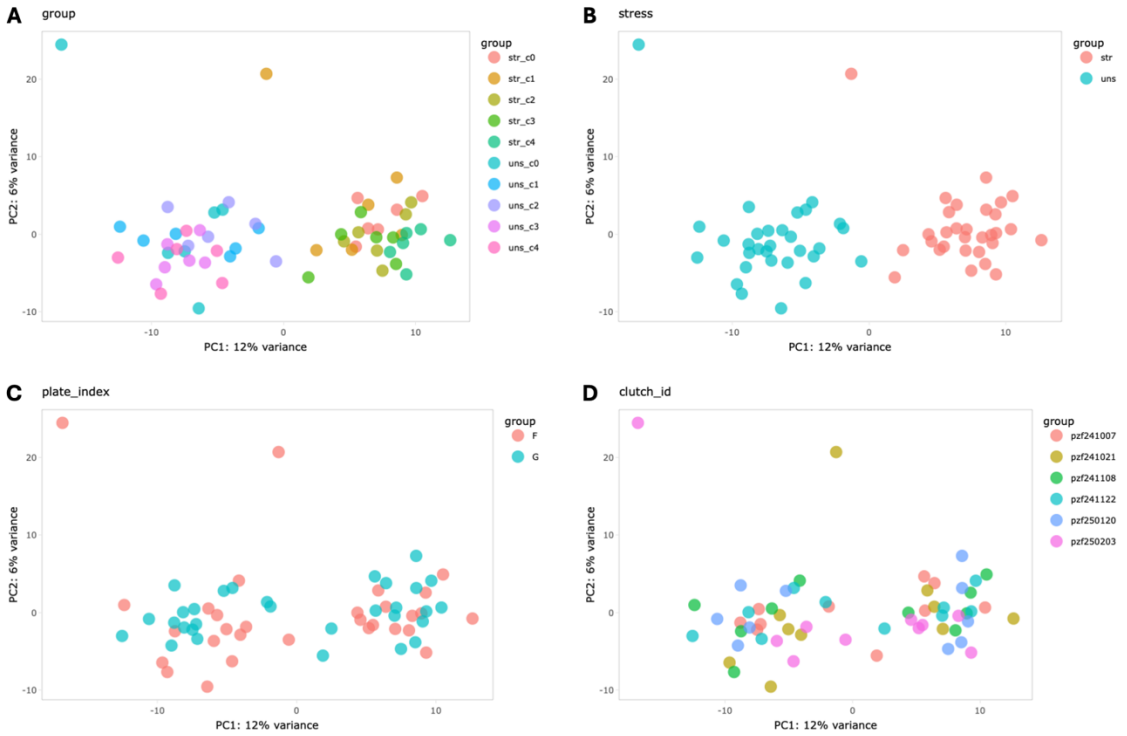

Supplementary Figure C.2. Variation between samples after batch effect normalisation.

Principal components analysis shows samples clustered by stress and concentration group (A), stress condition (B), library preparation plate index (C), and clutch identifier (D).

Supplementary Table C.2. Effects of sertraline exposure on hatching probability of SR4G zebrafish larvae.

Treatment	Predicted probability (95% CI)	Effect size (% ± SE)	z	*p*-value
3 days post-fertilization				
Vehicle control	0.94 (0.85 – 0.98)	N/A	N/A	N/A
Internal control	0.93 (0.84 – 0.97)	-0.56 ± 3.17	-0.216	0.995
SER 10 nM	0.93 (0.84 – 0.97)	-0.56 ± 3.17	-0.216	0.995
SER 50 nM	0.94 (0.86 – 0.98)	0.55 ± 2.76	0.223	0.994
SER 100 nM	0.94 (0.85 – 0.98)	0.00 ± 2.96	0.000	1.000
SER 500 nM	0.93 (0.83 – 0.97)	-1.13 ± 3.38	-0.425	0.969
4 days post-fertilization				
Vehicle control	1.00 (0.96 – 1.00)	N/A	N/A	N/A
Internal control	0.99 (0.93 – 1.00)	-0.57 ± 0.92	-0.971	0.752
SER 10 nM	1.00 (0.00 – 1.00)	0.27 ± 0.00	0.063	1.000
SER 50 nM	0.99 (0.93 – 1.00)	-0.57 ± 0.92	-0.976	0.749
SER 100 nM	0.99 (0.93 – 1.00)	-0.56 ± 0.92	-0.971	0.752
SER 500 nM	1.00 (0.96 – 1.00)	-0.01 ± 0.38	-0.017	1.000
5 days post-fertilization				
Vehicle control	1.00 (0.00 – 1.00)	N/A	N/A	N/A
Internal control	1.00 (0.96 – 1.00)	-0.32 ± 0.42	-0.111	0.999
SER 10 nM	1.00 (0.00 – 1.00)	-0.00 ± 0.00	-0.007	1.000
SER 50 nM	0.99 (0.93 – 1.00)	-1.06 ± 1.08	-0.119	0.999
SER 100 nM	0.99 (0.94 – 1.00)	-0.65 ± 0.72	-0.116	0.999
SER 500 nM	1.00 (0.96 – 1.00)	-0.33 ± 0.43	-0.112	0.999

Predicted hatching probability per treatment, and differences in hatching probability (%) between treatments and the vehicle control are derived from generalized linear mixed-effects models (binomial distribution, logit link) with experimental replicate included as a random factor.

Effect sizes are expressed as mean difference ± standard error (SE) on the response scale (probability). Values represent differences relative to the vehicle control group at each time point: positive values indicate increased hatching probability; negative values indicate decreased hatching probability. Statistical significance was assessed using treatment-vs-vehicle contrasts. *p*-values are derived from Wald z-tests.

Supplementary Table C.3. Effects of sertraline exposure on the mortality probability of 5 dpf SR4G zebrafish larvae.

Treatment	Predicted probability (95% CI)	Effect size (% ± SE)	z	*p*-value
Vehicle control	0.04 (0.02 to 0.09)	N/A	N/A	N/A
Internal control	0.01 (0.00 to 0.05)	-3.32 ± 0.67	-1.690	0.311
SER 10 nM	0.01 (0.00 to 0.05)	-3.32 ± 0.67	-1.691	0.311
SER 50 nM	0.03 (0.01 to 0.08)	-0.67 ± 1.57	-0.309	0.987
SER 100 nM	0.01 (0.00 to 0.05)	-2.66 ± 0.96	-1.373	0.498
SER 500 nM	0.01 (0.00 to 0.05)	-2.66 ± 0.96	-1.373	0.498

Predicted mortality probability per treatment, and differences in probability (%) between treatments and the vehicle control are derived from generalized linear mixed-effects models (binomial distribution, logit link) with experimental replicate included as a random factor.

Effect sizes are expressed as mean difference ± standard error (SE) on the response scale (probability). Values represent differences relative to the vehicle control group at each time point: positive values indicate increased mortality probability; negative values indicate decreased mortality probability. Statistical significance was assessed using treatment-vs-vehicle contrasts. *p*-values are derived from Wald z-tests.

Supplementary Table C.4. Malformation counts observed in 5 dpf SR4G larvae exposed to sertraline.

	Malformation counts					
Treatment	**Total**	**Head**	**Yolk sac**	**Edema**	**Trunk**	**Tail**
Internal control	0.00 ± 0.00	0.00 ± 0.00	0.00 ± 0.00	0.00 ± 0.00	0.00 ± 0.00	0.00 ± 0.00
Vehicle control	0.01 ± 0.01	0.00 ± 0.00	0.01 ± 0.01	0.00 ± 0.00	0.00 ± 0.00	0.00 ± 0.00
SER 10 nM	0.02 ± 0.02	0.00 ± 0.00	0.00 ± 0.00	0.01 ± 0.01	0.00 ± 0.00	0.01 ± 0.01
SER 50 nM	0.04 ± 0.03	0.01 ± 0.01	0.01 ± 0.01	0.01 ± 0.01	0.00 ± 0.00	0.01 ± 0.01
SER 100 nM	0.02 ± 0.02	0.01 ± 0.01	0.00 ± 0.00	0.00 ± 0.00	0.00 ± 0.00	0.01 ± 0.01
SER 500 nM	0.01 ± 0.01	0.00 ± 0.00	0.01 ± 0.01	0.00 ± 0.00	0.00 ± 0.00	0.01 ± 0.01

Data are reported as mean ± SEM (N = 6 experimental replicates; 24 individuals per replicate).

Supplementary Table C.5. List of all differentially expressed genes identified in 5 dpf SR4G zebrafish in response to the light/dark challenge.

Gene symbol	Description	FC	*p*-adj
abcg2d	ATP-binding cassette, sub-family G (WHITE), member 2d	2.0	1.6E-03
abhd4	abhydrolase domain containing 4	-1.2	1.3E-05
adipoqb	adiponectin, C1Q and collagen domain containing, b	2.3	1.4E-03
adipor2	adiponectin receptor 2	-1.2	3.2E-13
agla	amylo-alpha-1, 6-glucosidase, 4-alpha-glucanotransferase a	1.5	3.3E-03
arhgap29b	Rho GTPase activating protein 29b	1.4	6.7E-03
arnt	aryl hydrocarbon receptor nuclear translocator	1.3	2.8E-02
arntl2	aryl hydrocarbon receptor nuclear translocator-like 2	-1.3	1.3E-08
arr3a	arrestin 3a, retinal (X-arrestin)	-1.2	1.3E-09
arrdc3a	arrestin domain containing 3a	1.2	7.4E-03
arsg	arylsulfatase G	1.2	4.1E-02
axl	AXL receptor tyrosine kinase	1.5	2.2E-04
b4galt5	UDP-Gal:betaGlcNAc beta 1,4- galactosyltransferase, polypeptide 5	1.8	3.1E-03
bbs10	Bardet-Biedl syndrome 10	1.9	7.4E-06
bcl2l13	BCL2 like 13	-1.2	1.8E-12
bhlhe40	basic helix-loop-helix family, member e40	1.3	7.6E-10
blvra	biliverdin reductase A	-1.3	3.8E-09
bnip3	BCL2 interacting protein 3	1.7	4.6E-06
bphl	biphenyl hydrolase like	1.4	1.4E-03
btr18	bloodthirsty-related gene family, member 18	1.9	2.1E-03
btr20	bloodthirsty-related gene family, member 20	1.4	1.2E-02
btr26	bloodthirsty-related gene family, member 26	1.2	1.2E-03
btr29	bloodthirsty-related gene family, member 29	1.6	6.1E-03
c1r	complement component 1, r subcomponent	1.5	9.1E-05
camk1gb	calcium/calmodulin-dependent protein kinase IGb	-1.2	1.3E-04
carmil1	capping protein regulator and myosin 1 linker 1	1.3	4.5E-03
ccn4a	cellular communication network factor 4a	2.5	2.5E-04
ccnd3	cyclin D3	1.6	4.6E-03
cd4-1	CD4-1 molecule	1.4	1.0E-02
cd79a	CD79a molecule, immunoglobulin-associated alpha	2.9	3.9E-06
cdc45	CDC45 cell division cycle 45 homolog (*S. cerevisiae*)	2.0	3.7E-04
cdc6	cell division cycle 6 homolog (*S. cerevisiae*)	1.4	3.5E-03
cdc7	cell division cycle 7 homolog (*S. cerevisiae*)	1.2	4.4E-03
cdca7a	cell division cycle associated 7a	1.5	5.5E-34
cdkn1a	cyclin-dependent kinase inhibitor 1A	1.3	3.3E-02
cebpd	CCAAT enhancer binding protein delta	1.4	1.6E-07
cfhl5	complement factor H like 5	2.1	1.2E-04

chrna2a	cholinergic receptor, nicotinic, alpha 2a (neuronal)	1.2	2.2E-02
coasy	CoA synthase	1.3	2.3E-02
comtb	catechol-O-methyltransferase b	1.4	2.8E-02
cpt1b	carnitine palmitoyltransferase 1B (muscle)	-1.3	2.3E-06
pde4cb	phosphodiesterase 4C, cAMP-specific b	1.3	1.5E-06
cryz	crystallin, zeta (quinone reductase)	1.3	3.4E-02
cxcl19	chemokine (C-X-C motif) ligand 19	1.4	2.4E-02
cxcl8b.1	chemokine (C-X-C motif) ligand 8b, duplicate 1	1.9	1.8E-03
cyp19a1b	cytochrome P450, family 19, subfamily A, polypeptide 1b	2.1	9.3E-04
cyp2aa3	cytochrome P450, family 2, subfamily AA, polypeptide 3	1.4	1.0E-02
cyp2aa8	cytochrome P450, family 2, subfamily AA, polypeptide 8	1.6	3.8E-09
cyp39a1	cytochrome P450, family 39, subfamily A, polypeptide 1	1.6	5.7E-03
ddx3xa	DEAD-box helicase 3 X-linked a	-1.2	1.4E-06
dph2	diphthamide biosynthesis 2	1.5	1.3E-02
drap1	DR1-associated protein 1 (negative cofactor 2 alpha)	1.2	1.4E-03
drd6b	dopamine receptor D6b	1.7	2.3E-04
duox2	dual oxidase 2	1.7	3.9E-04
duox	dual oxidase	1.4	1.2E-02
e2f7	E2F transcription factor 7	1.6	5.8E-08
eif4ba	eukaryotic translation initiation factor 4Ba	1.2	3.0E-10
eprs1	glutamyl-prolyl-tRNA synthetase 1	1.3	2.4E-02
fabp1a	fatty acid binding protein 1a, liver	1.5	1.8E-03
fignl1	fidgetin-like 1	1.4	1.3E-04
fkbp5	FKBP prolyl isomerase 5	-1.7	4.2E-05
fosb	FBJ murine osteosarcoma viral oncogene homolog B	1.5	1.7E-02
g3bp1	GTPase activating protein (SH3 domain) binding protein 1	-1.2	1.7E-14
gabbr1a	gamma-aminobutyric acid (GABA) B receptor, 1a	1.2	1.9E-03
gadd45bb	growth arrest and DNA-damage-inducible, beta b	1.3	7.5E-06
gata4	GATA binding protein 4	1.2	3.0E-02
glod4	glyoxalase domain containing 4	2.7	7.2E-05
gnb3a	guanine nucleotide binding protein (G protein), beta polypeptide 3a	2.9	6.4E-08
gpr18	G protein-coupled receptor 18	1.3	4.4E-02
grb10b	growth factor receptor-bound protein 10b	-1.3	1.4E-06
GRB14	growth factor receptor-bound protein 14	1.8	3.5E-03
hif1al	hypoxia inducible factor 1 subunit alpha, like	-1.4	1.8E-15
hist1h2a5	histone cluster 1 H2A family member 5	1.3	1.3E-07
hmox1a	heme oxygenase 1a	-1.3	9.5E-08
hp	haptoglobin	1.7	4.5E-03
hsd11b2	hydroxysteroid (11-beta) dehydrogenase 2	-1.3	2.4E-10
hsp90aa1.2	heat shock protein 90, alpha (cytosolic), class A member 1, tandem duplicate 2	1.5	1.4E-48

hsp90b1	heat shock protein 90, beta (grp94), member 1	1.2	4.1E-17
hspa13	heat shock protein 70 family, member 13	1.3	6.8E-03
htr6	5-hydroxytryptamine (serotonin) receptor 6	1.3	3.8E-02
ido1	indoleamine 2,3-dioxygenase 1	1.3	2.0E-03
igf1	insulin-like growth factor 1	1.5	6.1E-03
igl4v10	immunoglobulin light 4 variable 10	2.2	4.3E-06
il6	interleukin 6 (interferon, beta 2)	1.6	6.7E-03
inha	inhibin subunit alpha	1.6	1.4E-02
ipcef1	interaction protein for cytohesin exchange factors 1	1.3	8.6E-07
iqgap1	IQ motif containing GTPase activating protein 1	1.3	6.8E-03
isg20	interferon stimulated exonuclease gene	-1.3	7.2E-14
jak2b	Janus kinase 2b	1.3	1.5E-02
kif15	kinesin family member 15	1.3	1.3E-02
l1cama	L1 cell adhesion molecule, paralog a	1.3	2.6E-02
lhb	luteinizing hormone subunit beta	2.0	1.4E-06
si:ch1073-185p12.2	si:ch1073-185p12.2 [Source:ZFIN;Acc:ZDB-GENE-110411-196]	1.9	2.4E-03
ggt1l2.2	gamma-glutamyltransferase 1 like 2.2	1.4	4.8E-03
si:ch211-22k7.9	si:ch211-22k7.9 [Source:ZFIN;Acc:ZDB-GENE-070424-160]	2.0	1.6E-32
si:dkey-14o6.1	si:dkey-14o6.1 [Source:ZFIN;Acc:ZDB-GENE-081103-51]	2.9	6.5E-30
si:ch211-226h7.5	si:ch211-226h7.5 [Source:ZFIN;Acc:ZDB-GENE-130531-3]	1.4	1.1E-02
pde6ha	phosphodiesterase 6H, cGMP-specific, cone, gamma, paralog a	-1.2	4.7E-07
dhx33	DEAH (Asp-Glu-Ala-His) box polypeptide 33	1.2	4.4E-02
si:ch211-161n3.3	si:ch211-161n3.3 [Source:ZFIN;Acc:ZDB-GENE-041210-102]	1.3	2.8E-02
lyrm1	LYR motif containing 1	1.3	2.6E-02
malt1	MALT paracaspase 1	1.5	5.5E-03
mapk13	mitogen-activated protein kinase 13	1.4	1.1E-02
bx248108.1	multidrug and toxin extrusion protein 1-like	1.7	2.1E-05
mmp19	matrix metallopeptidase 19	1.9	6.6E-08
mterf3	mitochondrial transcription termination factor 3	1.4	2.0E-02
mybl2b	v-myb avian myeloblastosis viral oncogene homolog-like 2b	1.3	2.6E-02
neu4	sialidase 4	1.9	9.1E-08
nmur1b	neuromedin U receptor 1b	1.9	4.1E-04
nod1	nucleotide-binding oligomerization domain containing 1	1.6	5.4E-03
nop58	NOP58 ribonucleoprotein homolog (yeast)	-1.3	8.0E-32
nr1d1	nuclear receptor subfamily 1, group d, member 1	1.2	3.1E-14
nr1i2	nuclear receptor subfamily 1, group I, member 2	-1.2	7.2E-18
nr5a1a	nuclear receptor subfamily 5, group A, member 1a	1.6	1.2E-03
pax8	paired box 8	1.3	2.2E-02
pfklb	phosphofructokinase, liver b	1.4	4.1E-03
pigp	phosphatidylinositol glycan anchor biosynthesis, class P	1.3	1.7E-02

pik3c2g	phosphatidylinositol-4-phosphate 3-kinase catalytic subunit type 2 gamma	2.3	1.0E-06
pmm2	phosphomannomutase 2	2.1	2.1E-03
poc1bl	POC1 centriolar protein homolog B (*Chlamydomonas*), like	1.5	5.8E-03
pora	P450 (cytochrome) oxidoreductase a	-1.2	4.6E-06
pparab	peroxisome proliferator-activated receptor alpha b	1.3	7.9E-03
prelid3b	PRELI domain containing 3	-1.2	1.2E-03
psmb10	proteasome 20S subunit beta 10	1.3	1.0E-02
lo018490.1	RAB31, member RAS oncogene family	1.4	7.5E-03
rbm15b	RNA binding motif protein 15B	1.3	3.0E-02
renbp	renin binding protein	1.4	5.6E-03
rrs1	ribosome biogenesis regulator 1 homolog	-1.4	6.6E-32
rsad2	radical S-adenosyl methionine domain containing 2	1.2	4.9E-02
saa	serum amyloid A	1.3	6.1E-03
samhd1	SAM domain and HD domain 1	1.6	7.8E-06
serpine2	serpin peptidase inhibitor, clade E (nexin, plasminogen activator inhibitor type 1), member 2	1.7	4.6E-04
sgce	sarcoglycan, epsilon [Source:ZFIN;Acc:ZDB-GENE-030724-1]	1.6	5.5E-05
mhc2a	major histocompatibility complex class II integral membrane alpha chain gene	1.4	1.1E-02
cabz01066312.1	si:cabz01066312.1 [Source:NCBI gene;Acc:100537698]	1.7	8.6E-04
si:cabz01093077.1	si:cabz01093077.1 [Source:ZFIN;Acc:ZDB-GENE-160113-45]	2.7	1.6E-04
SPSB2	si:ch1073-228j22.2 [Source:ZFIN;Acc:ZDB-GENE-110411-227]	2.3	1.6E-04
si:ch211-113a14.22	si:ch211-113a14.22 [Source:ZFIN;Acc:ZDB-GENE-121214-203]	1.4	3.2E-09
si:ch211-120g10.1	si:ch211-120g10.1 [Source:ZFIN;Acc:ZDB-GENE-130531-56]	1.3	3.0E-02
si:ch211-139g16.8	si:ch211-139g16.8 [Source:ZFIN;Acc:ZDB-GENE-100922-126]	1.6	2.6E-06
si:ch73-160i9.3	si:ch73-160i9.3 [Source:ZFIN;Acc:ZDB-GENE-141212-252]	1.4	6.8E-03
si:ch211-226o13.1	si:ch211-226o13.1 [Source:ZFIN;Acc:ZDB-GENE-081104-491]	2.0	3.2E-35
si:ch73-100l22.3	si:ch73-100l22.3 [Source:ZFIN;Acc:ZDB-GENE-141222-74]	1.4	1.2E-03
si:dkey-21h14.3	si:dkey-21h14.3 [Source:ZFIN;Acc:ZDB-GENE-041210-92]	1.8	4.4E-03
si:dkey-21h14.12	si:dkey-21h14.12 [Source:ZFIN;Acc:ZDB-GENE-110913-1]	2.4	6.5E-04
si:dkey-21h14.9	si:dkey-21h14.9 [Source:ZFIN;Acc:ZDB-GENE-110915-1]	1.7	7.4E-03
si:dkey-251i10.1	si:dkey-251i10.1 [Source:ZFIN;Acc:ZDB-GENE-060531-122]	1.3	1.9E-02
slc2a5	solute carrier family 2 member 5	1.3	2.4E-04
slc40a1	solute carrier family 40 member 1	1.5	2.1E-04
slc5a5	solute carrier family 5 member 5	1.2	4.1E-02
slc6a6a	solute carrier family 6 member 6a	1.8	6.7E-03
smtnb	smoothelin b	2.0	6.7E-05
socs1a	suppressor of cytokine signaling 1a	1.4	2.1E-03
socs3a	suppressor of cytokine signaling 3a	1.5	2.8E-04
spata6	spermatogenesis associated 6	1.5	2.0E-02
spc25	SPC25 component of NDC80 kinetochore complex	1.5	2.2E-03
star	steroidogenic acute regulatory protein	1.3	1.7E-04

tbc1d9	TBC1 domain family, member 9 (with GRAM domain)	2.1	9.2E-05
tek	TEK tyrosine kinase, endothelial	1.2	2.3E-02
tert	telomerase reverse transcriptase	1.9	3.2E-09
tgfb3	transforming growth factor, beta 3	1.5	2.0E-02
timd4	T cell immunoglobulin and mucin domain containing 4	1.5	9.0E-03
tlr1	toll-like receptor 1	1.4	2.9E-02
tnfsf13	TNF superfamily member 13	1.2	4.8E-02
tph1a	tryptophan hydroxylase 1 (tryptophan 5-monooxygenase) a	1.3	2.3E-02
trib1	tribbles pseudokinase 1	1.6	2.4E-03
trpc7a	transient receptor potential cation channel, subfamily C, member 7a	1.6	1.1E-02
ttc21b	tetratricopeptide repeat domain 21B	1.3	4.6E-02
ttk	ttk protein kinase	2.2	1.1E-06
vtg1	vitellogenin 1	2.2	1.3E-03
vtg2	vitellogenin 2	1.2	4.7E-02
vtg3	vitellogenin 3, phosvitinless	2.1	2.2E-03
vwf	von Willebrand factor	1.5	1.4E-03
wnt7bb	wingless-type MMTV integration site family, member 7Bb	1.5	1.0E-02
zgc:173581	zgc:173581 [Source:ZFIN;Acc:ZDB-GENE-080212-7]	1.3	1.3E-02
zgc:194990	zgc:194990 [Source:ZFIN;Acc:ZDB-GENE-081022-171]	1.3	6.4E-03
zgc:66313	zgc:66313 [Source:ZFIN;Acc:ZDB-GENE-040426-1606]	1.5	1.3E-02
znf367	zinc finger protein 367	1.6	3.8E-09
znf395a	zinc finger protein 395a	1.2	3.3E-02

All samples were pooled for DEG analysis. All significant DEGs were defined by p-adj ≤ 0.05 and an absolute linear fold-change (FC) ≥ 1.2 (after shrinkage).

Supplementary Table C.6. List of all differentially expressed genes identified in 5 dpf SR4G zebrafish in response to the light/dark challenge at each concentration tested.

Gene symbol	Description	FC	*p*-adj
Unstressed vs. Stressed – Vehicle control			
loc108183819	si:ch211-22k7.9 [Source:ZFIN;Acc:ZDB-GENE-070424-160]	2.1	4.7E-06
loc108184002	si:dkey-14o6.1 [Source:ZFIN;Acc:ZDB-GENE-081103-51]	3.4	8.4E-06
hsp90aa1.2	heat shock protein 90, alpha (cytosolic), class A member 1, tandem duplicate 2	1.5	8.4E-06
nr1d1	nuclear receptor subfamily 1, group d, member 1	1.4	8.4E-06
rgs2	regulator of G protein signaling 2	2.8	8.4E-05
rrs1	ribosome biogenesis regulator 1 homolog	-1.4	3.1E-04
cdca7a	cell division cycle associated 7a	1.4	1.1E-03
si-ch211-226o13.1	si:ch211-226o13.1 [Source:ZFIN;Acc:ZDB-GENE-081104-491]	1.7	1.8E-03
bnip3	BCL2 interacting protein 3	2.9	4.0E-03
hist1h2a5	histone cluster 1 H2A family member 5	1.5	7.9E-03
plac8.2	placenta associated 8, tandem duplicate 2	11.5	8.3E-03
smtnb	smoothelin b	4.6	1.1E-02
vwf	von Willebrand factor	3.3	1.1E-02
ifrd2	interferon-related developmental regulator 2	-1.7	1.1E-02
fosl1a	FOS-like antigen 1a	1.9	1.3E-02
axl	AXL receptor tyrosine kinase	2.2	2.0E-02
mterf3	mitochondrial transcription termination factor 3	4.6	2.1E-02
slc5a5	solute carrier family 5 member 5	3.9	2.3E-02
btr20	bloodthirsty-related gene family, member 20	4.0	2.5E-02
hp	haptoglobin	4.9	2.7E-02
tert	telomerase reverse transcriptase	2.2	3.6E-02
p2ry13	purinergic receptor P2Y13	2.8	3.9E-02
Unstressed vs. Stressed – Sertraline 10 nM			
hsp90aa1.2	heat shock protein 90, alpha (cytosolic), class A member 1, tandem duplicate 2	1.6	3.9E-09
si-ch211-226o13.1	si:ch211-226o13.1 [Source:ZFIN;Acc:ZDB-GENE-081104-491]	2.1	3.1E-06
loc108183819	si:ch211-22k7.9 [Source:ZFIN;Acc:ZDB-GENE-070424-160]	2.0	2.3E-05
rrs1	ribosome biogenesis regulator 1 homolog	-1.4	4.4E-05
nr1i2	nuclear receptor subfamily 1, group I, member 2	-1.3	4.4E-05
cdca7a	cell division cycle associated 7a	1.5	5.7E-05
nop58	NOP58 ribonucleoprotein homolog (yeast)	-1.3	1.1E-04
si-ch211-113a14.22	si:ch211-113a14.22 [Source:ZFIN;Acc:ZDB-GENE-121214-203]	1.5	2.2E-02
Unstressed vs. Stressed – Sertraline 50 nM			
hsp90aa1.2	heat shock protein 90, alpha (cytosolic), class A member 1, tandem duplicate 2	1.6	4.0E-10
cdca7a	cell division cycle associated 7a	1.5	3.4E-06
si-ch211-226o13.1	si:ch211-226o13.1 [Source:ZFIN;Acc:ZDB-GENE-081104-491]	2.0	1.5E-05
mrpl13	mitochondrial ribosomal protein L13	-1.4	1.5E-05
hsp90b1	heat shock protein 90, beta (grp94), member 1	1.3	4.0E-05
fkbp4	FKBP prolyl isomerase 4	1.3	5.2E-05

rrs1	ribosome biogenesis regulator 1 homolog	-1.4	6.3E-05
nop58	NOP58 ribonucleoprotein homolog (yeast)	-1.3	2.6E-04
znf367	zinc finger protein 367	2.0	7.7E-04
hif1al	hypoxia inducible factor 1 subunit alpha, like	-1.5	9.6E-04
loc108183819	si:ch211-22k7.9 [Source:ZFIN;Acc:ZDB-GENE-070424-160]	1.7	1.7E-03
ttk	ttk protein kinase	4.8	3.8E-03
loc108184002	si:dkey-14o6.1 [Source:ZFIN;Acc:ZDB-GENE-081103-51]	2.3	6.8E-03
hsd11b2	hydroxysteroid (11-beta) dehydrogenase 2	-1.4	2.2E-02
bphl	biphenyl hydrolase like	2.3	4.8E-02
fkbp5	FKBP prolyl isomerase 5	-2.4	4.9E-02
crtc1b	phosphodiesterase 4C, cAMP-specific b	1.5	4.9E-02
Unstressed vs. Stressed – Sertraline 100 nM			
hsp90aa1.2	heat shock protein 90, alpha (cytosolic), class A member 1, tandem duplicate 2	1.6	4.4E-09
nop58	NOP58 ribonucleoprotein homolog (yeast)	-1.4	4.3E-07
si-ch211-226o13.1	si:ch211-226o13.1 [Source:ZFIN;Acc:ZDB-GENE-081104-491]	1.9	1.3E-05
rrs1	ribosome biogenesis regulator 1 homolog	-1.4	1.3E-05
nr1i2	nuclear receptor subfamily 1, group I, member 2	-1.3	1.3E-05
bcl2l13	BCL2 like 13	-1.4	1.5E-05
adipor2	adiponectin receptor 2	-1.3	1.0E-04
epas1a	endothelial PAS domain protein 1a	-1.3	1.0E-04
loc108184002	si:dkey-14o6.1 [Source:ZFIN;Acc:ZDB-GENE-081103-51]	2.8	1.1E-04
cdca7a	cell division cycle associated 7a	1.4	1.6E-04
loc108183819	si:ch211-22k7.9 [Source:ZFIN;Acc:ZDB-GENE-070424-160]	1.8	1.3E-04
eif4ba	eukaryotic translation initiation factor 4Ba	1.3	1.6E-03
gnb3a	guanine nucleotide binding protein (G protein), beta polypeptide 3a	9.1	2.0E-03
g3bp1	GTPase activating protein (SH3 domain) binding protein 1	-1.3	2.8E-03
crtc1b	phosphodiesterase 4C, cAMP-specific b	1.7	4.1E-03
hif1al	hypoxia inducible factor 1 subunit alpha, like	-1.4	4.1E-03
mnd1	meiotic nuclear divisions 1 homolog (S. cerevisiae)	1.4	4.6E-03
hsd11b2	hydroxysteroid (11-beta) dehydrogenase 2	-1.4	9.0E-03
cyp2aa8	cytochrome P450, family 2, subfamily AA, polypeptide 8	1.8	9.4E-03
gins3	GINS complex subunit 3	1.6	1.2E-02
srp72	signal recognition particle 72	1.4	1.2E-02
rasgef1ba	RasGEF domain family, member 1Ba	-1.4	1.6E-02
e2f7	E2F transcription factor 7	2.0	1.8E-02
hmox1a	heme oxygenase 1a	-1.4	2.2E-02
adgrg6	adhesion G protein-coupled receptor G6	2.2	3.6E-02
cyp2aa4	cytochrome P450, family 2, subfamily AA, polypeptide 4	1.7	3.6E-02
arfip2b	ADP-ribosylation factor interacting protein 2b	-1.6	4.1E-02
Unstressed vs. Stressed – Sertraline 500 nM			
cdca7a	cell division cycle associated 7a	1.7	5.4E-11
loc108184002	si:dkey-14o6.1 [Source:ZFIN;Acc:ZDB-GENE-081103-51]	4.1	2.9E-09
cirbpb	cold inducible RNA binding protein b	-1.2	2.9E-09

si-ch211-226o13.1	si:ch211-226o13.1 [Source:ZFIN;Acc:ZDB-GENE-081104-491]	2.2	7.1E-09
loc108183819	si:ch211-22k7.9 [Source:ZFIN;Acc:ZDB-GENE-070424-160]	2.3	7.2E-09
nop58	NOP58 ribonucleoprotein homolog (yeast)	-1.4	3.6E-08
hsp90aa1.2	heat shock protein 90, alpha (cytosolic), class A member 1, tandem duplicate 2	1.5	2.4E-07
nr1i2	nuclear receptor subfamily 1, group I, member 2	-1.3	2.4E-07
hif1al	hypoxia inducible factor 1 subunit alpha, like	-1.6	7.0E-06
rrs1	ribosome biogenesis regulator 1 homolog	-1.4	9.5E-06
arntl2	aryl hydrocarbon receptor nuclear translocator-like 2	-1.5	2.7E-05
znf367	zinc finger protein 367	2.1	4.5E-05
neu4	sialidase 4	3.5	8.1E-05
prss59.1	serine protease 59, tandem duplicate 1	1.5	1.3E-04
ddx3xa	DEAD-box helicase 3 X-linked a	-1.5	2.0E-04
c1r	complement component 1, r subcomponent	2.7	5.2E-04
btr18	bloodthirsty-related gene family, member 18	10.0	6.0E-04
mmp19	matrix metallopeptidase 19	2.9	1.7E-03
dcp1b	decapping mRNA 1B	-1.3	1.8E-03
g3bp1	GTPase activating protein (SH3 domain) binding protein 1	-1.3	2.6E-03
bhlhe40	basic helix-loop-helix family, member e40	1.4	2.6E-03
tert	telomerase reverse transcriptase	2.5	3.5E-03
tbc1d9b	TBC1 domain family, member 9 (with GRAM domain)	5.1	4.0E-03
isg20	interferon stimulated exonuclease gene	-1.3	4.2E-03
e2f7	E2F transcription factor 7	2.0	6.1E-03
hsd11b2	hydroxysteroid (11-beta) dehydrogenase 2	-1.4	6.4E-03
slc40a1	solute carrier family 40 member 1	2.3	6.5E-03
si-ch211-139g16.8	si:ch211-139g16.8 [Source:ZFIN;Acc:ZDB-GENE-100922-126]	2.2	6.5E-03
ssbp2	single-stranded DNA binding protein 2	3.4	7.5E-03
hist1h2a5	histone cluster 1 H2A family member 5	1.4	7.7E-03
drap1	DR1-associated protein 1 (negative cofactor 2 alpha)	1.7	1.0E-02
pik3c2g	phosphatidylinositol-4-phosphate 3-kinase catalytic subunit type 2 gamma	4.4	1.3E-02
ptger4a	prostaglandin E receptor 4 (subtype EP4) a	3.7	1.7E-02
cyp2aa8	cytochrome P450, family 2, subfamily AA, polypeptide 8	1.7	1.7E-02
hmox1a	heme oxygenase 1a	-1.4	1.8E-02
nmur1b	neuromedin U receptor 1b	4.7	1.8E-02
mcm2	minichromosome maintenance complex component 2	1.4	1.8E-02
si-ch211-113a14.22	si:ch211-113a14.22 [Source:ZFIN;Acc:ZDB-GENE-121214-203]	1.5	2.3E-02
ccn4a	cellular communication network factor 4a	9.5	2.3E-02
gmpr2	guanosine monophosphate reductase 2	1.6	2.6E-02
gnb3a	guanine nucleotide binding protein (G protein), beta polypeptide 3a	4.1	2.8E-02
mate4	multidrug and toxin extrusion protein 1-like	2.3	3.2E-02
il11a	interleukin 11a	4.3	3.7E-02
sprb	sepiapterin reductase b	4.2	3.7E-02
zgc-173581	zgc:173581 [Source:ZFIN;Acc:ZDB-GENE-080212-7]	2.6	3.7E-02
blvra	biliverdin reductase A	-1.4	3.7E-02

cebpd	CCAAT enhancer binding protein delta	1.5	4.0E-02
tubb6	tubulin, beta 6 class V	2.1	4.4E-02
col11a2	collagen, type XI, alpha 2	-1.8	5.0E-02

All significant DEGs were defined by p-adj ≤ 0.05 and an absolute linear fold-change (FC) ≥ 1.2 (after shrinkage).

D. Application of the integrative testing design to fluoxetine and norfluoxetine

The experimental design presented in Chapter 4 was also applied to fluoxetine and norfluoxetine, to test whether it resolves compound-specific effects beyond sertraline. Transcriptomic analysis could not be performed on these samples, so Chapter 4 was focused on sertraline, the only compound for which behavioural, reporter and transcriptomic endpoints could be linked. The behavioural and reporter results for fluoxetine and norfluoxetine, and for the overnight cortisol and dexamethasone treatments as positive controls for the reporter induction, are reported here.

a. Summary of materials and methods

All procedures followed those described in Chapter 4 unless stated otherwise. Zebrafish husbandry, breeding and embryo sanitation were as described in Section 4.3.1, using the SR4G line (Tg(6xGRE:EGFP,myl7:TagBFP)mn48) (Krug et al., 2014). Fluoxetine hydrochloride and norfluoxetine hydrochloride (TargetMol) were prepared as DMSO stocks and diluted in facility water to nominal concentrations of 10, 50, 100 and 500 nM, with a final DMSO concentration of 0.02 % in all treatments. Hydrocortisone (CORT) and dexamethasone (DEX) (Tocris) were prepared in the same way and applied at 2 and 20 µM overnight. Fresh stocks were prepared for each experimental replicate, and exposure solutions were prepared daily before each medium change.

Exposures followed Section 4.3.3. Embryos were seeded individually in 96-well plates at 24 hpf in 200 µL of exposure solution and exposed to fluoxetine or norfluoxetine until 120 hpf, with daily semi-static renewal of half the volume. Each experimental replicate included a medium-only internal control and a vehicle control (0.02 % DMSO) and included two identical plates: one used for the photomotor assay (stimulated larvae) and one left undisturbed (unstimulated larvae). Hatching, mortality and malformations were monitored daily. For the glucocorticoid treatments, larvae were raised under the same conditions in vehicle until 4 dpf and treated with CORT or DEX overnight from ~105 to 120 hpf (treatment applied at 6:00 pm the day prior). For each plate, there were 12 embryos per treatment, and each treatment was performed in 3 to 6 experimental replicates.

Larval photomotor response was measured at 96 and 120 hpf on the stimulated plate as described in Section 4.3.4, using the ZebraBox video-tracking system (Viewpoint, Montréal, Canada): a 20-min acclimatisation under light followed by four cycles of 5 min dark and 5 min light, tracked in 1-min bins. Dead or malformed larvae and the acclimatisation period were excluded from analysis, and total distance moved and inactivity time were summed across the dark or the light phases for each larva (Section 4.3.5.2).

Sampling followed Section 4.3.6. At 120 hpf, 10 larvae per treatment were pooled into one biological sample, sampled 60 min after the light/dark challenge for stimulated larvae and directly for unstimulated larvae. Larvae were euthanised by rapid chilling in 4 °C facility water, preserved in RNA*later* and stored at -80 °C. Total RNA was extracted with the RNeasy Mini kit, quantified with a Qubit 4 fluorometer, and RNA integrity assessed on an Agilent 4150 TapeStation; all samples had RIN ≥ 9.0. Reporter transcription was measured by RT-qPCR as described in Section 4.3.7, using *d4egfp* and the reference gene *eef1a1l1* (Supplementary Table C.1). Relative eGFP expression fold-change was calculated with the $\Delta\Delta C_T$ method (Livak & Schmittgen, 2001) using the tidyqpcr R package (Wallace & Haynes, 2022).

Behavioural endpoints were analysed as described in Section 4.3.5.2, with linear mixed-effects models (LMM) fitted to log-transformed data, treatment, phase (light/dark) and their interaction as fixed effects, and animal ID and experimental replicate as random intercepts. Fixed effects were assessed with Type-III Wald χ^2 tests and pairwise comparisons within each phase were Holm-adjusted. Relative eGFP expression was analysed by two-way ANOVA with concentration and light/dark stimulus as factors (including the interaction term), followed by Holm-Šídák multiple comparisons for the fluoxetine and norfluoxetine experiments and Tukey's post hoc test for the glucocorticoid experiments.

b. Results

i. Larval photomotor response at 4 dpf in response to fluoxetine and norfluoxetine

At 4 dpf, larvae treated with fluoxetine exhibited a photomotor response, with increased locomotion during dark phases relative to light phases, that weakened with increasing concentration and over time of the assay (Supplementary Figure D.1A). Total distance moved was altered by fluoxetine treatment, by phase (light or dark), and by their interaction (LMM: treatment $\chi^2_4 = 48.68$, $p < 0.0001$; phase $\chi^2_1 = 78.15$, $p < 0.0001$; interaction $\chi^2_4 = 21.11$, $p = 0.0003$). In the dark, mean total distance travelled decreased from 2002 mm in vehicle-treated larvae to 1460, 1478, and 1157 mm at 50, 100, and 500 nM fluoxetine, respectively, whereas light-phase distance was unaffected (Supplementary Figure D.1B). Inactivity time was altered by treatment and by phase, with no interaction (LMM: treatment $\chi^2_4 = 10.97$, $p = 0.027$; light phase $\chi^2_1 = 11.12$, $p = 0.0008$; interaction $\chi^2_4 = 2.99$, $p = 0.56$) and only larvae exposed to 50 nM were more inactive than vehicle controls (Supplementary Figure D.1C).

At 4 dpf, larvae treated with norfluoxetine also exhibited a photomotor response that weakened with increasing concentration and over time of the assay (Supplementary Figure D.2A). Total distance moved was altered by norfluoxetine treatment and by phase, with no interaction (LMM: treatment $\chi^2_4 = 13.73$, $p = 0.008$; light phase $\chi^2_1 = 33.91$, $p < 0.0001$; interaction $\chi^2_4 = 4.80$, $p = 0.31$). In the dark, mean distance travelled decreased from 1654 mm in vehicle-treated larvae to 1163 mm at 500 nM, whereas light-phase distance was unaffected (Supplementary Figure D.2B). Inactivity time was altered by treatment only (LMM: treatment $\chi^2_4 = 17.32$, $p = 0.0017$; light phase $\chi^2_1 = 1.39$, $p = 0.24$; interaction $\chi^2_4 = 2.51$, $p = 0.64$): in the dark, larvae exposed to 100 nM were less inactive than those exposed to 50 and 500 nM, but no concentration differed from the vehicle control, and light-phase inactivity time was unaffected (Supplementary Figure D.2C).

ii. Larval photomotor response at 5 dpf in response to fluoxetine and norfluoxetine

At 5 dpf, larvae treated with fluoxetine or norfluoxetine exhibited a stronger photomotor response that was maintained throughout the assay (Supplementary Figure D.3A; Supplementary Figure D.4A). For fluoxetine, total distance moved was altered by treatment and by phase, with no interaction (LMM: treatment $\chi^2_4 = 16.82$, $p = 0.002$; phase

χ^2_1 = 156.18, p < 0.0001; interaction χ^2_4 = 9.29, p = 0.054). In the dark, mean distance travelled decreased from 2412 mm in vehicle-treated larvae to 1987 mm at 500 nM, whereas light-phase distance was unaffected (Supplementary Figure D.3B). Inactivity time differed between phases only (LMM: treatment χ^2_4 = 7.07, p = 0.13; light phase χ^2_1 = 60.93, p < 0.0001; interaction χ^2_4 = 4.95, p = 0.29) (Supplementary Figure D.3C).

For norfluoxetine, total distance moved was altered by treatment, by phase, and by their interaction (LMM: treatment χ^2_4 = 39.30, p < 0.0001; light phase χ^2_1 = 204.91, p < 0.0001; interaction χ^2_4 = 13.18, p = 0.01). In the dark, mean distance travelled decreased from 2123 mm in vehicle-treated larvae to 1720 mm at 500 nM, whereas light-phase distance was unaffected (Supplementary Figure D.4B). Inactivity time was likewise altered by treatment, by phase, and by their interaction (LMM: treatment χ^2_4 = 21.72, p = 0.0002; phase χ^2_1 = 59.41, p < 0.0001; interaction χ^2_4 = 11.591, p = 0.021): in the dark, larvae exposed to 500 nM were more inactive than those exposed to 10 and 50 nM, but no concentration differed from the vehicle control, and light-phase inactivity time was unaffected (Supplementary Figure D.4C).

iii. Larval photomotor response at 5 dpf in response to overnight glucocorticoid treatment

At 5 dpf, larvae treated overnight with cortisol or dexamethasone exhibited a strong photomotor response that was maintained throughout the assay (Supplementary Figure D.5A; Supplementary Figure D.6A). Cortisol treatment and phase both altered total distance moved, with no interaction (LMM: treatment χ^2_2 = 14.24, p = 0.0008; phase χ^2_1 = 212.22, p < 0.0001; interaction χ^2_2 = 1.79, p = 0.41): larvae exposed to 20 µM moved more than vehicle controls in both dark and light phases (Supplementary Figure D.5B). Inactivity time followed the same pattern (LMM: treatment χ^2_2 = 27.27, p < 0.0001; light phase χ^2_1 = 45.12, p < 0.0001; interaction χ^2_2 = 3.40, p = 0.18), with larvae exposed to 20 µM less inactive than vehicle controls in both phases (Supplementary Figure D.5C).

For larvae treated overnight with dexamethasone, only phase altered total distance moved (LMM: treatment χ^2_2 = 2.09, p = 0.35; phase χ^2_1 = 232.78, p < 0.0001; interaction χ^2_2 = 4.89, p = 0.08; Supplementary Figure D.6B). Inactivity time was altered by phase and by the treatment × phase interaction, but not by treatment alone (LMM: treatment χ^2_2 =

2.89, p = 0.24; light phase $\chi^2_1 = 91.34$, p < 0.0001; interaction $\chi^2_2 = 7.33$, p = 0.026): larvae exposed to 2 and 20 μM were less inactive than vehicle controls during the light phases only (Supplementary Figure D.6C).

iv. GRE-driven eGFP transcription at 5 dpf in response to fluoxetine and norfluoxetine treatment

Relative eGFP expression was significantly altered by the light/dark stimulus ($F_{1,49}$ = 48.4, $p < 0.0001$) but not fluoxetine concentration ($F_{4,49}$ = 2.10, $p = 0.09$) or their interaction ($F_{4,49}$ = 1.51, $p = 0.21$). he stimulus increased eGFP transcription in every treatment group except at 100 nM fluoxetine, where expression averaged 1.7-fold in unstimulated and 2.1-fold in stimulated larvae (Supplementary Figure D.7A).

Relative eGFP expression was likewise altered by the light/dark stimulus ($F_{1,49}$ = 38.2, $p < 0.0001$) but not by norfluoxetine concentration ($F_{4,49}$ = 0.81, $p = 0.53$) or their interaction ($F_{4,49}$ = 0.85, $p = 0.50$). The stimulus increased eGFP transcription in the vehicle, 50 and 500 nM groups, but not at 10 nM (1.1-fold unstimulated, 1.6-fold stimulated) or 100 nM (1.3-fold unstimulated, 1.6-fold stimulated) (Supplementary Figure D.7B).

v. GRE-driven eGFP transcription at 5 dpf in response to overnight glucocorticoid treatment

Overnight cortisol treatment altered relative eGFP expression through concentration ($F_{2,16}$ = 469, $p < 0.0001$) but not by the light/dark stimulus ($F_{1,16}$ = 0.004, $p = 0.95$) or by their interaction ($F_{2,16}$ = 0.27, $p = 0.77$). Expression was higher at 20 μM (unstimulated: 19.3-fold; stimulated: 18.9-fold) than at 2 μM (3.2-fold; 3.1-fold) and vehicle (1-fold; 1.5-fold), and unstimulated and stimulated larvae did not significantly differ within any treatment (Supplementary Figure D.8A).

Overnight dexamethasone treatment likewise altered eGFP expression through concentration ($F_{2,30}$ = 271, $p < 0.0001$) but not by the stimulus ($F_{1,30}$ = 0.58, $p = 0.45$) or by their interaction ($F_{2,30}$ = 0.13, $p = 0.88$). Expression was higher at 2 μM (unstimulated: 10.7-fold; stimulated: 10.9-fold) and 20 μM (28.9-fold; 30.4-fold) than in vehicle (1-fold;

1.8-fold), with no difference between unstimulated and stimulated larvae within any treatment (Supplementary Figure D.8B).

c. Figures

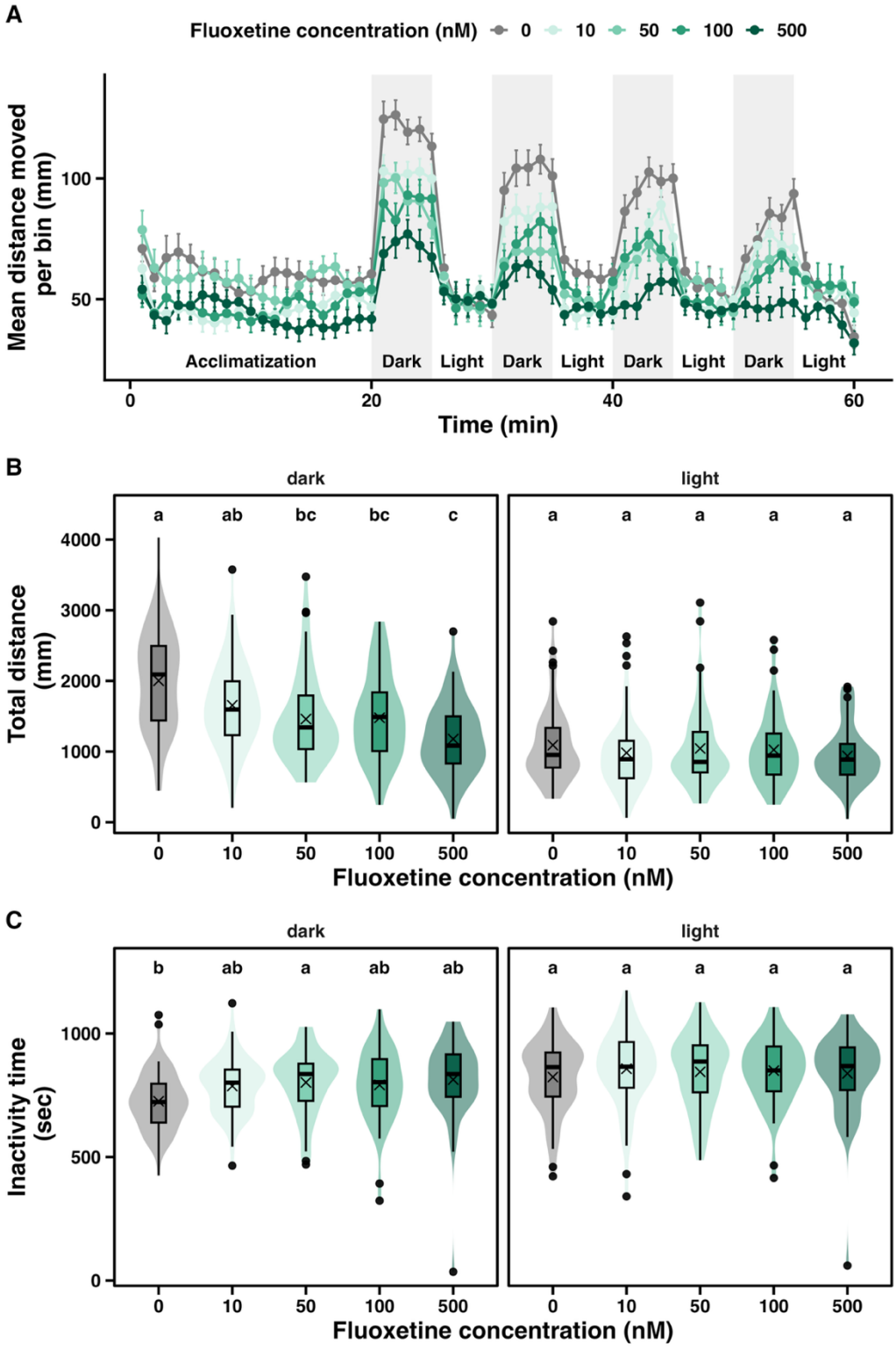

Supplementary Figure D.1. Effects of fluoxetine on 4 dpf SR4G zebrafish photomotor response.

(A) Mean distance moved per 1-min recording bin during a 20-min acclimatization period followed by four alternating 5-min dark and light phases. Grey shaded areas indicate dark phases. Data are shown as mean ± SEM for each concentration (0-500 nM). (B) Total distance moved per individual during dark and light phases. Violin plots represent the distribution density, and overlaid boxplots show the lower and upper quartiles with the mean (cross symbol), the median (bold line), the whiskers depict the minimum and maximum values, and outliers as single dots. (C) Total inactivity time per individual during dark and light phases, plotted as in (B). Statistical analyses were performed with linear mixed-effects models fitted on log-transformed data, with concentration, light condition, and their interaction as fixed effects, and experimental replicate and animal as random intercepts. Fixed effects were assessed using Type III Wald χ^2 tests. Estimated marginal means (EMM) were back-transformed for interpretation, and pairwise comparisons between treatments were conducted within each light condition using Holm correction. Letter superscripts indicate statistically different groups within each lighting context (letter "a" was assigned to the highest EMM).

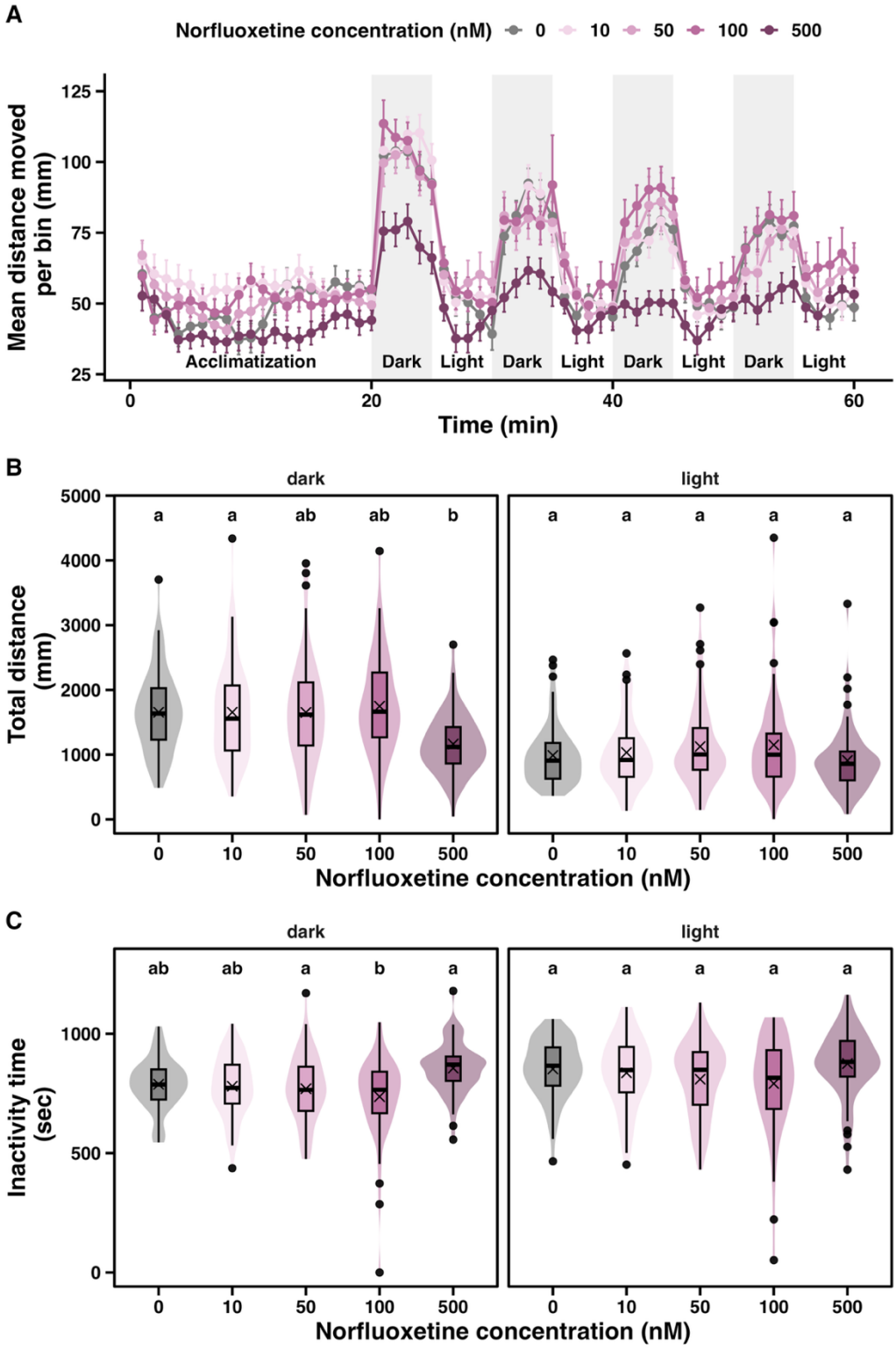

Supplementary Figure D.2. Effects of norfluoxetine on 4 dpf SR4G zebrafish photomotor response.

(A) Mean distance moved per 1-min recording bin during a 20-min acclimatization period followed by four alternating 5-min dark and light phases. Grey shaded areas indicate dark phases. Data are shown as mean ± SEM for each concentration (0-500 nM). (B) Total distance moved per individual during dark and light phases. Violin plots represent the distribution density, and overlaid boxplots show the lower and upper quartiles with the mean (cross symbol), the median (bold line), the whiskers depict the minimum and maximum values, and outliers as single dots. (C) Total inactivity time per individual during dark and light phases, plotted as in (B). Statistical analyses were performed with linear mixed-effects models fitted on log-transformed data, with concentration, light condition, and their interaction as fixed effects, and experimental replicate and animal as random intercepts. Fixed effects were assessed using Type III Wald χ^2 tests. Estimated marginal means (EMM) were back-transformed for interpretation, and pairwise comparisons between treatments were conducted within each light condition using Holm correction. Letter superscripts indicate statistically different groups within each lighting context (letter "a" was assigned to the highest EMM).

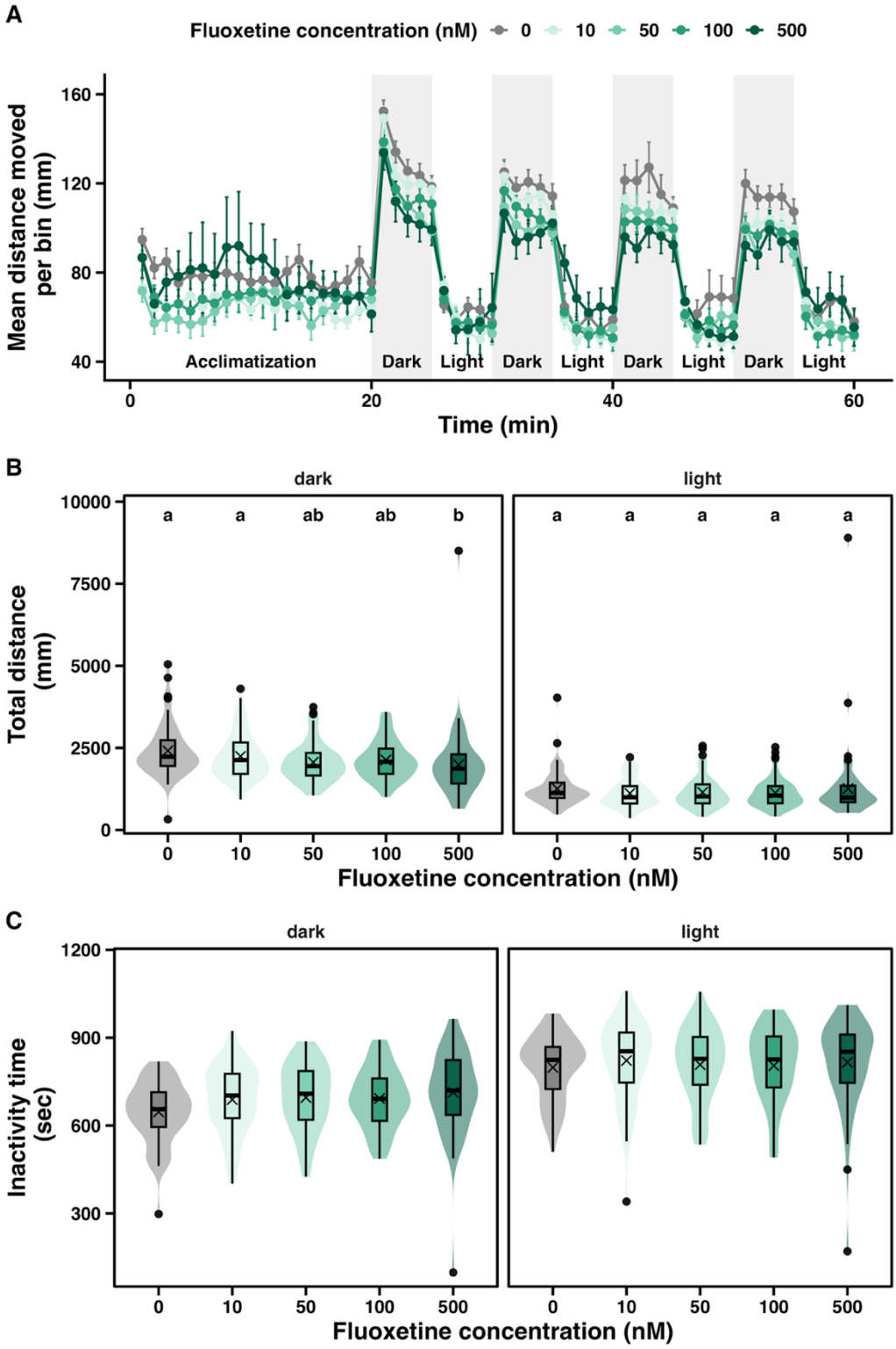

Supplementary Figure D.3. Effects of fluoxetine on 5 dpf SR4G zebrafish photomotor response. (A) Mean distance moved per 1-min recording bin during a 20-min acclimatization period followed by four alternating 5-min dark and light phases. Grey shaded areas indicate dark phases. Data are shown

as mean ± SEM for each concentration (0-500 nM). (B) Total distance moved per individual during dark and light phases. Violin plots represent the distribution density, and overlaid boxplots show the lower and upper quartiles with the mean (cross symbol), the median (bold line), the whiskers depict the minimum and maximum values, and outliers as single dots. (C) Total inactivity time per individual during dark and light phases, plotted as in (B). Statistical analyses were performed with linear mixed-effects models fitted on log-transformed data, with concentration, light condition, and their interaction as fixed effects, and experimental replicate and animal as random intercepts. Fixed effects were assessed using Type III Wald χ^2 tests. Estimated marginal means (EMM) were back-transformed for interpretation, and pairwise comparisons between treatments were conducted within each light condition using Holm correction. Letter superscripts indicate statistically different groups within each lighting context (letter "a" was assigned to the highest EMM).

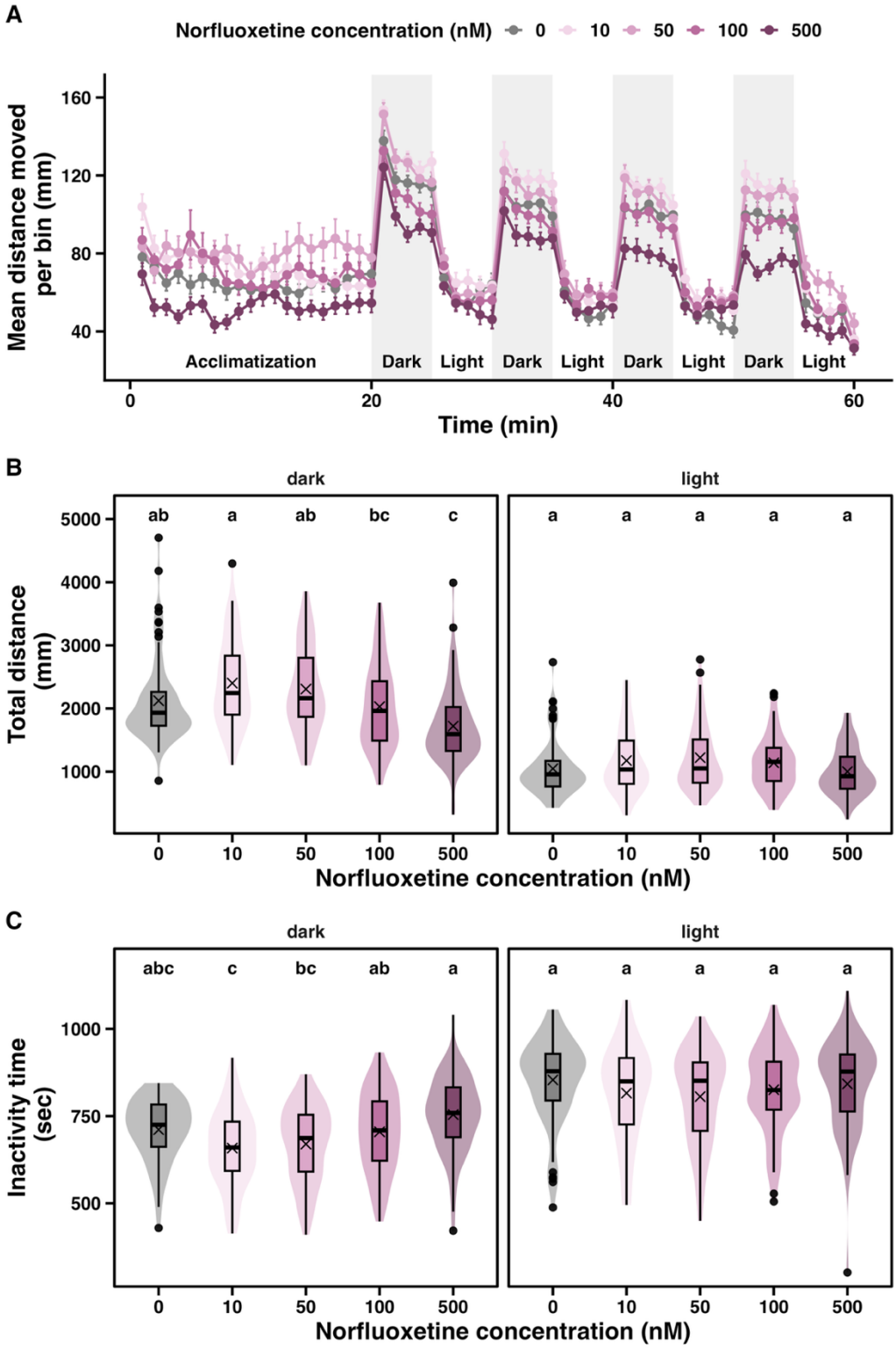

Supplementary Figure D.4. Effects of norfluoxetine on 5 dpf SR4G zebrafish photomotor response.

(A) Mean distance moved per 1-min recording bin during a 20-min acclimatization period followed by four alternating 5-min dark and light phases. Grey shaded areas indicate dark phases. Data are shown as mean ± SEM for each concentration (0-500 nM). (B) Total distance moved per individual during dark and light phases. Violin plots represent the distribution density, and overlaid boxplots show the lower and upper quartiles with the mean (cross symbol), the median (bold line), the whiskers depict the minimum and maximum values, and outliers as single dots. (C) Total inactivity time per individual during dark and light phases, plotted as in (B). Statistical analyses were performed with linear mixed-effects models fitted on log-transformed data, with concentration, light condition, and their interaction as fixed effects, and experimental replicate and animal as random intercepts. Fixed effects were assessed using Type III Wald χ^2 tests. Estimated marginal means (EMM) were back-transformed for interpretation, and pairwise comparisons between treatments were conducted within each light condition using Holm correction. Letter superscripts indicate statistically different groups within each lighting context (letter "a" was assigned to the highest EMM).

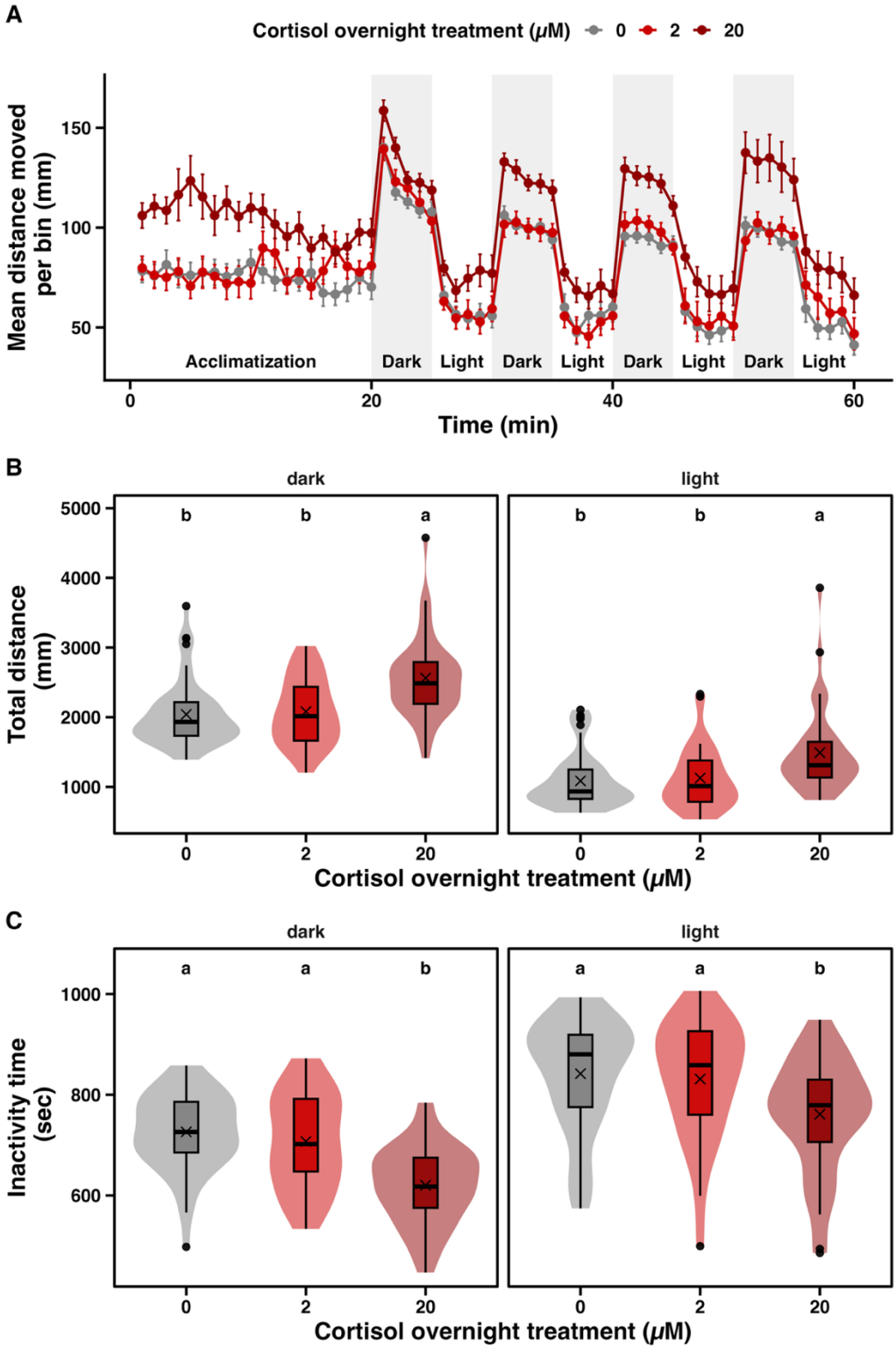

Supplementary Figure D.5. Effects of overnight cortisol treatment on 5 dpf SR4G zebrafish photomotor response.

(A) Mean distance moved per 1-min recording bin during a 20-min acclimatization period followed by four alternating 5-min dark and light phases. Grey shaded areas indicate dark phases. Data are shown as mean ± SEM for each concentration (0, 2, 20 µM). (B) Total distance moved per individual during dark and light phases. Violin plots represent the distribution density, and overlaid boxplots show the lower and upper quartiles with the mean (cross symbol), the median (bold line), the whiskers depict the minimum and maximum values, and outliers as single dots. (C) Total inactivity time per individual during dark and light phases, plotted as in (B). Statistical analyses were performed with linear mixed-effects models fitted on log-transformed data, with concentration, light condition, and their interaction as fixed effects, and experimental replicate and animal as random intercepts. Fixed effects were assessed using Type III Wald χ^2 tests. Estimated marginal means (EMM) were back-transformed for interpretation, and pairwise comparisons between treatments were conducted within each light condition using Holm correction. Letter superscripts indicate statistically different groups within each lighting context (letter "a" was assigned to the highest EMM).

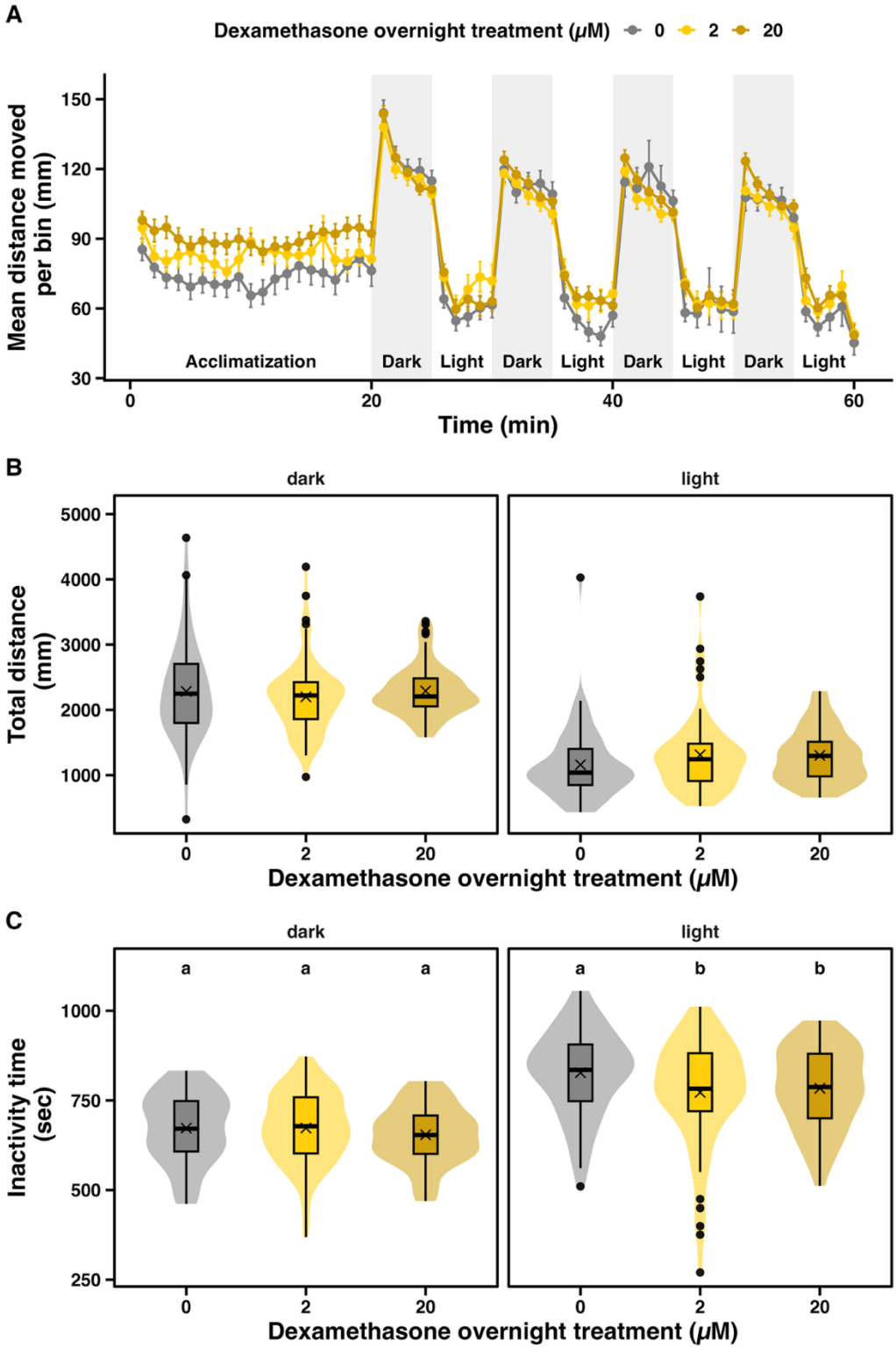

Supplementary Figure D.6. Effects of overnight dexamethasone treatment on 5 dpf SR4G zebrafish photomotor response.

(A) Mean distance moved per 1-min recording bin during a 20-min acclimatization period followed by four alternating 5-min dark and light phases. Grey shaded areas indicate dark phases. Data are shown as mean ± SEM for each concentration (0, 2, 20 µM). (B) Total distance moved per individual during dark and light phases. Violin plots represent the distribution density, and overlaid boxplots show the lower and upper quartiles with the mean (cross symbol), the median (bold line), the whiskers depict the minimum and maximum values, and outliers as single dots. (C) Total inactivity time per individual during dark and light phases, plotted as in (B). Statistical analyses were performed with linear mixed-effects models fitted on log-transformed data, with concentration, light condition, and their interaction as fixed effects, and experimental replicate and animal as random intercepts. Fixed effects were assessed using Type III Wald χ^2 tests. Estimated marginal means (EMM) were back-transformed for interpretation, and pairwise comparisons between treatments were conducted within each light condition using Holm correction. Letter superscripts indicate statistically different groups within each lighting context (letter "a" was assigned to the highest EMM).

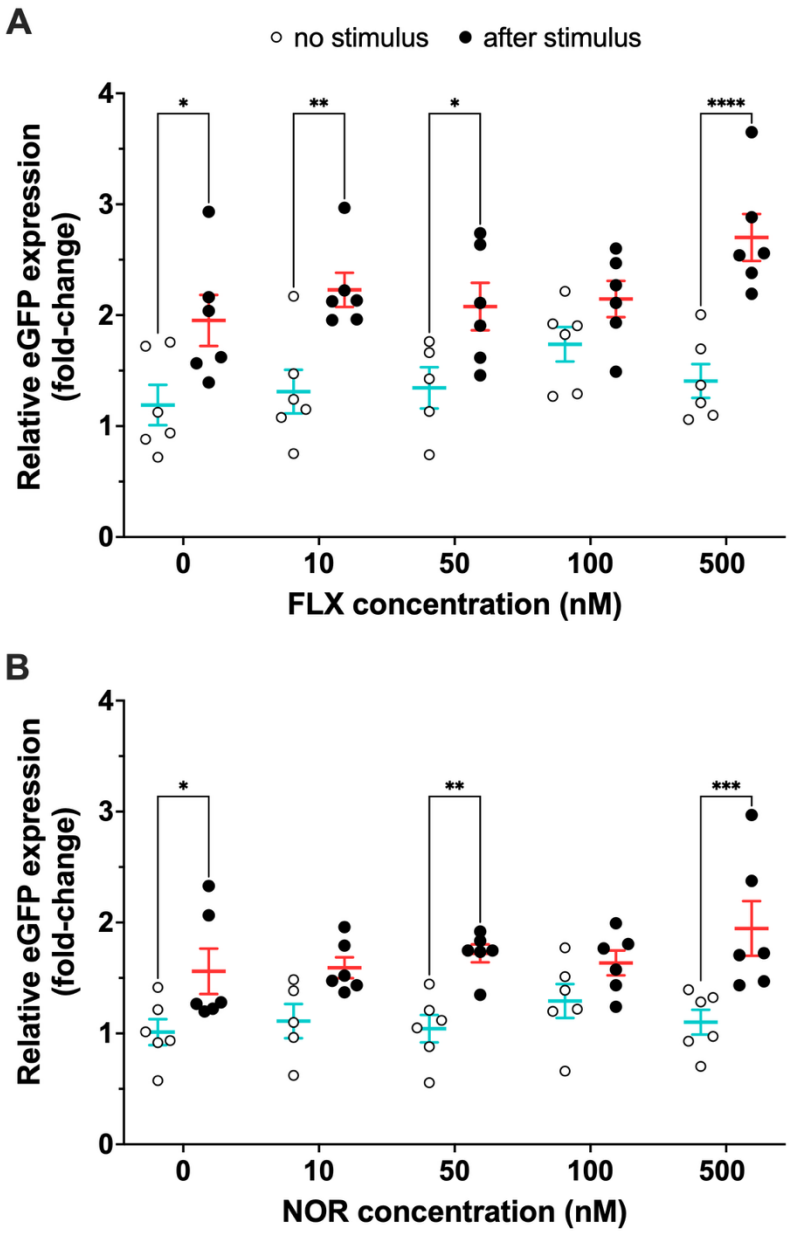

Supplementary Figure D.7. Effects of fluoxetine and norfluoxetine in combination with the light/dark challenge on eGFP relative expression in 5 dpf SR4G zebrafish.

Bars and intervals represent mean ± SEM (N = 6 biological replicates; sampling unit = 10 larvae/sample), with individual observations overlaid (no stimulus: white points, cyan intervals; after light/dark stimulus: black points, red intervals). Two-way ANOVA, followed by Holm-Šídák's multiple comparisons test, were used to identify significant differences between unstimulated and stimulated groups at each concentration. Asterisks indicate statistically significant differences (* $p < 0.05$, ** $p < 0.01$, *** $p < 0.001$, **** $p < 0.0001$).

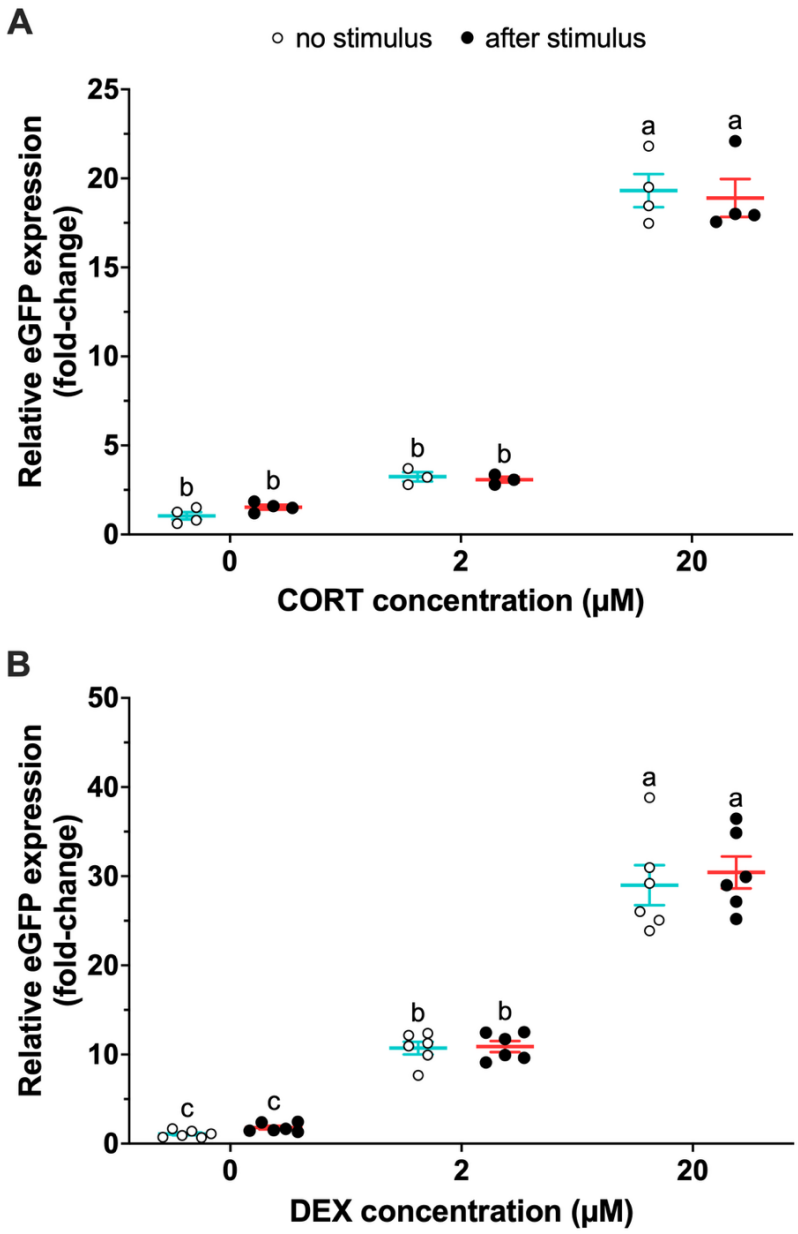

Supplementary Figure D.8. Effects of overnight treatment with cortisol or dexamethasone and the light/dark challenge on eGFP relative expression in 5 dpf SR4G zebrafish.

Bars and intervals represent mean ± SEM (N = 3-6 biological replicates; sampling unit = 10 larvae/sample), with individual observations overlaid (no stimulus: white points, cyan intervals; after light/dark stimulus: black points, red intervals). Two-way ANOVA, followed by Tukey's post-hoc test, were used to identify significant differences between all groups. Different superscripts indicate statistically significant differences.